Promotor	Prof. dr. Philippe Crombé
	Vakgroep Archeologie
Copromotor	Prof. dr. Marc Van Meirvenne
	Vakgroep Bodembeheer
	Dr. Tine Missiaen
	Vakgroep Geologie & Bodemkunde

Decaan	Prof. dr. Marc Boone
Rector	Prof. dr. Anne De Paepe

Kaftinformatie: Schuine luchtfoto van Doelpolder Noord door Wim De Clercq (Vakgroep Archeologie, UGent)

UNIVERSITEIT
GENT

Faculteit Letteren & Wijsbegeerte

Jeroen Verhegge

Spatial and chronological prehistoric landscape reconstruction using geo-archaeological methods in the Lower Scheldt floodplain (NW Belgium)

Proefschrift voorgelegd tot het behalen van de graad van
Doctor in de Archeologie

2015

Acknowledgements

This phd would not have been possible without help of various people and instutions.

First of all, I would like to thank the promotor of this doctoral dissertation, Prof. Dr. Philippe Crombé, for giving me the opportunity to study the subject of the prehistoric landscapes of the lower Scheldt floodplain. His expertise, guidance and support have been indispensable in more ways than describable.

Furthermore I thank the co-promotors of this doctoral dissertation, Prof. Dr. Marc Van Meirvenne and Dr. Tine Missiaen for their valuable support.

I also owe many thanks all (former) colleagues at the department of archaeology-prehistory research group (specifically Dr. Erick Robinson, Dr. Joris Sergant, Machteld Bats and Evy Van Cauteren) and other department members; at the department of soil management-Orbit research group (specifically Dr. Philippe De Smedt, Dr. Timothy Saey, Samuel Delefortrie, Valentijn Van Parys) and at the department of geology and soil science, marine geology research group (specifically Koen De Rycker, dr. Katrien Heirman, Wim Versteeg). All staff and students involved are kindly acknowledged for their assistance with field work.

A PhD bursary was provided by Research Foundation – Flanders (FWO) as part of the project entitled: "Archaeological exploration across the land-sea boundary in the Doelpolder Noord area (Westerschelde estuary): impact of sea-level rise on the landscape and human occupation, from the Prehistory to Medieval times" (Grand number G024911N).

The CITG of TUDelft is thanked for providing and introducing me to the GEM-2 and Supersting instruments, TNO for the EM31 & 34 instruments. CPTs and Sonic drill Aqualock cores were carried out by SGS. Thanks to Jan Lippens for his constructive support. Selection of the dated macro remains was performed by Hanneke Bosch (ADC) and Luc Allemeersch (GATE). Radiocarbon dating was carried out by the Royal Institute for Cultural Heritage. The Province of Antwerp-Department of Culture-Heritage Service and the City of Antwerp-Department Archaeology are thanked for providing us with important radiocarbon dates. The Flemish Nature and Forest agency, Natuurpunt and all local farmers are thanked for allowing us access to their grounds. The corings from

Chapter 7 were mostly carried out within the framework of a research project funded by the Special Research Fund of Ghent University, entitled “The Flemish wetlands. An archaeological survey of the Scheldt floodplains”. Most fieldwork was done by Machteld Bats in collaboration with numerous colleagues and students from Ghent University, who all are kindly acknowledged. Specific thanks also go to Hannah Brown for proofreading the manuscript of Chapter 1, to Lauren Tidbury for proofreading the manuscript of Chapter 3 and dr. Erick Robinson for proofreading the manuscript of Chapter 4. Anonymous reviewers of the papers are also kindly acknowledged.

Familie en vrienden, bedankt voor jullie steun.

Bedankt, Sofie Scheltjens, voor alle onvoorwaardelijke steun, geduld, aanmoedigingen en offers van de voorbije jaren.

Ik zou dit proefschrift dan ook graag aan haar opdragen.

Preface

This PhD dissertation is written in the context of an interdisciplinary FWO project (Grand number G024911N), entitled 'Archaeological exploration across the land-sea boundary in the Doelpolder Noord area (Westerschelde estuary): the impact of sea-level rise on the landscape and human occupation from the prehistory to medieval times' and supervised by Prof. Dr. M. De Batist (Ghent University), Prof. Dr. Ph. Crombé (Ghent University), Prof. Dr. J. Verniers (Ghent University) and Prof. Dr. T. Soens (University of Antwerp). The project investigates the transition between the present onshore and offshore coast in the Scheldt polders of NW Belgium, more specifically at the location of Doelpolder-Noord (Figure 1). Reconstructing the gradual drowning of the landscape and its effects on human occupation through time, starting from the earliest prehistory, was the principal aim of this project. Given the constant threat of destruction caused by the development of the Antwerp harbor, a survey strategy had to be developed allowing detailed and fast (geo-)archaeological assessment. This methodology should be applicable to other similar coastal areas in Belgium and abroad.

The tasks and responsibilities of the archaeological partners of this project, namely Prof. Dr. Philippe Crombé and myself, were archaeological drilling, analysis of archaeological finds, Ground Penetrating Radar (later replaced with electromagnetic induction survey and electrical resistance imaging), Cone Penetration Testing (via subcontract), ^{14}C dating (via subcontract) and landscape occupation modelling and reconstruction. This PhD dissertation is a result of the fulfilment of these responsibilities, with a major focus on the supratidal zone of the land-sea transition.

Fieldwork was challenged by accessibility issues of the nature reserve of Doelpolder-Noord, because it was specifically designed for bird nesting. As a result, the main 'field laboratory' of the project was only accessible in July and August. The impact on the environment of the selected methods had to be minimized as well. Nearby fields were not suitable as test survey areas because access was denied by farmers, who are threatened by the expansion of the harbor and weary towards researchers, despite argumentation and illustration of the non-invasiveness of near surface geophysical methods.

Nevertheless, some pastures could be surveyed aside from Doelpolder-Noord using a Dualem 421s sensor. These surveys are not included in this dissertation, because the results did not reveal prehistoric landscape features but rather badly drained (Post-) Medieval gullies and indications of brackish groundwater.

Due to the restricted accessibility in the Scheldt polders, Kerkhove Stuw was selected as an additional test site along the Middle Scheldt. Here, a prehistoric natural levee had already been mapped by gridded coring, providing excellent validation data. After ERI and EMI survey, however, it became clear that recent land raising with construction waste and asymmetric drainage of the levee due to water extraction impacted near surface geophysical results negatively. Therefore, only the CPT results were analyzed, published and included in this PhD (Chapter 3).

Finally, a large paleolandscape coring survey of circa 60 ha in a developer-led archaeological project at Verrebroek Schoorhavenweg prompted a third test-case. Here, circa 20 ha was selected for a Dualem21s survey. The results revealed a shallow prehistoric paleotopography, which was also recorded in gridded coring data. Furthermore, land division structures in two orientations were discovered. During development-led trial trenching at regular spacing, the archaeological contractor, namely GATE Archaeology bvba, kindly allowed small trial trenches to be dug targeted towards the geophysical results. The excavation results indicate that aside from the prehistoric landscape, two different phases of (late) medieval land division structuring were at least partly recorded in both Dualem 21s EMI survey. The targeted trial trenches proved to add vital interpretative information to the geophysical survey results. The preliminary results were included in the archaeological report of the archaeological contractor. Full publication awaits dating and paleo-ecological analysis and will be done in the future. Therefore this survey was not included in this PhD dissertation.

The papers in this PhD were often a multidisciplinary team effort. Although I delivered large contributions in most chapters, specific parts of them rely heavily on the co-authors. Most markedly, the seismic survey data in Chapter 1 were processed and interpreted by Dr. Tine Missiaen (Ghent University). Electromagnetic induction-, electrical resistance-, cone penetration testing- and archaeological coring results were largely my work. Tine Missiaen also processed and interpreted the CPT-U and CPT-S data of Chapter 3, while CPT-E analysis and subsurface modelling was done by myself. Chapter 4 was mostly my work. The paleo-ecological and archaeological interpretations in Chapter 5 would not have been possible without the help of respectively Dr. Koen Deforce (Royal Belgian Institute of Natural Sciences) and Prof. Dr. Philippe Crombé, while chronological Bayesian modelling was my main part of this paper. Chapter 6 is mostly my work. The EMI depth modelling routine was developed and applied by Dr. Timothy Saey (Ghent University). Chapter 7 is based on archaeological coring data collected through years of hard work by Machteld Bats (formerly Ghent University, now GATE Archaeology bvba).

This chapter consists of an empirical comparative analysis of her results. My contribution in this mainly consists of a quantitative and spatial analysis and interpretation of these augering data in view of developing a standard protocol for detecting sealed prehistoric sites.

Abstract

Since the last decades, well preserved Late Glacial dune formations containing numerous prehistoric sites buried deeply below peat, OM rich clays and marine clayey to sandy sediments have been discovered during extensive construction works in the harbor of Antwerp situated in the lower Scheldt river basin in northwest Belgium. Archaeological excavations have identified the first presence of the transitional Mesolithic-Neolithic Swifterbant culture, previously only known from sites in the Netherlands and one site in northwest Germany, and evidence for the presence of other Final Paleolithic to Early Neolithic cultural remains. High quality organic preservation at these sites have offered the opportunity to reliably place Swifterbant occupation within the absolute chronology of the Mesolithic-Neolithic transition in this region, as well as the reconstruction of Swifterbant subsistence practices, most notably the incorporation of cattle husbandry into a traditional hunting-fishing-gathering economy.

This PhD dissertation focuses on three aspects of prehistoric occupation in the wetland region of the lower Scheldt river basin, namely (1) the development of a protocol for mapping the buried paleolandscape in view of archaeological surveys, (2) the modelling of peat rise and the dating of a short expansion of the tidal influence as a tool for assessing the gradual drowning of the area and human response and (3) the refinement and the optimization of the archaeological sampling strategies.

1. Development of a protocol for mapping buried paleolandscape

Until recently, (hand-)coring used to be the main tool for mapping prehistoric landscapes in comparable wetlands. In this PhD a more effective approach, including near surface geophysical and geotechnical techniques, has been developed and tested, mainly at Doelpolder-Noord.

Firstly, electrical resistance imaging and shear wave land seismics are judged to be unproductive, due to the required effort and limited results.

Secondly, high resolution electromagnetic induction electrical conductivity survey provides a suitable approximation of the prehistoric landscape variability but is challenged by variations in groundwater brackishness and the presence of recent land rais-

ing or dumps. Qualitative maps of the total subsurface features could be made using single coil pair sensors. Using electromagnetic induction sensors with multiple coil spacings and configurations, the prehistoric paleotopography could be reconstructed quantitatively within the limits of the instrument's depth of investigation. This depth model could be separated from electrical conductivity variations created by more shallow (post-)medieval landscape structures.

Thirdly, cone penetration tests (CPT) can provide an alternative solution beyond the instrument's depth of investigation and in areas unsuited for electromagnetic induction survey. The use of CPT was investigated in estuarine and river floodplain environments as well as an intertidal saltmarsh. The efficiency, reliability and repeatability was evaluated against coring. These data have generally allowed highly accurate mapping of the paleo-topography of the transition from Pleistocene sediments to overlying Holocene peat sequences. Thin OM rich clay intercalations within the peat layers could often still be identified. Additional pore pressure, conductivity and seismic velocity data (from CPT-U, CPT-C and CPT-S) did not add much crucial information and their main use seems to lie in the added value for the interpretation of electromagnetic induction, electrical resistance imaging and shear wave land seismic survey results.

2. Modelling peat rise and dating of a short expansion of tidal influence

After developing a geological mapping strategy, chronological evolution of the regional prehistoric landscape was reconstructed and related to its contemporaneous land use. As a case study, the influence of hydrological dynamics in the occurrence of the Swifterbant culture in these wetland regions of the lower Scheldt floodplain is investigated. This is carried out by employing a Bayesian chronological modelling approach to integrate stratigraphic as well as radiometric chronological data from accurately datable archaeological remains and key horizons in peat sequences. An age-depth model has been developed of the peat formation driven by the rising groundwater and the timing was determined of a Middle Holocene increased tidal influence, resulting in a short period of OM rich clastic sedimentation.

Two different site types could be identified between the six excavated sites – dune and natural levee sites – which had contemporaneous periods of occupation, but different occupation histories. The integration of the archaeological and paleoenvironmental dates from both site types suggests a Swifterbant settlement system in the area. This could explain the specific tempo and trajectories of cultural and economic change in the Scheldt basin during the neolithisation well over a millennium later than in the nearby loess region.

This land use model consists of larger, more continuously occupied camps on natural levees or point bars along the river valley, resulting in complex palimpsest sites on the one hand and relatively specialized and temporarily inhabited cattle and hunting-fishing camps on the floodplain dunes on the other hand. Moreover, Bayesian chrono-

logical modelling suggests that the Swifterbant occupation of the dune sites has occurred shortly after the emergence of a brackish (supra-)tidal landscape replacing a freshwater marsh. The dated sites of Deurganckdok-Sector B and M were left shortly before being covered with organic sediments, which fits within the regional age-depth model of initiating peat formation.

The chronological relation between the end of the occupation of the dune sites and the disappearance of the (supra-)tidal landscape is still unclear due to a lack of dated dune sites with higher elevations. Therefore the area of Doelpolder-Noord suitable for prehistoric occupation was determined using the modelled subsurface.

3. Refinement and optimization of archaeological sampling strategies

Since the 90s and particularly in Dutch and Belgian wetland research, archaeological sampling using Dutch augers has increasingly become important for the detection of covered prehistoric hunter-gatherer sites, comprised mainly of scatters of lithic artefacts of variable size and find density. The archaeological results of eleven cored sites are analysed to develop a core sampling strategy for prospecting a broad range of prehistoric sites. The results indicate that augering within a 10m grid with a 10cm to 12cm diameter core and sieving through 1mm to 2mm meshes allows the detection of nearly all identified sites, even with a small area and a low find density. A two-step gridding approach is recommended to increase discovery rates.

This approach was followed at the reconstructed dune in Doelpolder-Noord. Part of it was archaeologically sampled in using the proposed methodology by Dutch hand augering on the top and Sonic Drill Aqualock coring on the flanks. Archaeological indicators for prehistoric occupation, such as burnt bone and flint fragments, were retrieved from these samples after sieving.

Samenvatting

Tijdens grote infrastructuurwerken in de haven van Antwerpen, gelegen in het bekken van de Benedenschelde in het noordwesten van België, zijn de voorbije decennia goed bewaarde, laatglaciale duinlandschappen met talrijke prehistorische sites aan het licht gekomen. Deze zijn begraven onder veen, organische klei en mariene kleiige tot zandige sedimenten. De archeologische opgravingen hebben de aanwezigheid van de Swifterbantcultuur uit de overgangsperiode van het mesolithicum naar het neolithicum aangetoond, die voordien uitsluitend vastgesteld is bij verschillende vindplaatsen in Nederland en een site in het noordwesten van Duitsland. Daarnaast zijn aanwijzingen voor de aanwezigheid van overige materiële culturen van het finaal-paleolithicum tot het vroeg-neolithicum aangetroffen. Dankzij de goede bewaring van organische resten afkomstig van deze vindplaatsen is niet alleen de aanwezigheid van de Swifterbantcultuur nauwkeurig gesitueerd kunnen worden in de absolute chronologie van de overgangsperiode van het mesolithicum naar het neolithicum in deze regio maar is ook de reconstructie mogelijk gemaakt van de occupatie en activiteiten van deze culturele groep, zoals de integratie van veeteelt in een samenleving van jagers-vissers-verzamelaars.

Dit onderzoek richt zich op drie aspecten van prehistorische aanwezigheid in de *wetlands* in het bekken van de Benedenschelde. Vooreerst komt de ontwikkeling van een strategie voor karteren van begraven paleolandschappen in functie van archeologische prospecties aan bod. Daarnaast worden de modellering van veenvorming door grondwaterstijging en de datering van occasionele sedimentafzettingen onder invloed van de getijdenwerking behandeld. Deze worden gebruikt voor de reconstructie van de geleidelijke 'verdrinking' van deze regio en de prehistorische occupatie in dit landschap. Ten slotte worden methodes voor archeologische prospectie en staalname verfijnd en geoptimaliseerd.

1. Ontwikkeling van een strategie voor karteren van begraven paleolandschappen

Tot nu toe zijn manuele boringen het meest gebruikte instrument voor het karteren van begraven prehistorische landschappen in *wetlands*, die vergelijkbaar zijn met het onderzoeksgebied. In kader van dit proefschrift is een meer doeltreffende strategie op

basis van geofysische en geotechnische methoden ontwikkeld en getest in Doelpolder-Noord. Ten eerste blijken elektrische weerstandsmetingen en schuifgolf landseismiek onproductief, wegens de vereiste fysieke inspanningen en de beperkte resultaten.

Ten tweede bieden elektrische geleidingsmetingen door elektromagnetische inductie (EMI) met hoge resolutie een geschikte benadering van de variabiliteit in de topografie van het prehistorische landschap. Deze methode wordt echter bemoeilijkt door variaties in de brakheid van het grondwater en aanwezigheid van recente landophogingen. Kwalitatieve kaarten van de totale ondergrondvariabiliteit zijn evenwel verkregen door middel van het gebruik van een instrument met één spoelenpaar. Toepassing van elektromagnetische inductiesensoren met meerdere spoelafstanden en configuraties heeft een kwantitatieve reconstructie van de paleotopografie mogelijk gemaakt binnen de beperkingen van de meetdiepte van het instrument. Dit dieptemodel kon worden gescheiden van variaties in elektrische geleidbaarheid door meer ondiepe, (post-)middeleeuwse landschapsstructuren.

Ten derde reiken *cone penetration tests* (CPT) een alternatieve oplossing aan voor gebieden die niet geschikt zijn voor elektromagnetische inductie en voor gebieden waar het prehistorisch niveau dieper gelegen is dan de meetdiepte van het instrument. Het gebruik van CPT is zowel onderzocht in een bedijkt overstromingsgebied van het estuarium en de zoetwater rivier als in een intergetijdengebied, zoals een schorre. De efficientie, betrouwbaarheid en herhaalbaarheid van CPT is vergeleken met boringen. In het algemeen laten deze data toe om de paleotopografie van de overgang van Pleistocene sedimenten naar bovenliggende, Holocene veensequenties nauwkeurig in kaart te brengen. Hierbij zijn dunne, organisch rijke kleilagen geïdentificeerd tussen de veenlagen. Bijkomende data van waterspanning, elektrische geleidbaarheid en seismische snelheid (CPT-U, CPT-C en CPT-S) hebben echter weinig informatie kunnen bijdragen. Het voornaamste gebruik betreft toegevoegde waarde voor de interpretatie van resultaten verkregen door elektromagnetische inductie, elektrische weerstandsmetingen en schuifgolf landseismiek.

2. Modellering van veenvorming door grondwaterstijging en datering van occasionele sedimentafzettingen door getijdenwerking

Na de ontwikkeling van een strategie voor geologische kartering, is de chronologische evolutie van het regionale, prehistorische landschap gereconstrueerd en gerelateerd aan het toenmalig landgebruik. Als voorbeeld is de invloed van de hydrologische dynamiek bij de opkomst van de Swifterbantcultuur in de *wetlands* van het overstromingsgebied van de Benedenschelde onderzocht. Hierbij is Bayesiaanse chronologische modellering toegepast om de stratigrafische en koolstof radiometrische gegevens van nauwkeurig dateerbare archeologische resten en horizonten in de veensequentie te integreren. Een tijd-diepte-model is ontwikkeld van het begin van de veenvorming als gevolg van grondwaterstijging en de toename van getijdenwerking tijdens het midden

Holoceen, wat resulteerde in kortstondige afzettingen van organisch-klastische sedimenten is gedateerd.

Twee verschillende typen van sites zijn herkend bij zes opgegraven vindplaatsen (duin- en oeversites), die gekenmerkt worden door gelijktijdige aanwezigheid maar verschillende occupatiegeschiedenis. Integratie van archeologische en paleolandschappelijke dateringen afkomstig van beide site typen suggereert de aanwezigheid van een nederzettingsysteem van de Swifterbantcultuur in de regio. Dit kan het specifieke tempo en verloop verklaren van culturele en economische veranderingen in het Scheldebekken tijdens de neolithisatie, meer dan een millenium later dan in de nabij gelegen leemstreek.

Het model voor prehistorisch landgebruik bestaat uit omvangrijke en meer langdurig bezochte kampementen op oeverwallen of kronkelwaardruggen langs riviervalleien, wat resulteert in complexe palimpsest-sites enerzijds en relatief gespecialiseerde en tijdelijk bewoonde jacht- en visvangstkampen met veeteelt op duinen in de overstromingsvlakte anderzijds. Bovendien suggereert de Bayesiaanse chronologische modellering dat de Swifterbantoccupatie van de duinsites heeft plaatsgevonden kort na de opkomst van een (supra-)getijdenlandschap met brakwater afzettingen, waarbij veenmoerasgebied met zoet water vervangen is. De gedateerde Swifterbant vindplaatsen Deurganckdok-Sector B en M werden verlaten kort voor ze afgedekt werden met organische sedimenten, wat binnen het regionale tijd-diepte-model van de start van veenvorming past. De chronologische relatie tussen het einde van de prehistorische bewoning op duinsites en het verdwijnen van het (supra-) getijdenlandschap is voorlopig onduidelijk, wegens het ontbreken van gedateerde sites op een hogere locatie in het landschap. Daarom is het gebied van Doelpolder-Noord met mogelijke vindplaatsen bepaald op basis van de gemodelleerde paleotopografie.

3. Verfijning en optimalisatie van archeologische staalname

Sinds de jaren ’90 wordt archeologische staalname door middel van edelmanboren steeds meer toegepast voor de detectie van afgedekte, prehistorische jagers-verzamelaarssites, voornamelijk in onderzoek naar *wetlands* in België en Nederland. Deze sites bestaan hoofdzakelijk uit concentraties van lithische artefacten van variabele omvang en densiteit. De archeologische resultaten van elf aangeboorde vindplaatsen zijn hierbij geanalyseerd, teneinde een boorstaalnamestrategie te ontwikkelen voor de prospectie van een breed scala aan prehistorische sites. De resultaten geven aan dat boren in een grid van 10 m met een boor met diameter van 10 cm tot 12 cm en zeven met een maaswijdte van 1 mm tot 2 mm toelaat om vrijwel alle geïdentificeerde vindplaatsen te detecteren, zelfs in geval van beperkte oppervlakte en lage vondstdensiteit. Een aanpak met verdichting van het grid in twee stappen is aanbevolen om ontdekkingskansen te verhogen.

Deze methode is toegepast op de gereconstrueerde duin in Doelpolder-Noord. Deze is archeologisch bemonsterd door middel van edelmanboringen op de top en door middel van Sonic Drill Aqualock-boringen op de flanken volgens de voorgestelde aanpak. De zeefstalen hebben hierbij archeologische indicatoren voor prehistorische bewoning, zoals vuursteenfragmenten en verbrand bot, opgeleverd.

List of abbreviations

A	Oxcal agreement index
A_{model}	Oxcal model agreement index
ABA	acid-base-acid treatment of a radiocarbon dating sample
AD	uncalibrated years *anno domini* or after the birth of Christ
ADW	archeologische dienst Waasland/Waasland archaeological service
AGIV	agentschap geografische informatie Vlaanderen/Flemish geographic information agency
BC	uncalibrated years before the birth of Christ
B.C.E.	see BC
Beta	radiocarbon date by Beta Analytic, Inc.
(yr) BP	(radiocarbon years) before 1950 (uncalibrated)
Cal AD	calibrated calendar years *anno domini* or after the birth of Christ
Cal BC	calibrated calendar years before the birth of Christ
(yr) cal BP	calibrated (calendar years) before 1950
CPT(-E)	(electric) cone penetration test
CPT-C	electrical conductivity cone penetration test with a dielectric cone
CPT-S	seismic cone penetration test
CPT-U	pore pressure piezocone penetration test
DEM	digital elevation model
DGPS	differential global positioning system
DGNSS	see DGPS
DPN	Doelpolder Noord research area
DOI	depth of investigation
GI-*i*	Greenland interstadial with identifier '*i*'
GPS	global positioning system
GS-*i*	Greenland stadial with identifier '*i*'
EC	electrical conductivity
$EC^*=\sigma^*$	modelled electrical conductivity
$ECa=\sigma_a$	apparent electrical conductivity

$EC_i=\sigma_i$	electrical conductivity of layer *i*
EM	Early Mesolithic
EM31	Geonics EM31 electromagnetic induction ground conductivity sensor
EM34	Geonics EM34 electromagnetic induction ground conductivity sensor
EMI	electromagnetic induction (survey)
EN	Early Neolithic
ERI	electrical resistance imaging (survey)
Est.	estuarine
FM	Final Mesolithic
FP	Final Paleolithic
f_s/fs	sleeve friction
GEM(-)2	Geophex GEM-2 electromagnetic induction ground conductivity sensor
GPR	ground penetrating radar
GrN	radiocarbon date by Centre for Isotope Research, University of Groningen
HCP	horizontal coplanar coil configuration
HH GPS	handheld GPS
IP	in-phase response to an induced electromagnetic field
IRPA	see RICH
K	Kerkhove research area
KIA	radiocarbon data by Leibniz-Labor Christian, Albrechts Universität, Kiel
LBK	*Linearbandkeramik* or linear pottery culture
LGW	local ground water level
LIN	low induction number conditions
LM	Late Mesolithic
LMHW	local mean high water level
MAEE	mean absolute estimation error
mb	mechanical boring location
MEE	mean estimation error
MHW	mean high water level
MM	Middle Mesolithic
MSL	mean sea level
Neo	Neolithic
NGI	nationaal geografisch instituut or national geographic institute of Belgium
NPP	Doel nuclear power plant core by Deforce (2011)
NZA	radiocarbon data by Rafter Radiocarbon Laboratory
OM	organic matter
Org.	rich in organic matter (=organic)
P	Oxcal outlier probability

P-wave	seismic compressional wave
pdf	probability distribution function
PRP	perpendicular coil configuration
q_c/qc	cone tip resistance
QP	quadradure phase response to an induced electromagnetic field
qt	corrected tip resistance
r	Pearson correlation coefficient
R^2	coeficient of determination
Rf	friction ratio
$R_i(z)$	cumulative electrical conductivity response (% of the measured signal relative to 1) from the soil volume above a depth z in *i* coil configuration mode
RICH	radiocarbon date by ^{14}C laboratory of royal institute for cultural heritage
RMSEE	root mean squared estimation error
RSL	relative sea level
RTK-GPS	real time kinematic global positioning system
s	transmitter receiver spacing (m) of an electromagnetic induction sensor
S-wave	seismic shear wave
SBT	soil behaviour type in soil classification chart by Robertson et al. (1986)
TAW	tweede algemene waterpassing= national ordnance level (mean low water tide level in Oostende)
u	in situ pore pressure, measured with CPT-U
UtC	radiocarbon data by the van de Graaf laboratory, Utrecht
VAA	archaeological site of Verrebroek Aven Ackers
VCP	vertical coplanar coil configuration
Vs	S wave seismic velocity
Watlab	Waterbouwkundig laboratorium van het Vlaamse departement mobiliteit en openbare werken/hydrological laboratory of the Flemish department of mobility and public works
Z-test	statistical Z score test with p-value as the sample results at a chosen significance level
z	depth
z*	modelled depth
z_i	depth of layer *i*
?	Oxcal outlier
σ	1 σ = standard deviation in radiocarbon pdf context, approximately 68 % 2 σ = date range at two standard deviations, approximately 95 %

List of tables

List of figures

Table of contents

Chapter 1 Introduction

1.1 Geological and geographic background

The presented research mainly focusses on the (embanked) floodplains covered with Holocene (peri-)marine sediments of the Lower Scheldt (see Kiden, 1991). Van Eetvelde and Antrop (2009) have characterized this landscape as the polderland of the Scheldt River (in short: the Scheldt polders). Doelpolder Noord, part of the Scheldt polders was selected as the most important field laboratory (Figure 1-top right). Other area of the Scheldt floodplain are also included: Chapter 3 includes the site of Kerkhove-Stuw, situated in the floodplain along the Middle Scheldt river (Figure 1-bottom left). Chapters 5 and 7 also include the results of various sites along the Middle and Lower Scheldt.

The Scheldt polders are situated at the transition from the Dutch estuaries of the Meuse, Rhine and Scheldt to the geographic regions of Sandy Flanders (within the Flemish valley (Antrop, 1995-2000; Antrop, 2000; Van Eetvelde and Antrop, 2009)) and the Campine region (National Committee of Geography of Belgium, 2012). The complex sedimentation history of the (Lower) Scheldt floodplain and more specifically the Scheldt polder landscape has resulted in a complex lithostratigraphy and consequently a complex prehistoric occupation history (Figure 2).

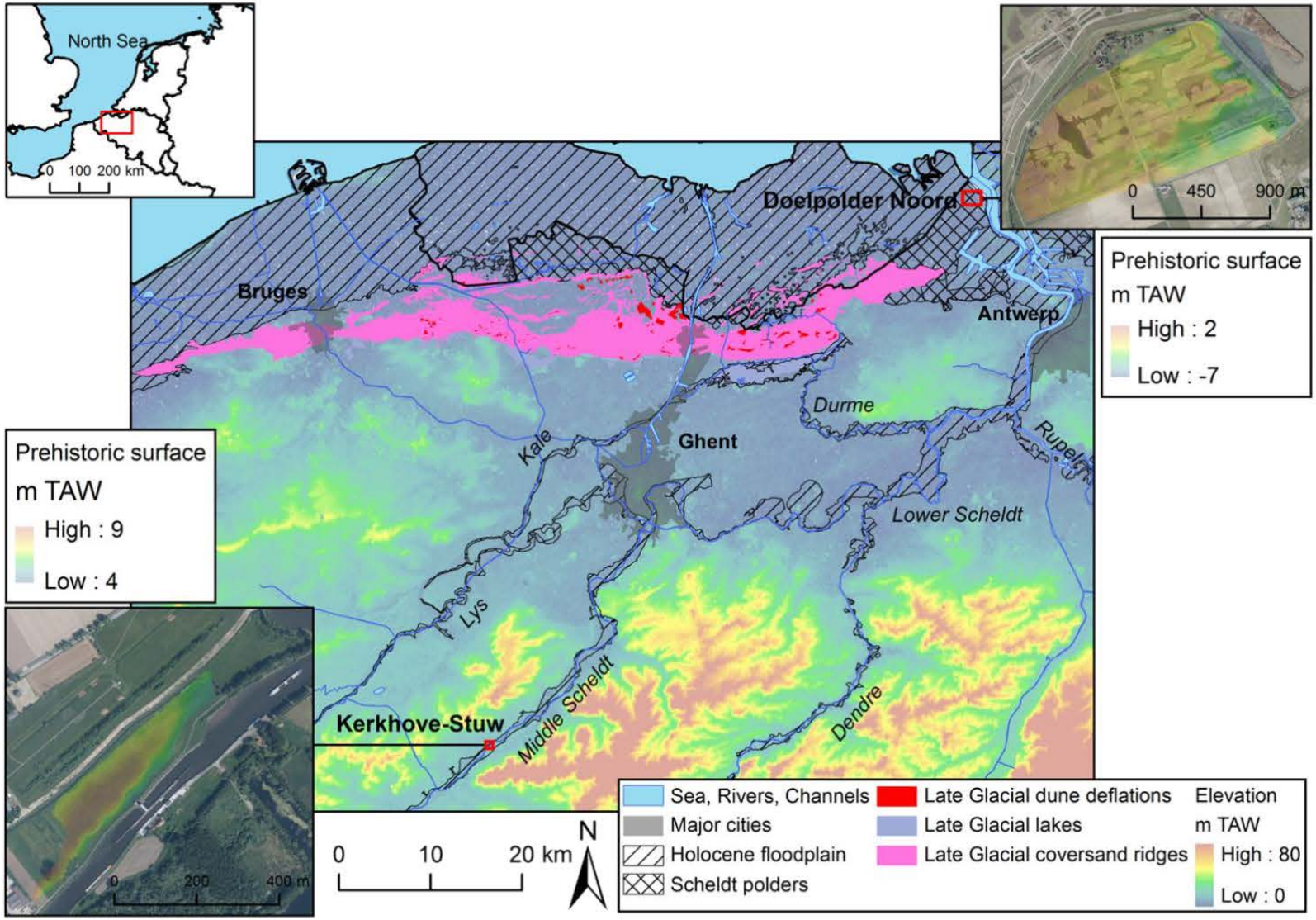
North Sea
0 100 200 km
Doelpolder Noord
0 450 900 m
Prehistoric surface
m TAW
High : 2
Low : -7
Bruges
Antwerp
Durme
Ghent
Kale
Rupel
Lower Scheldt
Prehistoric surface
m TAW
High : 9
Low : 4
Lys
Middle Scheldt
Dendre
Kerkhove-Stuw
0 200 400 m
0 10 20 km
N
Sea, Rivers, Channels
Major cities
Holocene floodplain
Scheldt polders
Late Glacial dune deflations
Late Glacial lakes
Late Glacial coversand ridges
Elevation
m TAW
High : 80
Low : 0

Figure 1: Map of NW Belgium indicating a selection of the largest outcropping geomorphological units (based on Heyse, 1979) and major rivers, which are relevant for prehistoric landscape reconstruction and mentioned in the introduction. Top left: location map of NW Belgium with inset of the central map in red. Top right: prehistoric surface = elevation model of the boundary between the top of the coversand and the base of the peat at Doelpolder-Noord. Bottom left: prehistoric surface = elevation model of the boundary between the top of the buried natural levee and the base of the organic material (OM) (-rich) sediments at Kerkhove-Stuw.

1.1.1 The formation of the coversand landscape

The formation of the Flemish coversand ridges (Figure 1), partially outcropping and partially buried below Holocene sediments, has started after the final incision and sedimentation of a Middle to Late Pleistocene (Pillans and Gibbard, 2012) Glacial paleovalley ('Vlaamse Vallei' and paleo-Scheldt valley) (De Moor, 1963; De Moor and Heyse, 1978a; Hijma et al., 2012; Tavernier, 1946). During the Late Weichselian (as defined by Svensson et al. (2006), i.e. the Late Pleniglacial and Late Glacial in Table 1), this repeatedly incised and infilled river valley was filled for the last time with fluvio-aeolian deposits of sand. These were eroded from the valley walls and deposited in a braided river system (Adams et al., 2002; Bogemans, 1997; De Moor and van de Velde, 1995; Kasse, 2002).

Major aeolian sedimentation occurred at the end of the Late Pleniglacial (GS-2a) and during the Bølling (GI-1e) and Older Dryas (GI-1d) (Greenland (Inter)Stadial: see Björck et al., 1998). The absence of permafrost allowed water infiltration and preservation of the horizontally deposited sand deposits and small dunes. During this period numerous sand ridges were formed by local reworking of Pleniglacial (Pillans and Gibbard, 2012) cover sands. Most of these ridges are relatively small, except for the "large coversand ridge between Maldegem and Stekene", which blocked the 'Vlaamse Vallei' from west to east (De Moor and Heyse, 1978b; Verbruggen et al., 1996). The small dunes are characterized by indications of a vertical drying out sequence and initiating vegetation development during the Bølling (Hilgers, 2007; Kasse, 2002; Schirmer, 1999). Simultaneously numerous shallow ponds, dune-slacks and lakes were created in deflated depressions between the dunes, forming important freshwater reservoirs (Bos et al., 2013). Aeolian sedimentation stopped at the start of the Allerød (GI-1c) (Björck et al., 1998) and was followed by birch- and later pine forest development (Hilgers, 2007; Kasse, 2002). A new and last episode of aeolian erosion occurred during the Younger Dryas (GS1), leading to the deposition of several meters of reworked sands mainly in former depression, and a local reversal of the topography (Crombé et al., 2012).

Table 1: ‘Timetable listing the chronostratigraphical units and archaeological periods of the last 20 ka. Ages are expressed in ka B.C.E. Chronostratigraphy of the Holocene is based on Terberger et al. (2006); the subdivision of the Pleistocene is based on radiocarbon dated pollen diagrams from the Netherlands, as revised by Hoek (2001). The time frame of the archaeological periods is expressed for the situation in Sandy Flanders. Note that at present, no traces of the Late Paleolithic and Ahrensburgian cultures have been reported in Sandy Flanders (Crombé et al., 2011c; Crombé and Verbruggen, 2002) The vegetation types are also indicated.’(Table and Caption from Zwertvaegher et al., 2013: figure 2).

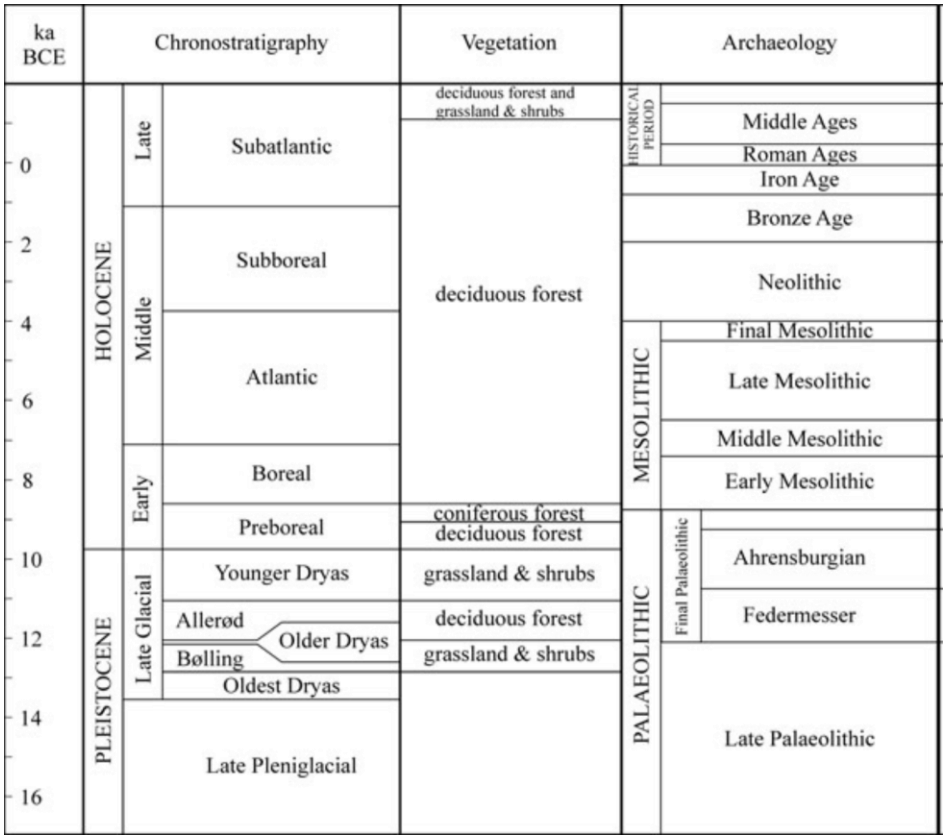

1.1.2 The formation of the Scheldt river

After having breached the cuesta of the Boom formation (Laga et al., 2001) near Hoboken, the Pleniglacial braided Scheldt river changed its flow direction from the ‘Vlaamse Vallei’ to its current trajectory through the cuesta (Kiden, 2006; Kiden and Verbruggen, 2001). A change to a meandering river system characterized by lateral migration forming large oxbow lakes took place during the Late Glacial. This transition started most likely before the onset of the Allerød (Bogemans et al., 2012), but was certainly completed before the end of the Allerød or the start of the Younger Dryas (Crombé, submitted). Downstream of Antwerp, meandering was less pronounced and lateral accretion deposits were formed with only one or two (or even none) fining up sequences (Bogemans, 1997). In contrast to other NW European river systems, the Scheldt river did not evolve

from a meander to anastomosing pattern during the Younger Dryas as observed in neighboring countries (Hilgers, 2007; Kasse, 2002). Instead the meandering channel system remained active during the Younger Dryas and the Early Holocene (Bogemans et al., 2012; Crombé et al., 2013a; Kiden, 1991). Nevertheless, due to reduced fluvial discharge, vertical sediment accretion of calcareous gyttja started at the end of the Allerød and the beginning of the Younger Dryas (Crombé, submitted; Meylemans et al., 2013). During the Younger Dryas (GS-1), the disappearance of vegetation cover and reduced fluvial discharge allowed the most outspoken (river) dune formation, reworking older coversand and sediments from the river interfluvia of the Scheldt valley (e.g. Kiden, 2006: fig. 2) (Bogemans and Vandenberghe, 2011; Hilgers, 2007; Kasse, 2002; Kiden, 2006). The resulting (river) dunes were the most important dry living surfaces which reduced in size throughout the Holocene as a consequence of the relative sea level rise.

During the Preboreal, fluvial discharge further decreased due to an increased evapotranspiration, resulting in a transition to shallow river water conditions and peat formation. The river system evolved into a locally anabranching (see Nanson and Knighton, 1996) pattern (Bogemans et al., 2012; Kiden, 2006). The reduced erosion and rising local groundwater allowed the formation of alder carr so-called basal (see Baeteman, 2004; Vos and van Heeringen, 1997) peat during the Early Atlantic period (Early and Late Atlantic as used by Deforce, 2014), first in the deepest channels and later covering the entire alluvial plain (Deforce, 2011; Kiden, 1991; Kiden, 2006; Vos and van Heeringen, 1997). At the start of the Late Atlantic period, the formation of the basal peat is interrupted by a sudden upstream expansion of the Scheldt estuary after the creation of the shorter Oosterschelde trajectory (Vos and van Heeringen, 1997). In the study region, occasional (brackish) water flooding resulted in the deposition of a intercalating layer of often OM rich so-called Calais clay (see Gullentops et al., 2001; Vos and van Heeringen, 1997) in the alluvial plain of the Scheldt (Kiden, 1991). During this period, the dry areas of the dunes are covered with alluvial hardwood forest (Crombé, 2005; Deforce et al., 2013; Van Neer et al., 2013). As a consequence of the closing coastal barrier, the tidal influence gradually decreased (Vos and van Heeringen, 1997). Sedimentation decreased and due to the rising groundwater table the formation of a wood peat bog (re-)started to form, later followed by a reed peat bog (Deforce, 2011). This lithostratigraphic unit is known as the 'Holland' peat by Vos and van Heeringen (1997). Bogemans (1997) identifies this unit as the Antwerp peat, but does not distinguish a basal peat layer or OM rich clay intercalation. Breaches in the coastal belt occurring from the sixth century BC onwards caused a renewed and gradually expanding marine influence with associated estuarine tidal deposition and erosion until this was halted by human intervention (Kiden, 2006; Vos and van Heeringen, 1997).

Because of the discussion about the Belgian lithostratigraphic nomenclature (Baeteman, 2004), the closely related nomenclature proposed by Vos and van Heeringen (1997) will be used in this dissertation. The latter accentuate that the formation of these

lithostratigraphic units is diachronic and does not reflect chronologically distinct periods of marine transgression or regression. This has led to a completely new nomenclature in the Netherlands (Weerts et al., 2006). Baeteman (2005b) suggested the introduction of the Streif classification system in Belgium, but this has not yet been adopted by the National Commission on Stratigraphy, which still uses Gullentops et al. (2001).

1.2 Archaeological background

Currently, no *in situ* evidence is known for human occupation in Sandy Flanders and the Scheldt valley before the Older Dryas (Crombé et al., 2012). However, in the same time period Late Magdalenian sites have been found more to the south in the loess region of Belgium and in caves along the Meuse (De Bie and Vermeersch, 1998).

Archaeological sites of the Late Magdalenian or Creswello-Hamburgian culture dating back to the Bølling interstadial period may, however, be present buried within the coversand ridges, beyond the reach of manual augering methods (Crombé et al., 2012). Indeed possibly attractive settlement locations were formed along dune deflations (Bos et al., 2013).

The earliest hunter-gatherer sites belonging to the *Federmesser* culture and date back to around the Allerød (13,900 to 13,700 cal. BP). These sites are mainly located close to the present day surface in the vicinity of the remnant of Late Glacial shallow lakes, like the Moervaart depression, and deflation dune slacks, especially along the south side of the 'great coversand ridge Maldegem and Stekene' (Bats et al., 2009; Bats et al., 2010; Crombé, submitted; Crombé and Verbruggen, 2002; Heyse, 1983). However, these freshwater lakes dried out before the end of the Late Glacial, most likely in response to the intra-Allerød cold phase making the area less attractive for hunter-gatherers (Bats et al., 2009; Bats et al., 2010; Crombé et al., 2012; De Smedt et al., 2013b).

The apparent absence of (Epi) Ahrensburgian and/or Epilaborian sites is not only caused by taphonomic factors but also by the prevalent cold, windy and dry conditions of the Younger Dryas. In addition finds from these cultural traditions are typologically similar to later Mesolithic artifacts and hardly distinguishable without context information (Crombé et al., 2014; Vermeersch, 2011). Therefore sealed contexts dating back to the Younger Dryas have significant archaeological scientific potential.

From the Boreal (= Early Mesolithic) onwards, the study-area testifies increased occupation and exploitation by highly mobile hunter-gatherers frequently revisiting the same parts of the "great coversand ridge Maldegem and Stekene" over longer periods of time (e.g. Crombé et al., 2011c: fig. 12). This goes together with an increased settlement

focus on the banks of the Scheldt and its tributary, the Kale/Durme (Crombé et al., 2013a; Perdaen et al., 2011).

The Middle and Late Mesolithic period, corresponding to the Boreal-Atlantic transition and Early Atlantic, is characterized by a reduced mobility and a preference for lower landscape parts such as natural levees or point bars along the Scheldt and its tributaries (Perdaen et al., 2011; Van Strydonck et al., 1995). Hardly any such sites are known further away from water ways (Crombé et al., 2013b; Crombé et al., in press-b). Re-occupation of inland coversand ridges occurred during the Swifterbant and Michelsberg cultural period situated in the 5th and 4th millennium cal BC (Crombé, 2005).

After this period, no traces of prehistoric human settlement are found in the Scheldt polders until the Roman period (De Clercq and Van Dierendonck, 2008; Sier, 2003). Crevasse splay deposits in similar alluvial sequences in the Netherlands have proven to be at least temporarily attractive for occupation from the Middle Neolithic period until the Bronze Age (van Dinter and van Zijverden, 2010). Despite renewed estuarine sedimentation, from the Middle Ages onwards, the region was attractive for pastural and subsequently agricultural exploitation (Van Roeyen et al., 2001). The thickness of the tidal sediments is determined by the chronology of variably successful land reclamations by embankments. The estuarine channel systems of older polders, such as Doelpolder, were formed in a large floodplain, resulting in smaller channels and less estuarine sedimentation. Conversely, more recent polders, such as Prosperpolder have a thicker estuarine sediment layer and a higher present day surface elevation, because larger tidal channel systems were active in the decreasing area of the estuarine floodplain. This proces is discussed extensively by Jongepier et al. (2015). As a result, older polders cover better preserved and less deeply buried prehistoric landscapes and sites.

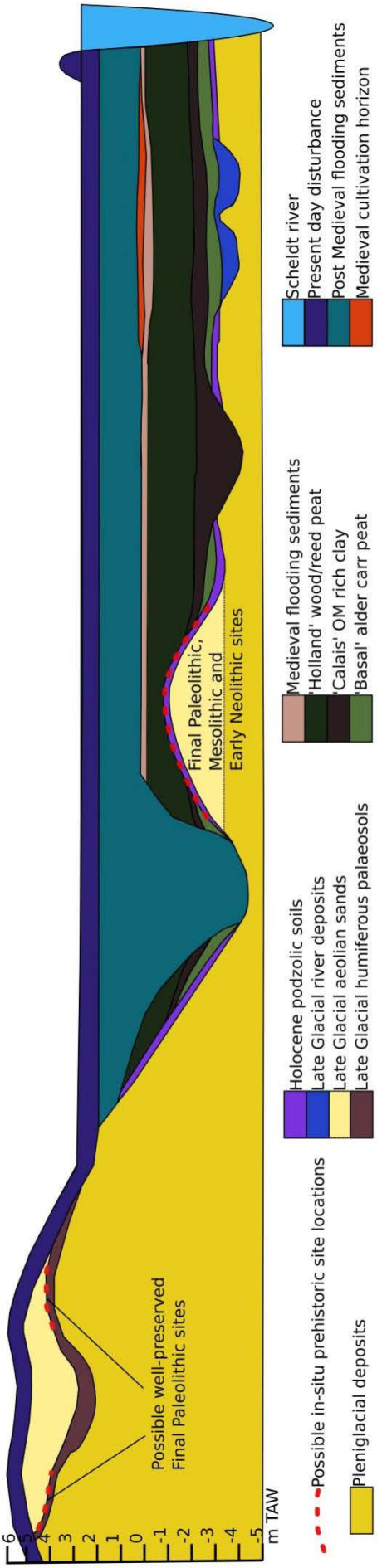

Figure 2: Schematic transect of the lithostratigraphy from the Scheldt polders to the surfacing coversand region with the possible locations of well-preserved prehistoric sites (an elaboration of Crombé (2005 Fig. 36) (not to scale).

1.3 Problem definition and aims

Prehistoric landscape reconstruction for archaeological purposes in this PhD has two major aims. Firstly, it could be aimed as a prospection tool for identifying and characterizing archaeological sites in order to decide about excavation or *in situ* preservation measures in a cultural resource management/development archaeology context. Therefore, our research in paleolandscape reconstruction and archaeological prospection strategies also has an economical, societal and heritage value aside from the scientific value. Secondly, paleolandscape reconstruction allows to evaluate existing archaeological site knowledge in its environmental context and to raise new purely scientific archaeological research questions about the prehistoric landscape occupation history of the region.

Since rescue excavations 15 to 20 years ago during the expansion of the Antwerp harbor, situated in the Lower Scheldt polders, the research group of prehistory at the archaeology department of Ghent University has underlined the importance of archaeological evaluation and prospection prior to the start of infrastructure works. The mainly prehistoric sites impacted by these subsurface interventions have scientific importance because they are rarely found with such degree of conservation closer to the surface. From the Early Atlantic onwards, basal peat started to cover the Pleistocene coversand ridges, sealing well-preserved prehistoric lithic scatter sites. Outside the polders, such sites are often disturbed by modern agricultural activities or other anthropogenic disturbances within the present day Ap-horizon (Figure 2). In addition, occasions to investigate such complete archaeological landscapes are very rare. In advance of these large infrastructure construction projects, including the construction of two large harbor docks – the Verrebroek and Deurganck docks (Crombé, 2005) - no archaeological evaluations could be done. As a consequence, excavations of accidentally discovered sites had to be performed under large time pressure, often literally ahead of the construction crew, without assessment of the find expectation and excavation costs.

Since 2002, however, the reformed Flemish heritage agencies started to implement the principles from the 'La Valletta Treaty' on archaeology enforcing constructors- and land- developers to fund salvage archaeological operations (De Clercq et al., 2012). Since the onset of the new Flemish heritage decree on January 1st 2015, this treaty has also been integrated in heritage legislation and cultural resource management. This evolution has been the reason to develop minimally invasive strategies to map buried landscapes and archaeological sites.

Such development is not an easy task as aeolian and alluvial/marine sediments do not only protect the buried archaeological remains but also make the latter harder to detect using standard prospection methods, such as field walking, oblique aerial pho-

tography, digital elevation model analysis or trial trenching. On top of that, the prehistoric sites in the (buried) coversand ridges are almost featureless due to the eluviation of prehistoric soil features, such as hearths or pits. As such the sites can be considered as artefact scatters (Sergant et al., 2006a), often forming palimpsests if the landscape locations were visited repeatedly by prehistoric people.

As a consequence, archaeological prospection of prehistoric landscapes and sites in such context ideally consists of a 2-phase/stage process. In a first phase, the buried sediments are mapped to reconstruct landscape development through time. In a second phase, well preserved strata in landscape locations suitable for prehistoric occupation (dunes, scroll bars, river and lake levees, etc.) are sampled and the retrieved samples checked for artefacts or other indicators of human occupation (Bats, 2007; De Clercq et al., 2011; Tol et al., 2004).

Over the last decades manual coring was generally applied to map the subsurface geology and paleosols and for subsequent archaeological sampling (Bats et al., 2006). This method was chosen because cheap and low-tech hand cores and augers had already been developed during the last century for geological mapping of the Quaternary and for pedological studies. However, the manpower required for these cheap and low tech methods has practical, ergonomic and physical sampling limitations. Therefore cost effective archaeological evaluation is impossible when the depth to the archaeological (in casu prehistoric) level and the complexity of the overburden increase (Soens et al., 2012). New industrial and infrastructural developments are planned in areas of NW Belgium with Holocene sedimentation regions (eg. Antwerp harbor expansion, nature compensation, flooding protection). In addition, alluvial and estuarine plains are preferred locations for large scale infrastructure works not only in NW Belgium but also elsewhere in river valleys and coastal plains (Brown, 1997; Vos et al., in press). Therefore the need for developing alternative methods to map subsurface prehistoric landscapes and their diachronic evolution is urgent. In this PhD, the effectiveness of various existing geophysical and geotechnical methods for paleolandscape mapping will be tested within two locations in the Scheldt valley, Doelpolder-Noord and Kerkhove-Stuw (Figure 1), to propose an improved paleolandscape evaluation strategy in the context of prehistoric archaeological evaluations.

Another research aim of this PhD dissertation is the precise dating and chronological reconstruction of the regionally changing sedimentary history in view of possible relations with the prehistoric occupants of these changing landscapes. In particular the relation between the 5th millennium Swifterbant culture and the gradual drowning of the area was further investigated. In this context the continuous growth of peat, induced by the rising groundwater and sea level, was reconstructed as an age-depth model of the uncompressed peat base within the study region as in the work by Kiden (1991). Vos and

van Heeringen (1997) have shown that such age-depth model is also an important variable for paleogeographic reconstruction of regions with Holocene sedimentation. Aside from developing a regional model of the growing peat, its local scale use in combination with efficient lithostratigraphic mapping for prehistoric landscape evaluations was also an important objective.

Recently user-friendly tools for advanced chronological modeling through Bayesian analysis have been developed (e.g. Bronk Ramsey, 2008; Bronk Ramsey, 2009a; Bronk Ramsey et al., 2006). Therefore, integration of a priori information (e.g. sedimentation rates, stratigraphic order) within the calibration procedure of radiocarbon dates is possible. This can result in more precisely modelled, posterior dates. In addition, Bayesian modelling allows advanced queries of the full probability distribution function (pdf) of the modelled dates. This can result in more accurate chronological analyses in comparison with analyses using e.g. mean values of calibrated radiocarbon dates.

Bayesian chronological modeling methods will allow a quantitative analysis of the chronological relations between the occupation of the prehistoric sites with the sedimentation environment of the contemporaneous landscape. The resulting information on the choices made by prehistoric humans to occupy certain parts of the contemporaneous landscape, will be used to optimize choices made for subsequent archaeological prospection through core sampling.

A final research aim of this PhD focuses on the refinement of the existing core sampling strategies for detecting prehistoric sealed sites. Current practice on grid sizes, coring diameters, etc. for archaeological core sampling is based on rationalized models of prehistoric sites (Groenewoudt, 1994; Verhagen et al., 2013). Based on these, a large number of prehistoric sites in the Scheldt valley have been evaluated using archaeological coring by Bats (2007). The resulting dataset allows a more empirical approach to derive broad range archaeological sampling strategies. The empirical basis of this research strategy could include more variables in the success of an archaeological coring project than using statistically modelled discovery probabilities (Tol et al., 2004; Tol et al., 2006). The objective of this empirical approach is to derive an archaeological core sampling strategy based on existing data. This strategy should include the appropriate grid size, core diameter and sieving mesh to detect a large variation of prehistoric site types.

1.4 Methodological background

The chances and challenges of paleolandscape reconstruction for archaeology in river floodplains are unquestionable, due to the attractiveness for humans, in particular pre-

historic hunter-gatherers, of these ecologically diverse and rich environments (Brown, 1997). Indeed, Howard and Macklin (1999) have pointed out the archaeological preservation issues in river floodplains and estuaries, but also the chances given to its researchers, because stable rivers systems and vertical accretion create multiple buried archaeological levels and because high waterlogging increases the degree of (organic) preservation both in paleochannels and depressions but also on ancient surface horizons.

Therefore, many river floodplains and estuaries are investiged in an interdisciplinary way to solve archaeological research questions by integrating techniques (and methods) from (other) geosciences, such as geomorphology, sedimentology, pedology, stratigraphy, geochronology (see discussion on defining geoarchaeology and archaeological geology in Waters (1992)). Examples of Northwest European geoarchaeological floodplain studies (used) for archaeological purposes are numerous: e.g. the Severn (Bell et al., 2000; Bell and Neumann, 1997), the Meuse-Rhine delta (Berendsen and Stouthamer, 2000; Berendsen and Stouthamer, 2002), Thames (Bates, 2000; Bates and Barham, 1995; Bates and Bates, 2000; Bates et al., 2007; Bates and Stafford, 2013; Bates and Whittaker, 2004), Trent-Soar (Howard, 2005; Howard et al., 2008; Knight and Howard, 2004), Scheldt (Bats, 2007; Bats et al., 2006; Meylemans et al., 2013).

Formerly, spatial geoarchaeological floodplain reconstruction was primarily based on interpretation of large numbers of corings (Bates, 1998; Bates et al., 2000). Recently, geological purpose mapping of deeply stratified alluvial sequences is increasingly done through integrated electromagnetic induction survey (EMI), electrical resistance imaging (ERI), Cone Penetration Tests (CPT) and various types of corings (e.g. Amorosi and Marchi, 1999; Baines et al., 2002; Gourry et al., 2003). Paleolandscape evaluation strategies for archaeological purposes using these combined methods were introduced by Bates et al. (2007, 2013) and Howard & Macklin (2008). Although the Scheldt polders have a comparable Holocene sedimentary sequence to the Thames (Bates and Stafford, 2013), the tertiary clay or glacial fluvial sandy substrate and high and brackish groundwater level will form additional challenges to the effective application of near surface geophysical techniques.

The (mechanical) CPT technique was developed for geotechnical analyses of pile foundations in the Netherlands, almost 80 years ago (Barentsen, 1936). A decade later electric penetrometer cones (CPT-E) were developed (Geuze, 1953). Formerly called, the 'Dutch sounding test' or 'Dutch deep sounding' (Meigh, 2013), CPT has been in use in Belgium for over 70 years (Lousberg et al., 1974). It is generally considered a fast, repeatable and economical method for geotechnical site investigation (Lunne et al., 1997). The CPT method allows investigators to obtain information regarding the mechanical properties of the subsurface strata in response to the penetration of a cone and registers

the tip resistance (q_c) and sleeve friction (f_s). The latter can be related to sedimentological and hydrological variability of the subsurface. In general, CPT is designed for penetrating softer soils, but good results have been achieved in stiff to very stiff soils with modern equipment (Lunne et al., 1997; Robertson and Cabal, 2012). Up to now, CPT has largely been ignored in geoarchaeological research, except for some rare studies (e.g. Bates and Stafford, 2013; Roozen et al., 2013; Brandenberg et al., 2009). Indeed, the use of CPT may provide a solution if near surface geophysical methods are disadvantaged by groundwater salinity, the peats, clay-rich top soil or heterogeneous or contaminated land raising.

Of all geophysical techniques, magnetometer survey is used most frequently in archaeology (Gaffney and Gater, 2003) but due to its limited depth range (Weston, 2001) in alluvial plains and the estuarine or peaty nature of the sediments in floodplain or polder landscapes (Kattenberg and Aalbersberg, 2004), other techniques with a higher depth of investigation (DOI) (but a lower resolution) have to be employed to detect prehistoric landscapes in the Lower Scheldt floodplain.

The sedimentology and geomorphology of river floodplains is theoretically well suited for direct current electrical methods because the sediments are mostly fine grained and badly drained (Baines et al., 2002; Challis and Howard, 2006; Gourry et al., 2003; Howard et al., 2008). Electrical resistivity imaging (ERI) records the apparent electrical properties of the soil, which vary in function of sediment texture and composition/pore size, water content and chemistry of fluids filling the pores and soil temperature (Schmidt 2013).

Electromagnetic induction survey (EMI) relies on eddy currents, induced in conductive soil elements by a primary magnetic field, to derive the apparent electrical and magnetic properties of a soil volume. This soil volume is determined by the soil conductivity, the induced field frequency, the sensor's coil separation-, height above ground and coil configuration (Reynolds, 2011). As a result, mobilized EMI sensors are well matched to map floodplain geomorphic units because they are interpretable by their shape in plan-view and have large variations in sedimentary facies (Conyers et al., 2008). Over the last decades, EMI has therefore been used to map (pre-)historic alluvial paleolandscapes of shallow river floodplains in Northwest Europe and the United States (Bates et al., 2007; Conyers et al., 2008; Gourry et al., 2003; Morin et al., 2009). In Belgium, EMI is increasingly applied since 2008 (Saey et al., 2008; Simpson et al., 2008). On the one hand, EMI is used to detect historic remains below a limited (alluvial) sediment cover (De Smedt et al., 2013c; De Smedt et al., 2011b; Simpson et al., 2008; Simpson et al., 2009a; Simpson et al., 2009b; Simpson et al., 2009c). On the other hand, EMI is also used to reconstruct the paleotopography of shallow buried (prehistoric) landscapes (De Smedt et al., 2013b; De Smedt et al., 2011a; Saey et al., 2008; Saey et al., 2010). The (simplified) depth response curves, employed for reconstructing these depths to sediment layers,

have been proposed by Keller and Frischknecht (1966) and McNeill (1980). These were applied on EMI datasets collected with mobilized instruments with multiple coil pairs by Santos et al. (2010); Triantafilis and Monteiro Santos (2013) and by Saey et al. (2008). Saey et al. (2008) also proposed an efficient procedure to create paleotopographical two layer models with calibration and validation of the modelled ECa data by layer depths derived from corings.

Chronological (prehistoric) landscape reconstruction during the Early to Middle Holocene period is mostly based on reconstructing relative sea level (and/or local groundwater level) rise through (basal) peat or other sediment dating (e.g. Berendsen et al., 2007; Hijma and Cohen, 2011a; Lespez et al., 2010; Van De Plassche et al., 2010). Recently these are combined increasingly with archaeological age-depth indicators (e.g. Pavlopoulos et al., 2010; Sjoerd et al., 2013). On this base, age-depth models of the covering of the Pleistocene sediments have been made on a scale ranging from a national level (Jelgersma, 1961; Shennan and Horton, 2002) to more local groundwater level variations of individual dune slopes (Van De Plassche et al., 2010). Mostly, these age-depth RSL models (groundwater curves) were derived from the mean and (2 σ) range values of calibrated dates and the elevation errors. These are visualized as horizontal and vertical error bars and a curve fitted to the minimal age and elevation values, which ignores the complexity of a full probability distribution function of a (radiocarbon) date.

Bayesian modeling of (radiocarbon) dates, integrating archaeological or other stratigraphic or depositional information has been introduced over two decades ago (Buck et al., 1991; Buck et al., 1992). In Bayesian chronological modelling (of radiocarbon and other dates), Bayes' theorem is used to include absolute *a priori* knowledge about a dated event or function into non-Gaussian probability distributions of the dates, in order to obtain a, preferably, more accurate and precise posterior probability distribution of this event. Possible priors include known age gaps (exact or with age uncertainty), exact and randomly varying sedimentation rates or only the order and contemporaneity of dated events (Bronk Ramsey, 2001, 2008). It was only after user friendly software was developed by e.g. Bronk Ramsey (1995, 2001; 2009a), Stuiver and Reimer (1993) and others that these techniques have become more widely and easily applied by archaeologists. Nevertheless, they have also been critically evaluated (Steier and Rom, 2000).

A lot of Bayesian modeling studies have been done on peat sequences of single cores with small relative depth errors (Blaauw et al., 2007; Yeloff et al., 2006). Due to peat compaction- (and other) issues (see Chapter 4), a single high resolution peat core cannot be representative for the groundwater rise or peat growth in the wider region. However, Bayesian modelling has not yet been applied to model regional groundwater rise or peat development curves using a single stratigraphic position from various cores.

Furthermore, the chronological integration of independently dated archaeological and geological sequence records using a Bayesian approach is not frequently done (eg. Gearey et al. (2009)), despite allowing quantitative analyses to test chronological correlation and order between archaeological site occupation and geological events or phases.

The results of chronological and spatial paleolandscape reconstructions are integrated in paleogeographic maps. The first paleogeographic reconstructions of the Holocene were mainly based on chronostratigraphic interpretations derived from corings on a countryscale and coupled subsurface mapping with age-depth models of RSL- and groundwater rise (e.g. the Netherlands by Jelgersma et al., 1970). Recently, more detailed regional scale paleogeographic reconstructions were made, integrating archaeological results (Baeteman, 2008; Berendsen and Stouthamer, 2000; Hijma and Cohen, 2011b; Lespez et al., 2010; Vos and van Heeringen, 1997). The extension of the regional paleogeography of Zeeland at important archaeological 'time slices' (Vos and van Heeringen, 1997) to the whole Netherlands (Vos et al., 2011; Vos, 2006), instigated the creation of regional 'archaeological expectation' maps from the Mesolithic and Neolithic period (Peeters, 2007; Peeters, 2008) and the use of paleogeographic reconstructions methods on a more local scale in archaeological projects (Boon et al., 2014; Chapman and Gearey, 2013; Vos et al., 2009; Weerts et al., 2012). In the study region the first paleogeographic maps were made by Heirman et al. (2013) in the tradition of Vos and van Heeringen (1997). In this PhD dissertation, local scale paleogeographic reconstruction, based on inverted electromagnetic induction data and an age depth model of the base of the peat, will be attempted for the first time in Chapter 6.

Based on the archaeological interpretation of paleogeographic maps, areas can be selected for more detailed archaeological prospection (e.g. Boon et al., 2014). Groenewoudt (1994) has developed coring based methods to detect prehistoric sites, based on the statistical models designed for shovel-/testpit sampling from the US (Banning, 2002; Krakker et al., 1983; Lovis, 1976; Orton, 2000; Shott, 1985). As a result, Groenewoudt has suggested to use large cores (25 cm diameter) in a staggered 22.5 m sampling grid and to sieve the soil samples through 1-2 mm meshes if using smaller diameter cores. More recently, Tol et al. (2004) and Verhagen et al. (2013) have compared theoretical models with grid excavation data from prehistoric sites the Netherlands and Belgium. Both studies refined core sampling strategies in relation to the expected size and find-density of the prehistoric sites. Since Groenewoudt's study, core sampling has increasingly been applied within Dutch archaeology, and also increasingly in Flanders (De Clercq et al., 2011), in floodplain contexts, forests, meadows, dunes or anthropogenic soils, but evaluations of the coring methodology based on the coring results will be done for the first time in Chapter 7.

1.5 Structure

The structure of this dissertation is shown in Figure 3 and further discussed below:

In Chapter 1, near surface geophysical and geotechnical methods are explored to map subsurface lithological variations as a cost-effective alternative for coring, specifically aimed at the subsoil conditions of the estuarine Scheldt polders. The resulting data are interpreted qualitatively resulting in maps of prehistoric geomorphic units or locations, which can be subsequently sampled and checked for the presence of prehistoric sites.

In Chapter 3, cone penetration tests are further explored as a tool for gridded mapping of prehistoric landscapes covered by peat, beyond the limits of near surface geophysical methods. Furthermore, the added value of CPTs with extra geophysical sensors to characterize the subsurface lithology or to calibrate and validate near surface geophysical data is investigated.

Chapter 4 is focused on the development of a regional age-depth model of the covering of the Late Glacial landscape with peat and dating the occurrence of a perimarine influence in relation to the human occupation at two nearby Final Mesolithic/Early Neolithic Swifterbant Culture sites, namely Doel-Deurganckdock Sector B and M.

Chapter 5 further interprets the geoarchaeological implications of the chronological results presented in Chapter 4 by including the stratigraphically modelled dates of a palimpsest site as a tool to start unravelling the complex occupation history of such sites. The relations between the (repetitive) nature of the Mesolithic-Early Neolithic occupation and the choices of paleolandscape locations for differing settlement types are further elaborated.

Chapter 6 combines the knowledge gained from the previous chapters. Multi coil spaced electromagnetic induction survey data (Chapter 1) are modelled into a subsurface elevation model of a small dune and extended with data from corings and cone penetration tests (Chapter 3). Subsequently, this model is related to the age-depth model of peat development (Chapter 4) to create a paleogeographic map selecting parts of the dune, where dated sites or features could fill in gaps in the occupation knowledge of dune sites (Chapter 5). This also provides sampling locations and depths for subsequent archaeological sampling (Chapter 7).

Chapter 7 is focused towards an evaluation of appropriate variables for archaeological prospection in the strict meaning of the word, namely to detect the sites themselves. Optimal grid size, core diameter and sieving mesh are evaluated, derived from existing archaeological core sampling projects and excavations of prehistoric sites in the broader study region.

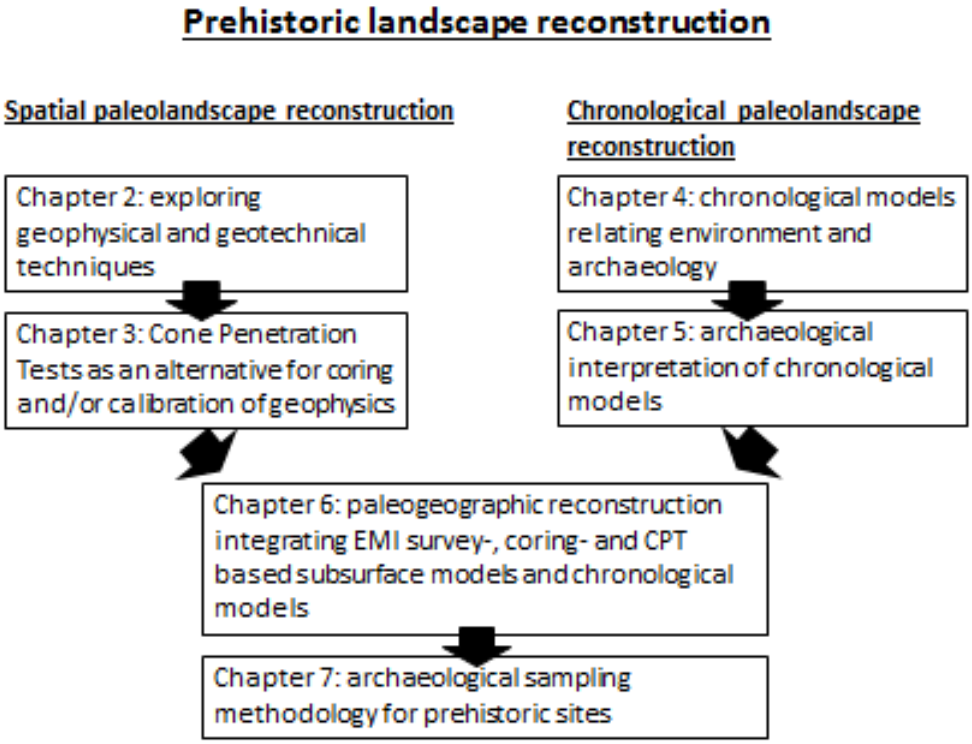

Figure 3: Dissertation structure and chapter ordering according to the principal research aims.

Chapter 2 Exploring integrated geophysics and geotechnics as a paleolandscape reconstruction tool: archaeological prospection of (prehistoric) sites buried deeply below the Scheldt polders (NW Belgium)

This chapter is adapted after Verhegge et al. (submitted-a) and Verhegge et al. (2012)

During extensive construction works in Antwerp harbour, well preserved Late Glacial dune formations were discovered buried deeply below the Scheldt polders and covered by peat, OM rich clays and marine clayey to sandy sediments. First, coring based archaeological prospection strategies for evaluating prehistoric occupation levels in wetland landscapes are reviewed. Next, a more effective approach including near surface geophysical and geotechnical techniques is proposed and tested in Doelpolder Noord. The results indicate that high resolution electromagnetic induction survey at multiple coil spacing provides a suitable approximation of the prehistoric landscape variability but is challenged by variations in groundwater brackishness. Gridded cone penetration tests provide a solution in such cases and serve as an excellent interpretation tool for the conductivity data in general. Due to the required effort, electrical resistance imaging and shear wave land seismics were judged inefficient. Finally, a small dune with indications of paleosol conservation and estimated suitability for Final Paleolithic to Early Neolithic occupation is sampled by Dutch hand augering and Sonic Drill Aqualock coring. Archaeological indicators for prehistoric occupation such as burnt bone and flint fragments were retrieved from these samples after sieving.

Keywords

Prehistoric buried landscapes, Electromagnetic Induction Survey, Electrical Resistance Imaging, Shear wave land seismics, Cone Penetration Test, Core Sampling

2.1 Introduction

2.1.1 Research context and archaeological relevance

In the past decades, large parts of the Waasland Scheldt polders have been destroyed in the context of the expansion of Antwerp harbour. Salvage excavations had to be performed *impromptu* as no archaeological evaluation had been done in advance (Crombé, 2005). A cost-effective archaeological evaluation strategy has to be developed that can be integrated within the construction process to evade such problems in future cases. These large scale projects potentially have an important scientific value as they are amongst the rare chances to investigate complete and well preserved archaeological landscapes in Flanders (De Clercq et al., 2012).

Both Howard and Macklin (1999) and Bates and Bates (2000) have demonstrated the archaeological preservation issues in estuaries and challenging survey and excavation circumstances. They also highlighted the chances given to researchers as the stable river systems and vertical accretion create multiple buried archaeological levels and high waterlogging. This increases (organic) preservation in paleochannels, depressions and on ancient surface horizons. Rescue excavations have shown that the undulating surface of the Late Glacial and Early Holocene landscape buried roughly between 1 and 10 m below the surface of the Scheldt polders is well preserved (Crombé, 2005). Many (micro-)sand ridges within this landscape are still untouched and covered with archaeological sites ranging from the Final Paleolithic to the Early/Middle Neolithic times (Crombé, 2005; Crombé et al., 2013b). Throughout this period, humans have chosen different settlement locations within this landscape, causing sites of varying size and find-densities. Except for small and often nearly invisible hearth(pit-)s, these sites often do not contain any structural features (Sergant et al., 2006a). In general, they consist of scatters of lithic artifacts, sometimes intermixed with burnt plant (mostly burnt hazelnut shells) and bone remains. Despite their ephemeral nature, these sites are of high scientific archaeological value because they are key to understanding hunter-gatherer responses to changing environment as well as the Mesolithic-Neolithic transition (Crombé, 2005). In contrast, the occupation history of the Late Neolithic to early historic

peat-landscape within the Waasland Scheldt polder is still insufficiently known, while the (post-) medieval occupation is mostly known from historic sources only.

2.1.2 Aims

This paper is aimed at evaluating the effectiveness of existing and widely available geophysical and geotechnical methods as paleolandscape mapping survey tools in the archaeological evaluation of deeply buried prehistoric sites, a process that currently solely uses coring methods. A series of methods were applied to investigate if the research questions in the initial evaluation stage of paleolandscape mapping can be answered in a more efficient manner. As such, this paper provides useful guidelines for heritage officers and commercial archaeologists working in these, or similar, polder environments.

2.1.3 Alluvial landscape and human occupation development from Late Pleistocene to present in the Scheldt polders

During the Weichsel Pleniglacial period, the Scheldt river system evolved from a braided river, depositing mostly acyclic fine sandy sediments, to a Late Glacial meandering river system. The present day eastward trajectory of the lower Scheldt in Belgium (inset maps on Figure 5) was certainly formed before the end of the Late Glacial period but cannot be dated more specifically (De Moor and Heyse, 1978b; Kiden, 1991). Downstream of Antwerp, the meandering river was just weakly winding. As a result, lateral accretion deposits were formed with just one or two fining up sequences, from fine sands to loam or clay deposits, or even singly clayey deposits (Bogemans, 1997). In this region, the river runs through a Late Glacial coversand ridge system, consisting of many SW-NE oriented (river-)dunes, made up of reworked marine and/or fluvial deposits. These geomorphic features determine the basic stable settlement locations throughout the Holocene. During this period these dry spots decreased in size and number as an indirect consequence of the continuous sea level rise. This reduction largely determined the nature of the changing human occupation in the region.

By the end of the Late Glacial and from the Preboreal onwards, the gradual infill of the meandering river channel started, first with the deposition of gyttja and later with peat (Kiden, 2006; Bogemans et al., 2012). Less erosion took place and the fluvial discharge decreased within the paleovalley, while the local groundwater level surfaced because of relative sea level rise (Kiden, 2006; Vos and van Heeringen, 1997). As a consequence, basal alder carr peat formed during the Early Atlantic (Deforce, 2011). This started in the deepest gullies but increasingly covered the wider alluvial plain (Kiden, 1991).

The first occupations known from the Scheldt polders date back to the Final Paleolithic and Early Mesolithic. Settlement locations are situated both at the edge of the alluvial plain on larger, relatively dry cover sand ridges, which were covered by open birch and pine forests (Crombé, 2005), and on natural levees along the river. At the start of the gradual drowning of the landscape, Mesolithic occupation clustered on levees (eg. Van Strydonck et al., 1995) along the paleochannels of the Scheldt, leaving the alder carr peat land unoccupied. The basal peat formation was interrupted at the start of the Late Atlantic after a shorter Scheldt trajectory downstream had expanded the estuary further upstream (Vos and van Heeringen, 1997). As a result, occasional brackish water incursions created a layer of OM rich clay deposits in lower landscape positions radiocarbon dated from 6530-6410 cal BP (2σ) onwards (Verhegge et al., 2014). Synchronic with this flooding event, the first semi-agricultural groups belonging to the Swifterbant and Michelsberg Cultures started to exploit the area, also settling on the top of smaller cover sand ridges which, by that time, were already decreasing in surface (Crombé, 2005; Crombé et al., in press-b) and covered with alluvial hardwood forests (Deforce et al., 2013; Van Neer et al., 2013).

Between 6090-5770 cal BP (2σ) (Verhegge et al., 2014), the tidal influence gradually decreased as the coastal barrier closed up, leading to a sedimentation stop. Hereafter, peat restarted to grow, resulting in the formation of first wood peat and subsequently reed peat (Deforce, 2011). So far, no traces of human occupation are known from this stage until the Roman period (De Clercq and Van Dierendonck, 2008; Sier, 2003). However, crevasse splay deposits within similar alluvial sequences in the Netherlands have proven to be at least temporarily attractive to occupation from the Middle Neolithic to the Bronze Age (van Dinter and van Zijverden, 2010). Breaching of the coastal barrier in the 6th century BC gradually created a renewed estuarine landscape (Vos and van Heeringen, 1997). This expanded into our study region around 500-600 AD during extreme high tides and stopped peat development (Kiden, 2006). Locally, however, peat continued to grow as indicated by a radiocarbon date between 890 and 1015 cal AD (2σ) (RICH-20045: 1095±29 BP) on *sphagnum* (Verhegge et al., 2014).

The first Medieval attempts to exploit the reed peat marsh for pasture or peat extraction in the 12-13th century AD are known from historic sources (Klinck et al., 2007; Mys, 1973) and excavated drainage ditches (Crombé, 2005; Meersschaert et al., 2006; Mys, 1973). The successive embankment attempts following storm surges or intentional levee breeches during wars, have created a complex sedimentation and occupation history in the following centuries.

From historic documents, it is known that the dikes creating Doelpolder were built erected as early as the 13th century explaining its lower topographic position (Klinck et al. 2007). Other parts of the polder were exposed to marine sedimentation until the 18th and 19th century. Depending on the time of this embankment, traces of landscape development can still be seen on historic maps or the present day digital elevation model

(Figure 4). The DEM is not reliable as a data source for prehistoric landscape variablity however (Soens et al., 2012).

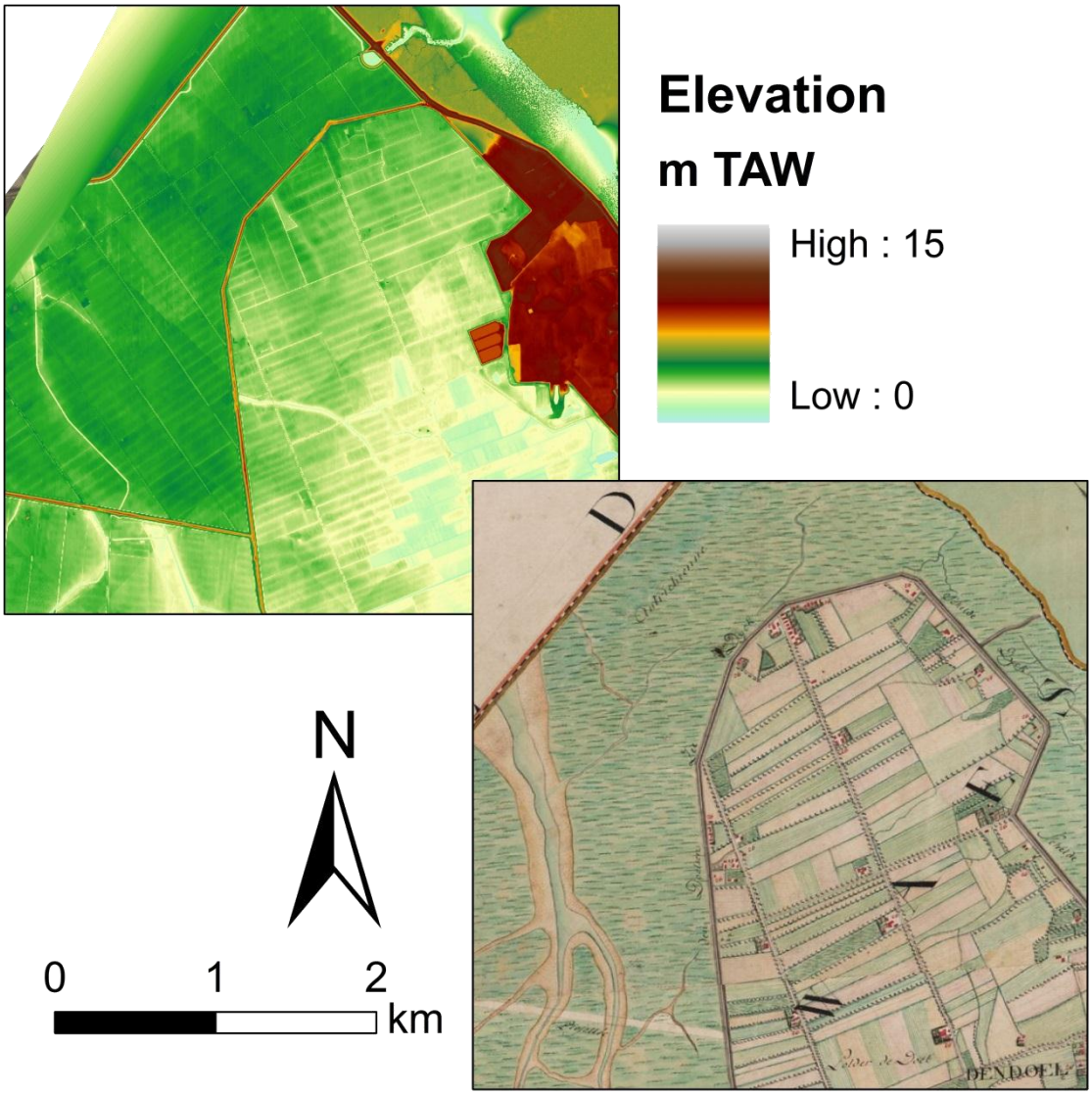

Figure 4: Doelpolder Noord on the Ferraris map (De Ferraris, 1771-1778) (top) and the Digital Elevation Model Flanders (AGIV, 2001-2004) showing Post Medieval land divisions and the tidal channel system but no prehistoric landscape units (e.g. Figure 5).

Overall, the (Post-)Medieval floods started in a high energy environment with the deposition of marine sands, and finished with a more clayey sedimentation. According to the soil map, the resulting polders consist of soils ranging from loamy sand or light sand-loam (17.5-35% clay content) in or next to badly drained old tidal gullies, to slightly better drained heavy clay (>35% clay content) on old tidal mudflats/saltmarshes closer to older polders (Van Ranst and Sys, 2000). Earlier embanked polders, such as Doelpolder, have a lower elevation and less developed tidal channel systems, resulting in a larger proportion of tidal mudflats and clayey top-soils. It is precisely these embanked tidal mudflats which cover the best preserved prehistoric landscapes.

2.1.4 Archaeological prospection methodology for prehistoric landscapes in the polders of the Low Countries

The importance of alluvial paleolandscape reconstruction for prehistoric archaeology has already been stressed by Brown (1997). But whilst protecting the deeply buried archaeological sites, the polder sediments also hamper detection using traditional surface based prospection approaches (e. g. field walking, LIDAR, trial trenching). In addition to the geological overburden, the nature of the archaeological remains forms an additional hindrance as prehistoric sites in the study area consist of featureless artifact scatters (Sergant et al., 2006a). Therefore, a traditional archaeological geophysical survey approach (eg. Gaffney and Gater, 2003) will not detect the prehistoric sites.

Current archaeological surveys of buried prehistoric sites in polder alluvial plains in the Low Countries optimally consists of a two phase process. First, the diachronological development of the paleolandscape is reconstructed (Bats, 2007; De Clercq et al., 2011; Tol et al., 2004) by mapping the geological strata through augering. A 30m-50m staggered grid spacing is required to map small river dunes. Field observations include contrasting soil colours and texture variations (Stein, 1986). As such, the preservation of the soil sequences is also assessed (Bats, 2007; De Clercq et al., 2011). Interpolating elevations of possible archaeological strata allows a rough paleotopographical model of the buried geomorphic units. Depending on the model accuracy, however, the sampling strategy in the subsequent archaeological evaluation phase can be prone to errors.

In a second phase, the modeled paleolandscape evolution guides an archaeological evaluation by soil sampling of the relevant archaeological strata at possible human occupation locations using 10-15cm diameter (eg. Schuldenrein, 1991) Dutch augers in a 10m staggered grid (Crombé and Verhegge, 2014). Samples are sieved wet on a 1-2mm mesh (Crombé and Verhegge, 2014) and the dried residue is checked for reliable archaeological indicators such as flint artifacts (mainly chips), ceramic fragments, (un)charred plant remains or (un)burnt bone fragments. If necessary, the grid size is reduced in between or surrounding positive samples (Bats, 2007; Groenewoudt, 1994; Verhagen et al., 2013). Based on these results, more invasive test pitting or full excavation is planned.

However, as the burial depth increases it becomes impractical and costly in both phases to perform large numbers of corings by hand. Below the ground water level, it is hard to reach the Pleistocene deposits without time consuming encased corings or expensive continuous mechanical coring equipment (Canti and Meddens, 1998; Hissel and Van Londen, 2004).

Alternative techniques are therefore needed to reduce the number of corings required in the paleolandscape evaluation phase and to guide the archaeological core sampling phase more accurately. The primary aim of these techniques is the detection of the variability of the depth to the base of the peat since this covers the major buried archaeological levels throughout prehistory. Secondly, indications of possible erosion of

these strata (eg. gullies) have to be mapped and the preservation of paleosols determined. A surface based geophysical survey strategy seems most appropriate. The limited vertical resolution of surface geophysics still, however, imposes a certain degree of depth sounding or coring data in order to interpret the geological facies and evaluate the paleosol preservation.

The main surface geophysical techniques for mapping alluvial geomorphology include ground penetrating radar (GPR), Electromagnetic Induction (EMI), electrical resistance imaging (ERI) and shear wave seismics. The results of GPR would provide the best models of the subsurface (eg. Bakker et al., 2007; Vandenberghe and van Overmeeren, 1999) but the method is hindered by the presence of clay and brackish groundwater (Olhoeft, 2003) and was therefore not suitable in our case. De Smedt et al. (2013b) and Conyers et al. (2008) have mapped shallow (pre-)historic paleolandscapes in alluvial plains in an archaeological context using frequency domain electromagnetic induction survey (EMI) supported by a limited number of handcorings. More deeply stratified alluvial sequences (Bates and Bates, 2000) have been mapped with the combined use of EMI or electrical resistance imaging (ERI), backed up by borehole data from Cone Penetration Tests (CPT) and mechanical corings (eg. Baines et al., 2002; Gourry et al., 2003). This approach was used on the floodplains of the Thames by Bates and Stafford (2013) and the Trent by Howard et al. (2008). The Scheldt polders add a number of additional challenges to EMI and ERI as used in these established approaches. First, our study region is marked by a comparable Holocene sedimentary sequence but the loose Tertiary and Pleistocene sediments have a smaller texture contrast. In addition, the embanked estuarine polder plains are often located below sea level, creating a possibly brackish groundwater level (Goes et al., 2009) impeding interpretation of EMI results. Finally, the complex (post-)medieval erosion and sedimentation history and the textural variability of these estuarine sediments could create more geophysical variation than the underlying Pleistocene landscape forms.

In addition to measuring sedimentological variations, EMI allows the detection of (post-)medieval landscape structures such as dikes, traces of peat extraction, drainage ditch systems and moated sites, and, if the in-phase signal is included, even brick structures buried below a limited alluvial cover (<2 m), if collected at a sufficiently high resolution (eg. De Smedt et al., 2013c; Saey et al., 2012a; Simpson et al., 2008). Detecting these features is problematic using magnetometers as Weston (2001) has shown, while Kattenberg and Aalbersberg (2004) have illustrated the variable magnetic contrasts of peat extraction features covered by badly drained estuarine deposits.

2.2 Survey area

The study area of Doelpolder Noord is situated north of Antwerp harbour on the left bank of the Scheldt river and at 1.5km from the border with the Netherlands (Figure 5). The top soils here range from heavy clay to clay with moderately bad to bad drainage and lack any soil profile development (Van Ranst & Sys 2000). The elevation data (AGIV, 2001-2004) show a variation between 2.5m and 4m above national ordnance level (TAW = mean low water tide level) (Figure 6). The lowest parts are related to (re-activated) Post Medieval tidal creeks or drainage ditches. Prior to its conversion into a bird reserve, which demanded tidal ditches to be dug out (Figure 5) and farmsteads to be torn down (topographic map on Figure 5), the buried Pleistocene paleolandscape had been reconstructed using more than 500 manual corings (Klinck et al., 2007). This makes it into an excellent testing ground for geophysical methods.

Based on the available (sub-)surface data, a 100m by 700m transect was selected containing maximal subsoil variability including the top of a Pleistocene micro-sand ridge (buried about 2m deep) flanked by a deep (up to 9m) depression to the south and a smaller depression to the north. Further north, the Pleistocene surface undulates between 4m and 6m depth (Figure 6).

Selected macroremains from the peat covering the dune were radiocarbon dated to reconstruct its diachronic coverage by peat (Verhegge et al., 2014). Results indicated that the top of this dune was covered with peat between ca. 800-555 cal BC (2σ) (RICH-20046: 2555±28 BP), while peat started to grow on its slopes from ca. 4230-3985 cal BC (2σ) (RICH-20057: 5265±30 BP) onwards. Peat development continued at least until between 890 and 1015 cal AD (2σ) (RICH-20045: 1095±29 BP) based on a radiocarbon date on s*phagnum* retrieved from the top of the peat on the flank of the dune. Corings on the top revealed subtle podsolization indicating a lack of erosion before its peat coverage, which was confirmed by the preservation of the ancient A-horizon as sandy to clayey peat. Therefore the preservation potential of possible prehistoric sites is high.

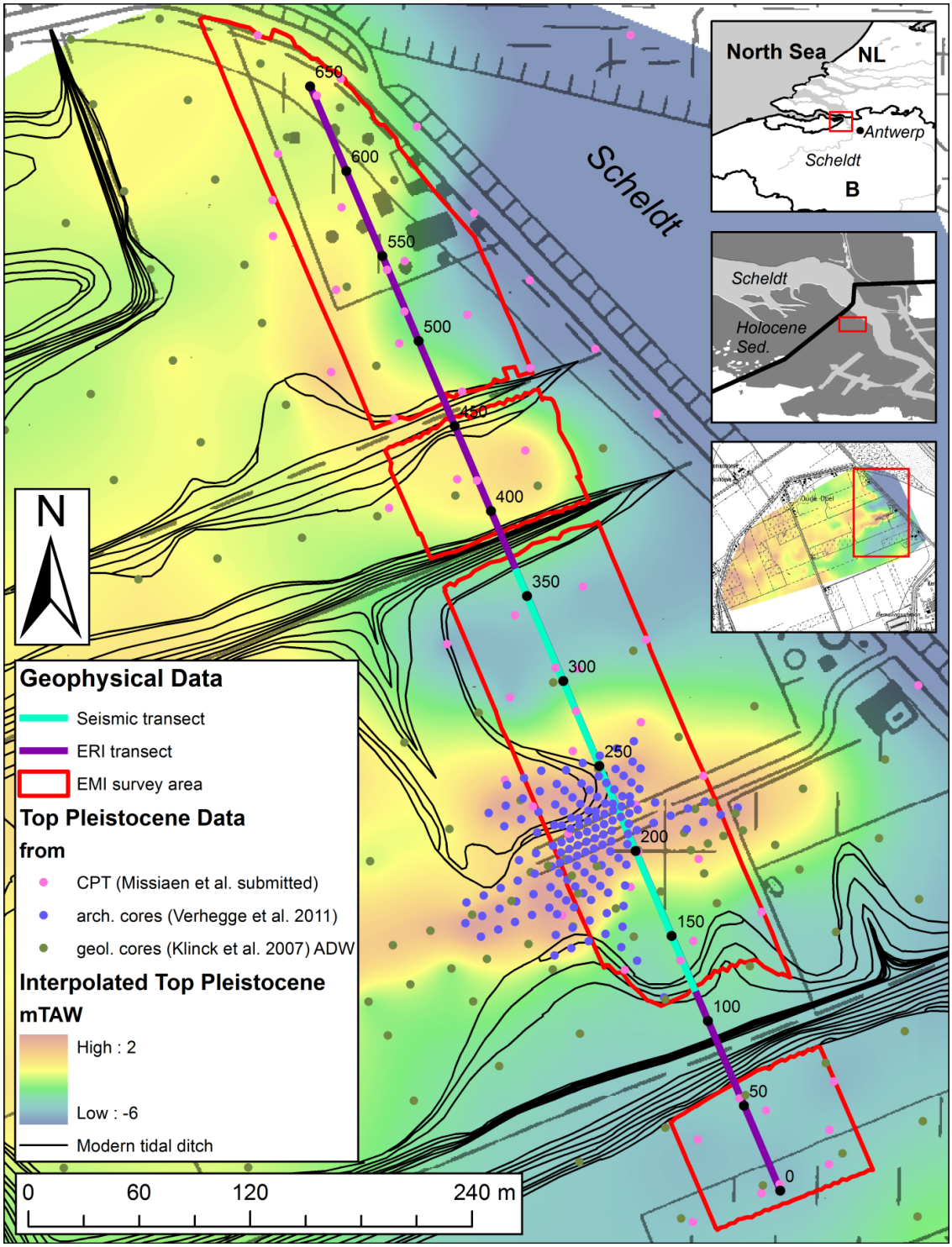

Figure 5: Location of the EMI survey area and ERI and Land Seismics transect (distances in m) on top of the Pleistocene surface elevation model based on geological and archaeological corings (Klinck, et al., 2007, Verhegge, et al., 2012) and CPTs (Missiaen, et al., submitted) (Modern tidal ditches were created recently; topographic map: copyright by NGI 1993). Top inset map: location of the Scheldt polders in Belgium; Middle inset map: location of Doelpolder Noord in the Scheldepolders, covered with Holocene marine and fluvial sediments; Bottom inset map: survey area selected in Doelpolder Noord across a Late Glacial (river) dune flanked by two depressions.

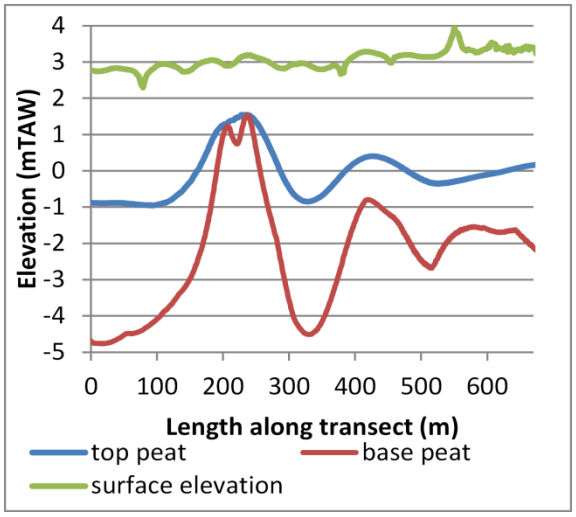

Figure 6: Southwest to Northeast transect across the survey area on the location of the ERI transect through Doelpolder Noord (Figure 5) showing the elevation of the surface (green), interpolated base and top of peat (resp. red and blue) based on corings and CPTs, revealing the surveyed (river) dune.

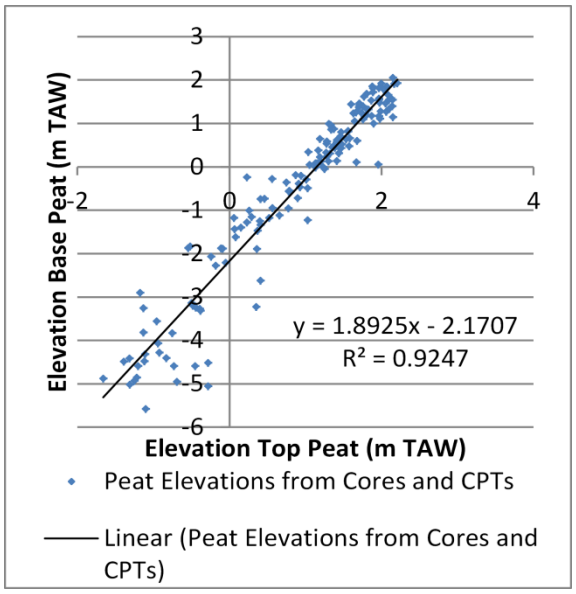

Figure 7: Correlation plot of the top and base of the peat elevation from corings and CPTs in the survey area (see Figure 5).

Figure 7 illustrates the linear correlation between the top and base of the peat that covers the Pleistocene sand, suggesting that the Late Pleistocene-Early Holocene topography largely determined the surface topography during the Middle to Late Holocene peat formation. This correlation decreases in lower topographic positions, indicating greater variability in the peat thickness. This could be due to erosion or due to increasing depth determination errors from the cores. Due to this linear correlation the prehistoric landscape reflected in the geophysical data could be simplified as a conductive layer (Holocene sediments) overlying a resistive layer (Pleistocene sands).

2.3 Methods

2.3.1 Electromagnetic induction

Slingram frequency domain EMI survey is used to measure apparent electrical (ECa) and magnetic properties of the subsoil without direct contact. The method relies on a primary magnetic field inducing eddy currents in conductive soil elements. The resulting secondary field is measured in a second passive coil (Reynolds, 2011). The measured soil volume depends on the primary field frequency, coil separation and orientation (McNeill, 1980; Reynolds, 2011). Apparent electrical conductivity values are derived from the quadrature phase response and well suited to map texture, moisture or electrolyte (salt) variations in clayey to sandy sediments. As such, EMI is well suited to map floodplain geomorphic units, because these have large sedimentary variations and are interpretable by their horizontal shapes (Conyers et al., 2008). However, as the electrical conductivity increases (roughly above 100 mS/m), the low induction number (LIN) approximation required to derive electrical conductivity linearly from the quadrature phase response gradually becomes invalid (McNeill, 1980). Nevertheless, Delefortrie et al. (2014b) have observed an acceptable signal to noise ratio in highly conductive saline environments, despite a reduced depth of exploration. Magnetic susceptibility was not measured.

Our sensor choice was oriented towards commercially available, widely applied and, due to vegetation, hand portable instruments. The sensor had to be able to detect the Pleistocene sand with a burial depth roughly from 2m to 8m. As such, the first choice of instruments (Table 2) was the Geonics EM31 and EM34 (McNeill, 1980). In addition a Geophex GEM-2 sensor was tested because it is claimed that this lightweight broadband multi-frequency sensor measures multiple soil volumes up to a depth of 10m in conductive areas (EC> 10 mS/m) (Won et al., 1996), although this is debated by McNeill (1996).

The spatial field data resolution was determined by the smallest features to be detected (small dunes), but was also related to the soil volume that is measured to avoid under- and over-sampling. If a 30 to 50 m line spacing is used (Eg. Bates et al., 2007; Orbons, 2011), the continuous measuring speed advantage of EMI is not fully used. If the spacing approaches the measured soil volume, a better interpretation of the buried landscape features is possible and the direction of the survey lines is of no consequence. In addition, small shallow (Post) Medieval features are also mapped.

The EMI survey area (Figure 5) was surveyed with all three selected sensors, albeit at different spacings. The GEM-2 sensor was hand-carried in a horizontal coplanar configuration (HCP) with five induced field frequencies corresponding with theoretical respective skin depths between roughly 3m and 11m in a 1000 mS/m conductive clay subsoil, according to Won (1980). Data in all frequencies were collected every 0.05-0.1 m along parallel transect, positioned 2.5 m apart. For practical reasons, two different EM31 sensors were used during the surveys. In 2011, the southern half of the survey area was measured using an analogue output sensor and stationary measurements were collected every 2.5 m along parallel lines located 5 m apart. During the second fieldwork season in 2012, digital output sensor measurements were positioned using a handheld GPS to locate the measurements. Finally, stationary EM34 data were collected in 10m vertical coplanar (VCP) configuration.

All EMI sensors were calibrated every two to three hours at the same location throughout both survey years. The time between survey period was no issue for different reason. Firstly the calibration procedure guaranteerd a constant base value. In addition, shallow groundwater made that variable precipitation between both summers only influences the upper meter of the soil volume. ECa variations in overlapping data of both years were negligible in view of the total ECa range. Grids were set out in the field using an RTK-GPS and subdivided using measuring tapes guiding the surveyor and positioning the data if no GPS tracking was available. All quadrature phase data were converted to ECa and interpolated in Surfer software to a 0.2m by 0.2m grid using the ordinary kriging (Goovaerts, 1997) with an elliptic search window with a length of four times the line spacing and a width of a single line spacing along the survey lines. Interpretations were done by vectorisation of interpreted anomalies (Schmidt, 2001) through comparison with other available coring (Klinck et al., 2007) or CPT information (Missiaen et al., 2015) using Arcinfo and Rockworks software.

Table 2: Meta data of the survey data collected with the following EMI sensors: GEM-2 in HCP configuration, EM31 in VCP configuration, EM31 in HCP configuration and EM34 in VCP configuration.

Sensor-coil configuration	Geophex GEM-2-HCP	Geonics EM31-VCP	Geonics EM31-HCP	Geonics EM34-VCP
Coil separation (m)	1.66	3.66	3.66	10
Primary field frequency (Hz)	41025-20025-9825-2175-925	9800	9800	6400
Approximate theoretical exploration depth (m)	3-11 (1000mS/m) Won (1980)	3	6	8
Coil center height	1	1	1	0.315
In line spacing (m)	~0.05	S:2.5; N: ~0.15	S: 2.5, N: ~0.15	5
Line spacing (m)	2.5	5	5	10
Measurement mode	Continuous	S: stationary; N: continuous	S: stationary; N: continuous	Stationary
Localization	D-GPS	S: Tape measure grid; N:HH gps	S: Tape measure grid; N: HH gps	Tape measure grid

2.3.2 Electrical resistivity imaging

Electrical resistivity imaging (ERI) transects map varying electrical properties and uses a 2D inversion to calculate resistivity (Schmidt, 2013). Electrical resistance data are collected by introducing a current into the soil through two electrodes and measuring the electrical potential in two different electrodes. By variation of the distance between the electrodes, the apparent resistivity of different soil volumes can be measured. These electrodes can be arranged in different arrays, each with a different geometrical coefficient influencing the calculation of apparent resistivity (Schmidt, 2013). These arrays also determine the signal to noise ratio, sensitivity to horizontal or vertical buried objects, depth of investigation and measuring speed. Linear ERI pseudo-sections are often collected using a multi-electrode cable, oriented perpendicularly across a medium assumed to be homogenous, which requires pre-existing subsurface knowledge (Loke, 2014; Loke et al., 2013; Samouëlian et al., 2005). Theoretically, polders are well-suited for direct current electrical methods because the sediments of these environments are mostly fine grained, badly drained and therefore well-conductive (Baines et al., 2002).

At Doelpolder-Noord, 2D electrical resistance imaging data (ERI) were collected using an AGI Supersting R8 (for location of the ERI line see Figure 2). An inverse Schlumberger configuration was chosen, because a conductive subsoil and horizontal and vertical sediment variability were expected. In addition, this array allows us to use the multichannel possibilities of the instrument, increasing survey speed. However, this configuration is more sensitive to telluric noise, although this was not expected. Electrodes were positioned 2m apart in order to obtain an estimated 1m resolution (Baines et al., 2002).

The resulting data were despiked and concatenated using Res2Dinv software (Loke, 2014). A robust-data constrained optimization algorithm was chosen, because large resistivity contracts were expected between the peat and overlying or underlying sediments. Sharp boundaries were defined at the base and the top of the peat as known from a series of CPT-Cs along the survey line (see further) to constrain the inversion. Because the polder topography is more or less flat no topographical correction was needed.

2.3.3 Reflection land seismics

Reflection seismic investigations involve the generation of a seismic pulse that travels through the sediments and is partially reflected back at the interface between two materials. The amplitudes and travel times of the returning waves are recorded at the surface. Knowing these and the velocity, an image of the subsurface can be reconstructed (Sheriff and Geldart, 1995). Apart from the common compressional (P-)waves, shear (S-)waves can also be generated. The latter have much lower velocities and therefore shorter wavelengths, resulting in an increase in resolution compared to P-waves (e. g. Ghose, 2003). However, they also often exhibit lower frequencies than P-waves which may partly cancel the increase in resolution (Telford et al. 1990). Other seismic responses may be recorded by the receivers complicating correct interpretation. Some of these waves (e.g. Rayleigh waves) can be attenuated by optimal survey design, whereas others (e.g. Love waves) are more difficult to remove, especially in shallow surveys (Miller et al., 1999).

Because of high groundwater saturation in polders, low attenuation of the seismic waves was expected, allowing a good resolution of shallow targets (e. g. Ghose et al., 1998; Missiaen et al., 2008). S(hear)-waves are not affected by the fluid content of the sediments and essentially respond to the lithologic contrast (Johnson and Clark, 1992). The seismic measurements in Doelpolder-Noord (performed by *Deltares)* therefore involved the use of a small portable S-wave vibrator source. This is advantageous because source frequency and source strength can be independently controlled (Ghose et al., 1997). The location of the seismic line is shown in Figure 5. For our measurements a

sweep frequency from 10 to 500 Hz and sampling rate of 0.1ms were used. In view of the reasonably flat polder topography and in order to increase the operational speed in the field, the seismic data were recorded using a so-called 'land streamer' containing 24 built-in 3-component geophones spaced 1m apart and a Geometrics geode seismograph. Minimum source-receiver offset was 5m and shot point interval was 1m. Because the resulting data largely determined data processing, this will be discussed in the results section.

2.3.4 Cone penetration tests

Electrical cone penetration testing (CPT) is an economical and generally repeatable geotechnical method to sound the composition of the subsurface (Lunne et al., 1997). A cone on the end of a series of rods is pushed into the ground and (continuous or intermittent) measurements are made of the resistance of the cone tip (q_c) and the friction on the trailing sleeve (f_s). Both tip resistance and sleeve friction and their ratio (friction ratio R_f) can be related to the subsurface lithology. Several studies have shown that in practice lithological interpretation of CPT results should best be accompanied by borehole verification or other sources of subsurface knowledge (Lunne et al., 1997). This is especially true in polder soils, often marked by intercalating peat and clay (Long and Boylan, 2012; Missiaen et al., 2015; Vos, 1982). Additional sensors can be added to the cone. For instance the *in situ* pore pressure or conductivity can also be recorded (Lunne et al., 1997).

The most widely used CPT soil classification (SBT) chart was suggested by Robertson et al. (1986), with an updated, dimensionless (normalized) version for large depths (>30 m) (Robertson, 2010). In polder areas, the automatic soil classification method is known to have difficulties in distinguishing peat and (OM rich) clay soils (Landva et al., 1983; Long, 2005; Long, 2008; Long and Boylan, 2012). Therefore, the approach suggested by Vos (1982) to identify peat merely from the friction ratio was adapted in our study (Eg. Missiaen et al., 2008).

Apart from conventional electrical CPTs (CPT-E) and a number of pore pressure CPTs (CPT-U), a series conductivity CPTs (CPT-C) with a dielectric cone (Frequency Domain method, 20 MHz) (Hilhorst, 1998) were also carried out and extensively discussed in Missiaen et al. (2015). The former were intended as a replacement for paleolandscape mapping by gridded corings (Missiaen et al., 2015), the latter as an interpretation tool for the near surface geophysical data relating ground mechanical properties, ECa and subsurface lithology from corings (this study). Finally, a couple of seismic CPTs were carried out, a.o. along the seismic transect (Missiaen et al., 2015).

2.3.5 Archaeological coring

Archaeological coring for mapping lithic artefact clusters used cores with a diameter of 10 cm in a 10 m grid and sieves samples over a 1-2 mm sieve (Crombé and Verhegge, 2014). This method was applied on the dune, which was previously mapped using geophysical and geotechnical methods. This presented results form a test-study using a combination of manual and mechanical archaeological sampling methods over a range of depths (arch. cores Figure 5). In a first phase, a Dutch auger with a 10cm diameter was used until between 2.5 and 3 m deep, directly below ground water level in a 10 m triangular grid. In a subsequent campaign, sonic drill aqualock coring was tested with a diameter up to 10 cm and a 2 m long core sampler and with both semi-continuous and discontinuous profile sampling on the flanks of the dune. The soil samples were retrieved from the transition from the top of the dune to the base of the peat and were sieved over a 1 mm mesh. The dried residue was checked for macroremains indicating the presence of a prehistoric site, such as pottery fragments, flint artefacts or -chips, (burnt) bone fragments or (charred) hazelnuts (e.g. Crombé and Verhegge, 2014).

2.4 Results

2.4.1 Electromagnetic induction

The descriptive data statistics of the EMI ECa data are summarized in Table 2 and Figure 8 shows a transect of the data along the ERI transect (for location see Figure 5). Figure 11-19 show the data plots of the GEM-2, EM31 and EM34 data and deduced interpretation.

Table 3: Descriptive statistics (Minimum, Maximum, Mean, Median and Standard Deviation) of the collected datasets of the GEM2, EM31 and EM34 sensors in Doelpolder Noord (ECa in mS/m, values clipped <600mS/m).

	GEM2-HCP925Hz	GEM2-HCP2175Hz	GEM2-HCP9825Hz	GEM2-HCP20025Hz	GEM2-HCP41025Hz	GEM2-HCPTotal	EM31 HCP	EM31 VCP	EM34 VCP
Minimum	0.09	0.04	31.63	39.38	37.23	20.90	5.80	27.30	43.00
Maximum	592.74	593.40	539.93	504.57	474.86	487.14	298.00	177.25	200.00
Mean	43.94	96.36	132.57	126.83	113.38	97.98	159.01	88.51	100.25
Median	4.04	62.55	100.06	98.79	91.26	67.19	161.50	86.00	87.00
Standard Deviation	72.94	88.36	74.62	67.01	57.87	69.60	41.96	26.17	33.76

The mean ECa values at the various GEM-2 frequencies seem to suggest a transition from high (at 41025 Hz and 20025 Hz) to very high (at 9825 Hz) and finally to lower (at 2175 and 925Hz) conductive sediments as the theoretical depth increases. This could reflect the transition from estuarine deposits to the peat and Pleistocene sands below. In Figure 8, it is apparent, however, that the 925 Hz and 2175 Hz responses are very noisy. The higher frequency data are stable but the 20025 and 40025 Hz do not add new anomalies compared to the 9825 Hz data. Figure 8 and Figure 14-19 also illustrate that despite the theoretically differing exploration depth, anomalies in the higher frequencies (20025 and 40025 Hz) appear just as strong in the lowest stable frequency (9825 Hz) and only the absolute measured values differ, raising questions about the multiple depth measurement claims. Due to the unstable 925 and 2175Hz data, attempts at inverting the data to create a 3-layer subsurface model using WinGEM software (Haoping and Won, 2003) were unsuccessful. The 9825Hz data seem to have the most stable results at the lowest frequency in our dataset (see Figure 8). Therefore, the GEM-2 performs similarly in our case study to other single frequency electromagnetic sensors in agreement with McNeill (1996).

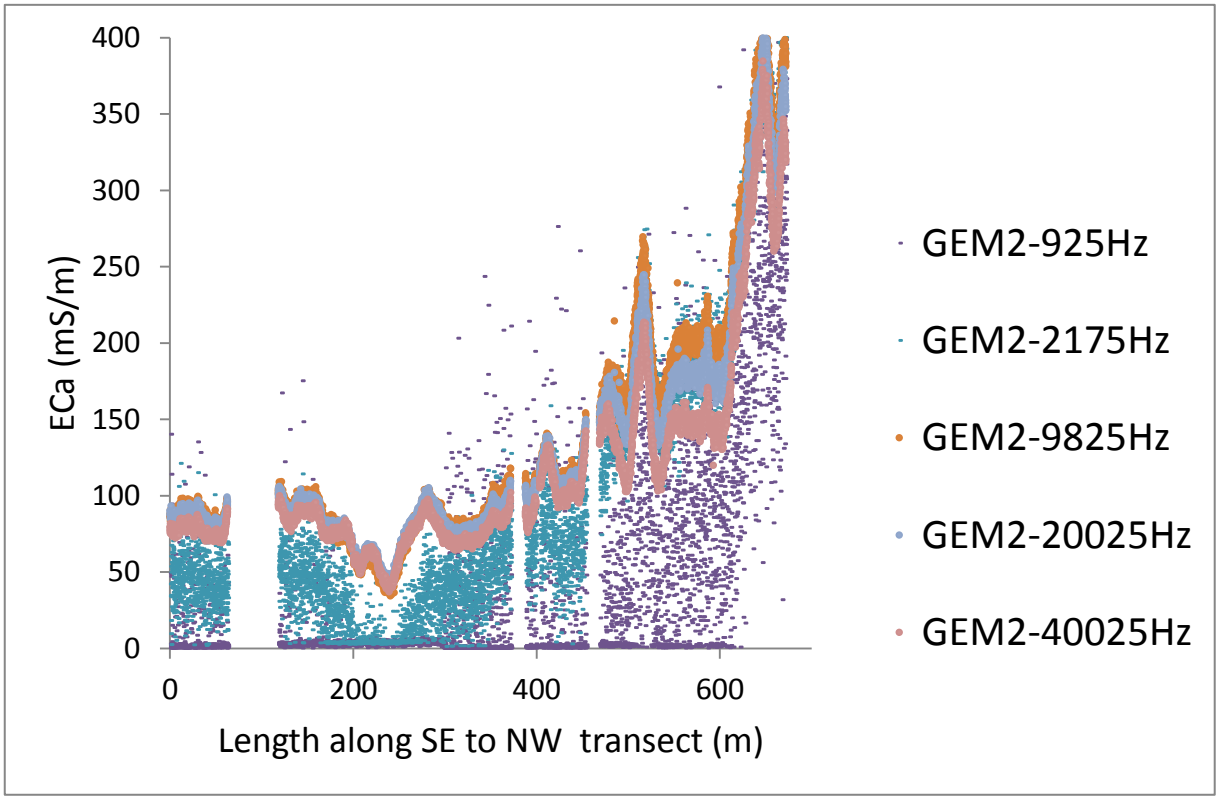

Figure 8: Transect of the GEM-2 ECa data on the location of the ERI transect through Doelpolder Noord (Figure 5).

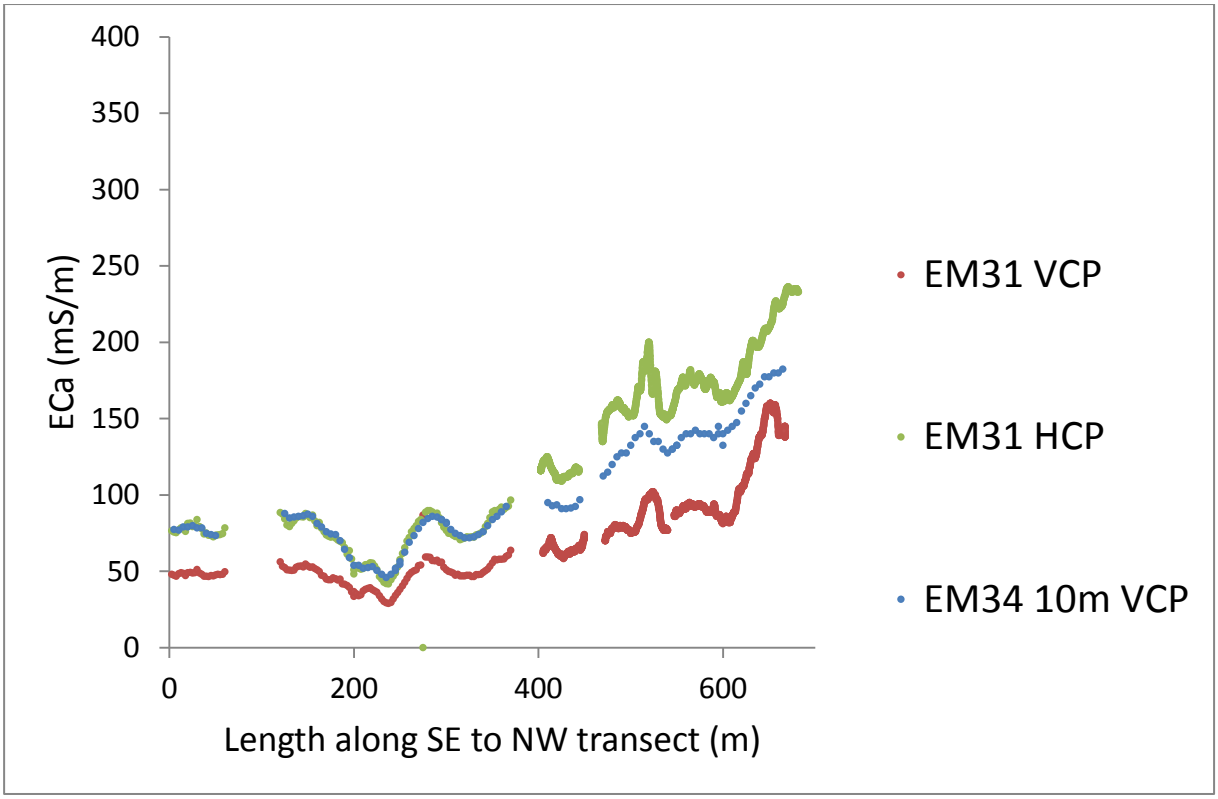

Figure 9: Transect of the EM31 and EM34 ECa data on location of the ERI transect through Doelpolder Noord (Figure 5).

The EM31 VCP registers significantly lower values and contrasts than the other EMI datasets (Figure 8 and Figure 11-18). This was to be expected because this sensor is most sensitive to the shallow variations. For this reason, the VCP configuration is not suited to be carried at waist height (McNeill, 1980). The EM31 HCP and EM34 register similar values to the GEM in the southern half of the survey area but do not register small variations due to shallow (Post) Medieval ditches and gullies (see further). In the northern half the EM31 HCP values increase a lot but reveal less variability than the GEM-2, indicating a lesser deviation of the LIN approximation. This is further confirmed by the even lower EM34 VCP ECa values in the northern half registering no shallow (Post) Medieval ditches or gullies. An alternative explanation for the lower EM34 ECa data could be the shallow depth of salt intrusion compared to the larger measured soil volume (see further).

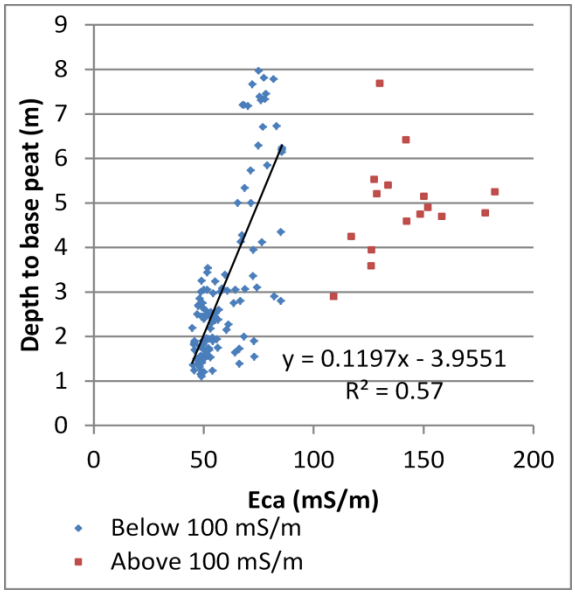

Figure 10: Relation between ECa of the EM34 sensor and depth to base of the peat at coring and CPT locations.

In all datasets, the highest ECa values were measured in the northern half of the survey area while the southern half is significantly more resistive (Figure 11-18). Plotting the ECa values against the depth of the base of the peat (Figure 10), a moderate linear relation can be observed. This correlation is only moderate as many other factors introduce variability, both in the sedimentology within stratigraphic units and in the elevation measurements (core sampling/measurement errors). The extremely high values towards the north of the survey area indicate the presence of salty or brackish groundwater intrusion (eg. Orbons, 2011) close to the Scheldt. Here, the ECa does not correlate with the depth to the Pleistocene sand but probably to the salinity of the groundwater or the proximity to the Scheldt (red versus blue dots in Figure 10 and Figure 11). Here, the quadrature phase response does not represent the actual ECa but rather a combination of magnetic and electric properties, due to the LIN approximation breakdown.

The problematic georeferencing of the handheld GPS of the northern EM31 (HCP and VCP) data has resulted in less sharply defined anomalies after interpolation. The EM31 HCP measurement resolution in the southern half was still sufficiently high to record the smaller geological anomalies such as a depression in the dune or a gully, but did not record the shallow ditches which could be observed in the GEM2 data. The EM34 results include major anomalies such as the dunes and the saltwater intrusion of the Scheldt, but smaller features are hardly visible, mainly due to the larger measured soil volume, but possibly also due to the limited spatial measurement resolution of this time consuming instrument.

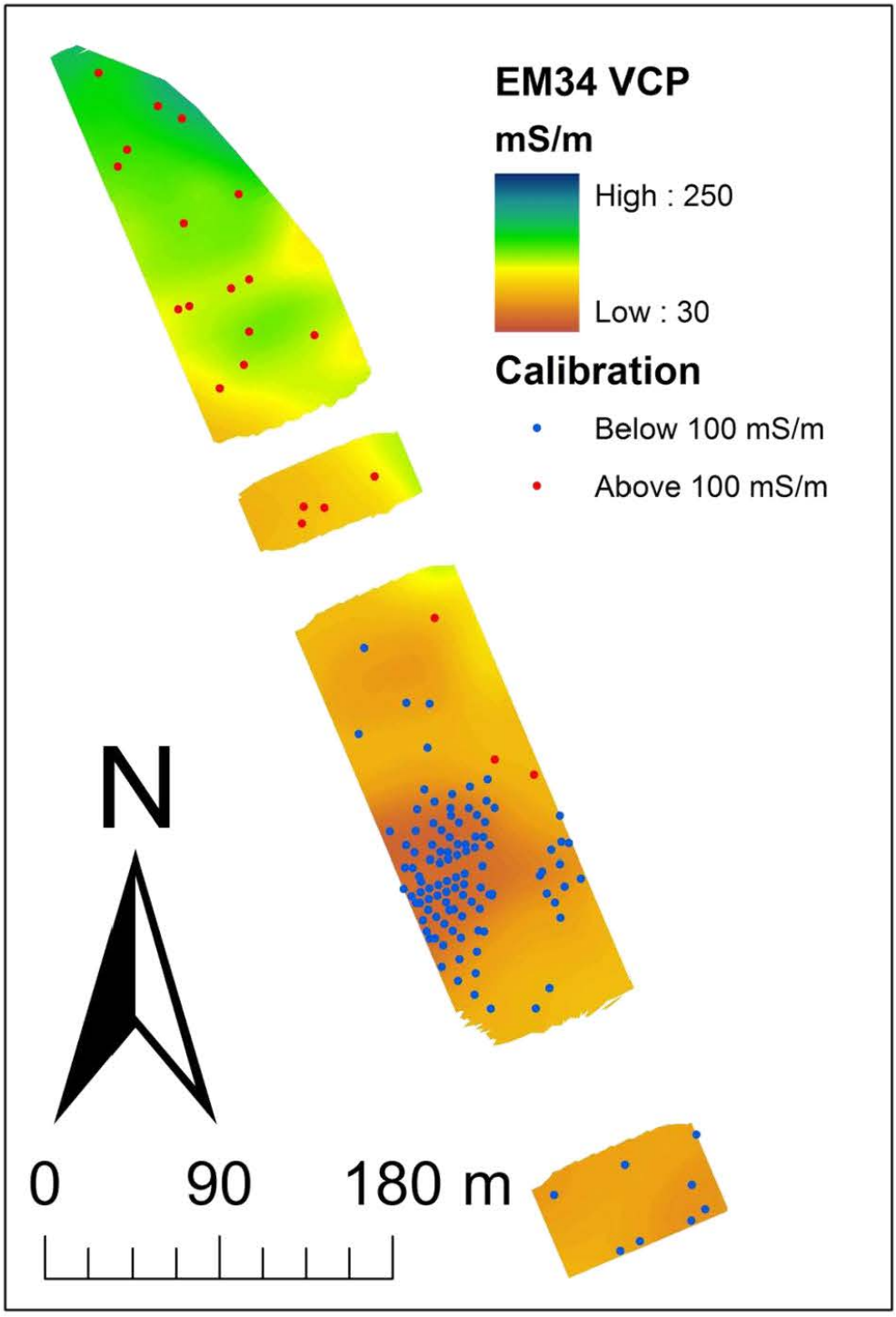

Figure 11: Interpolated EM34 ECa plot of the EMI survey area (Figure 5) in Doelpolder Noord; red and blue dots from calibration points (base of peat layer in corings and CPTs) above and below 100 mS/m (Figure 10).

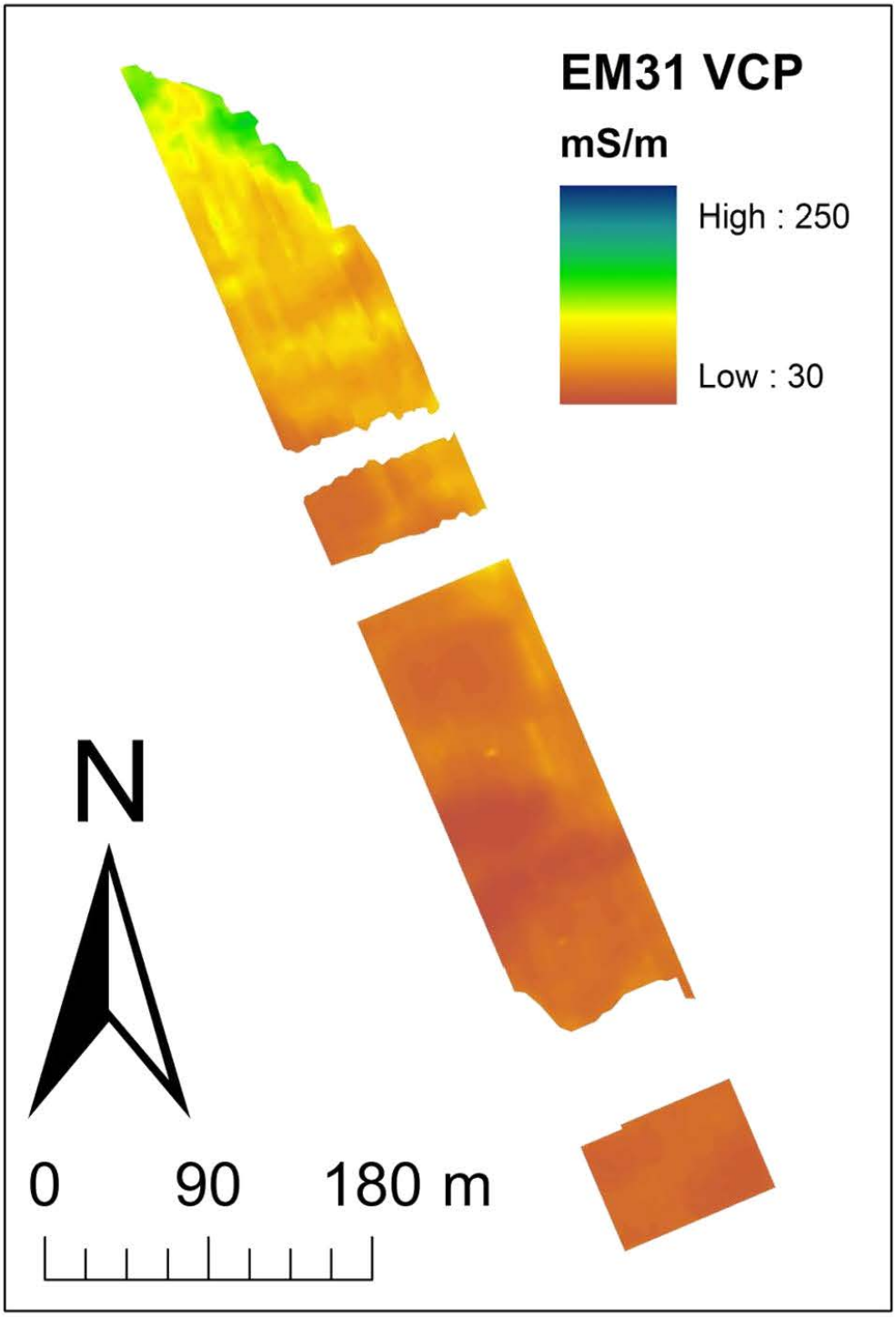

Figure 12: Interpolated EM31 VCP ECa plot of the EMI survey area (Figure 5) in Doelpolder Noord.

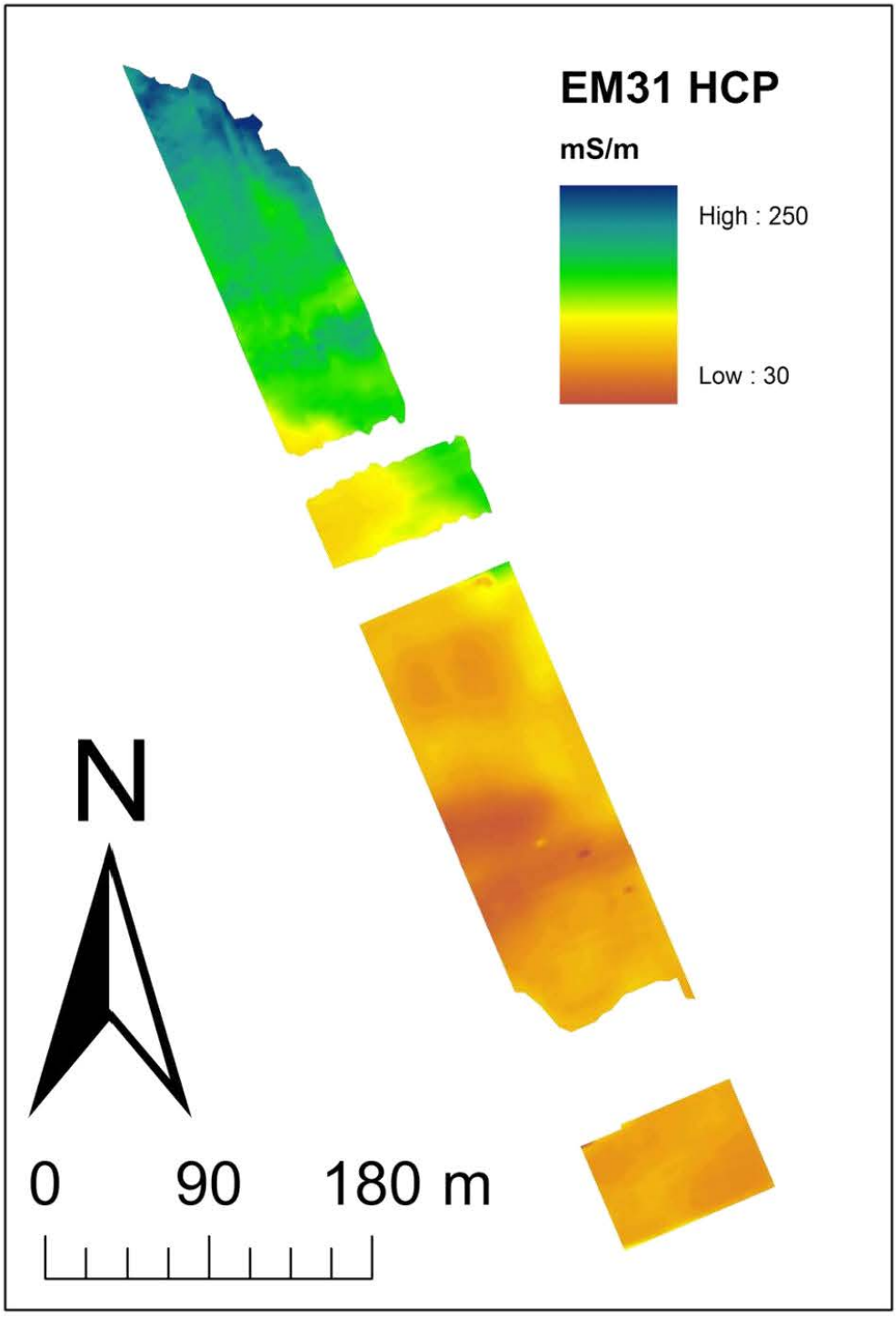

Figure 13: Interpolated EM31 HCP ECa plot of the EMI survey area (Figure 5) in Doelpolder Noord.

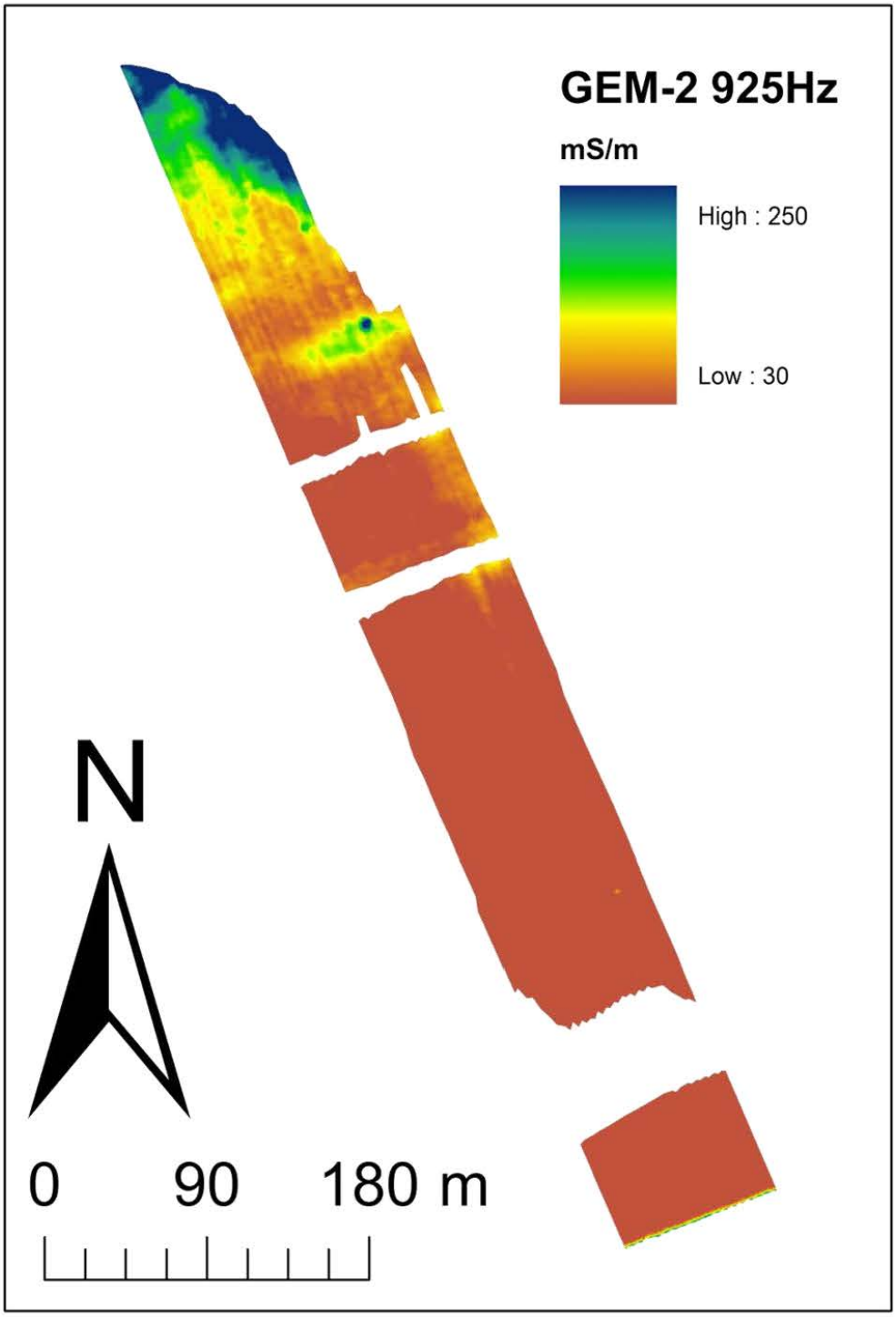

Figure 14: Interpolated GEM-2 ECa plot of the EMI survey area (Figure 5) in Doelpolder Noord at a 925 Hz induced field frequency.

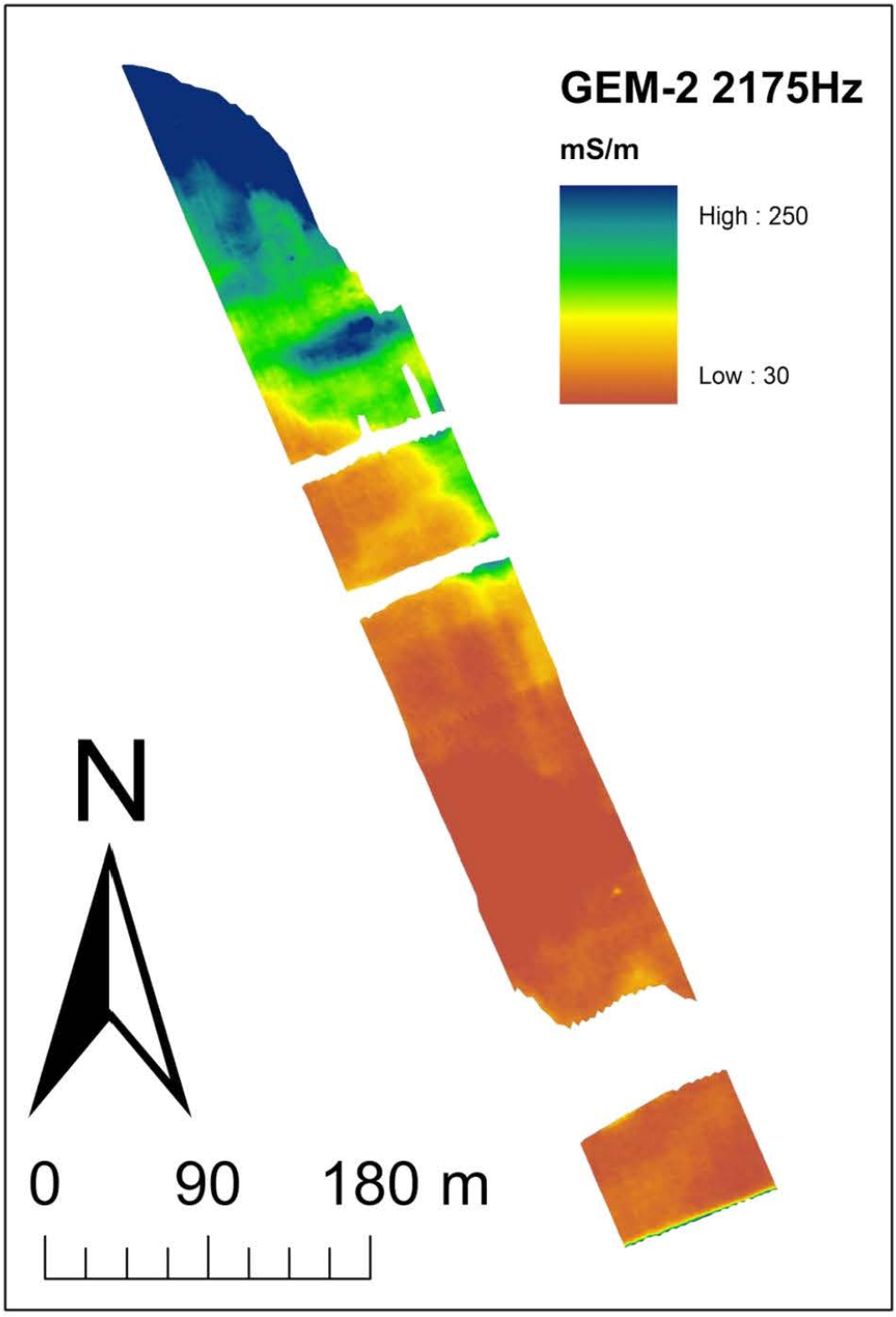

Figure 15: Interpolated GEM-2 ECa plot of the EMI survey area (Figure 5) in Doelpolder Noord at a 2175 Hz induced field frequency.

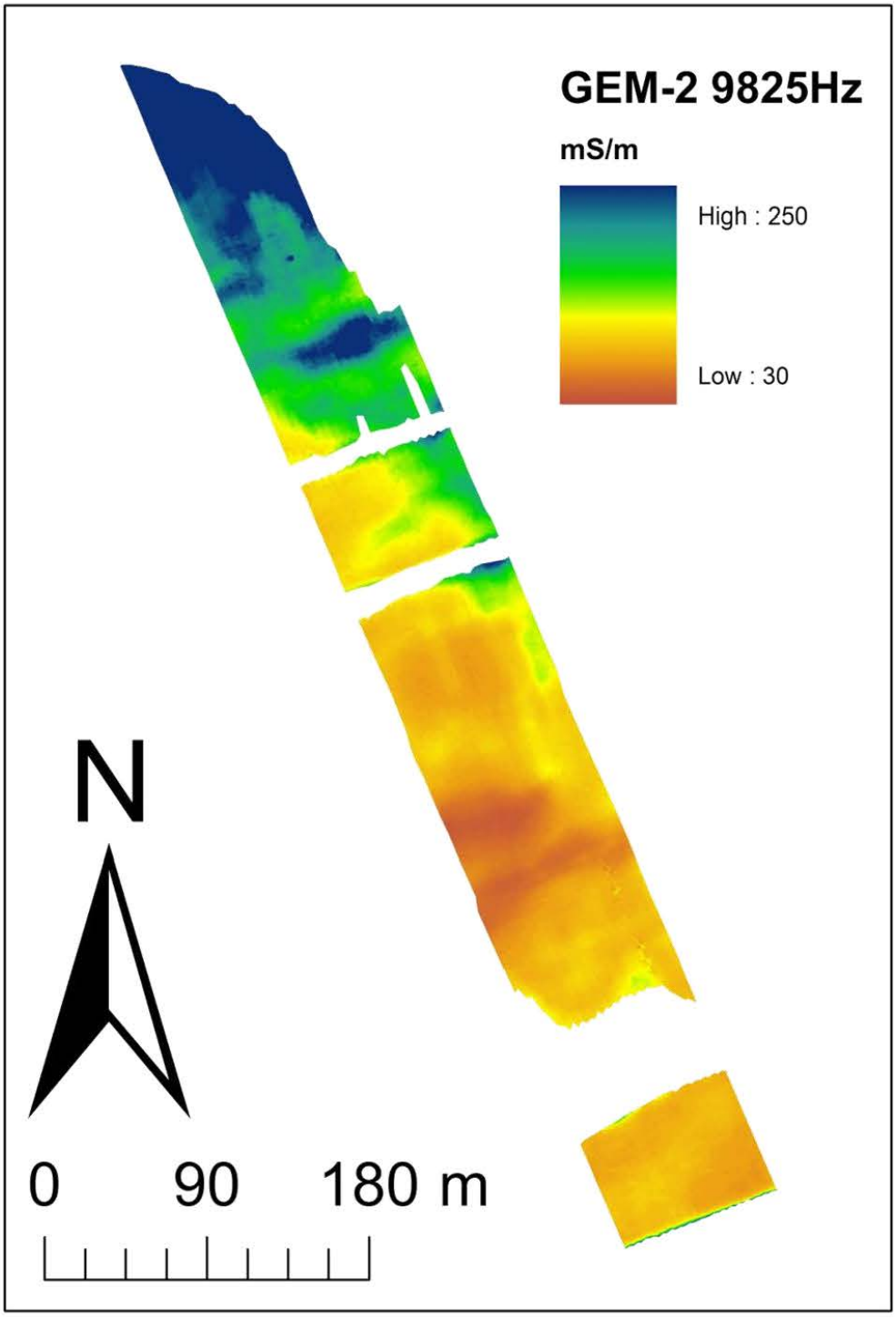

Figure 16: Interpolated GEM-2 ECa plot of the EMI survey area (Figure 5) in Doelpolder Noord at a 9825 Hz induced field frequency.

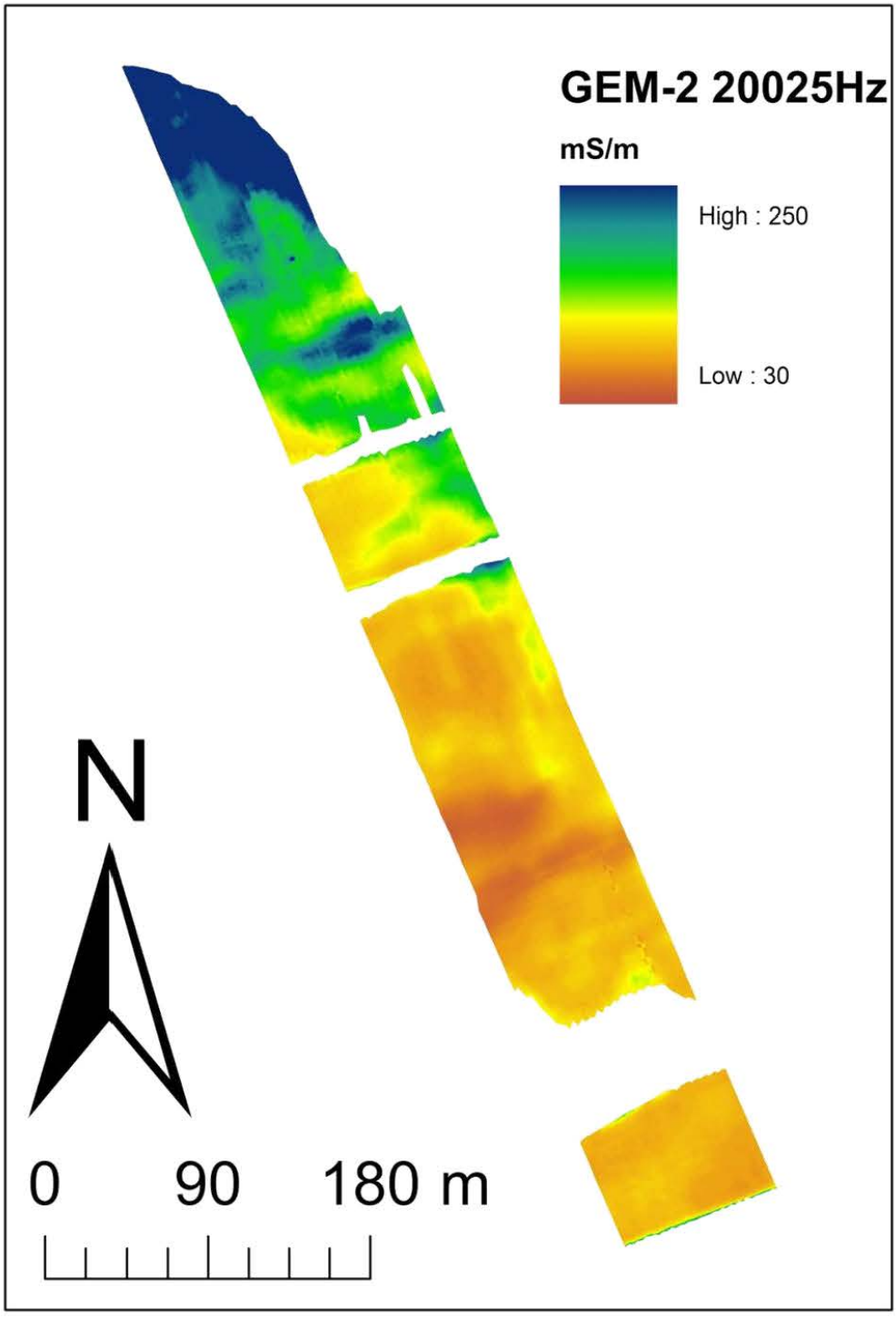

Figure 17: Interpolated GEM-2 ECa plot of the EMI survey area (Figure 5) in Doelpolder Noord at a 20025 Hz induced field frequency.

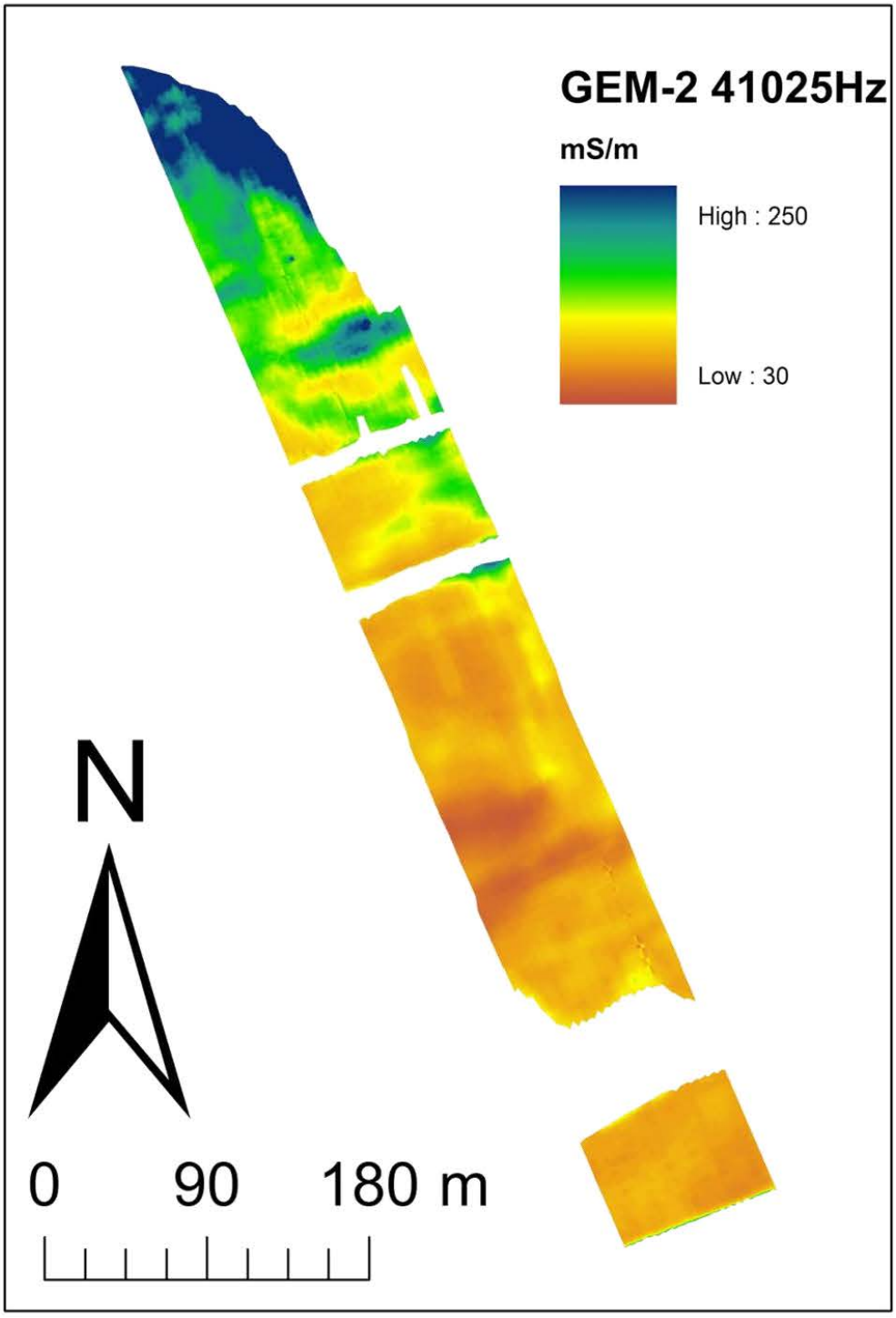

Figure 18: Interpolated GEM-2 ECa plot of the EMI survey area (Figure 5) in Doelpolder Noord at a 41025 Hz induced field frequency.

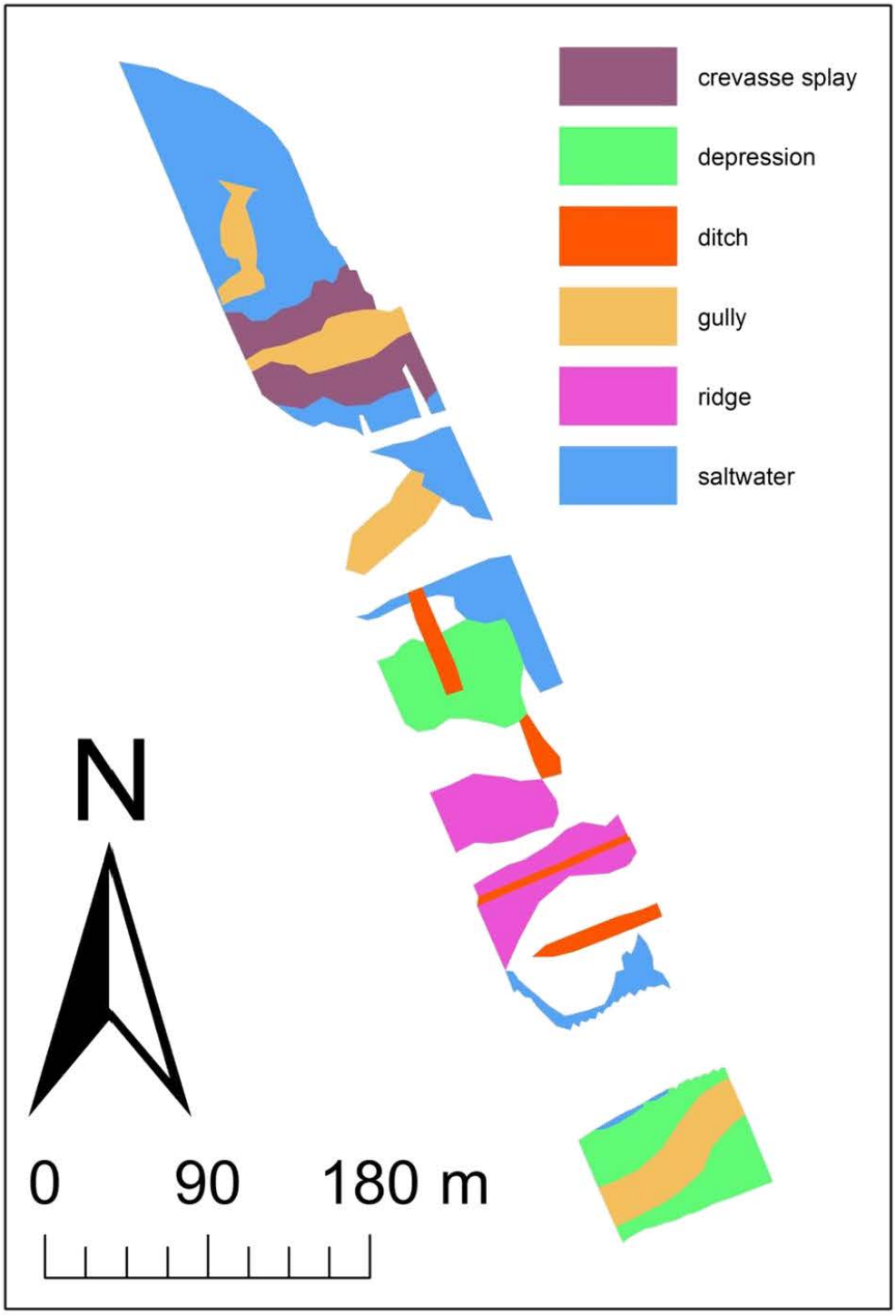

Figure 19: Graphical delineation and interpretation of the EMI survey (Figure 5) datasets in Doelpolder Noord, based on comparison with corings and CPT data.

After interpretation using available coring, CPT information and general knowledge, various features linked to modern fences, saltwater intrusion or drainage ditches could be mapped (Figure 19). Broad linear conductive anomalies traversing the study area visible on the GEM-2 data (Figure 16, 17, 18, 19: ditch) could be related to bad draining caused by the presence of (Post) Medieval ditch systems, still partially visible on digital elevation models. A major feature in all datasets is the semi-crescent shaped low conductivity anomaly in the southern half of the dataset (Figure 19). Details in its shape and sediment characteristics observed in cores and CPTs suggest a sandy (river-)dune. The small conductivity increase observed on the top of this dune is related to a small depression filled with peat (between 200 and 250 m in Figure 6) . This low conductivity anomaly is flanked by two areas of increased conductivity, correlating with flanks of the ridge, with most peat in the measured soil volume. The deepest part of the Pleistocene depression to the south of the dune coincides with a subtle increase in conductivity, which is most pronounced in the GEM-2 data, indicating the presence of a shallow clayey/badly drained gully (Figure 19: gully in depression). North of the dune, the deepest part of the Pleistocene depression correlates with a decrease in conductivity without indications of a gully (Figure 19: depression). The increased conductivity in the depressions is due to the thickness of the peat at the lower edge of the measured soil volume.

Towards the north a linear high ECa anomaly can be observed in the GEM-2 data indicating a possible (Post) Medieval gully (since the variability in ECa roughly >100mS/m is uncorrelated to the depth to the Pleistocene surface). Immediately north of this, two large low ECa anomalies flanking a linear high ECa anomaly can be seen. Correlation with CPT data (CPT-C 8 and 9 in Figure 24), indicates a crevasse filled with peat and clay, flanked by crevasse splay deposits covered with a thinner layer of peat and more sandy sediments. In the extreme north a high ECa anomaly is also interpreted as a (post-)medieval gully.

2.4.2 Electrical Resistivity Imaging

Data statistics of the ERI pseudosection are shown Table 4. Many spikey readings occurred, due to bad wiring or electrode contact with the dry clay topsoil. When inverting with a uniform starting model, no sharp resistivity contrast could be observed between the base of the peat and the top of the Pleistocene sands. Due to the low resistance of the peat, this transition cannot be mapped by ERI independently. Therefore, constraints were put on the forward model, putting resistivity transitions at the depth of the topsoil clay and the top and base of the peat as derived from CPTs and cores. In the resulting modeled pseudo-section (Figure 20: bottom), a conductive layer correlating with the peat can be recognized. The topographic variability of the paleosurface is largely determined by these imposed boundaries. The modeled resistivity contrast between peat

and underlying Pleistocene sand is limited to values below 4ohm.m in the peat and between 4 and 7.5ohm.m below the peat. A general south to north trend of decreasing resistivity is recognizable in the peat layer. In the northern part, this decrease can also be observed in the sediments above and below the peat, indicating that saltwater intrusion also occurs outside the peat layer. This correlates well with the increasing ECa in the EMI data regardless of the peat thickness.

Table 4: Descriptive statistics (Minimum, Maximum, Mean, Median, Standard Deviation) of the modelled ERI Supersting R8 data in Doelpolder Noord (resistivity in ohm.m).

Minimum	0.503
Maximum	105.27
Mean	10.92763
Median	5.1095
Standard Deviation	11.28938

Due to the limited data collection resolution, the small and shallow (Post) Medieval gullies and ditches are only subtly recognizable in the noisy and variable resistivity values above the low resistive peat layer. A large highly resistive zone, split in two (above 20ohm.m), disrupts the continuous conductive layer and coincides with the drier parts of the Pleistocene sand ridge. The separation between both peaks is caused by the depression on the top of the ridge. On the ridge the peat thickness is below the measuring resolution. The depressions flanking the dune are only visible where they are determined by the forward model. The northern crevasse observed on the EMI plots and CPT data is also recognizable in the ERI data, showing a locally decreased shallow resistivity above the peat layer. The crevasse splay deposits are hardly recognizable in the modelled data. It is remarkable, however, that these were more pronounced in the unconstrained data. This illustrates the dependence of the inverse modelled results on the information introduced in the forward model.

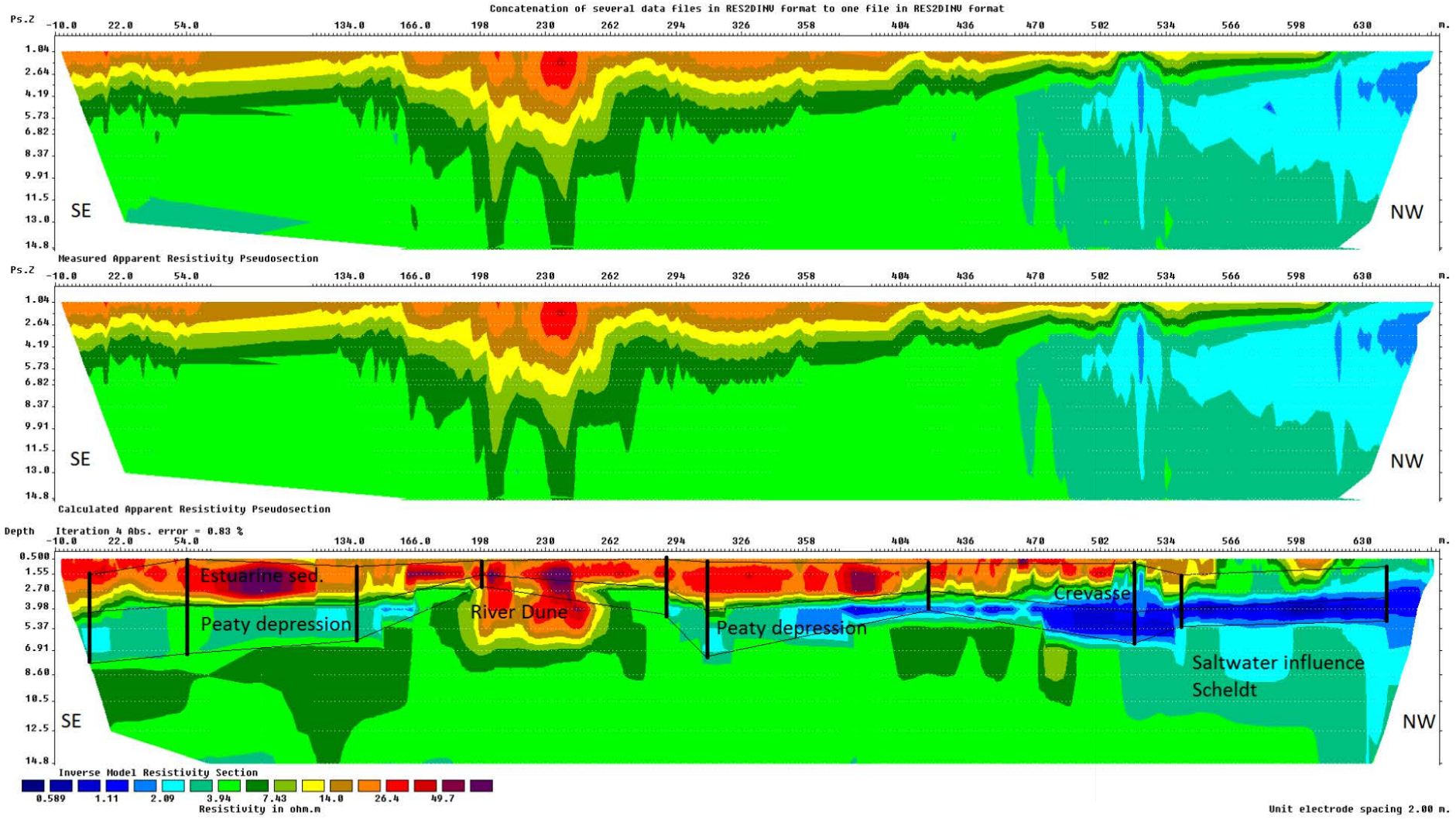
Concatenation of several data files in RES2DINV format to one file in RES2DINV format
Ps.Z
-10.0 22.0 54.0 134.0 166.0 198 230 262 294 326 358 404 436 470 502 534 566 598 630 m.
1.04 2.64 4.19 5.73 6.82 8.37 9.91 11.5 13.0 14.8
SE
NW
Measured Apparent Resistivity Pseudosection
Ps.Z
-10.0 22.0 54.0 134.0 166.0 198 230 262 294 326 358 404 436 470 502 534 566 598 630 m.
1.04 2.64 4.19 5.73 6.82 8.37 9.91 11.5 13.0 14.8
SE
NW
Calculated Apparent Resistivity Pseudosection
Depth
Iteration 4 Abs. error = 0.83 %
-10.0 22.0 54.0 134.0 166.0 198 230 262 294 326 358 404 436 470 502 534 566 598 630 m.
0.500 1.55 2.70 3.98 5.37 6.91 8.60 10.5 12.5 14.8
Estuarine sed.
Peaty depression
River Dune
Peaty depression
Crevasse
Saltwater influence
Scheldt
SE
NW
Inverse Model Resistivity Section
0.589 1.11 2.09 3.94 7.43 14.0 26.4 49.7
Resistivity in ohm.m
Unit electrode spacing 2.00 m.

Figure 20: Constrained (horizontal black lines) ERI section (top: measured apparent resistivity; middle: calculated apparent resistivity; bottom: inverse model resistivity); vertical black lines: forward model calibration points of the base of the topsoil, the top of the peat and the base of the peat, derived from 10 CPT-Cs, shown in Figure 24). Transect location in Doelpolder Noord: Figure 5.

2.4.3 Land seismics

Shear waves were only clearly visible in the seismic record below the surface wave train (>100ms (~75m)). Reflections shallower than 100ms could be due to Love waves and should be interpreted with care. Furthermore, some ringing occurred and additional surface waves were also observed, caused by the correlation of the raw seismic record with the signal sweep. The field geometry in the central part (between CMP's 310 and 350, see Figure 21) showed errors in the geometry spreadsheet. Here, the data could not be trusted.

Frequency analysis showed that the seismic reflection data were most dominant between 30-60 Hz. Love waves seemed to be dominant between 20-40Hz. Due to the frequency overlap, muting of the Love waves was done very carefully. A velocity model was created using semblance analysis, constant offset analysis and constant velocity panels and used for NMO correction. Furthermore, Bandpass frequency filtering, CMP stacking, time-depth conversion using the velocity model and a Surgical mute were applied.

Using the knowledge from the different data analyses, an interpretation was made of the seismic data. For this a combined shear wave reflection profile was made, consisting of a section where the surface waves were muted out of the field records before stacking, and a section where that has not been done. Horizons were drawn on features that were considered shear wave reflections. This picking had to be done carefully due to the ringing effect of the sweep correlation.

The resulting shear wave reflection profile (Figure 21) clearly shows the top of the Pleistocene topography and a large number of additional reflectors. A dome-like structure can clearly be seen in the central part. This structure is not caused by the velocity model that was used for creating the seismic stack and can be considered a genuine geological feature. This is fully confirmed by the paleotopography, which is marked by a buried sand ridge at this location.

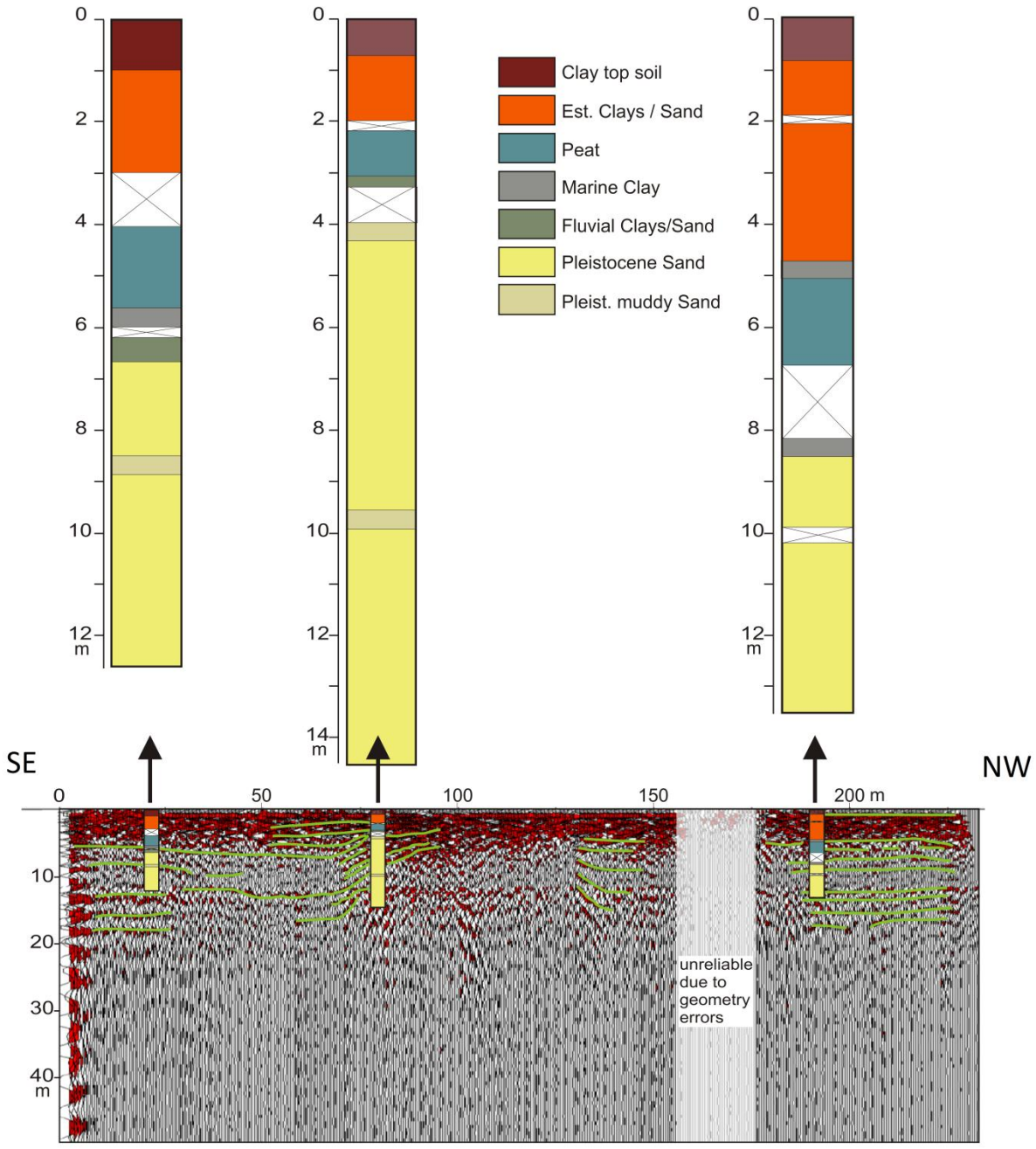

Figure 21: Interpreted seismic depth section trace plot (location on Figure 5) with lithostratigraphic core descriptions.

Correlation of the seismic data with the core was not easy in view of the limited length of the cores compared to the resolution and depth of the seismic section. Nevertheless, the transition from the peat deposits to the underlying cover sand correlates well with a prominent shallow reflector. In the topmost section, the seismic data resolution is not sufficient to allow a reliable correlation with the core data. A number of high-amplitude reflectors appear in the thick marine clayey-sandy sequence but these cannot be linked to changes in the core lithology.

2.4.4 Cone penetration tests

Comparing the tip resistance and friction ration to nearby located cores shows that both methods are able to map the major lithological units but the transitions may be somewhat ambiguous (Figure 22). This is caused by the depth uncertainties introduced by the (discontinuous) coring methods when the sample is pushed into the core and/or retrieved from the borehole. The depth errors of CPTs are limited and therefore the derived elevations of the sedimentary transitions are more accurate than in cores.

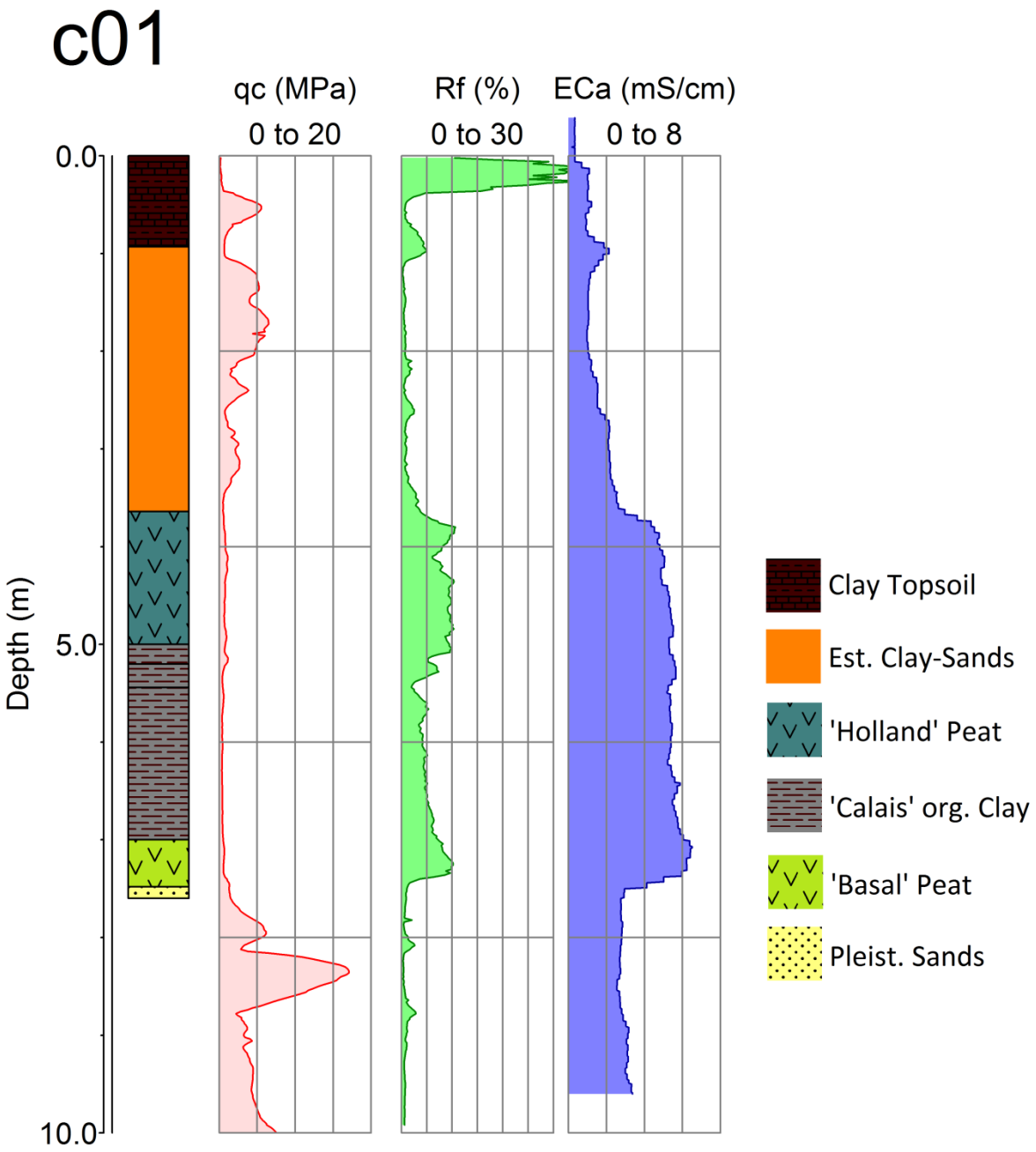

Figure 22: Conductivity CPT (CPT-C) plot with matching lithostratigraphic sediments from a nearby handcore.

(Automated) quantitative interpretation using the Roberston (1986) classification was only partly successful, as expected (cfr. Missiaen et al., 2015). Figure 23 shows that the friction ratio of the peat falls within and beyond the appropriate soil behaviour class, but the tip resistance values are too high and peat is therefore wrongly interpreted as clay. In general, it was found that the peats have a friction ratio above 5%, reaching values up to 12%. This could be due to its fibrous and/or compressed nature. If sufficient

'Basal' peat was present, a subtly lower tip resistance than the upper 'Holland' peat, can be observed suggesting a more amorphous and decomposed peat (Figure 23). If present in the sequence, the OM rich 'Calais' clay layer in between both peat layers (Deforce, 2011; Gelorini et al., 2006) is correctly interpreted as clay (Soil behavior type 3 in Figure 23). Intercalating peat and clay layers, sometimes as thin as 20cm, could be identified on the CPT logs thanks to the continuity of the layer between cores (Missiaen et al., 2015). The Pleistocene sands are correctly interpreted as sand to sandy silt/clayey silt (Figure 23). In a number of cases a thin transition layer seems to be present between the base of the peat and the top of the sand. This could be related to the OM rich sandy topsoil at the base of the peat (A-horizon). The marine clays and sands overlying the peat are also correctly interpreted, showing a large range of values, as expected in estuarine sediments. The topsoil friction ratio reaches values similar to peat, due to its unsaturation.

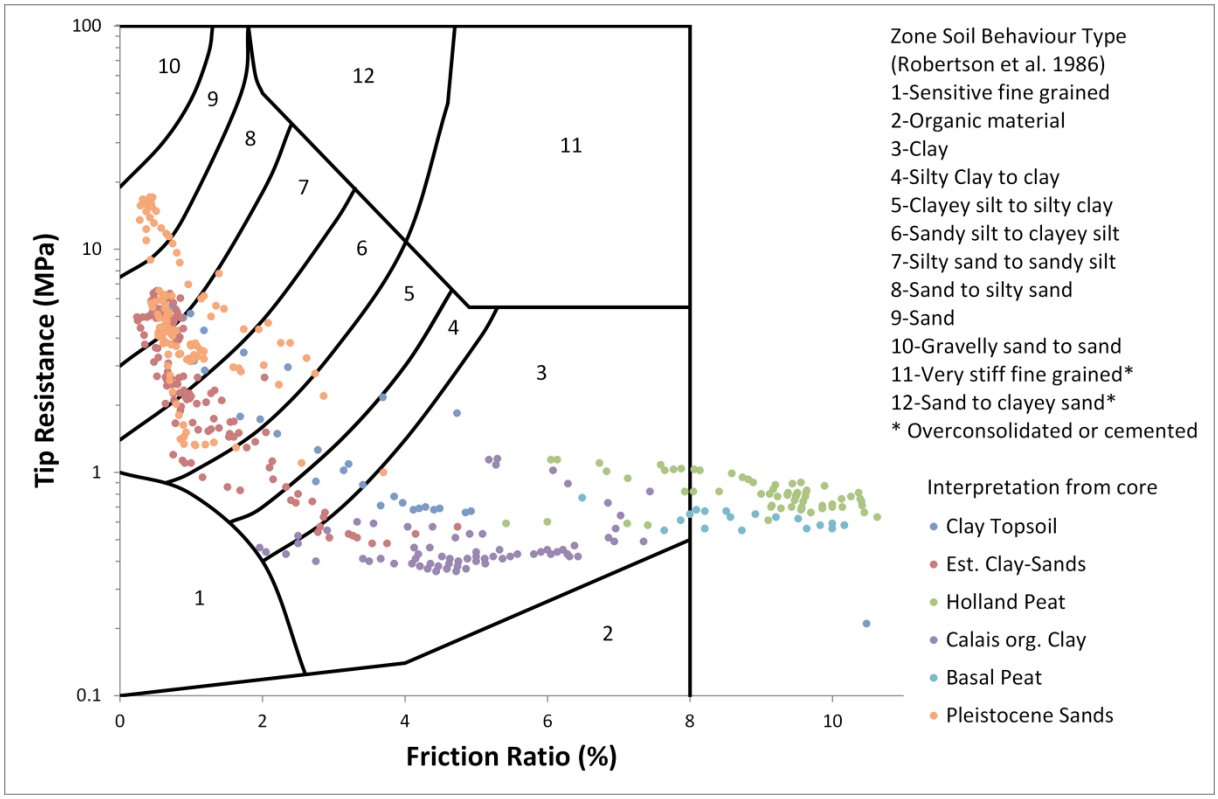

Figure 23: Lithostartigraphically interpretated CPT-E tip resistance and Friction Ratio values (from Figure 22) on soil behaviour classification chart by Robertson et al. (1986).

Because the base and top of the peat are such important transitions and could not be automatically mapped, interpretation was done manually. In this way interpretations could also include information derived from the stratigraphic continuity along CPT and coring transects (Figure 24). The derived elevations were integrated in the coring based subsurface paleosurface model without significant discrepancies (Figure 5) and used for interpretation of the geophysical data.

The conductivity (EC) data resulting from the CPT-C measurements did provide a definite peat indicator. A single increased conductive layer with varying thickness according to Pleistocene elevation correlated well with the peat in the corings and CPT-Cs. Therefore these EC data can be used to interpret both the EMI and ERI data. Figure 24 shows a CPT-C transect along the ERI section through the study area (for location Figure 5). An increasing EC of the non-peaty sediments northwards along the ERI section does not fit with the respective qc and Rf values. This indicates another source of increasing EC, such as brackish/saltwater intrusion closer to the Scheldt river.

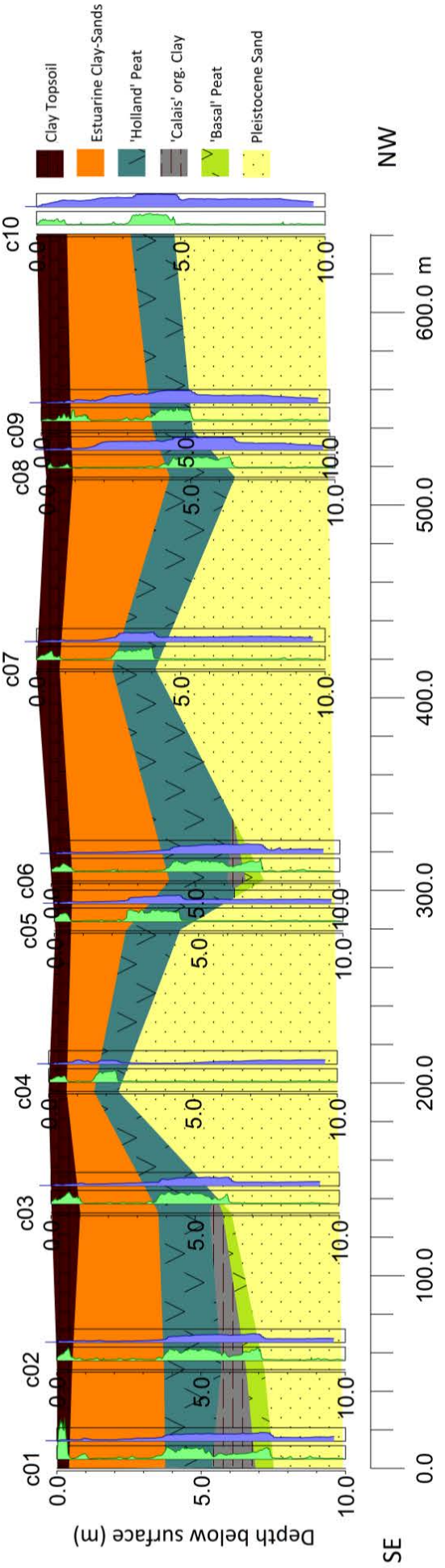

Figure 24: CPT-C transect along the ERI section (Figure 5) through study area (green: Rf (%) from 0 to 12, blue: EC (mS/cm) from 0 to 10) with the interpreted lithostratigraphy.

2.4.5 Archaeological coring

Based on the geophysical (see results), geotechnical (see results and Missiaen et al., 2015) and coring paleolandscape (Klinck et al., 2007) data, several topographically pronounced landscape positions could be estimated suitable for human occupation. Amongst these, the main feature was a well preserved small dune with steep slopes which was selected for archaeological evaluation through core sampling (Crombé and Verhegge, 2014).

Using the Dutch hand auger, samples could only be retrieved up to groundwater depth, with limited soil volume retrieval and laborious effort. During a second phase, the flanks were sampled mechanically resulting in larger, less disturbed sample volumes than a comparable Dutch hand auger, in agreement with Hissel and Van Londen (2004); Hissel et al. (2005). Aqualock coring did not result in perfectly continuous archaeological sampling because 0.2 m of sediment was lost between the sampler tubes (Hissel and Van Londen, 2004). This problem was resolved by using a 7 cm diameter core on the same location in a discontinuous manner, only opening the aqualock sampler directly above the top of the Pleistocene sediments.

Both methods retrieved several samples containing burnt bone and flint chips, which were considered good indicators for prehistoric archaeology (Figure 25). Both flint and burnt bone were found on only one coring location. This was also the only location where more than 3 indicators per borehole were found. If the spatial distribution of the 'positive' boreholes is taken into account, an possible interpretation tends towards the presence of small discrete artefact clustering, probably resulting from ephemeral activities. A temporal reconstruction of the occupation history of the site is not possible based on the retrieved site indicators. Further evaluation of the site requires test pits or trenches.

Furthermore, Late Medieval ceramic fragments were found in the top of the peat, indicating at least surface exposure and exploitation of this location during this period.

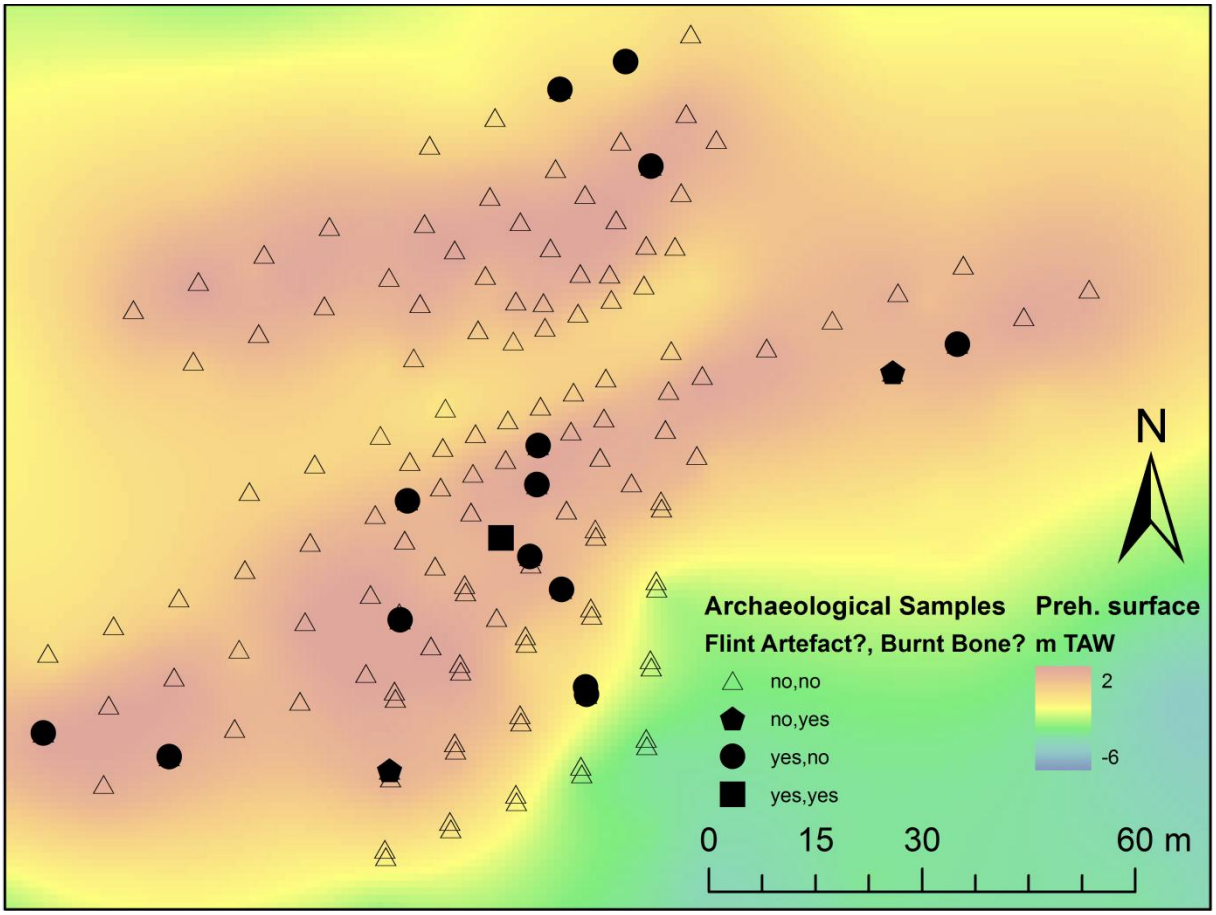

Figure 25: Results of the archaeological sampling with 10 cm diameter handaugering, 10 cm diameter continuous sonic drill aqualock coring and 7 cm discontinuous sonic dril aqualock coring. (arch. cores in Figure 5) (yes/no is the answer on the question if respectively flint artefacts and burnt bone fragments were found in the cored sieving residu).

2.5 Discussion

Bates and Stafford (2013) have already argued that a good archaeological survey strategy in buried landscape contexts should take both geological and practical variables into account. The first are related to the nature of the buried geological or geomorphological system. As Howard et al. (2008) had already suggested, prior information about subsoil lithology has to be obtained during a desk based assessment of the studied area. Based on this information, in our experience some methods can be estimated to be better suited to map buried Pleistocene and Holocene paleotopography for subsequent prospection of prehistoric sites, despite the individual merits of each method. The practical variables include the size of the area to be evaluated in relation to the time, budget and experience available. Both practical and geological variables should be considered in

relation to the aims of the study, for example the necessity of sample recovery or stratigraphic logging only. On this basis, a measuring and sampling strategy can be devised that takes into account the expected depth of burial, subsurface conditions and target size. This is required in order to employ the applied methods to their fullest extent in this challenging environment. Processing and analysis of the various data has to be conducted within a GIS environment, preferably capable of handling 3 dimensional data.

The primary aim of this paper was to evaluate existing geophysical and geotechnical methods that would improve the effectiveness of paleolandscape mapping for prehistoric archaeological prospection purposes. An interpretation of the resulting findings is summarized in Table 5. So far, prehistoric paleolandscape mapping has mainly been conducted by means of manual and/or, to a lesser extent, mechanical augering. The former is often confronted by problems related to depth, water saturation, compaction and interpretation, while the latter is restricted by discontinuity of the retrieved cores, possible sample disturbance and the high costs involved.

The simplest alternative to map subsurface variability is to use gridded conventional CPTs (Missiaen et al., 2015). Within our test-area the CPT method allowed a rapid registration of the soil mechanical properties over a large depth range at a single location. The method was very effective in reaching depths beyond the range of manual coring with a higher depth accuracy. In addition, modern day commercially available CPTs allow cheaper and more rapid sediment sounding than mechanical coring, while only one operator is required. Lithostratigraphical interpretation is possible after data collection by comparison with a limited number of cores, depending on the stratigraphical variability of the buried geomorphic system. Subsequently, a paleotopographical subsurface model can be constructed using gridded CPTs, similar to the coring approach. However, the resulting subsurface models are still dependent on the interpolation and resolution of the CPT grid as is the case with coring data. A possible improvement would be to use more geostatististical sampling (e.g. stratified random sampling) and interpolation methods (e.g. (co-)kriging) rather than simple staggered triangular grids (Goovaerts, 1997; Webster and Lark, 2013).

Another, more complicated, strategy could improve the quality of the resulting models by including surface geophysical methods and using depth sounding data at a single point (coring or cone penetration tests) only as calibration and validation. In our case study land seismics has had only limited results with regard to mapping extensive subsurface variability and the input effort. Firstly, both data collection and processing are very intensive, hindering the evaluation of large areas. Secondly, the best results are obtained at depths greater than 10m, which are rarely encountered in the study region. Similar arguments are partly valid for ERI. ERI data collection is slightly less time intensive than land seismics, while processing is relatively fast using available inversion software. Due to the presence of a large conductor (i.e. the peat) in the subsurface, the inversion procedure has difficulties in mapping the underlying sediments and con-

straints have to be introduced into the inversion procedure, requiring a significant number of corings or CPTs per ERI section. Nevertheless, ERI could resolve some geophysical interpretation with single coil EMI methods, but these issues could also be resolved by well-placed and relatively simple CPT-Cs.

Better suited to paleolandscape evaluation studies would be the use of mobile EMI sensors. Single coil spaced EMI methods would be suitable if pre-existing knowledge suggests that the subsurface variability of the study area falls within the measurement range of the system (McNeill, 1980). In this study, the multifrequency GEM-2 did not prove to be of significant additional value compared to the single frequency instruments. It is advisable to maximize the spatial resolution in relation to the measured soil volume, because the effort required to collect more EMI data is far less than if too many (coarsely defined anomalies) or too few (if small geomorphic features are missed) archaeological samples are taken subsequently. Well aimed corings or CPTs have to be used to define the nature of the detected anomalies as well as provide a rough depth estimate (Figure 10). If the geophysical anomalies cannot be explained using the latter, conductivity CPTs may provide an answer. In our study, brackish/saltwater intrusion in the sediment sequence created anomalous zones where the ECa variability was not related to the prehistoric landscape variability. Other sources of variability include (post-)medieval gully formation or land divisions, which are also valuable during the archaeological evaluation process. Similarly, modern interference by metal objects, power lines or artificial land reclamations, all of which often occur in polder landscapes, provide possible disturbances of the EMI results.

After evaluation of the preservation of possible archaeological levels and of diachronic landscape evolution, an archaeological sampling strategy can be devised. The geomorphological features mapped by single coil spaced EMI can be archaeologically sampled by gridded continuous core sampling. This can be done by hand using 10cm Dutch augers until the depth of subsoil saturation is reached, and below this by sonic aqualock coring with full sequence sediment retrieval in agreement with Hissel and Van Londen (2004).

Further developments to discontinuous mechanical coring of the individual prehistoric strata require a high resolution (maximal 5 m grid, accurate to ca. 0.5 m) depth model of the base of the peat. This can only be acquired by using high resolution multi-coil spaced EMI measurements, which are subsequently interpreted and modeled into paleosurfaces (Saey et al., 2008). The additional advantage is that this dataset also splits the modeled prehistoric paleotopography and (Post) Medieval landscape structures (eg. De Smedt et al., 2013c), resolving part of the issue with extensive systematic trial trenching prospection in wetlands/polders (De Clercq et al., 2011). Both the Dualem 421S and CMD explorer could prove useful sensors for these problems and will be the subject of future research.

Table 5: Summarized interpretation of the effectiveness of the tested geophysical and geotechnical methods for prehistoric landscape mapping in an archaeological evaluation context and the method proposed to be further investigated (see Chapter 6).

	Gridded hand/mechanical coring	Gridded CPT	Land seismics	Electrical resistivity imaging	Single frequency, single coil spaced emi	Multifrequency, single coil spaced emi	*Future: single frequency multiple coil spaced emi*
Data dimensionality	1-D vertical	1-D vertical	2-D vertical	2-D vertical	2-D horizontal	in theory 2.5-D, this study 2-D	*2.5-D (after inversion)*
Measurement speed	low	moderate	low	moderate	high	high	*high*
Depth resolution	high	high	moderate	moderate	low	low	*moderate*
Horizontal resolution	low	low	moderate	moderate	high	high	*high*
Additional technique necessary?	no	limited number of corings	multiple corings/cpts per transect	multiple corings/cpts per transect	corings/cpts trough variation of anomalies	corings/cpts trough variation of anomalies	*corings/CPTs trough variation of anomalies*
Advantages	sample retrieval; direct interpretation of soil variability and preservation	widely commercially available; additional geophysical sensors; depth accuracy	high resolution at large depths (>10 m)	widely commercially available; stratigraphic info	widely commercially available; hand carried	hand carried, light weight	*multiple soil volumes in one survey; depth discrimination possibilities*
Limitations	discontinous, limited depth range by hand, dependent on data grid; time consuming	dependent on data grid	limited availability; extensive processing	electrical current has difficulties in mapping below high conductor (peat)	nearly no depth info; possibly multiple surveys needed	no depth reliable depth discrimination; not widely available; low frequencies are noisy in this study	*not widely available, quad pulled*

2.6 Conclusion

The results obtained in this first test of different geophysical and geotechnical methods indicate that CPT and EMI are the best alternatives for manual or mechanical augering in view of mapping deeply buried prehistoric paleolandscapes in polder areas. The main advantage of CPTs is the high depth control and the high contrast between the peat layer(s) and the under- and overlying sediments. On the other hand, single coil spaced EMI offers a higher horizontal resolution map of the varying peat thickness/depth to Pleistocene within the measured soil volume, but also includes other sources of variations which can be desirable (e.g. the (Post) Medieval landscape divisions) or undesirable (e.g. saltwater intrusion).

Dependent on the specificities of the study area, either gridded CPTs or a combination of EMI calibrated and validated by CPTs provides a commercially widely available solution to map the paleolandscape variability, but this has to be backed up by geological coring to identify the degree of preservation of archaeologically interesting landscape locations in the following evaluation phase of archaeological coring.

2.7 Acknowledgements

The presented research was funded by Research Foundation Flanders (FWO) (Grand number G024911N) and the Interreg IVA 2 Seas project "Archaeology, Art and coastal Heritage" (08-019 Arch-Manche). The CITG of TUDelft is thanked for providing the GEM-2 and Supersting, TNO for the EM31 & 34. CPTs and Sonic drill Aqualock cores were carried out by SGS. Selection of the dated macro remains was performed by Hanneke Bosch (ADC) and Luc Allemeersch (GATE). ^{14}C dating was carried out by the Royal Institute for Cultural Heritage. All staff and students are kindly acknowledged for their assistance with field work. Our thanks also go to Hannah Brown for proofreading the manuscript..

Chapter 3 Potential of cone penetrating testing for mapping deeply buried paleolandscapes in the context of archaeological surveys in polder areas

This chapter is adapted after Missiaen et al. (2015)

Geoarchaeological mapping of wetlands conventionally involves extensive coring. Especially in wetlands marked by a deep paleosurface (> 3 m deep) this can be very difficult and time-consuming. In this paper we therefore present an alternative approach based on cone penetration testing (CPT) for structured, rapid and cost-effective evaluation of buried paleolandscapes. Both estuarine and river floodplain environments were investigated, including the water-land transition zone (marsh). The efficiency, reliability and repeatability of the CPT method was tested through the comparison with ground-truth core data. The CPT data generally allowed highly accurate mapping of the paleotopography of the prehistoric surfaces and the overlying peat sequences. Thin OM rich clay intercalations within the peat layers could often still be identified. Additional pore pressure, conductivity and seismic velocity data (from CPT-U, CPT-C and CPT-S) did not add much crucial information and their main use seems to lie in the added value for near surface geophysical measurements. The results of this research clearly illustrate the importance of CPT information for mapping of paleolandscapes in archaeology.

Keywords

CPT, paleolandscape mapping, archaeology, prehistoric wetlands

3.1 Introduction

The potential of wetlands, estuarine and riverine areas for understanding past human exploitation and paleolandscapes has been demonstrated by many studies (Bell, 2007; Coles, 1987; Rippon, 2000). These areas are often marked by thick peat deposits known to be a rich source of archaeological and paleoenvironmental information since they often include ecofacts and artifacts that are generally not preserved in other, dryland contexts (Coles, 1987). However, wetlands are also very complex and dynamic environments and understanding the processes of sedimentation and erosion is crucial in order to detect and study archaeological sites (Howard and Macklin, 1999).

Geoarchaeological mapping of wetlands usually involves two main phases (Bats, 2007; Bats and Crombé, 2007; Crombé and Verhegge, 2014; De Clercq et al., 2011; Groenewoudt, 1994; Tol et al., 2004). A first, crucial phase concerns the detailed mapping of the sealed paleoenvironment, especially the paleotopography, and its evolution (i.e. preservation) through time and in relation to the sediment dynamic regime. In a second phase, based on these results, directed archaeological surveys can be carried out on specific locations in view of detecting buried archaeological sites. Previous research in the coastal and riverine wetlands of N Belgium (Crombé, 2005; Crombé, 2006) and the Netherlands (Peeters, 2007) has shown that most prehistoric occupation sites are situated right below the peat on former higher Pleistocene grounds (river dunes, levees, scroll bars, etc.) and often along open water systems (river channels, creeks), whereas younger settlement sites are usually situated on top of the peat and in the covering clay sediments. Therefore detailed mapping of the peat deposits is crucial in order to reconstruct the paleorelief and hence to locate potential archaeological zones and levels within this buried landscape.

Until now geoarchaeological and paleoenvironmental mapping on land has commonly been achieved through manual coring and to a lesser extent by mechanical drilling set in narrow and fixed grids or in transects (Bats, 2007; Groenewoudt, 1994). Manual cores, using 3 cm gouge augers, are effective but very time-consuming, hard work and in the case of deeper layers (below 4–5 m) they are very difficult to obtain and seldom successful. In addition manual drilling below groundwater level and/or through certain sediments, such as coarse sands or woody peat, can be seriously hampered by the sedi-

ment texture or presence of large fragments of organic matter. Mechanical drillings (e.g. Sonic drill, Aqualock, Begemann) on the other hand are less affected by these problems but they are slow and the high costs can be a serious burden (Hissel et al., 2005). Furthermore paleotopographical modelling by interpolation of paleosurface depth points often does not allow accurate delineation of geomorphological features, possibly containing archaeological sites, making this sampling strategy prone to errors. Additional methods must therefore be explored which are less expensive, faster and allow accurate correlation between coring points. Recent work in the United Kingdom (Bates et al., 2007) has shown the advantages of such a mixed method approach.

In the framework of a recent Flemish research project we have tried to develop an alternative approach that allows structured, rapid and cost-effective evaluation of the buried paleolandscape in estuarine polder areas, including the water–land transition zone. This approach focuses both on the (combined) use of near surface geophysical methods such as seismic, electrical, and electromagnetic survey (Verhegge et al., submitted-a), as well as on geotechnical investigations such as cone penetration testing (CPT). Near surface geophysical methods can be hampered by variations in groundwater salinity in combination with the presence of peat (Orbons, 2011), a clay-rich heterogeneous or contaminated top-soil and the burial depth of the prehistoric landscape. In these cases, CPT investigations may provide an answer. The CPT method has been in use for over 70 years in Belgium (Lousberg et al., 1974) and is commonly recognized as a fast, repeatable and economical method for site investigation, but up to now it has largely been neglected in geoarchaeological research, except for a few occasional studies (e.g. Bates and Stafford, 2013; Brandenberg et al., 2009; Roozen et al., 2013).

3.2 Aims of the study

The main goal of this study is to assess the potential of the electrical CPT method for the paleotopographical and paleoenvironmental reconstruction of deeply buried prehistoric landscapes in estuarine polder areas in Flanders. This does not only regard mapping the depth of possible occupation horizons, which are often related to transitions in the sedimentary environment, but also the nature of the different depositional layers (i.e. lithostratigraphy) (Amorosi and Marchi, 1999). This paleotopographical and lithostratigraphic information is crucial for subsequent archaeological prospection as it will allow efficient sampling at the correct location and depth of possible archaeological sites locations.

Two study-areas within the Scheldt valley of NW Belgium were chosen as test sites (Figure 26): (1) the site of Doelpolder Noord located in the Waasland Scheldt polders in

the Lower Scheldt estuary, and (2) the alluvial site of Kerkhove located further upstream in the floodplain of the Middle Scheldt river. In both sites the base and top of the peat are known to be important reference horizons for (pre)historic occupation: the base of the peat reflects the relief of the underlying Pleistocene landscape (an important level for Stone Age sites), whereas the top of the peat is an important indicator related to more recent (early historic) occupation (Bats et al., 2008; Crombé, 2005; Crombé, 2006). In addition, the Scheldt polders are threatened by the continuous expansion of the Antwerp harbour and imposed nature compensation through coastal realignment. Hence there is an urgent need for a detailed, rapid archaeological and paleoenvironmental evaluation strategy. Therefore accurate mapping of the peat layers was crucial.

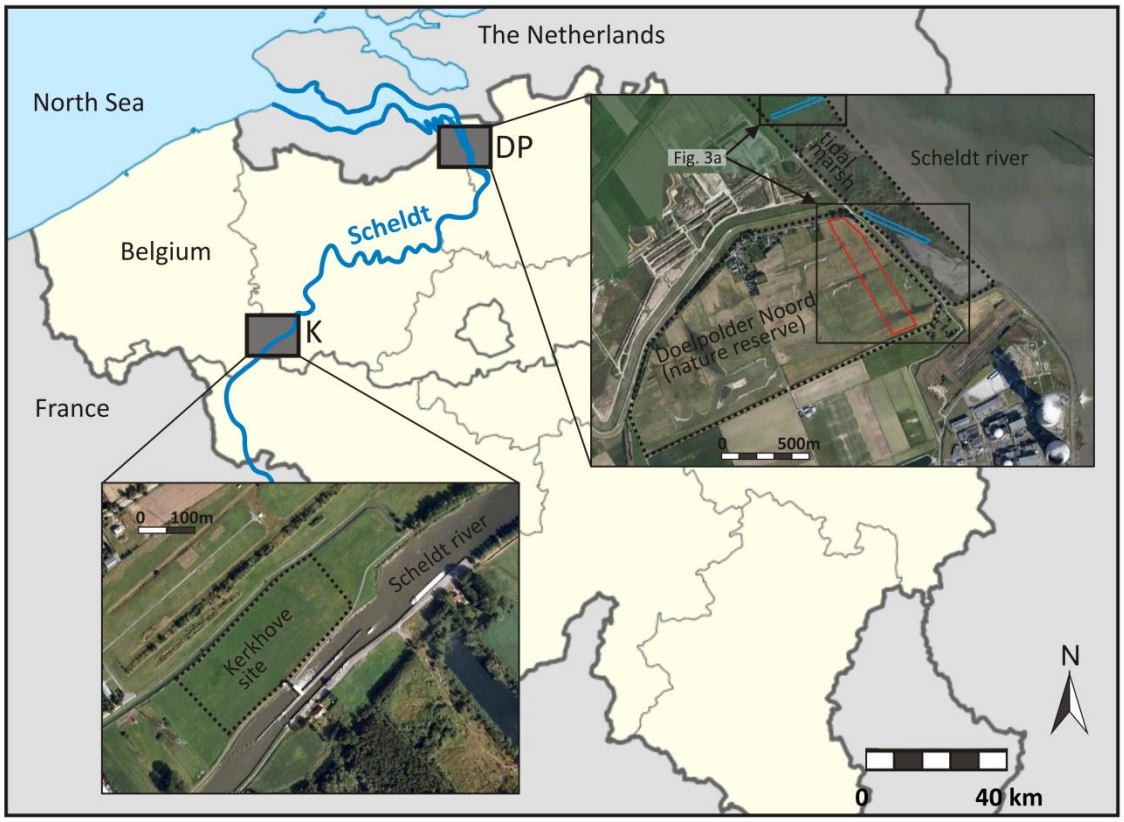

Figure 26: Overview map of the site locations of Doelpolder Noord (DP) and Kerkhove (K). The river Scheldt is marked in blue. Colour rectangles indicate the investigated areas in Doelpolder Noord (red: polder; blue: marsh). Aerial images © Agiv.

An important focus of this research is on the efficiency, applicability, reliability and repeatability of the applied CPT method. This is a.o. tested through the comparison with various ground-truth data (mainly shallow manual cores but also a few deeper mechanical cores) that were either available from previous (archaeological) investigations or newly obtained at the test site.

3.3 Shallow geology of the study area

The study area of Doelpolder Noord (Figure 26) is located in the Lower Scheldt polders in the NW of Belgium, near the Dutch border. The Tertiary geology here consists of a shelly sand (Formation of Lillo) and is covered by Late Pleistocene fluviatile sand (Bogemans, 1997; Jacobs et al., 2010a, b). These sandy deposits were reworked by wind activity in the Late Pleniglacial and Late Glacial, locally resulting in thick coversand ridges (Bogemans, 1997). In the lower depressions the sand is locally overlain by early Holocene deposits consisting of fluviatile fine sand or sandy clay deposits (Bogemans, 1997). During the Middle Holocene increased marine influence and rising ground water level changed the area into a large swamp, with the earliest basal peat growing from between 8345 and 7785 cal BP (Gilot, 1997). The lower regions were flooded by a peri-marine incursion starting between 6530 and 6410 cal BP (Verhegge et al., 2014) leading to the interfingering of (OM rich) clay into the peat deposits (Kiden, 2006; Kiden and Verbruggen, 2001). Recent Bayesian chronological modelling of this (OM rich) clay facies situates the restart of the peat growth between 6090 and 5770 cal BP (Verhegge et al., 2014). Late Holocene flooding turned the area into a tidal mudflat environment resulting in a thick layer of estuarine deposits consisting of an alternation of sandy and clayey sediments (Kiden, 2006; Kiden and Verbruggen, 2001).

Doelpolder Noord has been evaluated in recent years in the context of nature compensation works. According to an extensive handcoring campaign conducted in 2007 (Klinck et al., 2007), the buried coversand landscape in this area is well preserved. Our study focuses on a 100 m wide and 700 m long transect through the easternmost part, and the adjoining supratidal marsh (only flooded during spring tides) (Figure 26). The study area contains a micro sand-ridge buried about 2 m deep which is flanked by an 8–9 m deep depression in the Pleistocene sands, and surrounded by an undulating paleotopography of roughly 5–6 m deep.

The second test site is situated further upstream along the Middle Scheldt river near Kerkhove (see Figure 26). In the framework of planned construction works for a lock this site has recently been evaluated through a large number of shallow handcorings (Bats and Crombé, 2007). Similar as in Doelpolder Noord the site at Kerkhove contains a well preserved, paleotopography marked by an elongated ridge, the top of which is buried at least 3 m deep. This Late Pleistocene natural levee is made up of (locally OM rich) sandy clay deposits and flanked to the east by a depression 4–5 m deep, probably representing the onset of a paleochannel of the Scheldt. The natural levee and the flanking depression are covered by a locally thick (>3 m) peat layer (Bats and Crombé, 2007). The overlying deposits consist of alluvial, OM rich clay. Similar to Doelpolder Noord the peat layer is intercalated with peaty clay and/or OM rich clay deposits (Bats and Crombé, 2007).

3.4 Archaeological background

The sites of Doelpolder Noord and Kerkhove are known to be very rich in archaeology. At both sites the Late Pleistocene/Early Holocene paleolandscape is well preserved, and the local high topography make attractive locations for prehistoric occupation in the proximity of a river. Furthermore the relative deep burial depth of the paleolandscape and the wet conditions allow for good conservation of the archaeological remains.

During the last decade various excavations in the direct vicinity of Doelpolder Noord have revealed a number of well-preserved prehistoric settlements, all located on the tops and flanks of the Pleistocene sand ridges (Crombé, 2005). The oldest remains date back to the Final Paleolithic and Early Mesolithic (Crombé et al., 2013b; Crombé et al., 2011c), when the landscape was still a largely dry environment. A series of sites dating back to the Mesolithic–Neolithic transition (Crombé, 2005; Crombé et al., 2009a; Sergant et al., 2006b) and attributed to the Swifterbant culture (Crombé et al., 2011a), are contemporaneous with a period of increased tidal influence (Verhegge et al., 2014). So far no direct archaeological evidence of human activity has been found that dates from the Middle Neolithic to the Middle Ages, when the area was a large peat marsh, but archaeological records from nearby locations in the Netherlands suggest that occupation took place even in these wet environments (De Clercq, 2009; De Clercq and Van Dierendonck, 2008).

Archaeological appraisal of the Kerkhove site dates back to the early 20th century when several prehistoric discoveries were made in the area (Claerhout, 1921a, b). Research in the 80's and 90's mainly concentrated on the dry river bank, yielding remains from the Mesolithic to Early Medieval times (Crombé, 1986). Recent archaeological corings in 2007–2008 focused on the adjacent floodplain area and yielded numerous findings including lithic artefacts (burnt), animal bone remnants, hazelnut shells, and charcoal fragments (Bats and Crombé, 2007; Bats et al., 2008). The stratigraphic position of these finds suggests that the occupation of the site took place before the gradual inundation and formation of peat. Very little archaeological evidence was found in the overlying peat layer, although a nearby Roman and Merovingian site suggests a larger archaeological potential (Bats et al., 2008).

3.5 Materials and methods

3.5.1 General characteristics of CPT methodology

Cone penetration testing (CPT) is a geotechnical method to sound the composition of the subsurface. A cone on the end of a series of rods is pushed into the ground and (continuous or intermittent) measurements are made of the resistance of the cone tip (qc) and the friction on the trailing sleeve (fs) (Figure 27). The technique generally allows fast and continuous profiling for subsurface sediment characterization and stratigraphical analysis. It is primarily aimed at fine-grained, relatively soft soils, as penetration can be difficult or restricted in hard layers such as gravel or compact sand (Lunne et al., 1997; Robertson and Cabal, 2012).

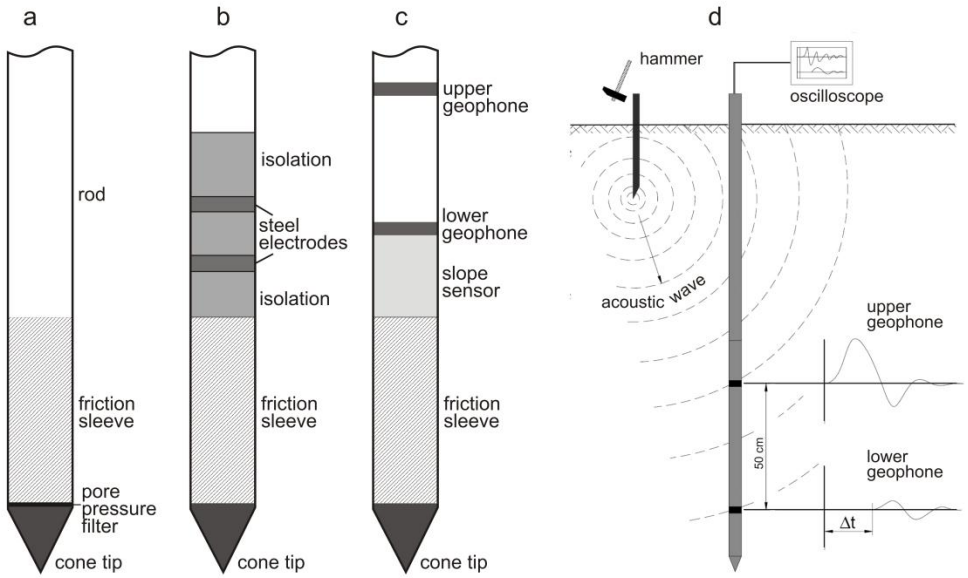

Figure 27: Schematic diagrams of different CPT cones (a: piezometric cone; b: resistivity cone; c: seismic cone) and principle of seismic CPT measurements (d) (adapted after Lech et al. 2008).

Additional sensors can be added to the cone. In piezocone penetrometer tests (CPT-U) also the in-situ pore pressure (u) is recorded, at the cone or just behind (Figure 27). Piezocone measurements are more time consuming than regular CPTs but the obtained pore pressure data may add valuable information on the presence of more, or less, permeable material within the soil matrix.

In conductivity (or resistivity) penetrometer tests (CPT-C) the electrical conductivity is also recorded, derived from the impedance between one or more pair(s) of electrodes attached to the sleeve section (Lunne et al., 1997) (Figure 27b). Since the conductivity is

related to various soil properties (e.g. water content, porosity, electrolyte content) this may give valuable information regarding the lithology (e.g. clay and organic matter will increase the conductivity). When working in estuarine environments one must keep into account that changes in salinity will have significant effects on the electrical conductivity. Since resistivity values are often comprised in overlapping ranges, interpretation is not straightforward and additional information will always be needed (Montafia, 2013). In dielectric cones also the electrical permittivity (dielectric constant) is obtained (Hilhorst, 1998). The latter is mainly used for contamination studies.

In seismic cone penetration tests (CPT-S) the sounding is combined with downhole velocity measurements using geophones installed into the cone rod (Figure 27c–d). CPT-S measurements are often used to determine the soil deformation and bearing capacity (since these are related to the seismic velocities) but in our case we wanted to see if any valuable added information could be obtained regarding the presence of peat. According to Silva and Brandes (1998) peat will lower the acoustic velocity due to increased compressibility (organic matter absorbs water and causes clay particles to aggregate, creating an open structure that is weak and relatively easy to deform).

3.5.2 Soil classification and the identification of peat

Both tip resistance and sleeve friction are related to soil type and moisture content, and the ratio of sleeve friction and cone resistance (friction ratio Rf) can be used to classify the soil. The most widely used CPT soil behaviour type classification (SBT) chart was suggested by Robertson et al. (1986) and an updated, dimensionless (normalized) version (Robertson, 2010). The normalization allows to compensate for the cone resistance dependency on the overburden stress, although for shallow depths (<30 m) this does not prove to be more advantageous (Fellenius and Eslami, 2000).

In the case of a uniform and well understood geology the predictions based on CPT results may be used singly for soil type identification. However this is rarely the case, and in practice CPT data must always be accompanied by data from boreholes, sampling and/or laboratory testing. This is especially the case for areas with variable and heterogenic geology (such as the present study sites) where interpretation of CPT data is not straightforward and ground-truth data are needed in order to verify local correlations (Lunne et al., 1997).

Automatic soil classification of peat for stratigraphic reconnaissance of polder areas is problematic, since most soil charts have difficulty in identifying peat and (OM rich) clay soils (Long and Boylan, 2012). Indeed how these are classified often depends on how fibrous or how amorphous the peat is (Landva et al., 1983; Long and Boylan, 2012). For instance fibrous peat, which has a higher net cone resistance than amorphous peat, may be classified as mixed silt and clay soil. Therefore, Vos (1982) suggest identifying peat

for Dutch (polder) soils merely from the friction ratio (Rf > 5%). Results from comparable areas along the German coast (Lunne et al., 1997) and at Saeftinge, a vast tidal flat north of Doelpolder (Missiaen et al., 2008) largely seem to confirm this approach.

3.5.3 CPT data acquisition

CPT soundings were carried out in Doelpolder Noord and Kerkhove between 2011 and 2014. In Doelpolder Noord a staggered grid of 41 CPT-E as well as 5 CPT-U, 10 PT-C and 3 CPT-S were obtained in a 90 m wide transect; in addition 12 CPT-E were carried out in the adjoining tidal marsh on the outside of the dyke (Figure 28a). In Kerkhove in total 12 CPT-E, 13 CPT-C and 5 CPT-U were performed in the same staggered grid as part of the existing handcorings (Figure 28b). The location of the non-gridded CPTs was determined by the paleotopography, the subsurface layering (heterogeneity), available geophysical and ground-truth data, and the accessibility of the terrain.

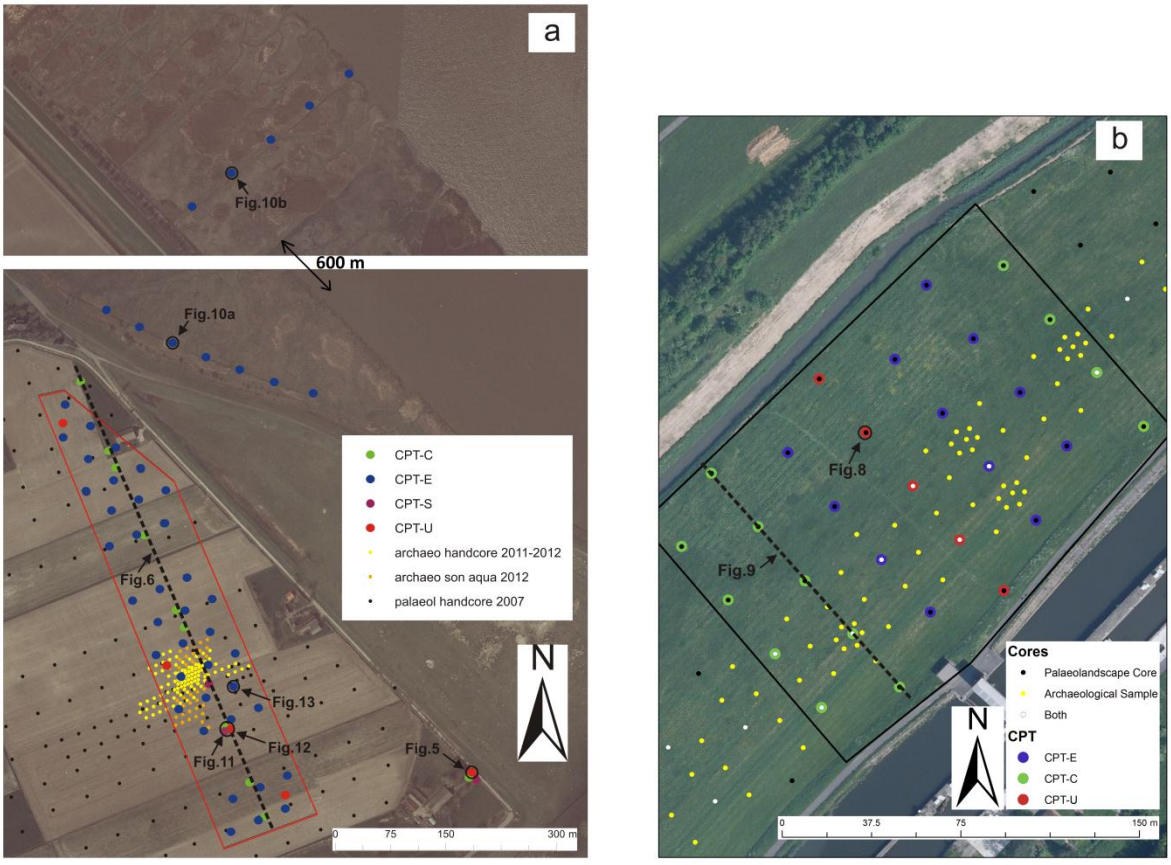

Figure 28: Overview maps showing CPT and core locations at (a) Doelpolder Noord (bottom) and Paardenschor 600 m to the NW (top); (b) Kerkhove. CPTs and cores discussed in the paper are marked. The red line marks the study transect in Doelpolder Noord. Aerial images © Agiv.

For the CPTs in Doelpolder Noord (inside the dyke) and Kerkhove a conventional CPT truck was used, in the saltmarsh at Doelpolder Noord, a mobile CPT rig was used that was installed on a small tracked vehicle (Figure 29a). Working on the marsh proved very risky due to hidden gullies and therefore only a limited number of soundings could be obtained here.

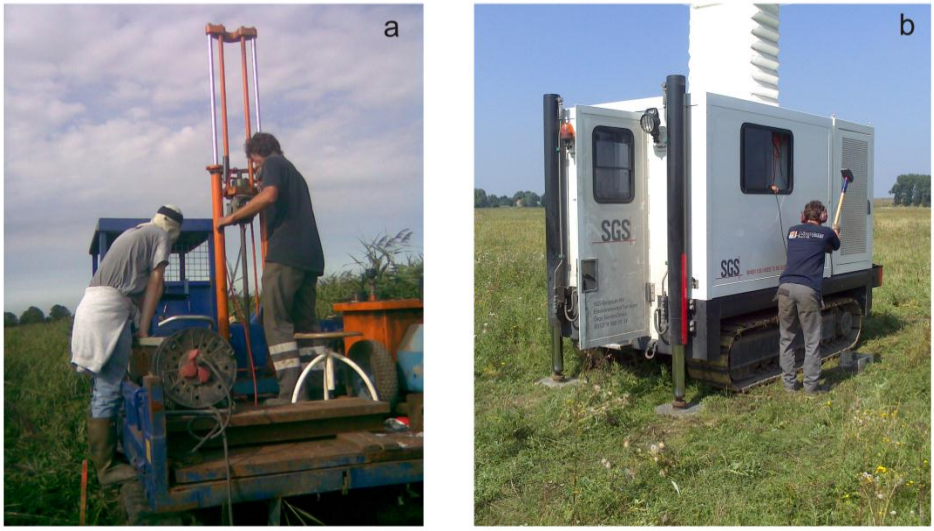

Figure 29: a: CPT measurements with a mobile rig on the marsh adjacent to Doelpolder Noord. B: Seismic CPT measurements at Doelpolder Noord.

Measurement intervals for all CPTs were 2 cm, allowing a good vertical resolution. Piezocone measurements (CPT-U) involved a pore pressure sensor located just behind the cone. CPT-C measurements were performed with a dielectric cone (Frequency Domain method, 20 MHz) using 2 insulated electrodes (spaced 4 cm apart) located roughly 40 cm behind the cone. The seismic cone was equipped with two geophones (50 cm spacing). A heavy plate and sledge hammer were used to generate the seismic waves. Lateral offset between source (plate) and sensor (cone rod) was 120 cm. Both P (primary) and S (secondary or shear) waves were generated by hitting the beam in different directions (Figure 29b). Measurements were carried out at depth intervals of 0.5 m. At each depth and for each direction between 4 and 8 hammer blows were recorded and stacked. Sampling frequency was set high enough to allow accurate velocity calculation in view of the small travel path.

3.5.4 Groundtruth data

In Doelpolder Noord three different ground truth datasets were available (for location see Figure 28a): (1) shallow hand cores (over 500 cores) obtained in the framework of previous archaeological mapping with concise field descriptions (Klinck et al., 2007). These cores reached up to the basis of the peat; (2) 40 Sonic Aqualock drill cores ob-

tained for archaeological sampling of the top of the coversands with rudimentary field descriptions and photographs; (3) 5 deep mechanical cores with detailed core descriptions and photographs available and reaching well into the Pleistocene sands (max. depth 14 m).

Due to compression of the peat the depth information obtained from the mechanical (Aqualock) cores at Doelpolder Noord was not always fully accurate. In a few cases contamination of samples from overlying layers was also observed. Since mechanical drilling was not possible on the tidal marsh (due to the difficult accessibility of the terrain) instead manual augering was tried out. However this proved to be extremely time consuming (one augering could take multiple hours) and largely unsuccessful since it allowed only to penetrate the upper few metres, well above the depth of the peat sequence.

In Kerkhove a large number of shallow manual augerings, drilled for paleolandscape mapping (95) and archaeological sampling (141) were available with concise field descriptions as well as a limited number of mechanical corings described and analysed in laboratory conditions (for location see Figure 28b) (Bats and Crombé, 2007; Bats et al., 2008; MOW, 2010). The cores reached the base of the peat.

3.6 Results and interpretation

3.6.1 Doelpolder Noord

Peat layers stood out markedly on all CPT profiles at Doelpolder Noord, with friction ratio values ranging between 4 and 12%. Locally two distinct peat layers (generally the lower peat layer being much thinner) were observed, separated by OM rich or peaty clay deposits (Figure 30 and Figure 31). In some cases extremely thin intercalating clay layers (about 20 cm thick) could still be identified. The clay intercalations are generally related to a thick peat sequence and often coincide with the lower parts in the paleotopography. On one occasion intercalating sand was observed within the peat (S13), indicating possible erosion of the ridge. Here the peat sequence was much thinner, and coincided with a higher paleotopography. In general there was a tendency towards lower cone resistance values for the lower peat layer, which could point towards a less fibrous (more amorphous) peat (Long, 2005).

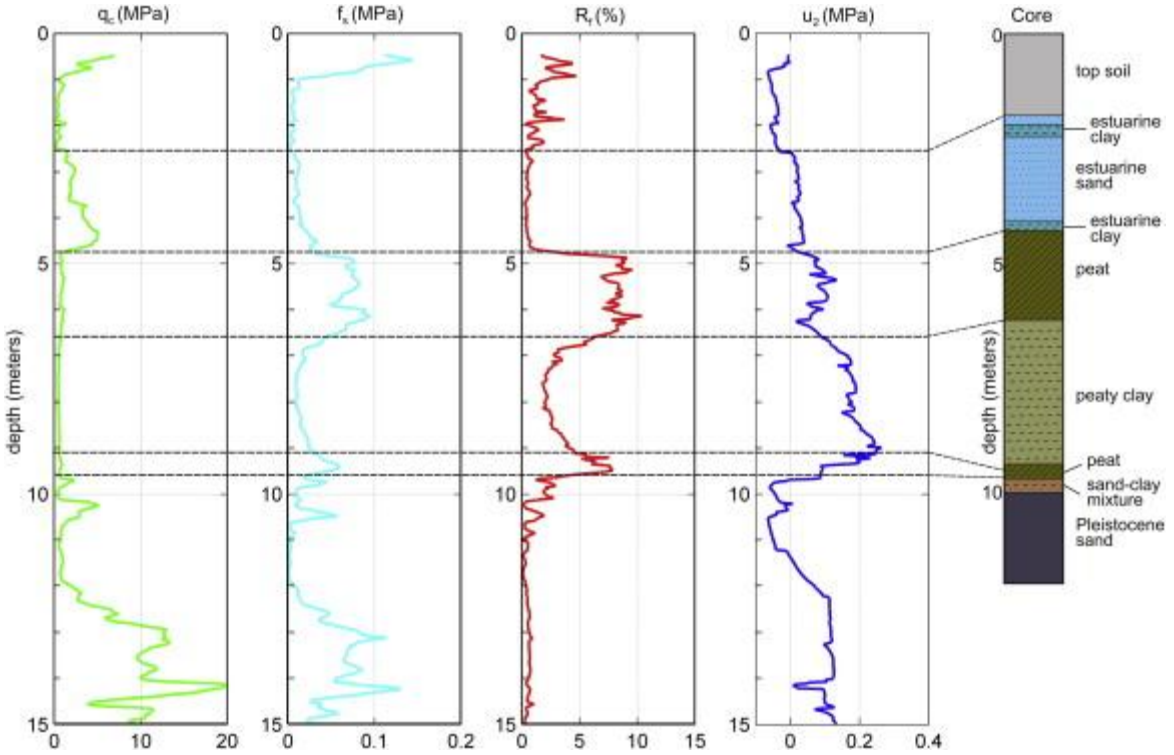

Figure 30: CPT-U log (piezocone) from Doelpolder Noord and the lithostratigraphic interpretation of a nearby core (U1, core P1). For location see Figure 28.

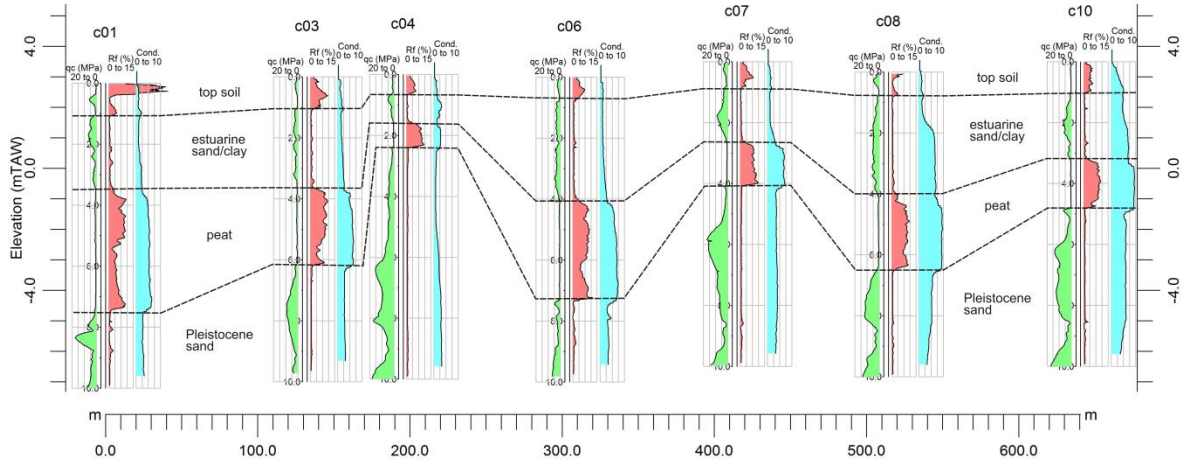

Figure 31: Transect of CPT-C logs (conductivity CPT, mS/cm) across Doelpolder Noord with lithostratigraphic interpretation. For location see Figure 28a.

The transition between peat and the overlying estuarine deposits, and also the underlying Pleistocene sand deposits, was generally very sharp and clear. In the lower parts of the paleotopography occasionally a thin transition-like layer between the peat and the Pleistocene sand seems to be present on the CPT logs. Neighbouring cores seem to point towards interfingering clay-rich and sand-rich deposits (Figure 30). Similar features were also observed in the surrounding Waasland polder area (K. Heirman, pers. comm.). The location (close to the Scheldt river) and paleotopography (lower than –2 m

TAW) suggest we could be dealing with Early Holocene fluviatile deposits from the meandering Scheldt river.

The estuarine sequence overlying the top of the peat is marked by a high vertical and horizontal variability (Kiden, 2006; Kiden and Verbruggen, 2001). Accurate mapping of this variability is an important challenge. However it turned out that the internal stratification of the estuarine sequence, largely made up of sandy deposits but locally also (intercalated with) clay layers, was not always easily resolved on the CPT logs. In some cases the sand and clay layers could be distinguished unambiguously, even for relatively thin intercalations (confirmed by cores), while in other places this was not the case (e.g. Figure 30). Most likely this was due to the fact that it concerns only minor changes in sand and clay content, but the thickness of the layers (too low to be resolved) may have also played a role.

Figure 31 shows a transect of CPT profiles across Doelpolder Noord (for location see Figure 28). On this transect we can clearly distinguish the Late Pleistocene cover-sand-ridge and the different strati-graphical layers (peat, clay, sand) above the cover-sand.

Figure 32 shows a map with the interpolated elevations of respectively the top and base of the peat sequence at Doelpolder Noord, based on the individually interpreted CPTs. Despite the differing locations of the datapoints, this model fits within the available coring model and even fills important gaps.

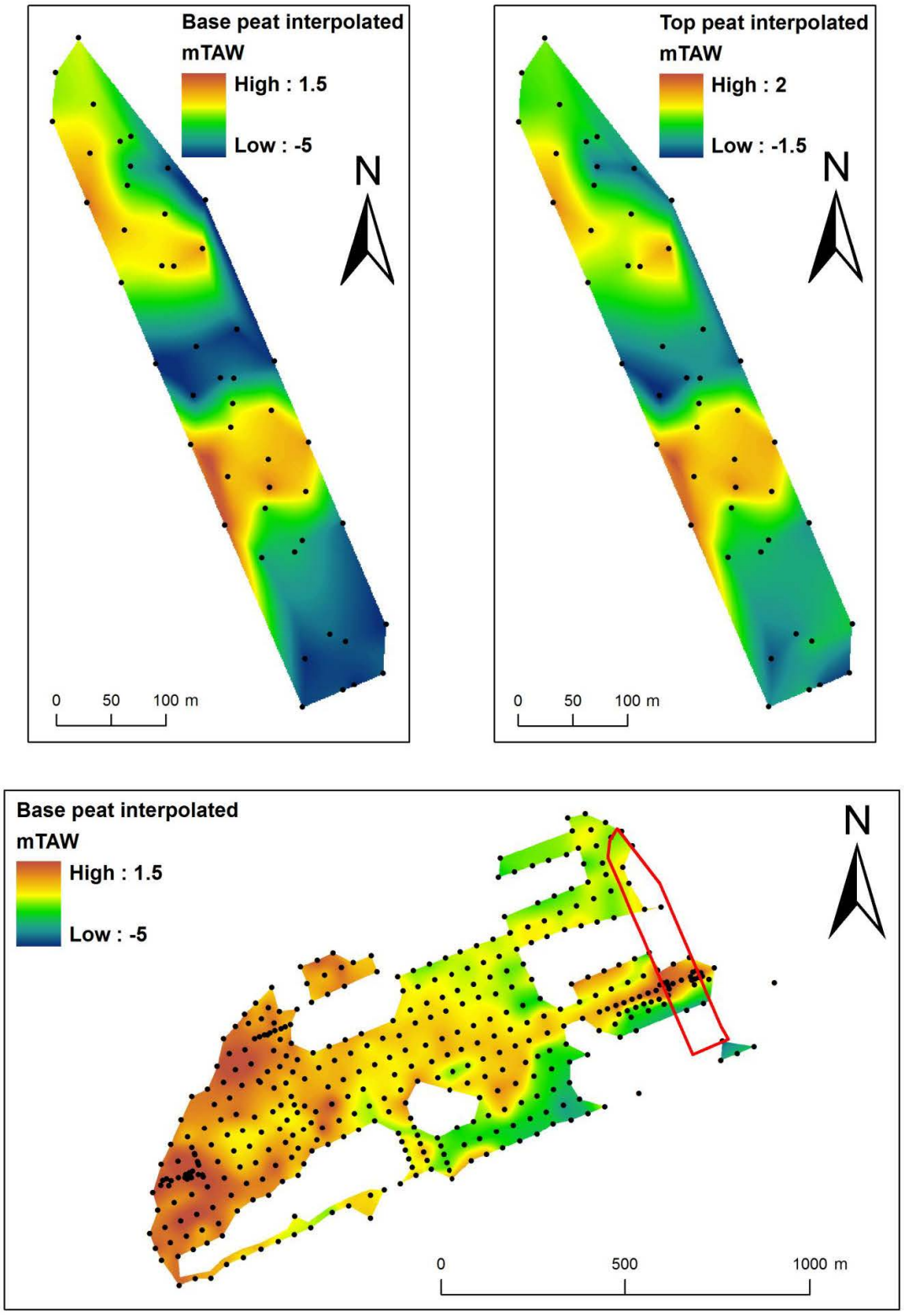

Figure 32: Top: Elevation maps of the top and base of the peat in the study transect at Doelpolder Noord (for location see Figure 26), as derived from the CPT data (in m TAW). Black dots indicate the CPT locations. Bottom: Base peat map at Doelpolder Noord derived from archaeological cores for comparison (in m TAW). Black dots indicate the locations of the archaeological cores. The red area marks the study transect.

3.6.2 Kerkhove

The identification of CPT data at Kerkhove was slightly more complicated. In a number of cases the peat stood out relatively well, with friction ratio values ranging here between 6 and 11%. In general the distinction between the peat layer and underlying sandy clay deposits was quite clear, whereas the transition from peat to the overlying organic clay deposits seemed to be more gradual and was not always clearly distinguishable on the CPT logs (Figure 33). Unlike Doelpolder Noord, the organic clay intercalations within the peat sequence were less apparent on the CPT logs (Figure 33). This could be due to their thickness (sometimes less than 20 cm) and/or a reduced difference in lithology (i.e. a more 'uniform' organic sequence of peat and clay deposits). It is not unlikely that the different environment at Kerkhove (fluviatile, freshwater) compared to Doelpolder Noord (estuarine, mainly brackish) and the hydrogenesis (e.g. 'Water rise mire/spring mire' vs. 'Fluvial flood mire', cfr. Meier-Uhlherr et al., 2011) may have played a role here.

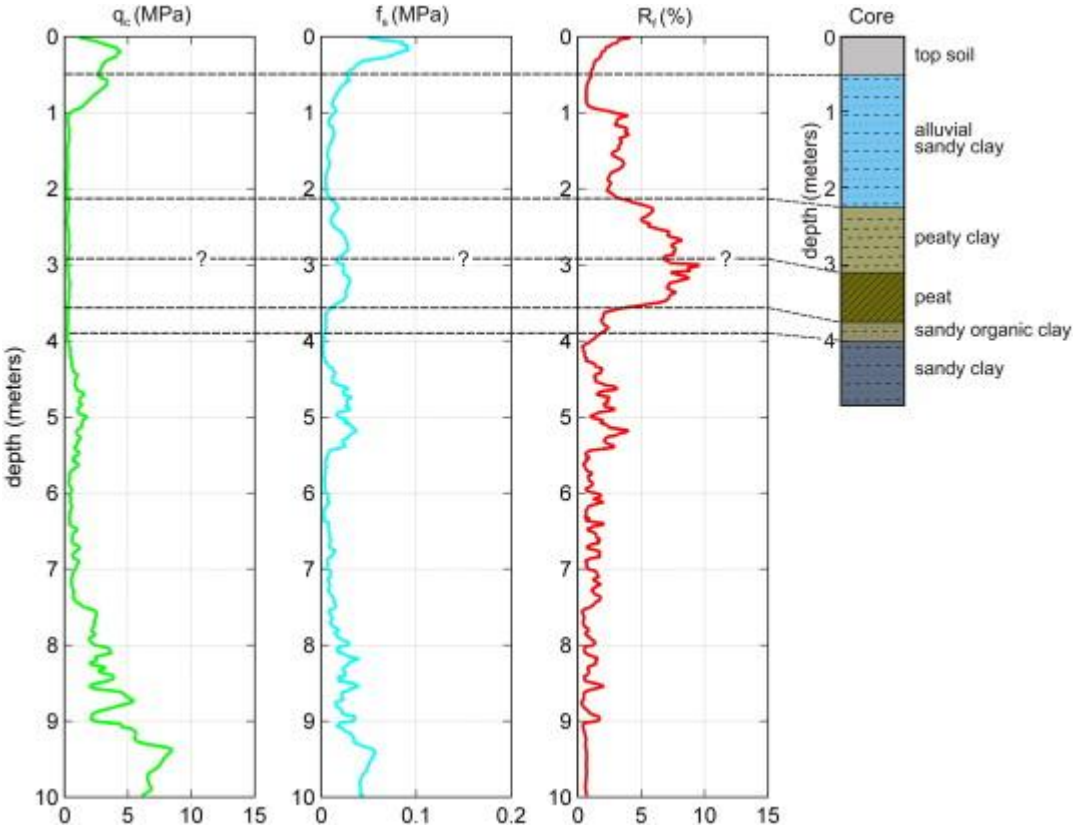

Figure 33: CPT-U (piezocone) log from Kerkhove and lithological interpretation of a nearby core (B52, core52+B4). For location see Figure 28b.

The transition between the top layer and the alluvial clay deposits at Kerkhove below stood out well on most data. Variations within the sandy clay river levee sequence could not always be clearly linked to lithological changes (as indicated by the cores), although in some cases a correlation with changing sand or clay content is suggested.

Figure 34 shows a transect of CPT profiles across Kerkhove (for location see Figure 28b). The sandy levee and peat sequence stand out relatively well on most logs. Stratification within the peat and the overlying sequence however is not clearly visible.

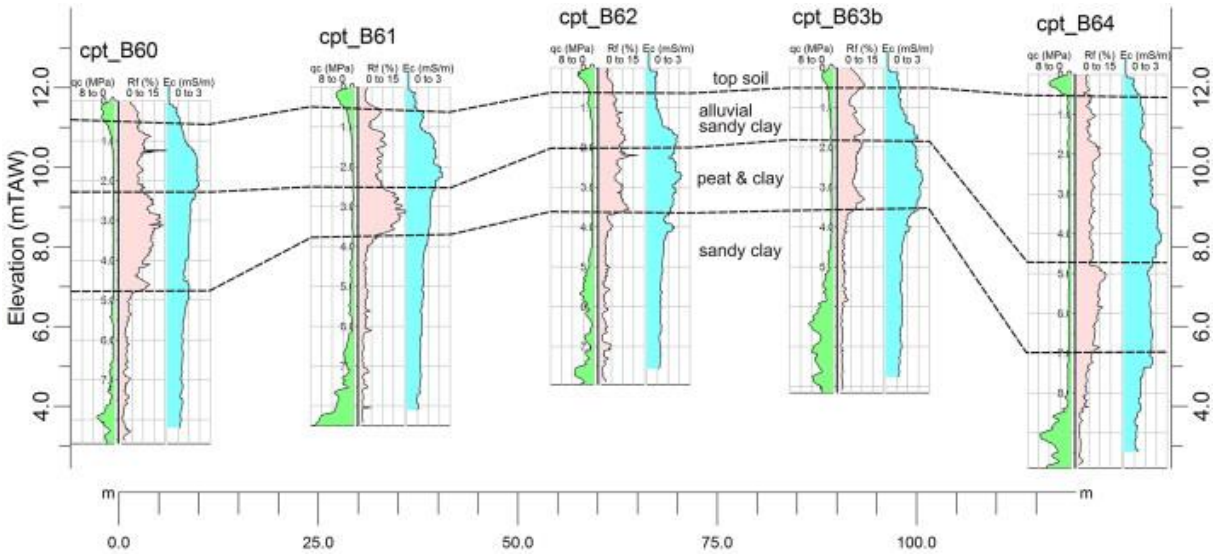

Figure 34: Transect of CPT-C logs (conductivity CPT, mS/cm) and lithological interpretation across the buried levee in Kerkhove. For location see Figure 28b.

3.6.3 CPT data on the tidal marsh

The CPT data on the marsh directly adjacent to Doelpolder Noord show largely similar results (Figure 35a). Again we can clearly observe two peat layers, separated by (supposedly) OM rich clay deposits (although (deep) core data are lacking on the marsh, the resemblance with the nearby polder data seems to justify this interpretation). The base of the peat is marked by a sharp increase in qc indicating a transition to sandy deposits. The uppermost metres of the marsh are marked by extremely low tip resistance (between 0 and 0.3 MPa) and sleeve friction (between 0 and 0.02 MPa), suggesting very soft muddy sediments. It is most likely that we are dealing with very recent tidal mudflat deposits. Unfortunately no cores were obtained here that were deep enough to reach the peat layer.

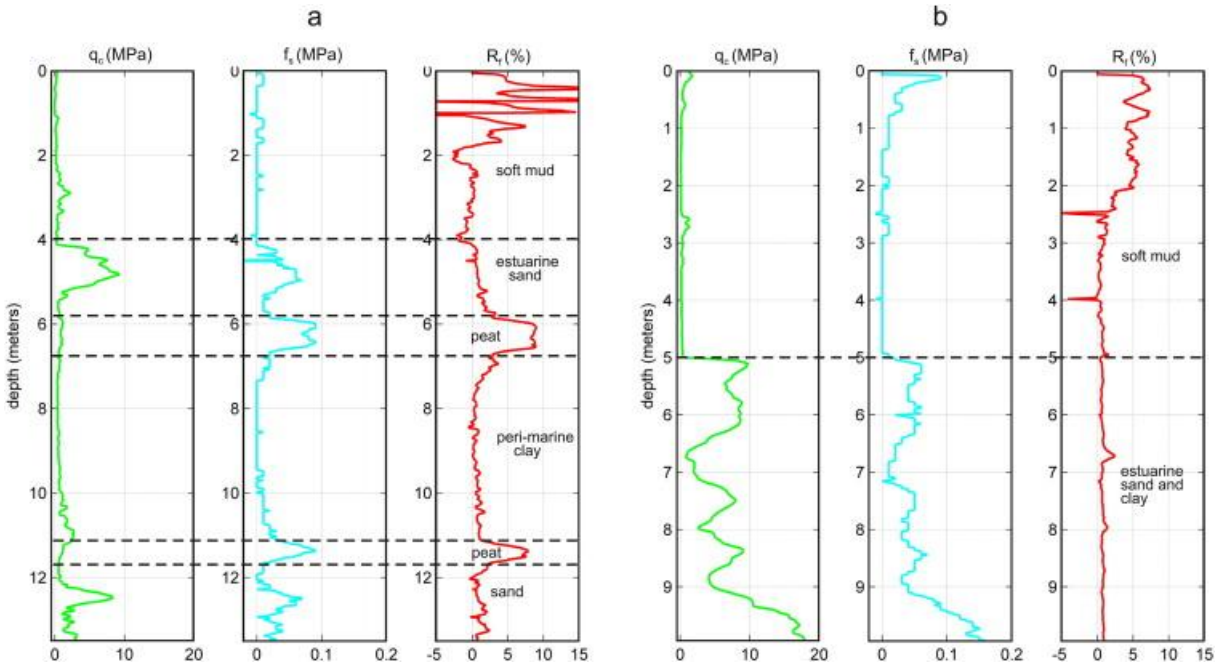

Figure 35: CPT logs and lithological interpretation from the tidal marsh adjacent to Doelpolder Noord. For location see Figure 28a.

The CPTs on the marsh further north, close to the Dutch border, show different results (Figure 35b). Here no peat seems to be present. It is not unlikely that peat deposits were once present here but that they were later eroded by (Post) Medieval tidal inlets. Again the upper 3–5 m is marked by extreme low resistance and sleeve friction values indicating very soft mud. Below the soft muddy layer the CPT data suggest the presence of sandy estuarine deposits with some possible clay intercalations. Nearby marine seismic data (unpublished) suggest we may be dealing with (Post) Medieval tidal channels. This is also confirmed by corings without peat from a transect in Prosperpolder perpendicular to and in the extension of this CPT transect (ADW, 2010).

3.6.4 CPT-U

Clay is known to exhibit a higher pore pressure compared to sandy sediments which show a pore pressure close to the hydrostatic pressure (a.o. Eslami and Fellenius, 2004). It was therefore interesting to see whether the pore pressure curves would allow a better definition of the estuarine deposits (i.e. distinction between sand and clay intercalations) overlying the peat at Doelpolder Noord. Unfortunately this proved not to be the case (Figure 30). This could be due to the relatively subtle changes in lithology (sand/silt/clay content). However, also at Kerkhove local sandy intercalations within the alluvial clay, as witnessed by the shallow cores, could not be traced back on the pore pressure data.

Identification of peat on pore pressure data is not always straightforward, since the pore pressure will strongly depend on the presence of sand or clay in the peat (sand will

lower the pore pressure whereas clay will increase it) and the decompositional state of the peat (very fibrous vs. amorphous) (Long and Boylan, 2012; Lunne et al., 1997). The latter suggested that fibrous peat will exhibit lower pore pressures (sometimes negative) compared to an amorphous peat. This pore pressure variability is clear in Figure 30, where the peat sequence is intercalated by a thick peaty clay/clayey peat layer. The latter is marked by an increased higher pore pressure indicating a more amorphous composition, whereas the actual peat layers show much lower values. The pore pressure data also confirm the more amorphous peat composition of the lower peat layer.

In Kerkhove the pore pressure data sometimes allowed a better distinction between the peat and OM rich clay deposits than the conventional data (qc/fs/Rf) (Figure 33). In general here the pore pressure data also indicates a tendency towards an increased decomposed state of the peat towards the bottom.

3.6.5 CPT-S

Both S-waves and P-waves were clearly observed on the recorded seismograms. Due to their lower velocity the S-waves showed a larger variation (with marked changes in the gradient) than the P-waves (Figure 36a). Identification of the arrival times was carried out with the direct time method, based on visual interpretation. In some cases unambiguous identification of S-waves was not easy. This could in principle be solved easily by comparing two signals from opposite sides of the beam (which will show opposite polarization) but unfortunately such ‘opposite signals’ were not recorded at Doelpolder. It is highly recommended or future measurements to record ‘opposite signals’ for identification of S-wave signals in seismic CPTs.

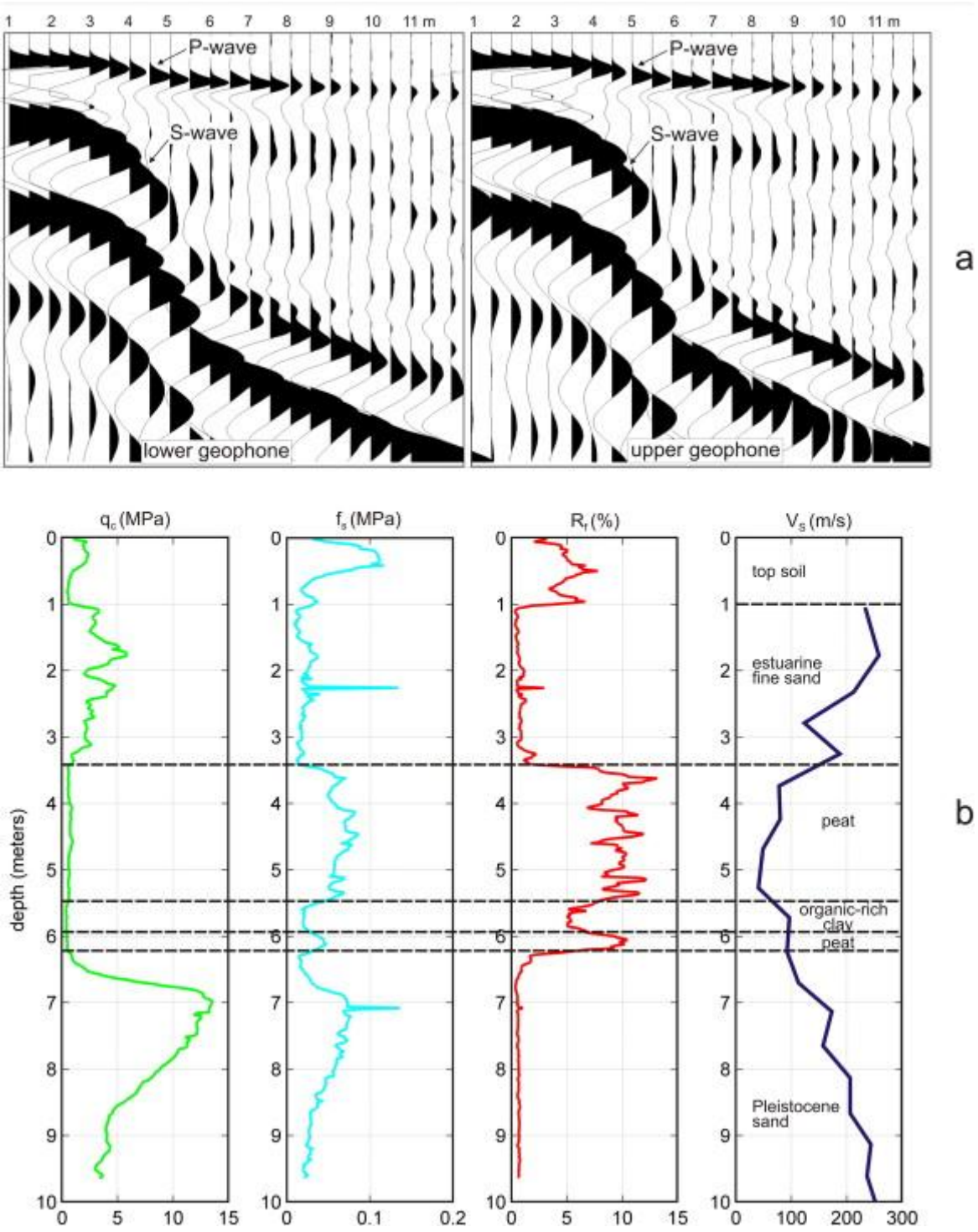

Figure 36: Results of seismic CPT tests at Doelpolder Noord; (a) Seismograms showing arrivals of P- and S-waves recorded on the upper and lower geophone in the cone rod (source z, receiver x); (b) CPT logs and calculated S-wave velocities. For location see Figure 28a.

The difference in arrival times between the two geophones allowed to calculate the interval velocity, taking into account the source-sensor offset and assuming that the origin of the source wave is in the middle of the beam. The high P-wave velocities did not allow accurate picking and therefore only S-waves were used. The results for CPT-S4

are shown in Figure 36b. The sharp drop in S wave seismic velocity (Vs), with velocities ranging between 40 and 100 m/s, correlates exactly with the presence of a peat layer at that dept (due to noisy data a reliable velocity estimation for the clay layer just below the peat was not possible). The measurement interval (0.5 m) did not allow to identify thin peat layers (less than a few dm). This may be overcome by decreasing the interval but this would have seriously increased the time to complete the CPT.

3.6.6 CPT-C

The conductivity data at Doelpolder Noord clearly show an increase caused by the peat, correlating well with the highest Rf values (Figure 31). However there seems to be no clear differentiation between other stratigraphic units. Both the average conductivity values of the complete sounding and the peak values caused by the peat alone increase towards the northern edge of the study area, due to the brackish Scheldt water seepage.

In Kerkhove, the clayey textures and peats have a small mechanical/geotechnical contrast. This is also reflected in the conductivity data, which have lower average values per sounding than in Doelpolder Noord but show a more continuous variation (Figure 34). The top of the peat is not recognizable as a conductivity shift, but continuous increasing values with the depth do indicate a transition to a more conductive substrate.

3.7 Discussion

3.7.1 Automatic soil classification

Since both test areas at Doelpolder Noord and Kerkhove are marked by relatively thick peat and OM rich clay sequences, automatic soil classification was expected to be problematic. Indeed in most cases the peat and OM rich clay layers could not be distinguished on the charts (both showing up as clay) (Figure 37a). It was hoped that normalization and corrected data using pore pressure information would result in a better (i.e. more reliable) soil classification, especially since the correction is believed to be increasingly important with decreasing grain-size (Coutinho and Mayne, 2012; Fellenius and Eslami, 2000). However this was not the case. Due to the very low pore pressure values that were recorded the corrected tip resistance values (qt) did not differ substantially from the uncorrected data (qc) (Figure 37b). The use of soil classification charts was

therefore abandoned and interpretation of the CPT data was mainly carried out manually, using the different measured parameters and knowledge of the local geology.

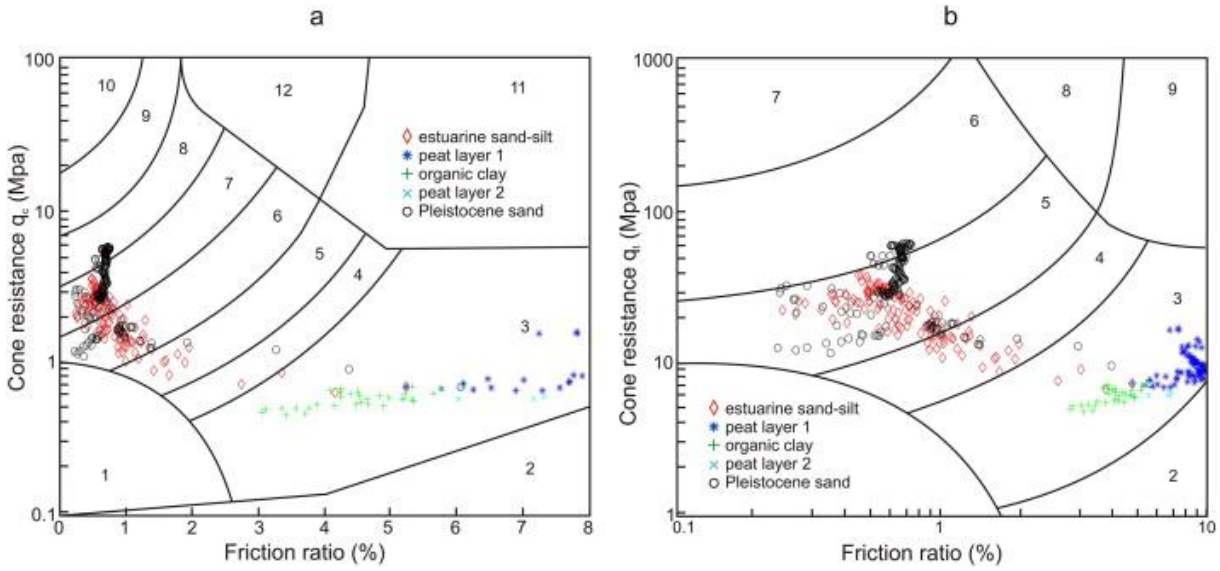

Figure 37: (a) Soil classification chart using uncorrected qc data (CPT-U3) (1: sensitive fine grained; 2: organic material; 3: clay; 4: silty clay to clay; 5: claeye silt to silty clay; 6: sandy silt to clayey silt; 7: silty sand to sandy silt; 8: sand to silty sand; 9: sand; 10: gravelly sand to sand; 11: very stiff fine grained*; 12: sand to clayey sand*. (b) Normalized soil classification chart using corrected qt data (CPT-U3) (1: sensitive fine grained; 2: clay - organic soil; 3: clays; 4: silt mixtures; 5: sand mixtures; 6: sands; 7: dense to gravelly sand; 8: stiff to clayey sand*; 9: stiff fine grained*. (*overcolsolidated or cemented) (after Robertson, 2010).

3.7.2 Layer thickness and resolution

One of the challenges in this study was the identification of thin layers, especially peat layers but also thin clay intercalations within the peat. Due to the nature of the CPT measurement this is not evident. Since the cone is influenced by the material ahead (and also behind) it will start to sense a change in soil material before it reaches it, and will continue to sense the soil even when it has entered a new material. This means that the tip resistance is actually an average value, taken over a certain zone around the cone tip. According to Lunne et al. (1997) the zone tends to be smaller for soft materials (possibly down to 2 times the cone diameter) but much larger for stiff materials (up to 10 or 20 times the cone diameter). This averaging effect is also the case for the sleeve friction which in fact measures an average value over the total sleeve (13 cm for a 10 cm² cone) and thus may smooth out the effects of very thin layers.

In Doelpolder Noord thin layers of intercalating peat and clay down to 20 cm in thickness could be identified correctly on the CPT logs. No noteworthy difference was observed in resolved layer thickness between 10 cm² and 15 cm² cones. Some software tries to take into account the averaging effect by using an average qc value, taken over

the length of the sleeve, for the calculation of the friction ratio. This did not seem to have any relevant effect on the results except for producing a faintly smoother Rf curve. Nevertheless it seems advisable to use the original data instead of an averaged value.

It was far more difficult to identify thin clay and sand intercalations in the overlying estuarine deposits. This could be due to the difference in stiffness between the two materials, as suggested by Lunne et al. (1997) which may lead to overestimation of strength in thin clay layers and vice-versa underestimation in thin sand layers. However, as stated before it could also be due to insufficient lithological difference between the sandy and clayey layers. The fact that relatively thick clay-rich intercalations within the sandy estuarine deposits could not always be detected also seems to support the latter.

3.7.3 Data repeatability and reliability

Overall the CPT data showed a good repeatability. Different CPT logs obtained at approximately the same location (maximum lateral deviation less than 2–3 m) were highly similar, and allowed an identical interpretation. However one remarkable feature stood out with regard to the data obtained at Doelpolder Noord in 2011 and 2013: in general the former showed lower friction ratio values for peat (on average 1.5 times lower). It is known that the CPT sleeve friction is generally less reliable than the cone tip resistance, and the main factors for this include a.o. (1) load cell design and calibration, (2) tolerance in dimensions between cone and sleeve, and (3) surface roughness of the sleeve (Lunne and Andersen, 2007). Since similar cones were used for the various CPT measurements in this study (carried out by the same company and involving the same calibration procedures), a worn sleeve in 2011 may have been the cause for the observed difference, as suggested by the lower sleeve friction values for peat (Figure 38). Yet the opposite trend observed in the sandy deposits above and below the peat seems to contradict this. Differences were also observed in the tip resistance data from 2011 to 2013. So far no clear explanation has been found for this. All in all, however, the problems in repeatability between the 2011 and 2013 measurements did not affect the interpretation of the data.

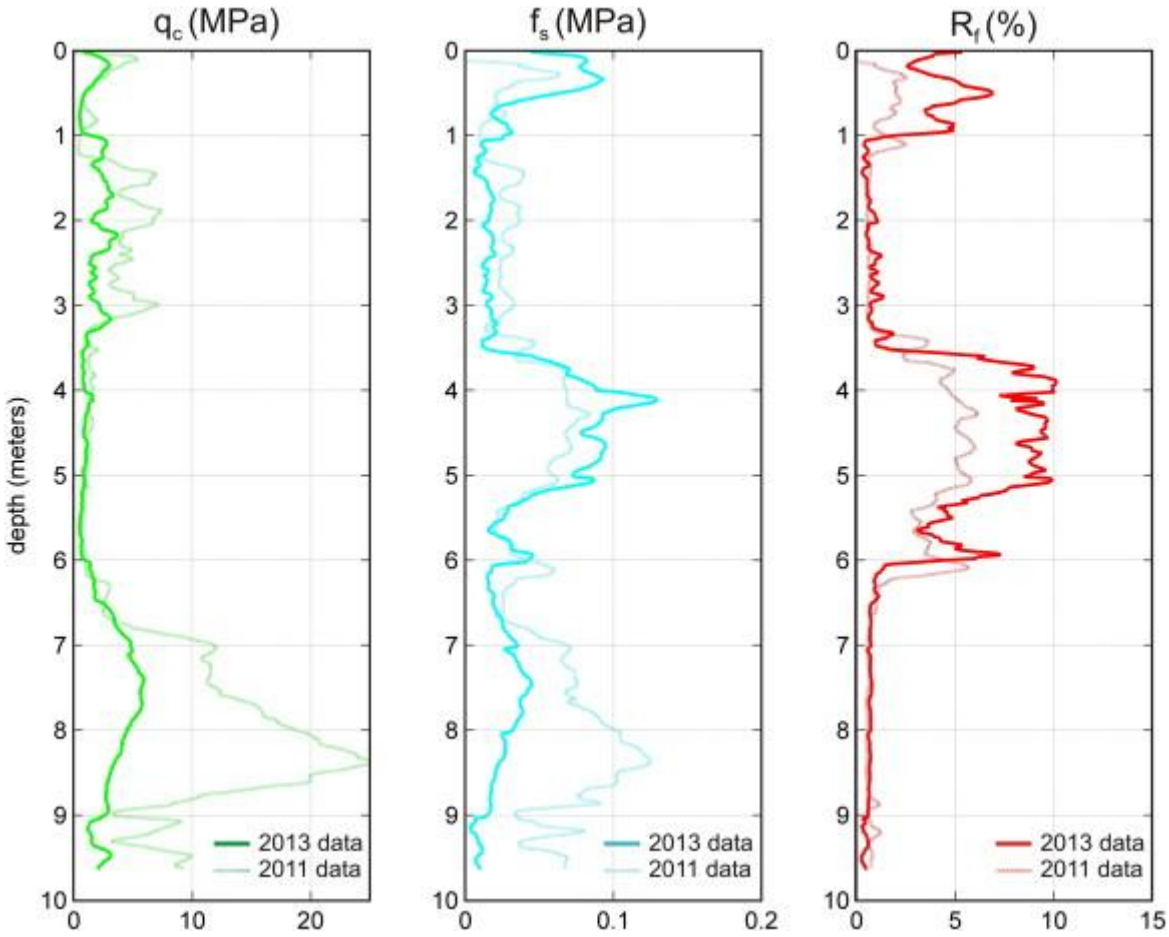

Figure 38: Comparison between CPT logs obtained in 2011 and 2013 at the same location in Doelpolder Noord (S8-CPT-C3). For location see Figure 28a.

The high friction ratio values observed in the upper metres on the tidal marsh (see Figure 35a and b) could at first sight suggest the presence of peat. However, they are the result of extremely low tip resistance and sleeve friction values (which on the contrary suggesting soft muddy sediments), and it seems therefore likely that the friction ratio values are erroneous since we are operating here at the limit of accuracy. Indeed most standard cones will have difficulty resolving extremely low resistance values (such as measured here) since these are close to the accuracy of the equipment.

3.8 Conclusions and recommendations

The results of this study show that CPT measurements are a reliable and accurate tool in determining the soil stratigraphy and paleotopography of covered prehistoric landscapes. Especially in wetlands marked by a deep paleosurface and thick peat (and clay) sequence the CPT method may well be more efficient than coring and may provide a

cost-efficient calibration tool for surface geophysical data or even a replacement when circumstances impede reliable results. As CPTs are frequently used within other disciplines (e.g. geology, construction, etc.) applying it for geoarchaeological purposes does not demand further technical refinement, except for the interpretation of CPT logs. This is ideally carried out manually, as our case-studies have shown that automated calculation of soil stratigraphy is often incorrect, especially when distinguishing peat and clay layers, and should be used with caution, if at all. Therefore we do not recommend relying on this software in polder areas. However, manual interpretation of CPT logs demands a good knowledge of the local geology and geotechnical background, which can be obtained by means of a limited number of sampling cores from nearby locations.

In this paper both estuarine (Doelpolder Noord) and alluvial (Kerkhove) polder environments were investigated. Overall the CPT data allowed highly accurate mapping of the paleotopography of the prehistoric surface (a Late Pleistocene sandy ridge/levee) and the thickness of the overlying peat sequence. Comparison with available coring or geophysical models at both sites showed a good correlation. At the estuarine site of Doelpolder Noord thin intercalating (OM rich) clay layers within, or just below, the peat sequence could still be identified. This was much less the case for the alluvial site of Kerkhove, possibly due to a lack of lithological difference. The latter was most likely also the case for the recent estuarine sand and clay deposits at Doelpolder Noord which were seldom distinguished.

The use of a lightweight, mobile rig allowed to obtain CPT data on the tidal marsh. Also here the buried paleosurface and peat sequence were clearly identified. However some caution must be taken with the identification of the (often very thick) soft muddy top layer, typical for marsh environments. The extremely low tip resistance of these soft sediments may result in high friction ratio values which could wrongly suggest the presence of peat.

Piezometric CPT data did not add significant information compared to conventional CPTs. At most the pore pressure data seemed to suggest a less or more fibrous state of the peat, although this needs to be taken with caution. Given the extra effort required to perform piezometric CPT measurements, their use is not recommended for archaeological paleolandscape studies. Also additional conductivity data generally did not add much crucial information regarding the peat layer(s) or buried paleosurface, although in some cases subtle changes in lithology (e.g. increase in sand or clay content) may be detected. The main use of conductivity CPTs seems to lie in their added value for surface geophysical measurements (calibration and interpretation of EMI and/or ERI data) (Verhegge et al., submitted-a).

The velocity information obtained from simple seismic CPT measurements showed a remarkably good correlation with the CPT logs and nearby cores regarding the presence of peat. The resolution (i.e. minimum thickness of the identified peat layer) and reliability of the seismic CPT method will however largely depend on the acquisition parame-

ters (seismic wave generation, beam hit direction, measurement and geophone interval, etc.). In general a higher accuracy will require more effort and more time, and therefore seriously affect the cost-efficiency.

The collection of (conventional) electric CPTs is generally quicker than the collection of sediment cores (on average 15 soundings of 10 m deep were obtained in 8 h time). Overall the time benefit will be greater for increasing depth (it is estimated that for depths >3 m CPTs are likely to be more advantageous than coring). CPTs also only involve a limited technical staff in the field, whereas drillings are labour intensive (especially hand augering) and demand an additional specialist to interpret the stratigraphy of the cores in the field. If cores are transported to the laboratory, e.g. in plastic tubes, there are additional costs of transport and opening of the tubes. Finally the depth accuracy of CPTs is often greater than for corings, especially in wetlands since peat has the tendency to expand after coring, resulting in erroneous depth measurements of the subsurface layers.

A major disadvantage of CPTs (and geophysical survey methods) however is that they do not provide data about the preservation of the different lithostratigraphical levels, which is important for assessing the quality of the prehistoric sites potentially present within these sediments. Information about possible erosion, truncation and/or bioturbation of sediment levels can only be achieved through coring. Conventional coring will therefore still be needed, but the paleotopographical and lithostratigraphic information obtained from CPT data will allow a much more efficient (i.e. less) coring and sampling strategy.

3.9 Acknowledgements

The presented research was funded by Research Foundation Flanders (FWO). Co-funding was obtained from the EU Interreg 2 Seas programme (project “Arch-Manche”). CPTs, Sonic Aqualock drill cores and mechanical corings were carried out by SGS. We thank Jan Lippens from SGS for his constructive support. Stanislas Delivet, Oscar Zurita Hurtado, Jonas Vandenberghe, Brecht Imbo, Mike Creutz, Kris Van Quaethem and Daphné Veraart are kindly acknowledged for their assistance with field work.

Chapter 4 Chronology of wetland hydrological dynamics and the Mesolithic-Neolithic transition along the Lower Scheldt: a Bayesian approach

This chapter is adapted after Verhegge et al. (2014)

The Mesolithic-Neolithic transition in the wetland margins of the southern North Sea basin occurred well over a millennium after the transition in neighboring loess regions. In this paper we investigate the possible role of hydrological dynamics in the occurrence of the last hunter-gatherer-fishermen in these wetland regions. A Bayesian modeling approach is used to integrate stratigraphic information and ^{14}C dates both from accurately datable archaeological remains and key horizons in peat sequences in the Scheldt floodplain of northwestern Belgium. We test whether the Swifterbant occupation of the study area was contemporaneous with hiatuses in peat growth caused by OM rich clastic sedimentation due to increased tidal influences and local groundwater rise. The results suggest that the appearance of this culture followed shortly after the emergence of a brackish tidal mudflat landscape replacing a freshwater marsh.

4.1 Introduction

During the last decade large-scale salvage excavations in the lower Scheldt river basin have revealed at least three well-preserved settlements dating (n° 4, 7 and 8 on Figure 39) back to the Mesolithic-Neolithic transition (Crombé, 2005; Crombé et al., 2009a; Sergant et al., 2006b). These sites have been attributed to the Swifterbant culture (Crombé et al., 2011a), which indicates a gradual adaptation from a hunter-fisher-gatherer economy to an extended broad spectrum economy that involved cattle-breeding and small-scale cereal cultivation (Louwe Kooijmans, 2010; Raemaekers, 1999). These wetland sites constitute key-sites in the study of the neolithization of the sandy lowlands along the southern North Sea basin. A series of radiocarbon dates obtained from carbonized plant remains (seeds and fruits) and charcoal from surface-hearths and hearth-dumps situate these transitional sites in the second half of the 7th millennium cal BP, specifically between ca. 6550 cal BP and ca. 5950 cal BP (Boudin et al., 2009; Crombé et al., 2011a). In order to reconstruct the environment in which this economic transition took place, intensive multi-proxy paleo-ecological investigations have been conducted on peat sequences from these sites and within their immediate vicinities. This paper presents the radiocarbon dates from these sequences in order to investigate the relationship between the archaeological occupation of the dated sites and the development of a peat marsh and occurrence of a tidal regime in the region.

4.2 Aims

This study will focus on:
1° Dating of the peat development using radiocarbon dates from the basis of the Basal peat at varying elevations and landscape positions in the floodplain surrounding two archaeological sites of the Swifterbant culture to derive a regional time-depth model.
2° Dating the beginning and ending of a first flooding period, using dates from *in situ* peat related to intercalating OM rich tidal clay deposits.
3° Relating 1° and 2° to radiocarbon dates directly attributable to the occupation of the Final Mesolithic (FM)/Early Neolithic (EN) Swifterbant sites of Doel Deurganckdok sector B and M (n° 8 and 4 on Figure 39).

4.3 Paleo-environmental situation

The two Swifterbant sites concerned are situated on the left bank of the lower Scheldt in northwestern Belgium. They were discovered at the municipality of Doel between 2000 and 2003, during the construction of the Deurganck dock in the Antwerp harbor (Crombé, 2005; Crombé et al., 2009a). Both sites are situated on top of relatively narrow (cover)sand ridges at a depth of 0.5-1.0 meter below national ordnance level (TAW = mean low water tide level in Oostende).

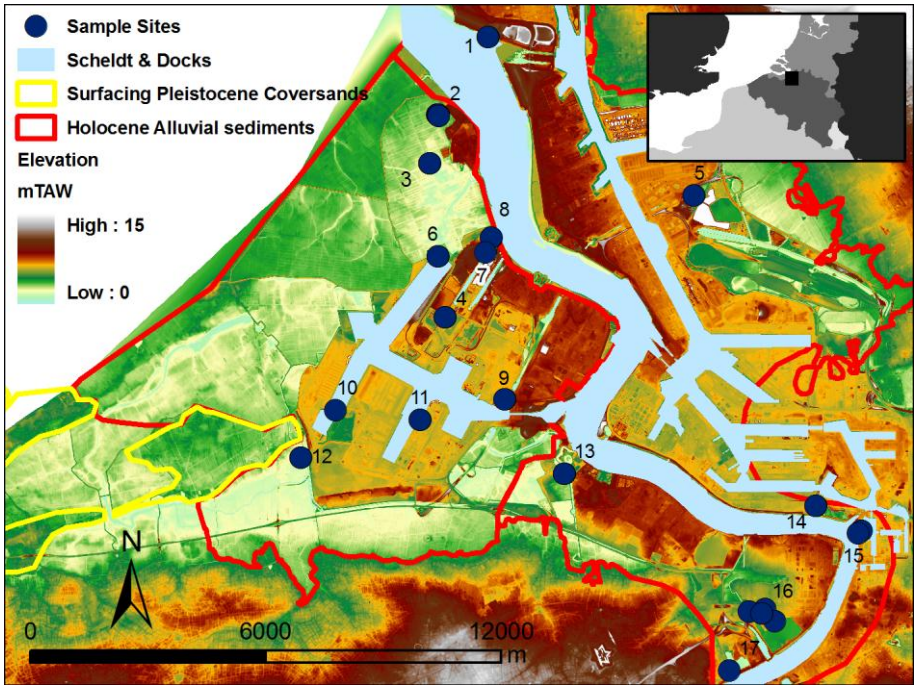

Figure 39: Site locations of dated samples (names and bibliographic references in appendix 1 & 2) in the study area (background Elevation data from AGIV).

Over the past few decades peats and OM rich clastic sediments have been sampled and analyzed on different locations both on- and offsite in the lower Scheldt valley for geological and paleo-ecological investigation (pollen, seeds and fruits, diatoms, mollusks, etc.) allowing detailed regional paleoenvironmental reconstructions (Bastiaens et al., 2005; Deforce, 2011; Gelorini et al., 2006; Van Neer et al., 2013). Awaiting better Belgian geological nomenclature for the Antwerp peats (Baeteman, 2004; Bogemans, 1997; Gullentops et al., 2001) and for ease of reference to older literature, the established nomenclature will be used lithostratigraphically without implying a fluctuating sea level rise (Figure 40).

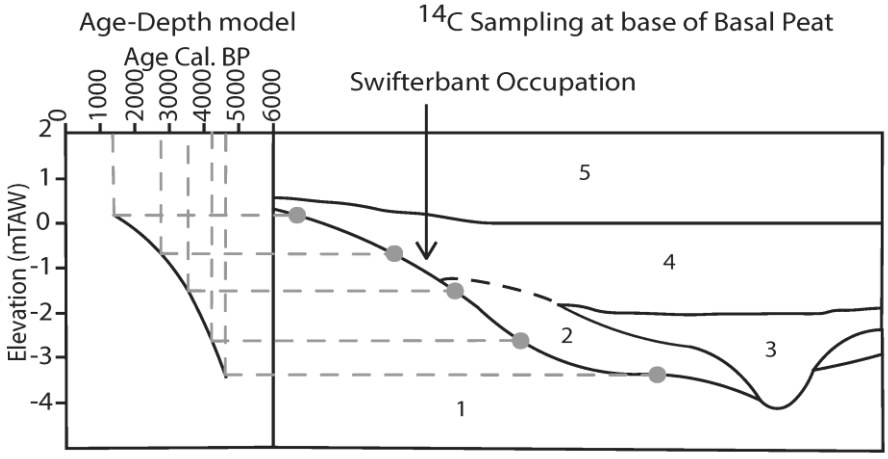

Figure 40: Basic principle of MHW/base of the peat reconstruction and applied lithostratigraphic terminology (1: Pleistocene Sands 2: Basal Peat 3: Calais Deposits 4: Holland peat 5: Estuarine Dunkirk Deposits).

As soon as the local ground water table reached the surface of the Pleistocene (cover)sands, eutrophic basal peat started to develop in a fen carr environment in the depressions. It started in the lowest depressions and developed to cover the entire area and eventually even the highest dunes, which were occupied by hunter-fisher-gatherer societies.

Locally, peat growth was interrupted by flooding of brackish water (formerly known as the Calais transgressions), which led to the deposition of OM rich tidal clastic sediments ('Calais deposits'). Pollen samples indicate that the region was situated in a transitional zone between brackish and freshwater environments (Deforce, 2011; Gelorini et al., 2006). The botanical and zoological evidence recovered from contemporaneous Swifterbant hearths (Deforce et al., 2013; Van Neer et al., 2013) at some localities suggests freshwater conditions, while at other locations evidence of a brackish water environment suggest sandy elevations within the floodplain to be covered with an alluvial hardwood forest, only incidentally touched by inundations.

Aside from the continuous relative sea level (RSL) rise, this flooding was caused by a combination of the local post-Pleistocene topography, the availability of marine and fluvial sediments in combination with a negative sedimentary balance (Beets and van der Spek, 2000), and the re-opening of old tidal gullies (Baeteman, 2005a). As a result, the dating of this (flooding) phase in one tidal basin cannot be compared to another. Because this tidal influence creates a specific ecological landscape surrounding the Deurganckdok sector B and Sector M sites, dating its occurrence is a requisite to investigate the relation with the (dis-)appearance of Swifterbant culture in the region.

When the tidal influence decreased, a fen carr back-barrier lagoon shifted from eutrophic to mesotrophic conditions. As a result, the Holland peat evolved from a sedge and sphagnum peat (Deforce, 2011; Gelorini et al., 2006). Finally, a new tidal phase took place that resulted in the deposition of several meters of marine sediments (formerly

'Dunkirk deposits') and lasted until dike construction protected the alluvial plain from floods (Bogemans, 1997).

4.4 Reconstructing paleogroundwater rise by peat dating

Because the basal peat layer that covered the well-drained Pleistocene sand was formed diachronously under the influence of rising groundwater, radiocarbon dating of samples at the base of this formation approximates the contemporaneous surfacing local ground water (LGW) level (Figure 40). However ground water drainage is hampered below mean high water (MHW) in tidal back-barrier lagoons. As a result, basal peat growth is generally initiated around MHW level. This allows the reconstruction of local mean high water level (LMHW) and the RSL through time, which was first applied by Jelgersma (1961). Assuming that both modern and earlier mean sea level (MSL) did not differ more than 10 cm between the Belgian and German North Sea coast Kiden et al. (2008), later comparison between differing LGW curves has revealed a series of influencing variables (eg. Berendsen et al., 2007; Kiden, 1995; Kiden et al., 2008; Makaske et al., 2003; Roeleveld, 1974; Van De Plassche, 1982; Van De Plassche et al., 2005; Van De Plassche et al., 2010; Van Dijk et al., 1991).

A first source of variation between RSL curves is subsidence. Tectonic subsidence is relatively small and constant throughout the Holocene (0.008-0.15 m/ka) (Vink et al., 2007). Glacio-isotatic and/or hydro-isostatic subsidence is the largest source of variation between RSL curves along the North Sea coast during the Early Holocene (~2.67m/ka. between 9 and 7.5 cal ka. BP) but has decreased since 5000 cal BP (~0.4m/ka. between 7.5-5 cal ka. BP) and is currently almost relatively negligible (Kiden, 2002; Vink et al., 2007). Secondly, if the coastal barrier is opened, the tidal wave can enter the back barrier easily and coastal MHW level equals the local MHW. If the gaps in the beach ridges decrease, the tidal wave is hampered and the local tidal amplitude decreases (Local MHW= MSL) (Makaske et al., 2003). This tidal damping is called the 'floodbasin effect' (Van De Plassche, 1982; Van De Plassche et al., 2010). Furthermore, on the one hand the estuary floodplain of the Scheldt decreases in size downstream of Antwerp, creating a tidal bulge (amplification). On the other hand, upstream of this 'bottleneck', the tidal wave is dampened, caused by the more shallow meandering Scheldt, which dissipates tidal flow into its tributaries and wider alluvial plain (extinction) (Kiden, 2006). Van Dijk et al. (1991) also illustrates that as a consequence of the rising MSL and increasing sedimentation, the effect of the decreasing river gradient is visible in local Basal peat curves along the Rhine-Meuse (see Cohen, 2003, fig 2.3). Finally, if the riverbed cuts through its natural levees to create a more favorable river gradient, this creates a short term increase

followed by a steady decrease in the speed of local MHW rise, superimposing the long term RSL rise (Berendsen et al., 2007).

4.5 Sampling and dating

4.5.1 Data collection

A database of legacy radiocarbon dates on bulk peat samples and selected terrestrial peat macro-remains was assembled from the literature (Appendix 2, Figure 39). If possible, both sample location and elevation were included. Further dates were included from a new dating program, yielding twenty new dates (Appendix 2, Figure 39). These dates were only performed on small AMS samples of terrestrial macro-remains according to Tornqvist et al. (1992). Suitable macro-remains were selected by Hanneke Bos (ADC).

4.5.2 Paleogroundwater dates

Samples have to be selected directly on top of the Pleistocene substratum as these are not compacted and at the original elevation. Through a series of dates at different elevations, a LGW rise curve can be constructed. The earliest peats were not necessarily formed under the influence of RSL rise because peat is also formed above MHW due to surfacing of the ground water (=groundwater gradient effect) (Denys and Baeteman, 1995; Van De Plassche, 1982). Therefore, sample locations with a high Pleistocene surface gradient such as Late Glacial floodplain dunes or paleovalley flanks are preferred (Van De Plassche, 1982).
Various sources of error complicate the reconstruction of local groundwater rise curves using Basal peat dates. Vertical errors in the age-depth plot can be introduced by several factors (Berendsen et al., 2007): the assumed depth of the sample is imprecise because of 1) sample elevation measurement (0.05 m error), 2) the in-core measurement (0.03 m error), or 3) through the sample thickness (0.02 m error). Vertical errors due to compaction are minimal but can be approximated as an upward error of twice the vertical distance to the Pleistocene sand according to Van De Plassche et al. (2005). Further vertical errors are caused by the complex relation between a Basal peat sample and actual groundwater depth elevation. This is estimated to be 0.1 m by Makaske et al. (2003), but can vary considerably depending on the peat vegetation. For example, *Phragmites* grow up to 30 cm below the water table and were excluded, as well as rain-fed *Spaghnum* peats

(van der Spek, 1997). Wood peat, on the other hand, develops closer to the local groundwater level (0.2 m error). Using the method proposed by Berendsen et al. (2007), a vertical standard deviation error of 0.21 m was estimated.
Horizontal (age) errors can be introduced if conventional bulk dating samples are contaminated by inclusion of aquatic macro-remains in the bulk sample, such as underlying older paleosols where there has been penetration by roots of younger plants. These can partially be accounted for during dating sample selection but are hard to estimate. Analytical errors during laboratory measurements are shown through the standard deviation value of the ^{14}C age.

4.5.3 Calais dates

Dating organic remains in the Calais sediment itself would result in unreliable dates, because this sediment was deposited in a mobile fluvial and/or marine environment, allowing the deposition of aquatic or older organic remains eroded from elsewhere. It is impossible to create a regional age-depth model using dates related to the tidal deposits as compaction could have caused vertical movement of the samples.
Dating the top of the Basal peat directly below only provides a *terminus post quem* for the start of the tidal sedimentation. Age errors are introduced if the top of the Basal peat is eroded (e.g. by tidal channels). On the other hand, peat marsh micro-topography can introduce a later start of sedimentation than the first tidal influence in the region. Therefore, only the oldest peat dates without an erosive transition to the Calais deposits were chosen as reliable indicators for regional appearance of a tidal environment.
The end of this tidal influence was dated through peat samples located at the base of the Holland peat. It has been observed by Vos and van Heeringen (1997) that the transition from the tidal Calais sedimentation to the restart of freshwater Holland peat development is a rather slow process. Therefore, it can be expected that the end of the tidal influence will be less precisely defined.

4.5.4 Archaeological dates

Two archaeological sites with artifacts mainly belonging to the Swifterbant material culture were selected. The occupation of these sites has been dated using short-lived plant macro-remains recovered from hearths and hearth pits directly relatable to the sites' occupation (eg. charred hazelnuts, seeds or charcoal from twigs) (Boudin et al., 2010; Van Strydonck, 2005) (Table 2).

4.6 Modeling and results

Calibration, analysis and Bayesian modeling of the dates were performed using Oxcal 4.2 (Bronk Ramsey, 2009a) and the IntCal09 curve (Reimer et al., 2009).
Other packages are also suitable to create deposition models of chronological records such as Bpeat (Blaauw and Christen, 2005) or Bchron (Haslett and Parnell, 2008). All three of them have been compared by Parnell et al. (2011) and have shown to have their individual (dis)advantages. Oxcal's capabilities to model and query both archaeological and geological data from different sequences. However, Oxcal has the disadvantage of not including the sample thickness (Bronk Ramsey, 2008) in its age-depth models while Bchron does (Parnell et al., 2008). Nevertheless, our central question was the relationship of the various peat sequences to the Swifterbant occupation of the area, for which OxCal was most amenable.

4.6.1 Outlier detection

Two steps of outlier detection were employed. First, potentially erroneous dates were marked as outliers manually after critically evaluating the available context information. Secondly, outlying dates were rejected from the model, using an overall model agreement index below 60% as an outlier indicator according to Bronk Ramsey (2009b). As such, a balance was sought between rejecting dates to fit models. The remaining basal peat dates were analyzed automatically for temporal outliers in a sedimentary sequence according to Bronk Ramsey (2009b).

4.6.2 Initiation of peat growth under influence of local groundwater rise

Age depth modeling of Basal peat growth is usually carried out for reconstructions of groundwater rise to derive RSL rise. Throughout its history, the research has been refined from models of a country's coastal plain (Jelgersma, 1961) to defining the variability between single duneflanks (Berendsen et al., 2007; Cohen, 2003). Such high-resolution date series were not available for the dunes surrounding the Deurganckdok sector B and M sites and the topographic setting of the dated samples could not always be accurately determined. Therefore, our aims were to reconstruct the spread of peatland in the regional prehistoric landscape surrounding the archaeological sites (roughly between Antwerp and the Belgian-Dutch border). The whole possible chronological and elevation range of the samples is relevant, including the regional variability in peat de-

velopment, rather than merely providing a linear paleo-groundwater curve. The resulting age-depth model can be considered a regional 'error envelope' of the minimal and maximal age-depth of the starting peat growth.

In most publications on basal peat dating, the age-depth position of a dated sample is determined by a simple error box, defined by the date range and estimated total vertical error (eg. Makaske et al., 2003). An advantage of the Bayesian approach allows deposition modeling of chronological records that includes both the full probability distribution function (pdf) of the radiocarbon or other dates and prior knowledge about exactly known or randomly varying sedimentation rate, stratigraphic order, or gaps in the sedimentation sequence (Bronk Ramsey, 2008). Such Bayesian models have been made on peat sequences of single cores with small depth errors (Blaauw et al., 2007; Yeloff et al., 2006), but rarely have they been applied to model the diachronic evolution of a single stratigraphic position from various cores.

Unfortunately the various local factors that influenced the determination of the elevation and time at which peat starts to develop could not entirely be included in the prior model. Therefore, the initiating peat growth age-depth plot has a wide vertical and horizontal range of non-sequential dates. Hence, constructing a single sequence including a maximal amount of data would still result in many outliers being excluded. Therefore a minimal (upper, earlier) and maximal (lower, younger) age-depth sequence was constructed. Both sequences included as many dates as possible while reaching a sufficient overall model agreement index for upper and lower sequence of the error envelope.

First, a simple OxCal sequence model was tested by using just the elevation of the dates as an ordering prior. This sequence was insufficient because it did not allow interpolation between dated elevations. An Oxcal P-sequence was therefore chosen because this model assumes a random deposition rate with approximate proportionality to the elevation. The degree of proportionality can be set using the 'k' parameter reflecting the number of random deposition events per 'z'-unit. In this paper the latter is defined by the sample elevation but the 'k' parameter is harder to define. In a single core sequence it can be related to the granularity of the sediments or the size of the deposition events (Bronk Ramsey, 2008). This cannot be applied in this paper because the samples do not represent accumulating peat at a single coring location. They rather refer to a possibly 0.21 m (at 1σ) (see errors section) sized age-depth point in the regional accumulation model of peat over the Pleistocene surface. As such the 'k' parameter was set at 5 resulting in a small proportionality between the elevation and deposition rate. Between dates, only 10 interpolated dates per meter have been calculated to limit computer processing time. If basal peat dates had been selected from a core or profile with other dated stratigraphic positions, these were included in the model using the 'before' or 'after' command defining additional *termini ante/post quos* in the prior model.

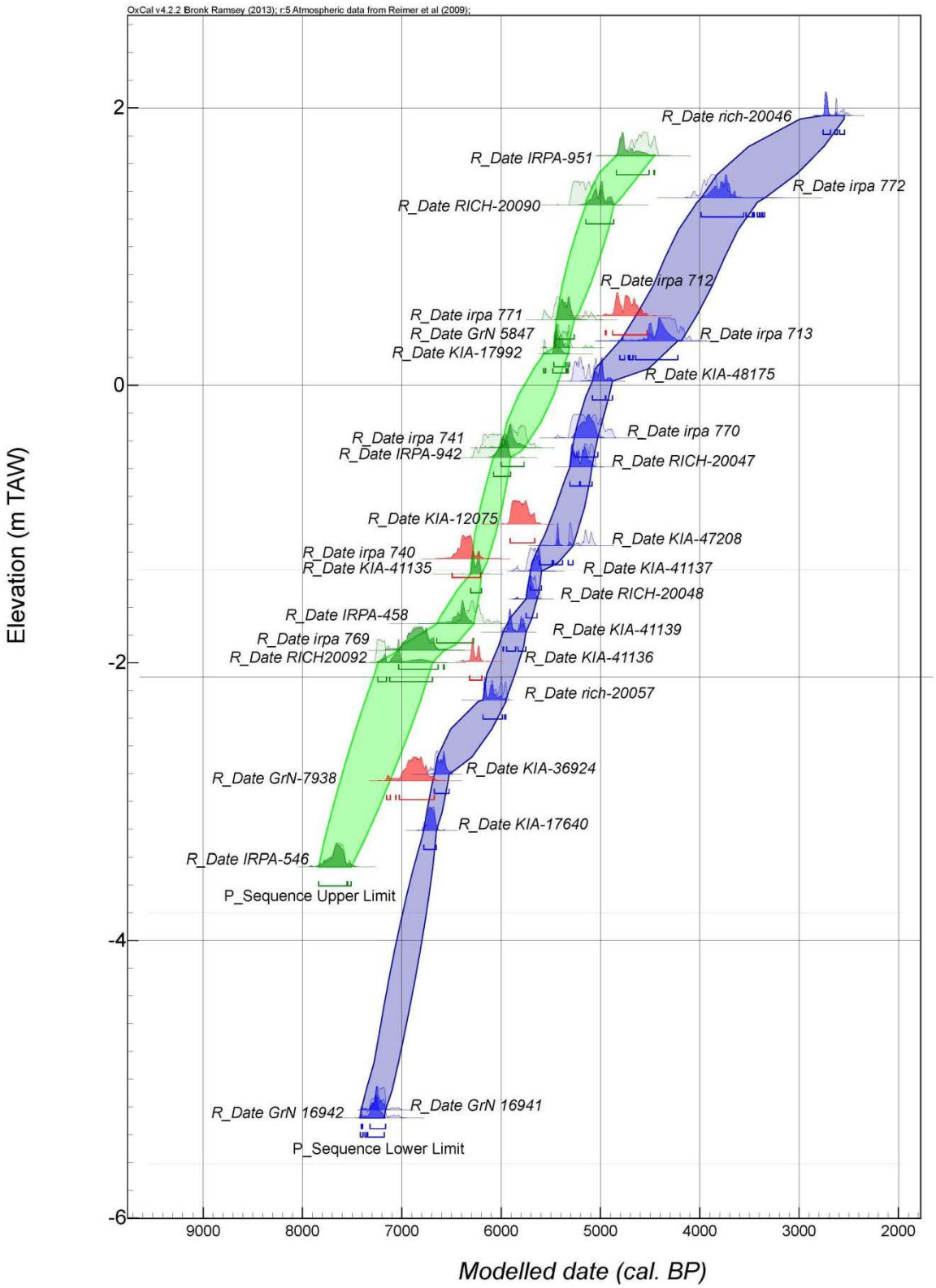

Figure 41: Age-Depth plot of the collected base of the peat dates: upper P-sequence (green interpolation) and lower P-sequence model (blue interpolation) enveloping the dates excluded from the sequences in between (red) (cal. date ranges at 2 σ).

As a result, two acceptable P-Sequences could be created (Figure 41). The upper sequence includes twelve dates while fifteen dates fit in a lower sequence. Four dates (KIA-41136, KIA-12075, GRN-7938, IRPA-712) had to be considered outliers to the upper and lower sequence. Nevertheless, they are located inside the error envelope. A fifth outlying date (IRPA-740) was statistically marked as an outlier but falls only partially out of the error envelope.
Both the upper and lower curve show a decrease in the peat development surrounding the start between 7000 and 6500 cal BP, while it increases again afterwards. This shift is attested between samples KIA-36924 from the Doel-NPP core (Deforce, 2011) and RICH-20057 from Doelpolder-Noord. Both have a position on a dune flank close together on the paleovalley of the Scheldt, assuring their reliability as groundwater indicator. In the upper P-sequence this shift is defined between IRPA-458, retrieved from an intact peat profile in the Doeldok (Minnaert and Verbruggen, 1986) and IRPA-769 (Kiden and Baeteman, 1989) from the slope of the Scheldt paleovalley and therefore also considered reliable indicators. The start of this decrease could possibly be related to the delaying MSL rise (Tornqvist and Hijma, 2012) combined with the closing coastal beach ridges. The increase after 6500 cal BP could relate to the appearance of the tidal Calais sedimentation (see further), neutralizing a tidal damping effect possibly existing before.
The newly gathered dates between 6000 and 5500 cal BP are filling a gap in the published dates in the Scheldt paleovalley and allow better comparison with the data from Zeeland. The lower time-depth of these dates confirms the observation by Kiden (1995) that the development of peat in the Scheldt valley was more directly influenced by the effects of MSL rise than the Zeeland peat, which was developed higher due to the groundwater-effect.
The size of the error envelope is probably a result of the large variability in undulating Pleistocene topography, changing flood basin, estuary and river gradient effects. Because even dates from the same core or section fit in both sequences, it can be concluded that spatial and temporal resolution of the dates was not yet high enough to disentangle all of these more local effects as observed by Makaske et al. (2003).

4.6.3 The occurrence of Calais sedimentation in the Scheldt polders

Inherent problems with summed probability functions to date geomorphological events have already been described by Chiverrell et al. (2011). Therefore, the chronology of appearance and disappearance of the tidal Calais landscape was reconstructed using a Bayesian approach including the following *a priori* information.
The first assumption is that in all dated sequences the Calais sediments belonged to a single but continuous lithostratigraphic unit and that the Holland peat did not start to grow before the latest basal peat development was interrupted. Therefore, it can be as-

sumed that the top of the Basal peat is older than the base of the Holland peat. All dates belonging to the top of the Basal peat are assumed to be unordered as well, allowing them to be grouped in a phase. The same was done for all dates of the base of the Holland peat. Secondly, it was assumed that the tidal influence was present during a distinct period and not a short event. As a consequence, the boundaries between both phases were modeled sequentially (Bronk Ramsey, 2009a). Because the first appearance of the tidal landscape is sought, the end boundary is required from the oldest top of the Basal peat dates. This boundary should refer to the event that started the expansion of tidal influence in the study area (Kiden, 2006). The restart of peat growth happened as soon as this (inter-)tidal sedimentation reached a level above high water tide and tidal influence decreased. This continuous process was treated as a single broad phase. If other dates were available from the same core or profile, their stratigraphic information was included using the before and/or after function with the Calais related datings.
Manual outlier selection excluded two samples related to the tidal clay deposits as they revealed an age inversion in the profile (IRPA 454 and IRPA-457) (Minnaert and Verbruggen, 1986). Furthermore, a sample from a disturbed Basal peat layer in a tidal channel (IRPA 946) (Van Strydonck et al., 1995) was considered unreliable as well. One date (IRPA-947) of the basis of the Holland peat was excluded because the pollen data indicated a hiatus between the deposition of the underlying tidal clay and the covering Holland peat (Van Roeyen et al., 1991). The remaining dates were considered reliable for the prior model. One sample from the top of the Basal peat was excluded because it did not result in an sufficient model agreement index (RICH-20091). This sample was recovered near the top of an aeolian sand ridge.

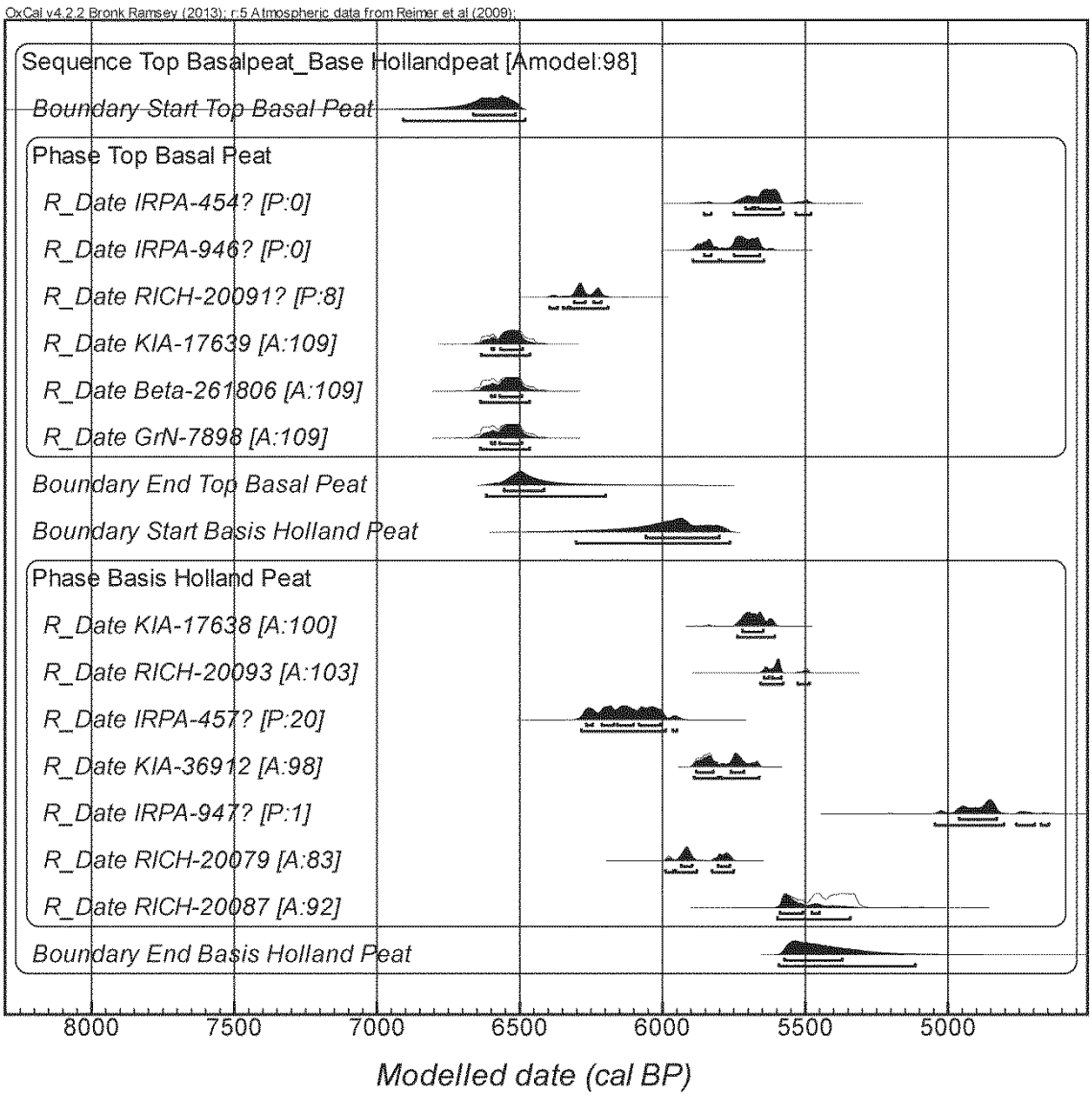

Figure 42: Oxcal plot of Bayesian sequence of all available Top of Basal Peat phase dates followed by the Basis of Holland peat phase dates with sequential boundaries (A: agreement index; outliers:'?'; P: outlier probability).

Using the remaining dates, a sufficient posterior model could be established (Figure 42). The end boundary of the top of the Basal peat dates revealed the start of the earliest (inter-)tidal influence between 6620 and 6200 cal BP (2 σ). Similarly the start boundary of the base of the Holland peat revealed the renewed peat growth starting between 6300 and 5760 cal BP (2 σ).

The start of this sudden upstream expansion of the estuary of the Scheldt into Belgium coincides with the supposed breakthrough period of a tidal channel preceding the present day Oosterschelde (Kiden, 2006; Vos and van Heeringen, 1997). This new estuary that broke through the coastal barrier possibly caused an increase in tidal influence, which decreased tidal damping.

The end date range of the Calais sedimentation period is less well defined as this was probably a more complex transition. Because the study area comprizes the most inland extension of the tidal influence, it was probably also amongst the first to be effected by the reduced tidal range and development of Holland peat.

4.6.4 Swifterbant culture occupation at the Deurganckdok sector B and M sites

The occupation of the sector B and M sites has also been modeled as a single phase, consisting of two possibly overlapping sub-phases of sector B and M. The start and end boundaries of the overall phase were used to estimate the start and end of Swifterbant occupation.
The Bayesian modeling of the occupation revealed an individually outlying date in sector B (NZA-12076) (Van Strydonck, 2005)(Figure 43). Upon closer examination, it was found that this date was retrieved from a hearth situated higher on the sand ridge which could be related to the peat development (see further). As a result the posterior model of sector B and M revealed the occupation started between 6550 and 6390 cal BP (2 σ) and lasted until between 6170 and 5950 cal BP (2 σ).

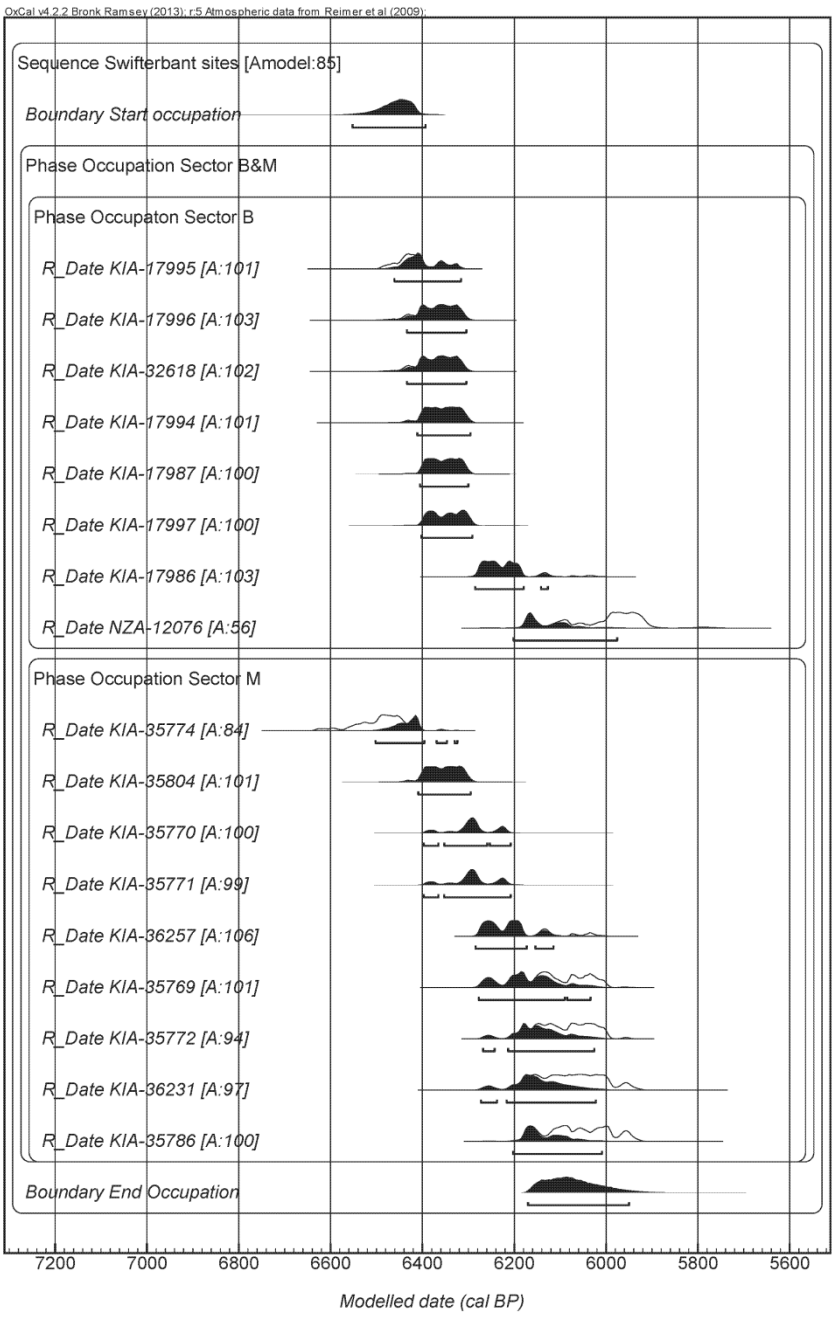

Figure 43: Oxcal plot of Bayesian model of the occupation phases of sector B and M sites dated on terrestric macroremains, recovered from excavated hearths (A: agreement index).

4.6.5 Integrating the initiation of peat-growth error envelope, the occurrence of the Calais landscape and archaeological dates

Integrating independently dated archaeological and geological sequence records using a Bayesian approach is rarely done (eg. Gearey et al., 2009). This study will do so by testing correlation and order between archaeological occupation and geological events, such as individual dates or boundaries of contemporaneous phases and/or chronological se-

quences. The elevation of the Basal peat at the start and end of Swifterbant occupation is relevant as it determines the amount of available 'dry' land. However, querying a probability range of elevation values in the initiating peat growth sequences at the boundaries of the Calais sedimentation phase or Swifterbant occupation was not yet possible using Oxcal 4.2. Therefore a simple plot of the archaeological dates in the Basal peat age-depth model (Figure 44) was made that nevertheless revealed some key insights.

It seems that at the start of the Swifterbant occupation, the hearths were situated at least 1 m above the maximal envelope of the initiating peat growth. This means that the site inhabitants settled (temporarily) in the supratidal area of the floodplain, only accidently touched by tidal flooding and too highly elevated for peat development. This is confirmed by the reconstruction of an alluvial hardwood surrounding the well-drained sites (Deforce et al., 2013).

It appears that through time the rising peat caught up with the level of occupation. At that time, the tidal zone (roughly below the lower boundary of the error envelope) was still about 1 m below the sites. This could explain the observed gap between the end boundary of the dated hearths and the start boundary of Holland peat growth. It also shows that the end of the Swifterbant occupation at sector B and M was determined by the disappearance of the tidal environment. Whether this meant the end of the Swifterbant culture in this part of the Scheldt valley remains unclear as it could well have continued at higher topographic positions. Unfortunately chronological evidence from higher positioned archaeological sites in the study region is currently missing (Crombé et al., 2011b).

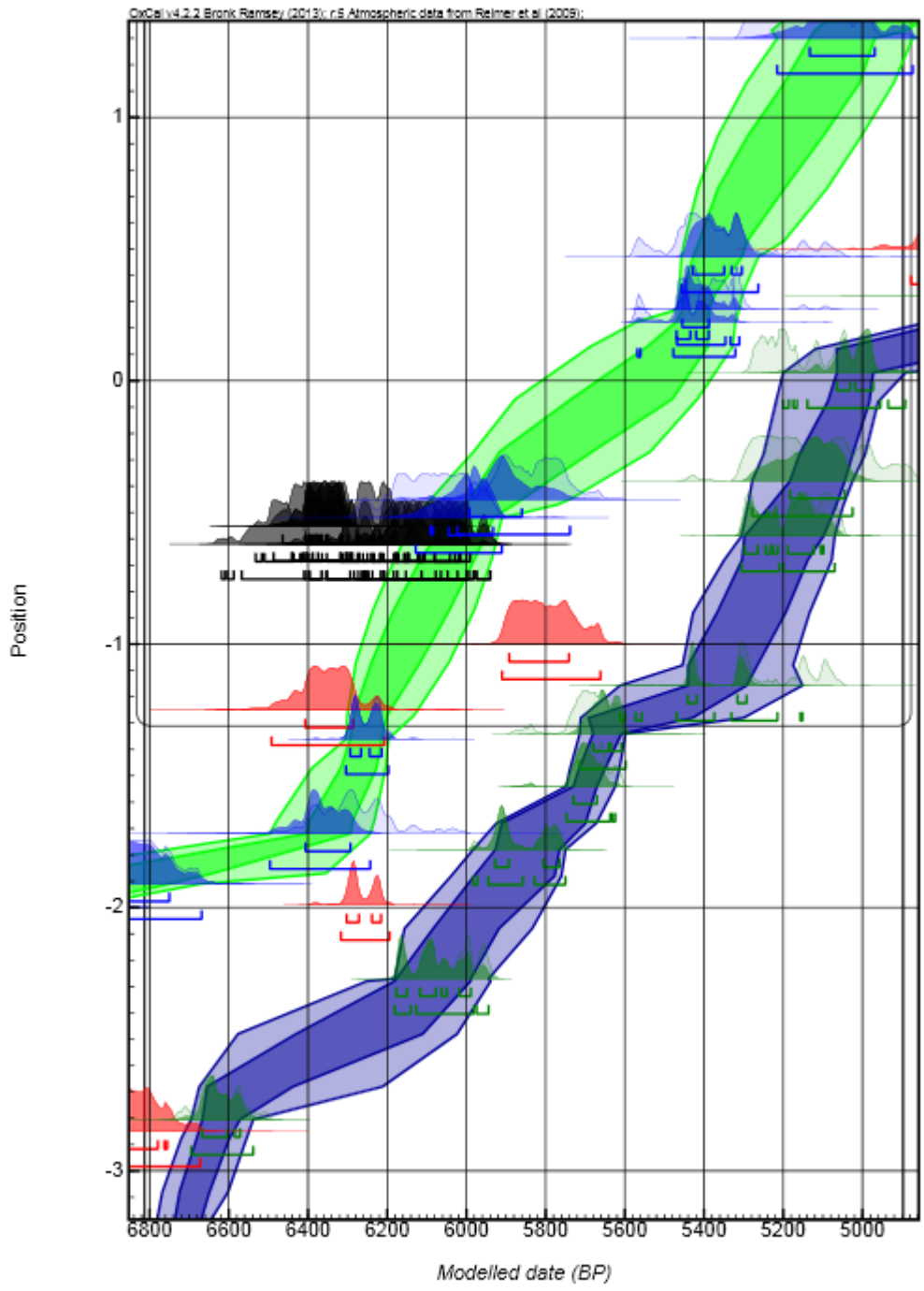

Figure 44: Detail of the age-depth model of the base of the peat layer (see Figure 41), archaeological Swifterbant dates (see Figure 43) are included at the respective elevations of sample retrieval (black).

The relationship between the (inter-)tidal Calais sedimentation and the Swifterbant occupation of the region was investigated using the Oxcal correlation plot and order query functions.

The correlation plot between the End Boundary of the top of the Basal peat and the Start Boundary of the Swifterbant occupation reveals a large correlation between around 6500 cal BP and 6430-6480 cal BP (Figure 45). Combined with the 61 % probability

that the start of the Swifterbant occupation followed the end of Basal peat formation, it can be concluded that the Swifterbant occupation of the sites started shortly after the appearance of a tidal environment. This suggests that the choice to start setting up camp on the excavated sand-ridges might have been at least indirectly influenced by the appearance of this tidal environment. This is further corroborated by the occupational gap between Early Mesolithic and the Swifterbant Culture, attested on both sand ridges (Boudin et al., 2010). Apparently, these dunes were not attractive for occupation during the period of peat development preceding the tidal influence.

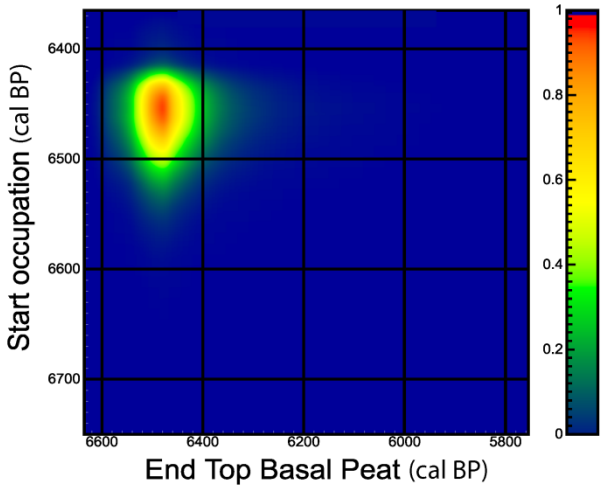

Figure 45: Oxcal Correlation plot of Top of Basal peat growth-End Boundary pdf (from Figure 42) and Swifterbant occupation-Start Boundary pdf (from Figure 43).

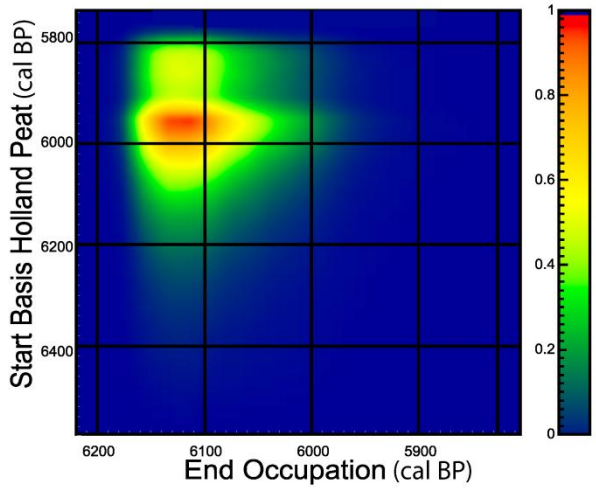

Figure 46: Oxcal Correlation plot of Swifterbant occupation-End Boundary pdf (from Figure 43) against the Base of Holland peat growth-Start Boundary pdf (from Figure 42).

A broader correlation peak indicates a lower degree of correlation between the end of Swifterbant occupation and the restart of Holland peat growth (Figure 46). In combination with an 80% probability of the Swifterbant occupation ending before peat growth

restarted, it can be concluded that a gap exists between the end of the archaeological data-record and the disappearance of the tidal environment.
The chronological models clearly suggest that the occupation of sector B and M happened when the tidal Calais landscape was surrounding the sites, which is further confirmed by paleobotanical and archaeozoological evidence (see earlier) (Crombé, 2005; Deforce et al., 2013; Van Neer et al., 2013).

These results allow the dates for site occupation to be included in a chronological sequence model between the top of the Basal peat- and the base of the Holland peat dates. A contiguous boundary is suitable to model the first transition samples, and a sequential transition was the optimal solution to model the gap between the Swifterbant dates and the base of the Holland peat samples. The resulting model (Figure 47) refines the boundary between the end of Basal peat growth and the Swifterbant occupation between 6530 and 6410 cal BP (2 σ). The end of occupation is modeled between 6180 and 5980 cal BP (2 σ) and the restart of Holland peat growth between 6090 and 5770 cal BP (2 σ).

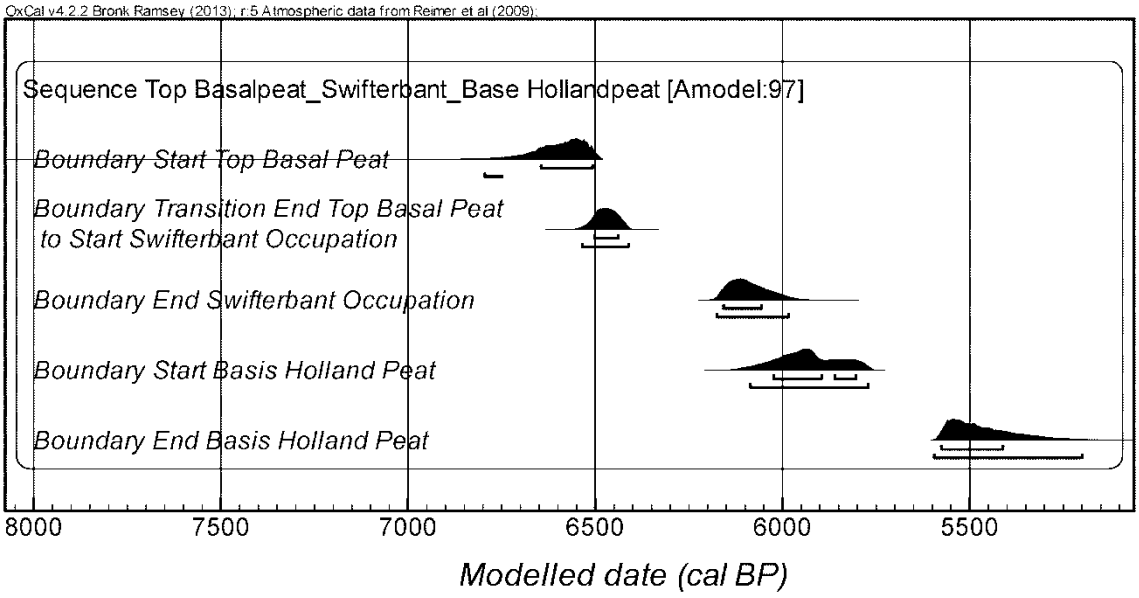

Figure 47: Bayesian model of the contiguous boundaries from a sequence of the beforementioned phases: Top Basal Peat; Swifterbant Occupation and Basis Holland Peat.

4.7 Conclusions

Regarding the first aim of this paper, the basal peat results show that a maximal error envelope for a regional model of the start of peat accumulation was obtained, using a dataset of diverse origin. This model was able to add new dates to existing groundwater

curves which confirms the differing hydrological dynamics between the Scheldt paleovalley and the rest of Zeeland before they became part of the same floodplain. Further refinements could be made if high-resolution radiocarbon date sequences of Basal peat are collected, such as along separate aeolian coversand ridges along the Scheldt river to study more local factors determining the initiation of peat development.
Secondly, the sudden expansion of the tidal influence in the Scheldt river floodplain could be accurately dated and situated within the proposed timing of the development of the later Oosterschelde estuary more downstream. The end of this OM rich clastic environment is chronologically less sharply defined.
Finally, the near-contemporaneity of start of the (inter-)tidal influence in the region with the arrival of the Swifterbant culture at the sector B and M sites could be proven, and further supported by tidal indications during the occupation of the sites in the archaeo-zoological and archaeo-botanical remains (Crombé, 2005; Deforce et al., 2013; Van Neer et al., 2013). The regional paleogroundwater model suggests that site occupation started well above ground water and ended when the earliest peats could start to develop at the site. The gap between the end of the occupation of the sites and the end of the tidal influence could be explained by the retreat of the Swifterbant inhabitants to slightly higher, currently unexcavated areas.
Future applications of the results include paleogeographic landscape reconstruction at specific time intervals (eg. Vos and van Heeringen, 1997) or an interpolation including variability in three dimensions, rather than elevation only (eg. Cohen, 2003). The results also generate new research questions regarding the archaeological occupation of the alluvial plain of the lower Scheldt.

4.8 Acknowledgments

The authors thank the Scientific Research Foundation Flanders (FWO) (Project title: Archaeological exploration across the land-sea boundary in the Doelpolder Noord area (Westerschelde estuary): impact of sea-level rise on the landscape and human occupation, from the prehistory to medieval times); the Province of Antwerp-Department of Culture-Heritage Service and the City of Antwerp-department archaeology and our colleague Erick Robinson for their support. The local farmers and the Flemish Nature and Forest agency are thanked for allowing us access to their lands.

Chapter 5 Wetland landscape dynamics, Swifterbant land use systems and the Mesolithic–Neolithic transition in the southern North Sea basin

This chapter is adapted after (Crombé et al., in press-b)

Over the last decade, excavations in the lower Scheldt river basin (NW Belgium) have identified the first presence of the transitional Mesolithic–Neolithic Swifterbant culture, previously only known from the Netherlands and one site in northwest Germany. These excavations have also yielded the first evidence for the presence of Early Neolithic Linearbandkeramik, Limbourg, Blicquy and Epi-Rössen cultural remains in these wetland landscapes. High quality organic preservation at these sites offered the opportunity to reliably place the Swifterbant within the absolute chronology of the Mesolithic–Neolithic transition in this region, as well as the reconstruction of Swifterbant subsistence practices, most notably the incorporation of cattle husbandry into a traditional hunting-fishing-gathering economy. Two different site types could be identified between the six excavated sites – dune and natural levee sites – which had contemporaneous periods of occupation, but different occupation histories. The integration of the dates from these different site types with the paleoenvironmental dates provides an initial model of the Swifterbant settlement system in the area and its role in the specific tempo and trajectories of cultural and economic change that occurred during the neolithisation of the Scheldt basin. This model consists of relatively specialized and temporarily inhabited cattle and hunting-fishing camps on the dunes and larger, more continuously occupied levee camps along the river valleys. Bayesian statistical modeling suggests that Swifterbant occupation of the dune sites occurred during a brackish water flooding period and that occupation of the levee sites was more continuous.

Keywords

Neolithization; Swifterbant culture; alluvial geoarchaeology; Bayesian chronological modelling; Northwest Europe; Belgium

5.1 Introduction

The chronology and nature of the transition from a hunter-gatherer-fisher to an agricultural lifeway in the sandy lowlands of the southern North Sea basin was hardly understood until recently. This was due mainly to an almost complete lack of well-preserved (Late) Mesolithic and (Early) Neolithic sites, as most sites are severely affected by ploughing, bioturbation, and organic decay (Crombé and Vanmontfort, 2007; Verhart, 2000; Vermeersch, 1994). In the last decade, however, developer-led archaeological research in the Lower Scheldt floodplain conducted mainly by Ghent University has provided the first reliable data, allowing us to research the neolithization process in much more detail. To date, six transitional sites have been excavated, which were protected from later disturbance thanks to a covering with peat and (peri-)marine deposits. These sites not only yielded the first Early Neolithic cultural remains (Linearbandkeramik, Limbourg, Blicquy, and (Epi)Rössen pottery) in the region, but also the first evidence of the Final Mesolithic Swifterbant Culture (Crombé et al., 2011a; Crombé et al., 2002; Crombé and Sergant, 2008; Crombé et al., 2011c), until then only known from the Netherlands and one site in northwest Germany (Raemaekers, 1999). Excavations of these transitional sites have generated large amounts of botanical and animal remains that enabled reconstruction of their subsistence practices (Deforce et al., 2014a; Deforce et al., 2013; Deforce et al., 2014b; Van Neer et al., 2013) and of the local environmental contexts of these settlements (Bastiaens et al., 2005; Deforce et al., 2014a; Deforce et al., 2013). In addition, the wider environmental context and alluvial dynamics can be inferred from paleoecological studies from contemporary alluvial deposits and peat (Deforce, 2011; Deforce et al., 2014a; Deforce et al., 2014b; Gelorini et al., 2006; Janssens and Ferguson, 1985; Kuijper, 2006; Meylemans et al., 2013; Minnaert and Verbruggen, 1986). These organics offer the opportunity to investigate the relationships between changes in settlement and subsistence practices during this transitional phase with hydrological changes that occurred in these highly dynamic wetland landscapes. In this paper we present the results of a Bayesian chronological modelling project that sought to integrate the dates from the archaeological sites with the environmental dates for

different flooding events. Two different site types could be identified between the six different sites, which had contemporaneous periods of occupation, but different occupation histories. The integration of the dates from these different site types with the paleoenvironmental dates provides an initial model of the Swifterbant settlement system in the area and its role in the specific tempo and trajectories of cultural and economic change that occurred during the neolithisation of the Scheldt basin.

5.2 General Setting

The six excavated sites are situated within the Waasland Scheldt polders, a low-lying area (mean 2–3 m TAW = mean low water tide level in Oostende) in the vicinity of Antwerp on the left bank of the river Scheldt (Figure 48). From the Middle Holocene onwards this area was exposed to a gradual increase of water tables as an indirect result of Postglacial relative sea level (RSL) rise. This resulted in repeated phases of peat growth and deposition of estuarine clayey sediments, which came to an end when people started to drain and embank the area with intermittent success from the 13th century AD onwards (Figure 49 and Figure 51).

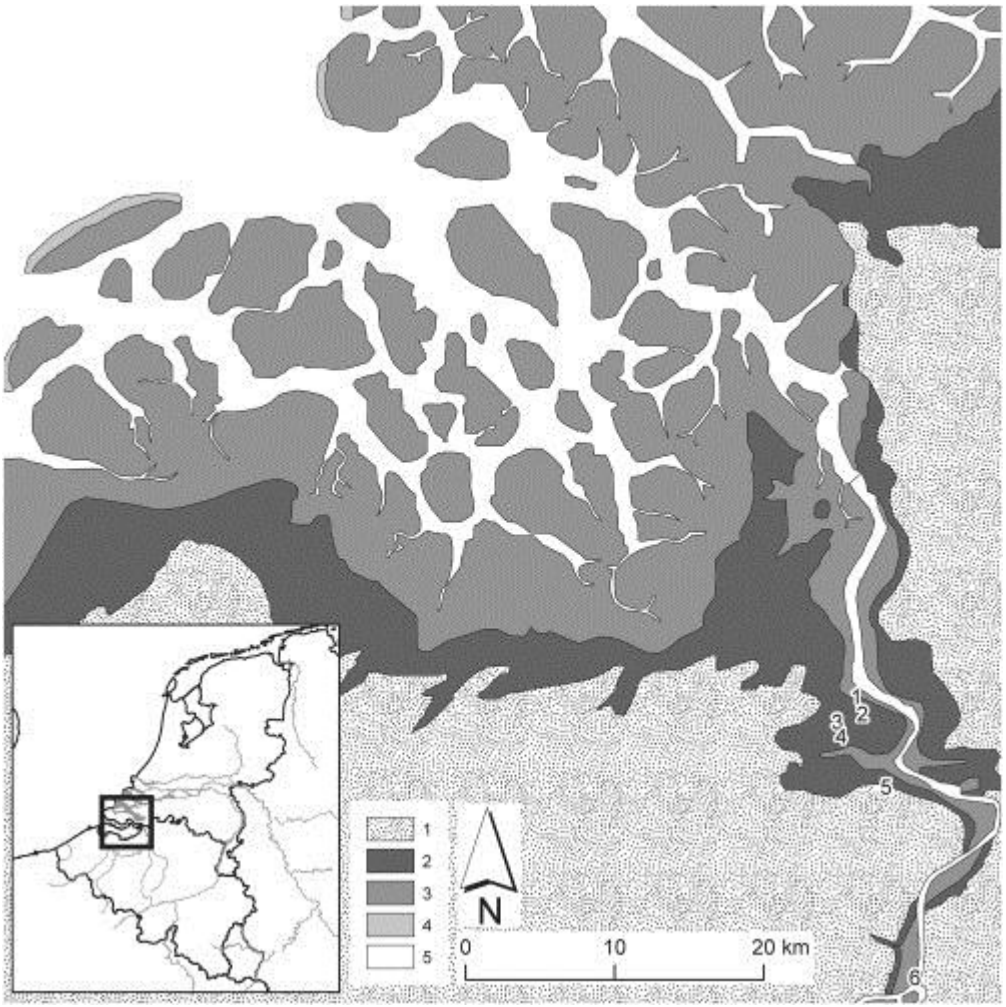

Figure 48: Paleogeopgraphical map of the Scheldt estuary around ca. 6300 cal BP (modified after Vos and van Heeringen, 1997) with indication of the prehistoric sites mentioned in the text: Doel-Deurganckdok- sector B (1), C (2), J/L (3) and M (4); Melsele-Hof ten Damme (5) and Bazel-Stuw (6). Key: 1. Pleistocene coversand area; 2. Peatland; 3. Tidal area (mudflats and saltmarshes); 4. Beaches and dunes; 5. North Sea, tidal inlets and tidal channels.

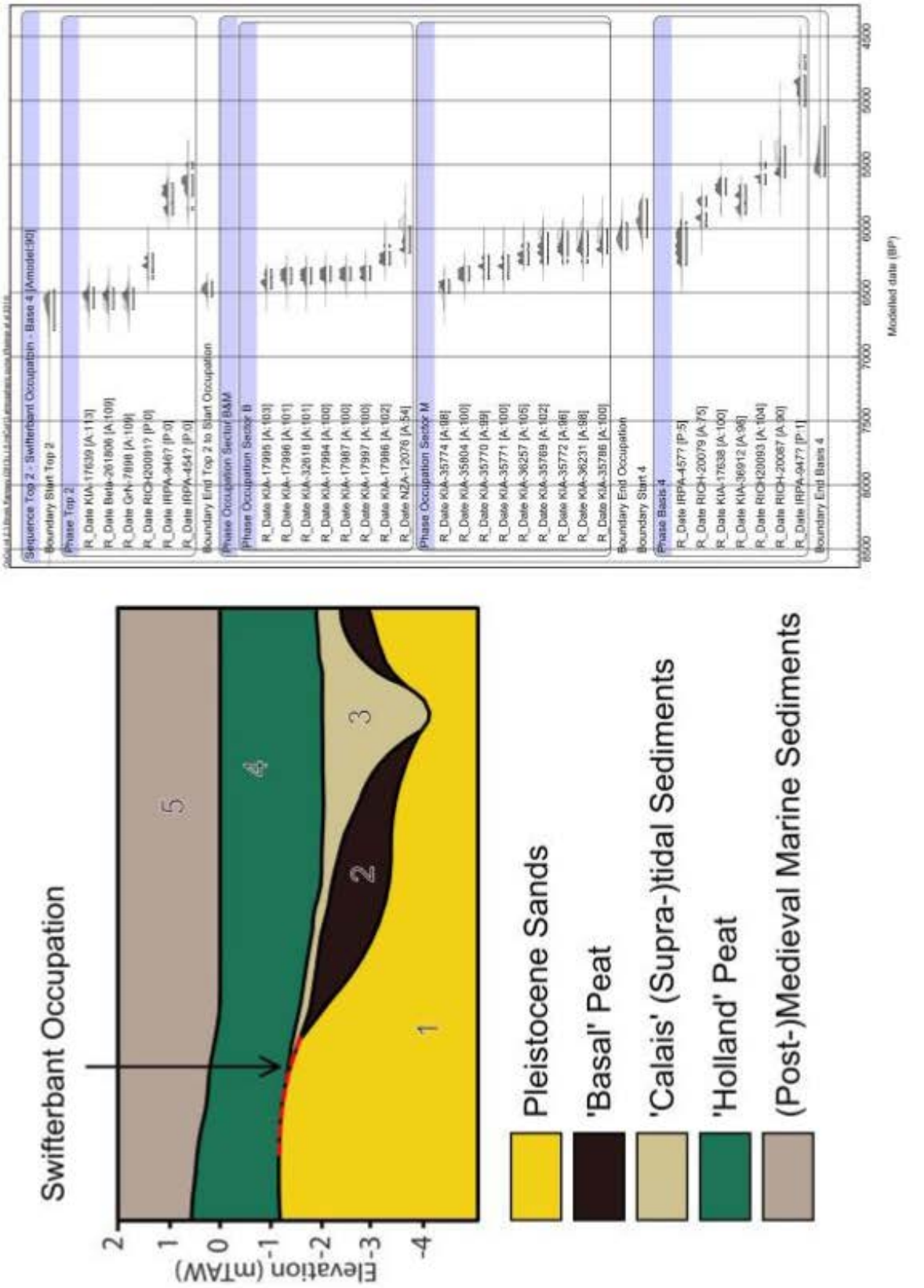

Figure 49: Reference profile (not to scale) from Doel-Deurganckdok showing the main lithostratigraphic units and the chronologically modelled phase numbers at the dunes sites. To the right the results of the Bayesian modeling (calibrated date ranges at 2σ).

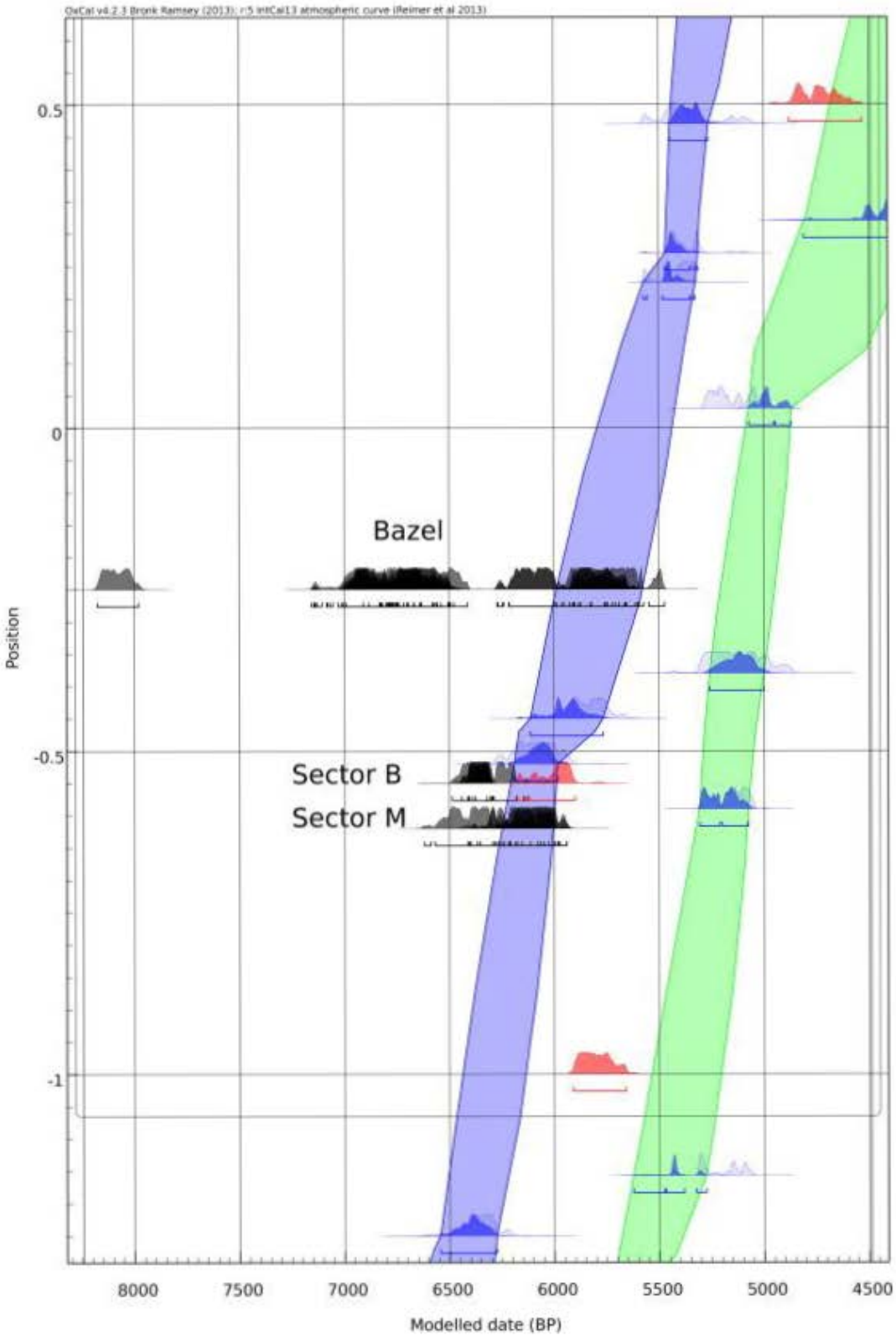

Figure 50: Extract of the regional paleogroundwater curve of the Scheldt polders (Agreement indices and labels in Verhegge et al., 2014: figure 3) with the Swifterbant dates (black, bottom) and Bazel dates (black, top) plotted at the respective elevations. Age-depth plot of upper P_Sequence (green interpolation) and lower P_Sequence model (blue interpolation) enveloping the dates excluded from the sequences in between (red) (calibrated date ranges at 2σ).

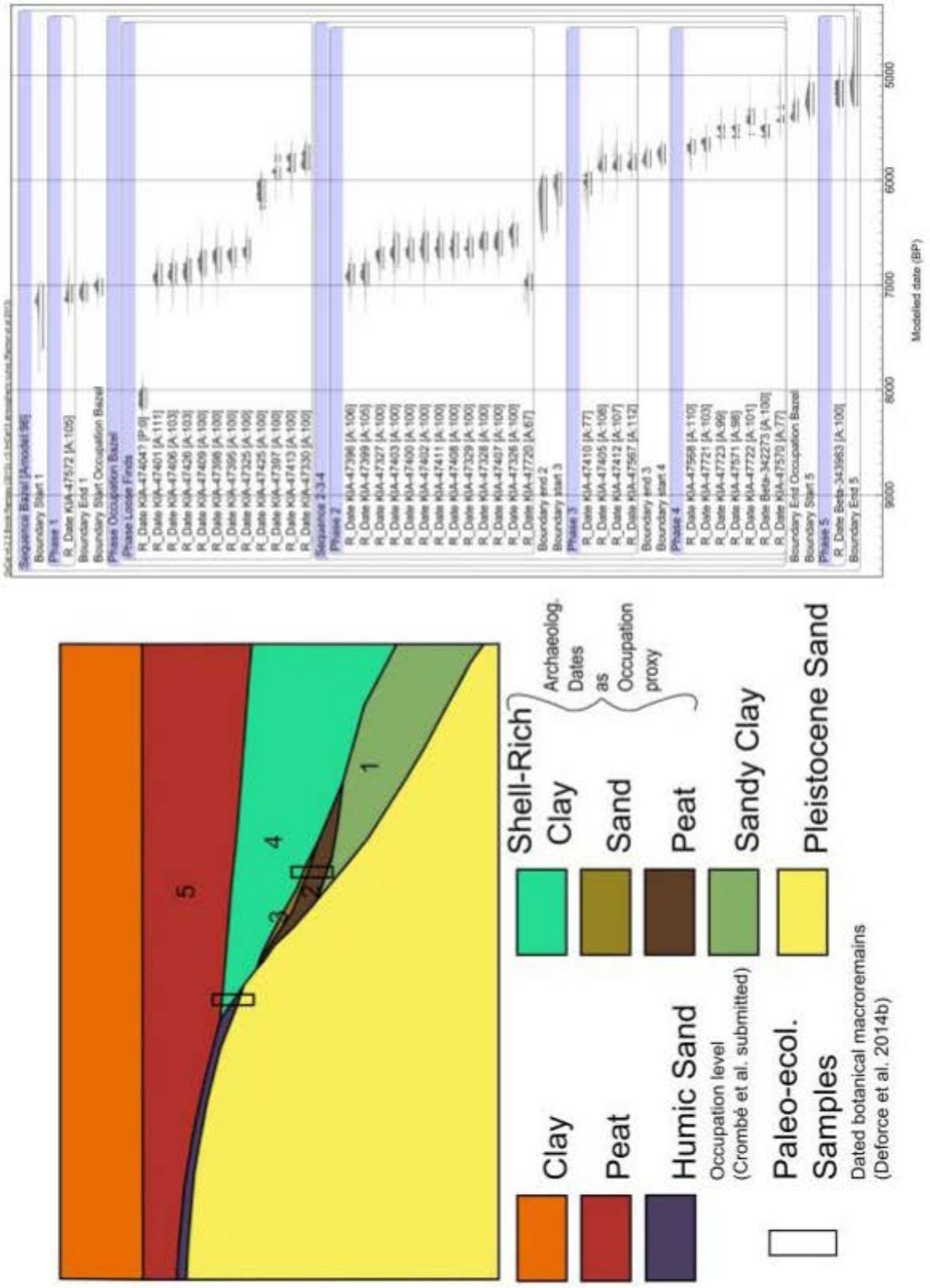

Figure 51: Reference profile (not to scale) from the levee site of Bazel showing the main lithostratigraphical units and chronologically modelled phase numbers. To the right the results of the Bayesian modeling (calibrated date ranges at 2σ).

As soon as the local ground water table reached the surface of the Pleistocene (cover-) sands, eutrophic basal peat started to develop in a fen carr environment in the depressions. Kiden (1995) used basal peat dates as RSL rise indicators in the Scheldt paleovalley. The limited indicator density for the Late Mesolithic and Early Neolithic periods was recently resolved by collecting several additional dates (Deforce, 2011; Verhegge et al., 2014) and a new regional basal peat rise/local groundwater rise age-depth model for the polder area has been developed in a Bayesian statistical framework (Verhegge et al., 2014).

Over a short period, peat growth was interrupted locally by the deposition of estuarine sediments (formerly known as 'Calais deposits') (Kiden, 2006). Microfossils from these sediments indicate that the region was situated in the transitional zone between brackish and freshwater environments (Deforce, 2011; Gelorini et al., 2006). Aside from the continuous RSL rise, this flooding was caused by a combination of the local post-Pleistocene topography, the availability of marine and fluvial sediments in combination with a negative sedimentary balance (Beets and van der Spek, 2000), and the re-opening of old tidal gullies (Baeteman, 2005a). The regional occurrence of this estuarine environment has been statistically modelled by integrating all available dates of the top of the basal peat and base of the Holland eat respectively between 6620 cal BP and 6200 cal BP (2 σ) and 6300 cal BP and 5760 cal BP (2 σ) coinciding with the largest expansion of estuarine influence downstream of our study area (Kiden, 2006; Verhegge et al., 2014).

When the estuarine influence decreased, a fen carr back-barrier lagoon shifted from eutrophic to mesotrophic conditions. As a result, the Holland peat evolved from a sedge to a *sphagnum* peat (Deforce, 2011; Gelorini et al., 2006). Finally, a marine flooding phase took place that resulted in the deposition of several meters of marine sediments ('Dunkirk deposits') and lasted until dike construction protected the alluvial plain from floods (Bogemans, 1997).

Table 6: List of the excavated sites within the Lower Scheldt floodplain with the attested chronological phases based on diagnostic artifacts (lithic artifacts and pottery). (FP) Final Paleolithic (Federmesser Culture); (EM) Early Mesolithic; (MM) Middle Mesolithic; (LM) Late Mesolithic; (FM) Final Mesolithic (Swifterbant Culture); (Neo) Neolithic (Michelsberg Culture). The chronological division is based on Crombé and Cauwe (2001), Robinson et al. (2011) and Robinson et al. (2013).

Site	Excavated surface (m²)	FP	EM	MM	LM	FM	Neo
Dune sites							
Doel Deurganckdok B	±3500	X	X			X	
Doel Deurganckdok C	±570						X
Doel Deurganckdok J/L	±3300		X			X	
Doel Deurganckdok M	±800		X			X	
Levee sites							
Bazel	±800		X	X	X	X	X
Melsele Hof ten Damme	±100			X	X	X	X

Prehistoric occupation (Table 6) occurred mainly on the higher grounds within this overall wet landscape. All six sites are situated between ca. 0.5–1.0 m below national ordnance level. Two different types of sites can be distinguished based on their different topographical locations (Figure 48). The first are situated on relatively large Late Glacial coversand dunes, some distance away (up to 4 km) from the Scheldt river. This site type includes all sites discovered at Doel Deurganckdok. The second type of site is situated on relatively narrow levees or point bars along a former channel of the Scheldt. The sites of Bazel and Melsele represent this second site-type. The archaeological remains from these sites indicate clear differences in occupational histories (Table 6). The dune sites are characterized by a discontinuous occupation, with well-attested human presence during the Allerød (Federmesser Culture), Early (Boreal) Mesolithic, and Final (Late Atlantic) Mesolithic. Despite the extensive excavations, thus far no clear evidence of Middle and Late Mesolithic occupations have been found, creating an occupational hiatus of almost three millennia (mid 10th to mid 7th millennium cal BP) (Crombé et al., 2013b). In contrast, the evidence from the levee sites, in particular from the more recently and thoroughly investigated site of Bazel, point to a longer occupation history starting from at least the Early/Middle Mesolithic until the Neolithic (Michelsberg Culture). Another difference between the dune and levee sites is the spatial preservation of the cultural remains. As the inland dune sites are located on relatively large coversand ridges, the occupational remains are usually found in spatially discrete clusters, probably representing separate occupation phases (Crombé et al., 2013b). According to Bailey's (Bailey, 2007) typology these sites can be classified as ‘spatial’ rather than ‘cumulative palimpsests’. Repeated occupation on the narrower levees, on the other hand, resulted in dense accumulations of human waste, leading to the formation of complex cumulative palimp-

sests. However, detailed spatial analyses have revealed the existence of a latent stratigraphy, probably resulting from intense and continuous bioturbation and trampling (Crombé et al., in press-a). The latter is confirmed by the generally smaller size of potsherds at the levee sites. Unfortunately, at the present moment we have not been able to dissect this latent stratigraphy in order to potentially separate different occupation events. Future research must take on this formidable challenge by carrying out more in-depth raw material (geo-chemical) and techno-typological analyses that might yield further chronological information.

5.3 Material and methods

5.3.1 Archaeological sampling

Due to the absence of unburnt organic remains, the dune sites were radiocarbon sampled on residue found within discrete clusters of heavily burnt material, interpreted as possible surface-hearths or hearth-dumps (Crombé, 2005; Sergant et al., 2006a). Samples of calcined bones, charred fruits and seeds, as well as charcoal, were selected after identification (Table 7). In addition, charred foodcrusts preserved on potsherds have been sampled in order to provide direct dates.

The dating of the levee sites (Table 7), on the other hand, could benefit from a better preservation of organic material, at least locally. At Bazel radiocarbon dating, which is still ongoing, mainly focused on unburnt bone and antler remains, among which a few tools (mattocks, chisel, etc). Most of these items were found intermixed with cultural remains, such as pottery fragments and lithic artifacts, within a max. 0.7 m thick peaty layer along the channel bank, interpreted as a dump area. So far no samples were selected from the levee top, where only charred remains occur. Hence, the obtained chronology might be biased to a certain degree. Further bias may come from the severe erosion and bioturbation (trampling) of the peat top in the dump area. The sharp boundary and the coarse sand texture of the sediment overlying this peat indicate an increase in fluvial activity which is likely to have caused partial erosion, at least in this lower part of the site (Deforce et al., 2014b). The most shallow dated finds were retrieved from a shell-rich clay layer covering the fluvial sand and peat.

The dating of the Melsele site, conducted in the late 1980s and early 1990s (Van Strydonck et al., 1995), is somewhat problematic. Most samples consist of charcoal retrieved from either natural pits (e.g. treefalls) or the coversand deposits, without clear anthropogenic connection, except for two samples of bark which were attached to the walls of a deep pit, tentatively interpreted as a storage-pit (Van Berg et al., 1992).

Site	Charcoal	Carbonized hazelnut shell	Bone	Calcined bone	Antler	Charred seeds	Foodcrust	Cereal grain	Wood/bark	References
Doel "Deurganckdok" B	3	2	–	9	–	3	16	–	–	Boudin et al. (2009) and Boudin et al. (2010).
Doel "Deurganckdok" C	–	–	–	–	–	–	–	1	–	Van Strydonck and Crombé (2005).
Doel "Deurganckdok" J/L	–	–	–	–	–	–	2	–	–	Boudin et al. (2009) and (Boudin et al., 2010).
Doel "Deurganckdok" M	2	3	–	6	–	4	4	–	–	Deforce et al. (2013).
Bazel "Sluis"	–	–	16	–	10	–	–	3	1	http://radiocarbon.kikirpa.be/
Melsele "Hof ten Damme"	10	1	–	–	–	–	–	–	4	Van Strydonck et al. (1995)

Table 7: List of radiocarbon dates related to the Final Mesolithic and Neolithic occupations of the excavated sites, classified according to dating material

5.3.2 Paleoenvironmental sampling

In the course of the last decades, numerous samples have been taken from the sediments covering the Pleistocene landscape, both on the prehistoric sites and on off-site locations. These were mainly used for studying the paleoenvironment through the analysis of various biotic remains, such as pollen, seeds and fruits, diatoms, and mollusks. A selection of these soil samples was also used for radiocarbon dating. In particular four levels have been intensively sampled: 1° the base of the basal peat; 2° the top of the basal peat; 3° the base of the Holland peat and 4° the top of the Holland peat (Figure 49). Because the basal peat layer that covered the well-drained Pleistocene sand was formed diachronically under the influence of rising groundwater, radiocarbon dating of samples at the base of this formation approximates the contemporaneous surfacing local mean high water level (LMHW) and the RSL through time. Since direct dating of the tidal Calais sedimentation is not feasible due to the potential presence of allochthonous organic material eroded from elsewhere, the top of the basal peat and the basis of the Holland Peat directly below and above the Calais deposits have been sampled. In our Bayesian model these samples provide a *terminus post quem* and *ante quem* respectively for the start and end of tidal activity. Dating the end of the peat growth is somewhat problematic since the top of the Holland peat could have been impacted by local erosion, peat digging, oxidation, etc. (Deforce, 2011; Denys and Verbruggen, 1989). Hence, dates from the peat top need to be interpreted as *terminus post quem*.

5.3.3 Dating

All samples were prepared using the conventional ABA (acid base acid) method. The vast majority was combusted and transformed into graphite at the Royal Institute for Cultural Heritage (Van Strydonck and van der Borg, 1990-1991). The oldest (bulk) samples were dated conventionally. AMS dating was performed at different laboratories, e.g. at Utrecht (UtC), New Zealand (NZA), Kiel (KIA) and recently also in Brussels (RICH).

All archaeological samples, except some from Melsele (Van Strydonck et al., 1995), were AMS-dated using identified single entity samples (Crombé et al., 2009b; Van Strydonck and Crombé, 2005). The quality of the environmental samples, on the other hand, is less consistent as sampling was done over a considerable period, starting in the eighties. Hence, the first dates have been conducted on bulk samples from peat, resulting in an average date. In addition most of these early dates still possess relatively large standard deviations, ranging between 75 and >100 BP years. More precise dates have been achieved when AMS dating was performed, reducing standard deviations to 30–40 years. More secure dates, however, have been obtained only recently using AMS dating

of identified terrestrial macrofossils (Verhegge et al., 2014). The results of these dating programs are listed in Appendices 3 and 4.

5.3.4 Bayesian modeling

Calibration, analysis and Bayesian modeling of the dates were performed using Oxcal 4.2 (Bronk Ramsey, 2009a) and the IntCal13 curve (Reimer et al., 2013). Bayesian modeling was only applied to the sites which yielded a considerable series of reliable radiocarbon dates, i.e. the dune sites of Doel Deurganckdok sector B and M and the levee site of Bazel (Table 7).

5.3.4.1 Doel Deurganckdok sector B and M

Comparative analyses at the Doel sites (Boudin et al., 2009; Boudin et al., 2010; Crombé et al., 2013c) have demonstrated quite convincingly that the radiocarbon dates obtained from samples of foodcrusts or calcined bones are highly problematic. Foodcrusts systematically produce older dates compared to charred plant remains, most likely a consequence of a reservoir effect resulting from the processing of freshwater fish in the vessels. The dates from calcined bones are even more problematic as some are compatible with the plant dates, while others are too old or too young. At present there is no conclusive explanation for these anomalies, but carbon exchange from the fuel might be partly responsible. Based on these observations, Bayesian modeling was only applied on the charred plant dates from Doel Deurganckdok sector B (8 dates) and M (9 dates) (Appendix 1).

Diagnostic artifacts at the dune sites of Doel Deurganckdok sector B and M indicate that they were occupied solely by the Swifterbant culture and no admixture with later Neolithic remains occur. The occupation area of these dune sites in a drowning landscape is limited by the rising groundwater, causing peat formation. Therefore Bayesian statistics was used to model the paleogroundwater rise using basal peat (Figure 49–2) samples from directly above the Pleistocene sediments (Figure 49–1). This resulted in the construction of an age-depth model with a regional ‘error envelope’ of the minimal and maximal age-depth of the starting peat growth modelled as a P-sequence with a k-factor chosen in relation to the elevation errors (Verhegge et al., 2014). The archaeological dates were simply plotted within this age-depth model (Figure 50).

The Swifterbant occupation of both sites has been modeled as a single Phase, consisting of two possibly overlapping sub-phases of the sector B and M sites, because no relation could be observed between them. The start Boundary and end Boundary, which are undated events determined by the dates within the Phase (Bronk Ramsey, 2001; Bronk Ramsey, 2009a), are used to estimate the start and end of Swifterbant occupation on the dunes.

These events could be further investigated because the paleo-environmental finds suggest the presence of a (supra-)tidal environment near the excavated hearths, causing the deposition of the Calais sediments. Therefore, Verhegge et al. (2014) have also analyzed the chronology of appearance and disappearance of this landscape using a Bayesian approach, assuming that the basal peat (Figure 49–2) growth ended diachronically with the intrusion of the tides in the lower parts of the landscape. If these tidal sediments are present in the sequence it can also be assumed that basal peat growth ended before the upper peat layer (Figure 49–4) restarted to grow. Therefore sequence was modelled as a phase of the peat dates from the top of (Figure 49–2) followed by a phase of the dates of the base of (Figure 49–4), separated by a sequential boundary.

Upon querying the order of the end boundary of the basal peat (Figure 49–2) (as a proxy for the start of Calais sedimentation (Figure 49–3) and the start boundary of the Swifterbant occupation of sector B and M, it was found that both were nearly contemporaneous. A similar query indicated that the end boundary of the Swifterbant occupation was followed distinctly later by the start boundary of Holland peat formation, which was also corroborated by the fact that a thin layer of Calais sediments covered the Swifterbant site at Doel Deurganckdok sector M.

Therefore both archaeological and sedimentological dates were integrated in a single sequence in order to be able to refine the chronology despite the lack of direct *in situ* stratigraphical relation (Figure 49). Based on the query results from the independently modelled archaeological and peat dates at Doel, the Swifterbant occupation phase of the dunes was modelled in a chronological sequence after the phase of the top of the basal peat with a contiguous boundary and before the base of the Holland Peat phase with a sequential transition boundary (Verhegge et al., 2014).

5.3.4.2 Bazel

At Bazel no dating problems are reported, hence all dates could be included in the Bayesian modeling. The archaeological dates were performed on materials recovered from either the peat (Figure 51–2), sand (Figure 51–3), or shell-rich clay (Figure 51–4). Most of the finds could be attributed to a single one of these sedimentary facies, the remainder (Loose Finds) could not be contextualized more precisely than originating from either one of these three (Appendix 1).

The dated ecological macro-remains were recovered from the sandy clay (Figure 51–1), peat (Figure 51–2), sand (Figure 51–3), shell-rich clay (Figure 51–4) and upper peat layer (Figure 51–5) (Deforce et al., 2014b; Appendix 2). The samples were assumed to be stratigraphically ordered between sedimentary facies but multiple dates from a single sediment were assumed to be randomly ordered. Furthermore, chronological gaps were assumed to be present between the dated sediments.

The Bayesian model assumed no chronological difference between archaeological dates and dated natural macroremains within as single stratigraphic context. As such the general model consisted of a sequence of 5 phases representing the deposition order of the stratigraphic units with sequential boundaries allowing for gaps in between. The phases of the stratigraphic units containing the archaeological artefacts were grouped as a single 'Bazel occupation' phase. The loose finds were modelled as a single phase chronologically overlapping with phases of units 2, 3 and 4 (Figure 51) within the occupation phase.

5.4 Results

The Bayesian modeling of the occupation revealed an individually outlying date in Doel Deurganckdok sector B (NZA-12076; Appendix 1). Upon closer examination, it was found that this date was retrieved from a hearth situated higher on the sand ridge, which could be related to the peat development (see further). As a result the posterior model of sector B and M revealed the occupation started between 6555 and 6395 cal BP (2 σ) and lasted until between 6170 and 5950 cal BP (2 σ) (Table 8, Figure 49). If the occurrence of an estuarine environment is included as a prior, the start can be refined to between 6535 and 6410 cal BP (2 σ) and the end to between 6175 and 5985 cal BP (2 σ) (Table 9). It is also clear that the first occupation is situated well above the regional peat level but the site terminates by the time or shortly after the regional ground water level surfaces at the elevations of the dunes (Figure 50).

Bayesian modeling of the Bazel data indicated one clear outlier date on a sample of a dog bone (KIA-47404: 7260 ± 50 BP; Appendix 1). However the stable isotopes (δ13C: -23.4; δ15N: 12.0) suggest a possible reservoir effect of this sample, explaining its older age (Ervynck et al. in prep.). Compared to the dune sites, the occupation at the levee site of Bazel lasted longer. It started between 7120 and 6885 cal BP (2 σ) and ended between 5605 and 5385 cal BP (2 σ) (Table 8, Figure 51). Unfortunately due to the advanced admixture, the radiocarbon dates at Bazel can be linked to specific cultural events or cultures only to a limited extend. Hence, the precise chronological range of the Swifterbant (or any other) occupation at Bazel cannot be determined. Remarkable, however, is the significantly lower frequency of radiocarbon evidence from the second half of the 7th millennium cal BP, coinciding with the main Swifterbant occupation of the nearby dune sites (Figure 51). The sequential boundary between dates recovered from the peat and the sand covering it, indicate a chronological gap in the archaeological finds starting between 6510 and 5995 cal BP (2 σ) and ending between 6280 and 5935 cal BP (2 σ) (Table 10). This gap is not precise, but seems to correlate with the occurrence of the Cal-

ais sediments in Doel and could relate to erosion (or a lack of occupation?). We hope that future dating of carbonized remains from the uneroded top of the levee will help us in solving this chronological problem.

Clearly the occupation at Bazel lasted longer than on the dune sites, but this is most likely due to its slightly higher topographical position (between ~0 and 0.5 m below mean low water tide level in Oostende) resulting in a somewhat later drowning of the levee. The youngest dates (ca. <6000 cal BP) are most likely connected with a Michelsberg culture occupation phase. A similar date KIA-14334: 5110 ± 35 BP (Van Strydonck and Crombé, 2005) has been obtained on a foodcrust sample at the nearby Michelsberg site of the dune site Doel Deurganckdok sector C. Despite the mentioned problems with this kind of sample, the bulk stable carbon and nitrogen isotopes of the residues of this site suggest processing of herbivore products and/or plant material, hence a reservoir effect can most likely be excluded (Craig et al., 2007).

Table 8: Modelled boundary dates of Bayesian model of the occupation at Doel and the occupation at Bazel (modelled years in cal BP).

Name	Modelled (cal BP)		
	From	To	%
Boundary Start Occupation Doel	6555	6395	95.4
Boundary End Occupation Doel	6170	5945	95.4
Boundary Start Occupation Bazel	7120	6885	95.4
Boundary End Occupation Bazel	5605	5385	95.4

Table 9: Modelled boundary dates of Bayesian model with the contiguous boundaries from a sequence of phases at Doel as prior (modelled years in cal BP).

Name	Modelled (cal BP)		
	From	To	%
Sequence Top basal peat_Swifterbant_Base Holland peat			
Boundary Start Top basal peat	6810	6480	95.4
Boundary Transition End Top basal peat to Start Swifterbant Occupation	6535	6410	95.4
Boundary End Swifterbant Occupation	6175	5985	95.4
Boundary Start Basis Holland peat	6085	5770	95.4
Boundary End Basis Holland peat	5595	5190	95.4

Table 10: Modelled boundary dates of Bayesian model including the stratigraphic sequence of dated macroremains of archaeological and geological origin at Bazel as prior.

Name	Modelled (cal BP)		
	From	To	%
Sequence Bazel			
Boundary Start pre-occupation	7340	6965	95.4
Phase Clay 1			
Phase OM rich Clay 1			
Boundary End pre-occupation	7140	6940	95.4
Boundary Start Occupation Bazel	7050	6885	95.4
Phase Occupation Bazel			
Phase Loose Finds			
Sequence peat-sand-clay2			
Phase peat			
Boundary end peat	6510	5995	95.4
Boundary start sand	6280	5935	95.4
Phase sand			
Boundary sand-clay2	5865	5680	95.4
Phase clay2			
Boundary End Occupation Bazel	5595	5445	95.4
Boundary Start post-Bazel	5575	5340	95.4
Phase OM rich Clay2			
Phase Wood Peat			
Boundary End post-Bazel	5300	4940	95.4

5.5 Discussion

One of the main conclusions of this study relates to the differential occupation dynamics between the inland dune sites and the levee sites. The chronology deduced from the analysis of cultural remains (Table 6) could be confirmed and further refined by Bayesian statistical modeling of the radiocarbon evidence. Although the dunes already attracted hunter-gatherers from as early as the Late Glacial and Early Holocene, and thus long before the drowning of the landscape started, there was a three millennia hiatus in their occupation that lasted from the mid-10th till the mid-7th millennium cal BP. They apparently waited until large areas of the landscape were inundated to set up camp. According to paleoecological analyses, the vegetation prior to this Middle Holocene estuarine influence maximum consisted of an alder carr in the lower areas and *Quercus* (oak), *Tilia* (lime) and *Corylus* (hazel) on higher elevations. Herbaceous species, such as *Cyperaceae* (sedge family) and *Poaceae* (grass family) only occurred in very small numbers, indicating a dense tree cover. It is well known that not all types of wetlands are equally diverse and productive (Nicholas, 1998). The dense leaf cover and absence of main open water systems not only resulted in limited undergrowth but probably also affected the game population. Herbivores in dense temperate forests mainly concentrate in small clearings and along the forest edges, the latter mostly situated along river valleys (Crombé et al., 2011a; Crombé et al., 2011c; Spikins, 1999; Svenning, 2002; Whitehouse and Smith, 2010). Dense tree cover would therefore not only decrease overall species abundance within this resource niche, but also increase its patchiness in space. Therefore, this environment was likely less productive to hunter-gatherers during the later Boreal and Early Atlantic periods than the resource niches forming along the larger clearings of the river valleys.

The vegetation during the subsequent period of increased estuarine influence is much more difficult to reconstruct by means of pollen due to the presence of allochthonous palynomorphs (Deforce et al., 2014a). Analysis of carbonized plant remains found at the prehistoric sites of Doel Deurganckdok sector B and M (Deforce et al., 2014a; Deforce et al., 2013) enables a fairly detailed picture of the vegetation on the dunes and in their direct vicinity. According to this evidence, the vegetation on the duneshad evolved into an alluvial hardwood forest dominated by *Quercus* sp., *Tilia* sp., *Ulmus* sp. (elm) and *Fraxinus excelsior* (ash) with a rich shrub layer (Figure 52). The presence of several lianas, e.g. *Hedera helix* (ivy) and *Clematis vitalba* (Old man's beard), and many light demanding shrubs, e.g. *Cornus sanguinea* (dogwood), *Ligustrum vulgare* (wild privet), *Craetagus monogyna* (common hawthorn), *Prunus spinosa* (sloe) furthermore suggests that much light penetrated to the trunk and ground level probably due to an uneven canopy. In the lower areas, however, *Alnus* woodland persisted. Alluvial forests like this occur under specific hydrodynamic conditions, i.e. in areas within a river floodplain that are

only very incidentally touched by inundations of short duration. The frequency of these inundations ranges from one time every few years to a few times in one year. More importantly, these alluvial forests are characterized by the highest species richness, productivity, and structural and successional complexity within the temperate forest ecosystems (for references, see Deforce et al., 2014a; Deforce et al., 2013; Deforce et al., 2014b). This might have been the main reason for the renewed human interest on these dunes. Archaeobotanical analysis (Deforce et al., 2013) demonstrated that the Swifterbant groups who settled on these dunes mainly consumed seeds, nuts and fruits from the trees and shrubs growing on the dunes, e.g. *Quercus sp.* (acorns), *C. sanguinea* (dogwood berries), *Corylus avellana* (hazelnut), *Malus sylvestris* (crab apples), *P. spinosa* (sloe plums) and *Viburnum opulus* (guelder rose berries). The presence of fish also constituted a supplementary value to the dune area. Thousands of calcined fish remains have been collected during excavations, the analysis pointing to the presence of large creeks with stagnant to slow running freshwater (Van Neer et al., 2013). Fishing focused mostly on cyprinids, among which road was the most prominent species. Anadromous marine fish species such as flatfish, thin-lipped mullet, and shad were also caught (and were particularly prominent in some hearths at Doel Deurganckdok sector M), which suggests temporary connections with the Scheldt river.

topographical position	valley floor	lower sand ridge	upper sand ridge	lower sand ridge	valley floor
substrate	peat/peaty clay	sand	sand	sand	peat/peaty clay
wetness	permanent wet	intermediate	dry	intermediate	permanent wet
inundation frequency	low	low	rare	low	low
vegetation type	alder carr	lower hardwood alluvial forest	upper hardwood alluvial forest	lower hardwood alluvial forest	alder carr
dominant trees	*Alnus glutinosa*	*Alnus glutinosa, Fraxinus excelsior, Ulmus*	*Tilia platyphyllos , T. cordata, Quercus*	*Alnus glutinosa, Fraxinus excelsior, Ulmus*	*Alnus glutinosa*
dominant shrubs	*Rhamnus cathartica, Viburnum opulus, Frangula alnus*	*Cornus sanguinea, Corylus avellana, Crataegus monogyna, Malus sylvestris, Prunus spinosa, Ligustrum vulgare*			*Rhamnus cathartica, Viburnum opulus, Frangula alnus*

Figure 52: Schematic reconstruction of the vegetation in relation with its topographical position and inundation frequency for the environment of the dune sites of Doel Deurganckdok sector B and M between ca. 6500 and 6000 cal BP (from Deforce et al., 2014a; Deforce et al., 2014b).

Also, the availability of *Viscum album* (mistletoe) and *Hedera helix* (ivy) might have contributed to the attractiveness of these sites. The large numbers of charcoal from *Viscum album* (mistletoe) and seeds from *Hedera helix* (ivy) at both dune sites, have been interpreted as an indication for animal husbandry from the mid of the 7th millennium cal BP onwards (Deforce et al., 2013). Both plants are evergreens, and were commonly used as winter leaf fodder during (pre)historic times, as documented by plenty of archaeobotanical and historical data. Unfortunately the high degree of fragmentation of

the thousands of burnt mammal remains does not allow us to test this hypothesis, but the existence of animal husbandry in the Lower Scheldt basin at least from ca. 6250-6000 cal BP, if not earlier, has been demonstrated by several radiocarbon dates from the levee site of Bazel (Ervynck et al. in prep.; Appendix 1). One bone fragment of a possible domesticated pig (determination Anton Ervynck) was dated to ca. 6900–6700 cal BP (KIA-47395; Appendix 1). However, further analyses are in progress in order to confirm the domesticated character of this find.

The end of the dune occupations coincided with renewed peat growth in the area ca. 6300 and 5760 cal BP. Peat gradually covered the higher parts of both dunes, replacing the hardwood forest vegetation by alder carr and making further human settlement impossible. At the dune site of Doel Deurganckdok sector M, the Swifterbant occupation was already confined to a small zone hardly 15–20 m wide, leaving not much extra space. Moreover, the presence of a very thin layer of estuarine sediments covering the settlement remains indicates that probably the Swifterbant occupation came to an end already before peat growth resumed. At the other dune site in sector B, the radiocarbon evidence demonstrates a gradual shifting of the Swifterbant occupation towards the higher parts of the dune at the end of the 7th millennium cal BP. From the start of the 6th millennium cal BP occupation was no longer possible except on the few highest sand dunes within the area, such as in sector C at Doel Deurganckdok. Here a small Michelsberg site, dated to around 5930-5740 cal BP, was found, situated ca. 0.5 m higher than the adjacent Swifterbant site. The currently available archaeological data indicates that hereafter human occupation in the dune area ceased until (late) Medieval times (Crombé, 2005).

The radiocarbon evidence, combined with the cultural data, demonstrate that the occupation of the levee sites started much earlier and had greater potential for continuous settlement compared to the dune sites. Despite not being able to determine the specific durations of settlement due to bioturbation, diagnostic material culture evidence at the site of Bazel suggest that the site was occupied throughout all stages of the Mesolithic till the start of the Neolithic. Here too the end of the occupation coincides perfectly with the drowning of the levee, which started around ca. 5250 cal BP with the deposition of Holland peat. The important role of these levee sites for Mesolithic and Early-Middle Neolithic settlements can most probably be explained by the presence of a paleochannel, providing constant drinking water, transport facilities, and also high potential for prey aggregations and biodiversity along its productive margins. In addition, a hardwood alluvial forest was already present on these levees from at least ca. 7060 cal BP (Deforce et al., 2014a), which indicates a more stabilized and therefore productive resource niche for almost half a millennium earlier compared to the dune sites (Figure 53).

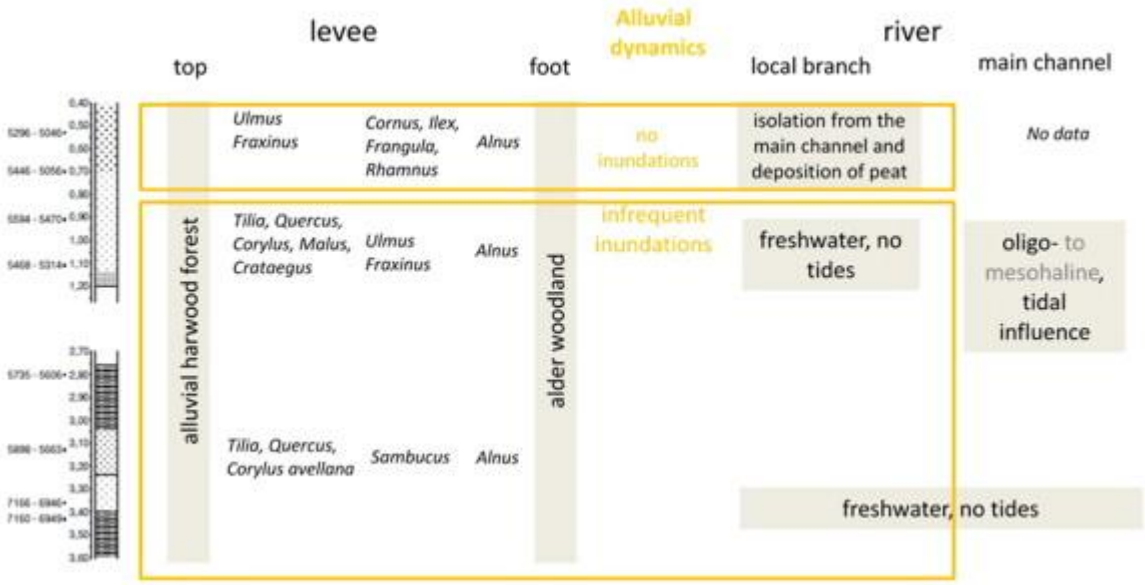

Figure 53: Synthetic presentation of the alluvial dynamics and associated vegetation types on the top and flanks of levee site of Bazel and in the nearby river Scheldt.

The importance of the Scheldt for transport and communication is evidenced by the presence of exotic pottery on both levee sites. At Bazel numerous potsherds have been recorded that, based on techno-typological (form, temper, etc.) and decorative features, can be linked to different Neolithic groups living in the southern loess area of the Upper and Middle Scheldt, such as the Late LBK, Limburg pottery tradition, and (Epi)Rössen (Crombé et al., in press-a). At Melsele the presence of decorated pottery related to the Blicquy tradition has been reported (Van Berg et al., 1992). These finds clearly point to repeated contact between local foragers and southern farmers along the Scheldt floodplain from at least ca. 7000 cal BP onwards. These contacts probably played an important role in the gradual neolithization of the area through the exchange of valuable commodities and technological transfers. One of the first steps in this process was probably the local production of (Swifterbant) pottery, at least from ca. 6500 cal BP onwards. Based on techno-typological similarities and the presence of decorated exotic pottery it is assumed that pottery knowledge was adopted from contemporaneous (Epi)Rössen farmers from the southern loess area (Crombé et al., in press-a). Simultaneously (cf. botanical evidence) or slightly later (cf. faunal evidence) stock-breeding of cattle, pig, and sheep/goat was practiced, followed by local agriculture around ca. 6000 cal BP.

The complete absence of exotic pottery on the dune sites is remarkable, but may point to functional or seasonal differences between the two types of sites. One hypothesis is that the Swifterbant settlement system during the second half of the 7th millennium cal BP consisted of a combination of semi-permanent base camps situated on the levees and temporary camps on the inland dunes. Alternatively, both site types may have been functionally similar but just represent seasonal differences in occupation. Choosing between these two models is currently unlikely for two reasons. First, seasonality analyses have not yet been conducted for both levee sites. Secondly, seasonality of

the dune sites can only be deduced from carbonized remains, which gives a biased picture as some seasonal indicators might not have been preserved. Furthermore, most of the studied charred seeds and fruits have been collected for food and might have been stored for a certain period of time. However, mistletoe and ivy seeds are reliable indicators for winter/early spring as during other seasons, much better suited taxa are available as fodder (Deforce et al., 2013; Van Neer et al., 2013). This is in agreement with seasonal information deduced from the anadromous fish remains, especially at Doel Deurganckdok sector M, which also points to a (late?) winter/spring occupation(s) (Van Neer et al., 2013). Especially shad is a good seasonality indicator because these species start their spawning run in spring. However, all this does not necessarily imply that humans did not visit the dunes during other seasons.

Despite all these restrictions, the land use model with levee base-camps and specialized dune camps seems more plausible but needs to be further tested by direct evidence. The dune sites could be viewed as temporary camps, visited by herders that left the levee base camps with their cattle in search for additional leaf fodder while carrying out hunting (wild boar, red deer and roe deer) and fishing (Figure 54). They did this specifically during winter and spring when other possible sources of fodder had become scarce. The relatively small size of these dunes means that they would have been highly predictive resource niches for terrestrial prey, and therefore would have required low energy expenditure to hunt, process, and return the acquired prey back to camp. The majority of the evidence for fishing comes from very small species ranging from ca. 10–15 cm in length, which suggests the use of stationary fishing gear such as traps and nets (Van Neer et al., 2013). While fish might have provided relatively low protein yields, the nature of the fishing was also such that traps or nets could be set while other activities such as hunting were carried out. The complete absence of exotic pottery also corroborates the status of these sites as non-residential rather than residential settlements. One may expect that exchanged goods were highly valuable and thus were not taken along during expeditions in the surrounding area.

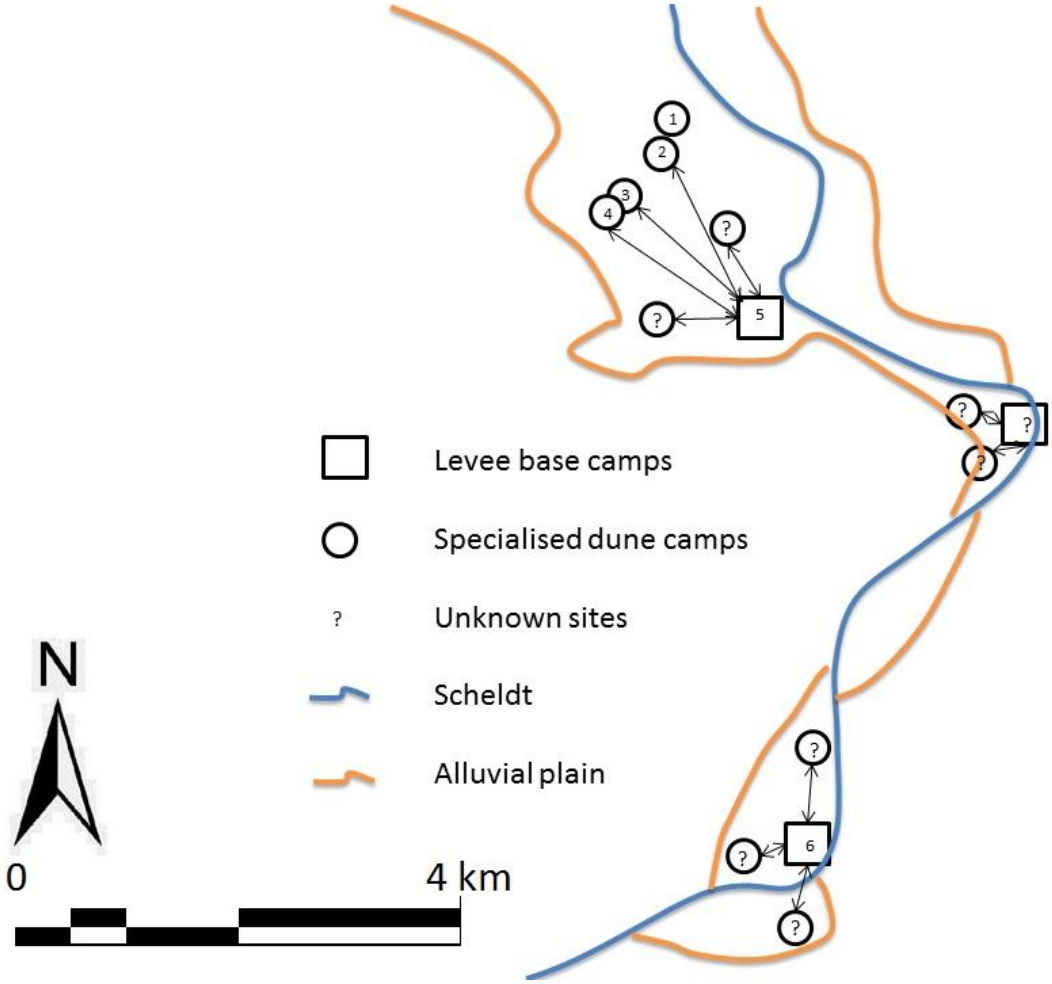

Figure 54: Tentative and schematic reconstruction of the Swifterbant settlement system in the Lower Scheldt floodplain.

The preliminary model that we propose here can be verified by future excavations of new levee and dune sites and comparative analyses of the lithic assemblages from all six previously excavated sites. We expect that more dune sites can be found, for example, around Melsele, and other levee and dune sites can be found at other locations along the Scheldt valley (Figure 54). In terms of the lithic assemblages, on the dune sites we expect minimal cortical and primary stage debitage, alongside high tool-flake ratios and a preponderance of microdebitage. We also expect a greater diversity of (exotic) lithic raw materials at the levee sites. Further petrographical and geochemical research is required not only for the lithic finds but also the ceramic finds, as these studies will help test and refine the model. We must also contend with the problem of dissecting the latent stratigraphy at Bazel by means of raw materials and techno-typological diagnostics.

5.6 Conclusion

Recent excavations in the lower Scheldt basin have helped advance our knowledge of the role of the Swifterbant culture during the Mesolithic–Neolithic transition in the southern North Sea basin. In this paper we integrated dates from six Swifterbant sites with dates from peat sequences in order to understand the chronological relationships between the occupation of levee and dune sites and hydrological changes in the surrounding wetland landscape. Bayesian statistical modeling suggests that Swifterbant occupation of the three dune sites occurred during a brackish water flooding period and that the levee sites were more stable and could sustain populations throughout the later part of the Mesolithic to the Middle Neolithic. This evidence for differential occupation histories of levee and dune sites enabled the development of a preliminary land use model for the Swifterbant occupation of this area. This model consists of relatively specialized and temporarily inhabited cattle and hunting-fishing camps on the dunes and larger, more continuously occupied levee camps along the river valleys.

We do not intend this model as a general model of Swifterbant land use systems throughout the entire geographical and chronological range of this culture, but rather as a specific model for Swifterbant occupation in the lower Scheldt basin. We agree with Raemaekers (1999) that the Swifterbant had many different kinds of mobility and land use strategies, and that we should not expect to find a single form of Swifterbant mobility. The six sites excavated in the lower Scheldt not only help us better place the Swifterbant within the chronological spectrum of the Early-Middle Neolithic LBK/Limbourg, Blicquy, Epi-Rössen, and Michelsberg cultures, but also give us the best picture thus far of a Swifterbant land use system from different types of neighboring sites that were inhabited during the same "middle phase" Raemaekers (1999).

Ideally, our model will not only be tested by further research in the lower Scheldt, but also extended to tests in other micro-regions throughout the entire Swifterbant cultural distribution. These further tests will help to refine the model and hopefully get us closer to understanding the specific ways in which indigenous Mesolithic foragers interacted with farmers and incorporated agriculture into their traditional socioecological systems in different regions along the southwestern North Sea basin.

Chapter 6 Reconstructing Early Neolithic paleogeography: EMI-based subsurface modelling and chronological modelling of Holocene peat below the lower Scheldt floodplain (NW Belgium)

This chapter is adapted after Verhegge et al. (submitted-b)

Well-preserved prehistoric landscapes and sites have been found, buried deeply below the Holocene peat or floodplain deposits of Waasland Scheldt polders. During the Middle to Late Holocene, Late Weichselian (river) dunes within the floodplain and river flanks were favored locations for Final Early Neolithic occupation. Available living space was determined by the dune topography and elevation of the peat at that time. Therefore an elevation model of the peat base was created using multi-receiver electromagnetic induction survey data. Electrical conductivity data of dune were collected and 1-D inverted within a 3-layered soil model with variable electrical conductivity of the top layer and variable depth to the base of the middle layer (i.e. the peat). The modelled peat base depth was calibrated, validated and eventually replaced by depth data from coring and cone penetration measurements wherever depth modeling from inverting the EMI measurements proved inaccurate. Using the resulting peat base elevation model, a paleogeographic map at the time of the modelled end date of Mesolithic-Neolithic transitional Swifterbant culture sites nearby was by chronologically modelleing the peat elevation at that time. The developed paleogeographic mapping methodology can be used for subsequent archaeological prospection by core sampling or to contextualize excavated sites.

6.1 Introduction

Large parts of the prehistoric landscapes buried deeply below the alluvial and estuarine plain of the lower Scheldt have been destroyed over the last decades in the context of Antwerp harbor expansion. Rescue excavations of prehistoric sites dating from the Final Paleolithic to the Early Neolithic often had to be done on the spot during construction of harbor docks due to a lack of preliminary prospection and failing legislation (Crombé, 2005). Current and future expansions in the region are an incentive to develop adequate prospection strategies (De Clercq et al., 2012; De Clercq et al., 2011), starting with lithostratigraphic and paleotopographic subsurface mapping, followed by a chronological landscape reconstruction and finally by archaeological core sampling (Bats, 2007; Crombé and Verhegge, 2014; De Clercq et al., 2011) to determine the presence of well-preserved but mostly featureless, lithic scatter sites (Sergant et al., 2006a). The reconstructed paleolandscapes can also be used to contextualize known prehistoric sites (Vos et al., in press).

6.1.1 Landscape evolution and prehistoric archaeology of the study region

The wider study region of this paper is the Waasland Scheldt polders geomorphological unit (De Moor and Pissart, 1992). During the Late Weichselian Pleniglacial period, a large Pleistocene valley (a.o. the precursor of the lower Scheldt valley), called the "Flemish Valley" (Vlaamse Vallei), was gradually filled with fluvioglacial sediments (De Moor and Heyse, 1978a; Heyse, 1979). At the end of this period, during the Older Dryas and Bølling, the valley sediments were reworked into large coversand ridges by aeolian activity. The flanks of these ridges were subsequently occupied by humans from the Federmesser culture during the Allerød period (Crombé et al., 2013a).

During the last Pleniglacial, the braided Scheldt river, settled in its present day trajectory via Antwerp after having breached the Paleogene cuesta near Hoboken (Kiden, 2006; Kiden and Verbruggen, 2001). An evolution to a meandering river system with oxbow lakes took place before and during the Allerød (Bogemans et al., 2012; Crombé, submitted). Despite the reduced fluvial activity at the end of the Allerød and during the Younger Dryas, the Scheldt did not leave is meandering channels. Nevertheless, vertical sedimentation of calcareous gyttja started in the deepest channels of the Scheldt from the Younger Dryas onwards (Crombé, submitted; Kiden, 2006; Meylemans et al., 2013). During the Younger Dryas, renewed aeolian activity resulted in local reworking of the coversand ridges and river interfluvia of the Scheldt valley into (river) dunes (Bogemans and Vandenberghe, 2011; Hilgers, 2007; Kasse, 2002; Kiden, 2006). These were favored

settlement locations throughout the later (pre-)history, because the floodplain was gradually wetting during the Holocene (Crombé, 2005; Vos and van Heeringen, 1997) as a consequence of sea level rise (Kiden, 1995; Kiden et al., 2002). During the early Holocene period alder carr peat started to develop, starting in the river channels peat and gradually invading the floodplain. Peat first covered the deepest depressions (Deforce, 2011), while dry landscape positions were occupied by the Early Mesolithic humans. Occupation of the dunes ceased during the Middle and Late Mesolithic when peat started to cover the wider floodplain (Crombé et al., in press-b).

Due to erosional coastal processes downstream, a (supra-)tidal influence of the Scheldt estuary expanded into the study region between 6620-6200 cal yr BP (95%) (Verhegge et al., 2014), resulting in the occasional deposition of OM rich clay on top of the peat in the floodplain and on the flanks of the dunes (Deforce, 2011; Gelorini et al., 2006). The resulting alluvial hardwood landscape (Deforce et al., 2014a) made dry landscape river dunes attractive to seasonal Final Mesolithic/Early Neolithic Swifterbant occupation from the start of the (supra-)tidal influence (Verhegge et al., 2014). This resulted in the formation of spatial palimpsest dune sites, while levee sites along the Scheldt are characterized by a more continuous occupation starting before and ending after this period, which resulted in cumulative palimpsest sites (Crombé et al., in press-b; Deforce et al., 2013; Deforce et al., 2014b; Van Neer et al., 2013).

The estuary retreated gradually as the coastal barrier restored itself and peat formation renewed (Vos and van Heeringen, 1997) between 6300-5760 cal yr BP (95%) (Verhegge et al., 2014). No indication about prehistoric occupation in the floodplain during the period of renewed peat formation has been found.

An important gap in our knowledge of local prehistory still exists, as the dated Swifterbant occupation on the excavated dune sites of Doel Deurganckdok sector B & M (Crombé et al., in press-b) (Figure 55: bottom inset map), apparently stopped before peat started to grow again. At sector M the end of the occupation probably was caused by (occasional) flooding of the dune top (Verhegge et al., 2014). It is assumed that occupation shifted to higher locations, which have not been archaeologically explored so far. Investigation of these potential (more elevated) Swifterbant- or Middle Neolithic Michelsberg sites could add valuable information about the relation between the changing landscape and its changing occupation patterns.

During the (early) Middle Ages, marine incursions gradually halted peat formation and resulted in the formation of tidal mudflats, with clayey sedimentation, and erosive tidal channels, characterized by more sandy sedimentation (Jongepier et al., 2015). This estuarine landscape was reclaimed during various embankment attempts from the (Post) Middle Ages onwards (Mys, 1973).

6.1.2 Prospecting buried prehistoric archaeological landscapes and sites

Over the past years, survey strategies have been developed for paleolandscape mapping, using mechanical coring and/or manual Dutch and gauge augering with a diameter of maximally 6 cm, and for archaeological survey, using Dutch augers with a diameter of minimally 10 cm (Bates and Bates, 2000; Bats, 2007; Crombé and Verhegge, 2014; De Clercq et al., 2012). Using this strategy, large physical and financial efforts are required to cover the lateral variability of large areas comprehensively. These efforts rise exponentially as the required coring grid size decreases and the core sampling depth increases.

As not all lithostratigraphic information from every gridded core is useful for paleotopographic mapping, alternative methods to map the prehistoric topography on a landscape scale are investigated, as part of an interdisciplinary project exploring the archaeology at the land-sea transition using both geophysical- and geotechnical methods (Verhegge et al., 2012). A more limited number of calibration and validation corings are always required to allow a lithostratigraphic interpretation of both methods, however.

(Gridded) cone penetration testing (CPT) was already investigated as a suitable and direct alternative to conventional coring in the Scheldt floodplain. Using CPT, greater depths are reached more rapidly and the depth of lithological transitions can be determined more accurately (Missiaen et al., 2015). Near-surface geophysical methods have a smaller depth resolution compared to corings, but the non-invasiveness allows higher lateral data densities. Such methods are widely employed for mapping of river floodplains both in geological (Gourry et al., 2003) and in archaeological contexts (Howard et al., 2008). Theoretically, ground penetrating radar would be the best alternative to coring in dry sandy river floodplains (Vandenberghe and van Overmeeren, 1999), to map lithological transitions with a high depth resolution (Conyers, 2013). In our study region, the radar pulse would be attenuated by clayey soil material and shallow groundwater, however. Therefore, electrical resistance- and electromagnetic induction (EMI) survey is often used to map buried river floodplains (Bates and Bates, 2000; Bates et al., 2007; Bates and Stafford, 2013; De Smedt et al., 2013b; De Smedt et al., 2011a; Howard et al., 2008). EMI derived apparent electrical conductivity (σ_a) maps delineate clear geometric patterns of the depositional floodplain units (Conyers et al., 2008) and of buried sedimentary litho-facies ranging from dune or levee sand to floodplain clay or peat (Brown, 1997).

Electrical resistivity-, shear wave seismic- and EMI survey methods have been explored already by Verhegge et al. (submitted-a) in the Scheldt polders. Success is challenged significantly by the depth of burial, the complexity and sedimentary contrast of the overlying (post-) medieval estuarine landforms (e.g. Jongepier et al., 2015). Furthermore, the variability of the level and brackishness of the local groundwater (Goes et

al., 2009) sometimes masks sedimentary σ_a contrasts. Nevertheless, the results from Verhegge et al. (submitted-a) showed that qualitative interpretation of σ_a data from a single EMI coil pair already improved the lateral mapping of buried (prehistoric) landscape units significantly, if integrated with information from corings or CPTs.

Simultaneous registration of σ_a from multiple soil volumes using a mobile EMI instrument with multiple coil configurations allows a more quantitative interpretation of the results through 1-D depth modelling of simplified subsurface layering (Saey et al., 2008). Recently such instruments and modelling approaches have been applied to model the depth of (Post) Medieval gullies in estuarine floodplains (De Smedt et al., 2013a; Saey et al., 2012b) and to 'depth slice' moated sites (Saey et al., 2012a). Due to the beforementioned issues, modelling the depth to the prehistoric landscape (i.e. the base of the peat layer) below the polders is even more challenging in our study region.

If inverted depths from the interfaces between different stratigraphic layers could be acquired however, this would be a reliable base to create local paleogeographic maps of the Holocene, as already created on a larger scale in the Netherlands (Vos et al., 2011; Vos et al., in press; Vos and van Heeringen, 1997). Due to the cost of (mechanical) coring, generally a selection has to be made of the reconstructed paleolandscape for subsequent archaeological sampling (Crombé and Verhegge, 2014). The strong link between prehistoric land use choices and the contemporaneous landscape (e.g. Crombé et al., in press-b), permits that such selection is made using paleogeographic and/or geogenetic mapping in combination with knowledge and knowledge gaps of the regional prehistoric occupation history (Vos et al., in press).

Identifying the presence of actual prehistoric sites is only possible through soil sampling of possible archaeological strata. After sieving, the sample residue is checked for archaeological site indicators such as flint artefacts (e.g. chips), charred plant remains (e.g. hazelnut shells) and (burnt) bone fragments (Bats, 2007; Crombé and Verhegge, 2014; De Clercq et al., 2011; Groenewoudt, 1994; Verhagen et al., 2013). Because of the large diameters (min. 10 cm) and dense grids (max. 10 m) required, expensive mechanical coring is required for archaeological sampling at depths below 2-3 m, or underneath the ground water table, if a sandy overburden is present. Therefore, the vertical and horizontal extend of the soil layering has to be reconstructed as accurately as possible in the first place. Based on such models, efficient continuous coring of the archaeological strata is possible. Discontinuous mechanical coring could further increase mechanical coring efficiency if only possible archaeological strata are sampled and the core sampler is kept closed while penetrating the geological overburden. An accurate depth model of the base of the peat is required to allow discontinuous coring to sample Final Mesolithic to Early Neolithic levels in the study region. Such model needs a lateral resolution of 10 m or less, as this is an appropriate coring grid for detecting a broad range of prehistoric sites (Crombé and Verhegge, 2014). The maximal vertical (depth) error to

allow discontinuous sampling of the peat base is related to the thickness of the archaeological strata and the length of the core sampler sections used.

Assuming that the thickness of the archaeological strata is 0.5 m and a 2 m long core sampler is used, the surface model of the peat base should have an overall absolute depth modelling error below 0.75 m to allow discontinuous core sampling of the complete vertical spreading of the finds. If the errors are larger, continuous coring methods have to be used for archaeological sampling, retrieving the full lithostratigraphic sequence.

6.2 Aims and objectives

The main aim of this paper is to establish the potential of depth modelling of multi-receiver EMI in the study region through comparison of the inverted depths with coring and CPT results, beyond the qualitative interpretation of single coil spaced EMI, imposed by the regional geological complexity (Verhegge et al., submitted-a). Specific objectives are to model the base of the peat integrating the surface-covered EMI-derived simultaneous σ_a measurements, employing corings and CPT's as calibration and validation tools on a prehistoric dune site, which is representative for the larger study region and beyond. Radiocarbon dating of the basis of this peat layer should aim at a local paleogeographic reconstruction.

6.3 Survey area

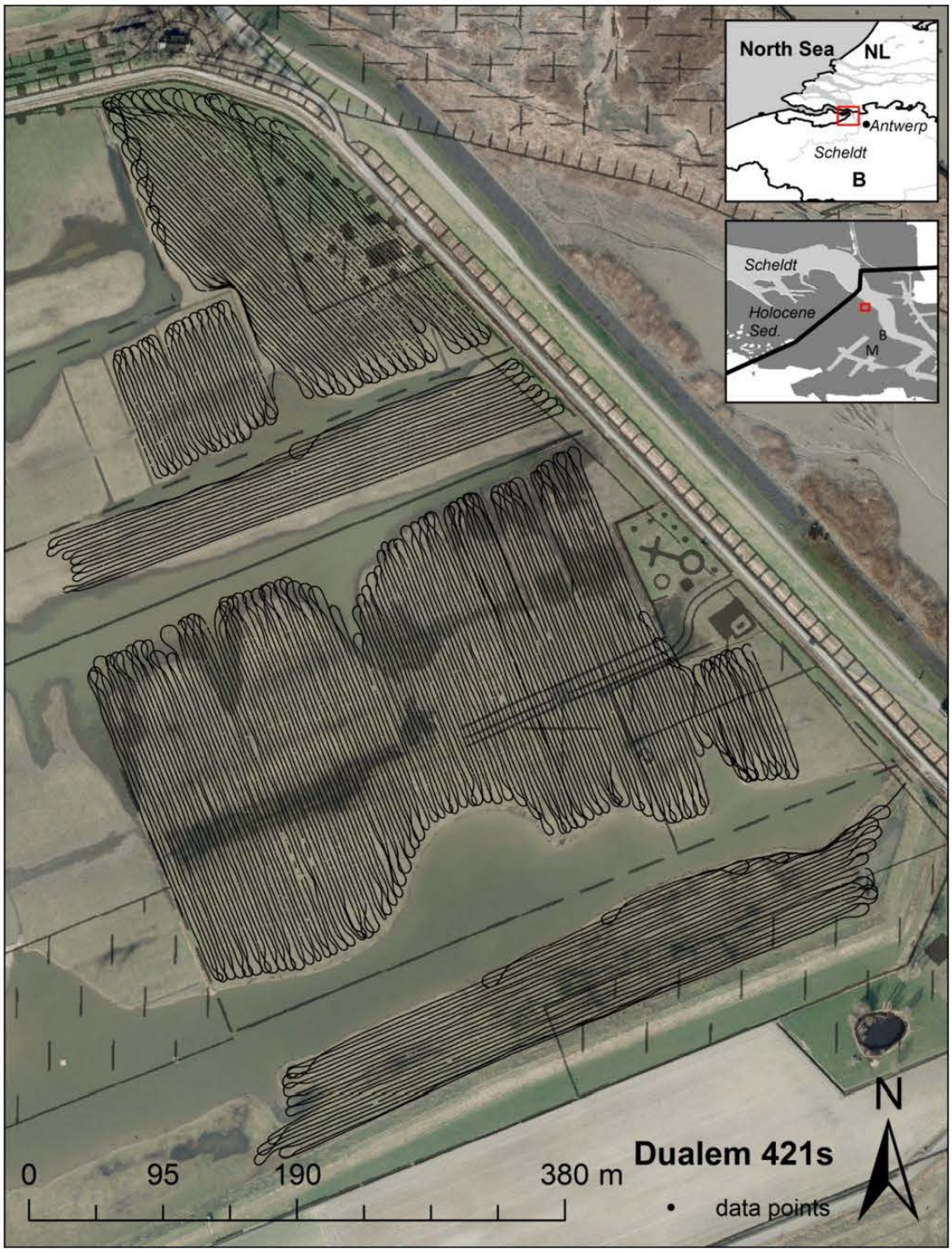

Figure 55: Survey lines measured with Dualem 421s instrument on top of midscale orthophoto (©AGIV, winter 2014) and topographic map (©NGI, 1993). Inset maps: top: location of the study region of the Scheldt polders, Bottom: location of the survey area within the Holocene marine sediment region (Polders) of the Scheldt floodplain; B/M: Doel Deurganckdok sector B and M site respectively.

The selected survey area is part of the nature reserve of Doelpolder Noord. Doelpolder is amongst the earliest remaining embanked floodplains (i.e. polders) on the left bank of the Scheldt river (Jongepier et al., 2015; Mys, 1973). This has resulted in a well-preserved underlying prehistoric landscape. Doelpolder Noord is situated north of the Antwerp harbor, in close proximity to the border between Belgium and the Netherlands (Figure 55-top inset map). Recently, tidal ditches were dug based on the (Post) Medieval drainage ditches during its conversion to a nature reserve. The local top soils are moderately bad to badly drained, clay to heavy clay according to the Flemish soil map (Van Ranst and Sys, 2000). The digital elevation model (DEM) of the survey area (Figure 64c) ranges roughly between 2.5 and 3.5 m above national ordnance level (TAW = mean low water tide level in Oostende) and is determined by (Post) Medieval to modern filled-up tidal creeks and drainage ditch systems (AGIV, 2001-2004; Klinck et al., 2007). Manual coring data obtained during the geoarchaeological evaluation of Doelpolder Noord, prior to its conversion, revealed a dune buried between 2 and 6 m deep, flanking a large depression with the (peat) base reaching up to 9 m below the surface. Both are covered with peat and estuarine sediments (Klinck et al., 2007). Because of the known attractiveness of such dunes to prehistoric humans, this area was chosen as a geophysical and geotechnical survey laboratory. The proximity of the Scheldt estuary, the variable depth and estuarine nature of the geological overburden of the prehistoric landscape, make the survey area representative for the challenging conditions in other embanked estuarine floodplains as well.

6.4 Materials and Methods

6.4.1 Dualem 421s survey

Using a mobilized Dualem 421s (Dualem inc., Milton, Canada) low frequency domain electromagnetic induction sensor (Figure 56), σ_a data from multiple soil volumes were collected on 1st, 2nd and 5th of August 2013. Low and high tide on the Scheldt, just outside the embankments, ranged between 0.09 and 5.15 m TAW during the survey (Watlab, 2013) but did not influence the survey results.

The Dualem 421s instrument records both in-phase (IP) and quadrature phase (QP) response to an induced field with a frequency of 9 kHz. Data are registered both in horizontal coplanar (HCP) coil configuration with 1, 2, 4 m separation and in perpendicular (PRP) coil configuration at 1.1, 2.1 and 4.1 m separation between the one transmitter coil and six receiver coils. σ_a is derived linearly from QP within low induction number conditions (LIN) (McNeill, 1980).

The instrument was mobilized in a quad pulled and metal-free sled. The axis between transmitting and receiving coils was oriented parallel with the survey lines and elevated 16 cm from the surface. Responses were registered at 8 Hz while driving 7-8 km/h on parallel lines every 3 m. Positioning was achieved in the Belgian Lambert '72 coordinate system using an Omnistar DGNSS antenna, accurate to about 0.1 m. The antenna was mounted on the pulling vehicle.

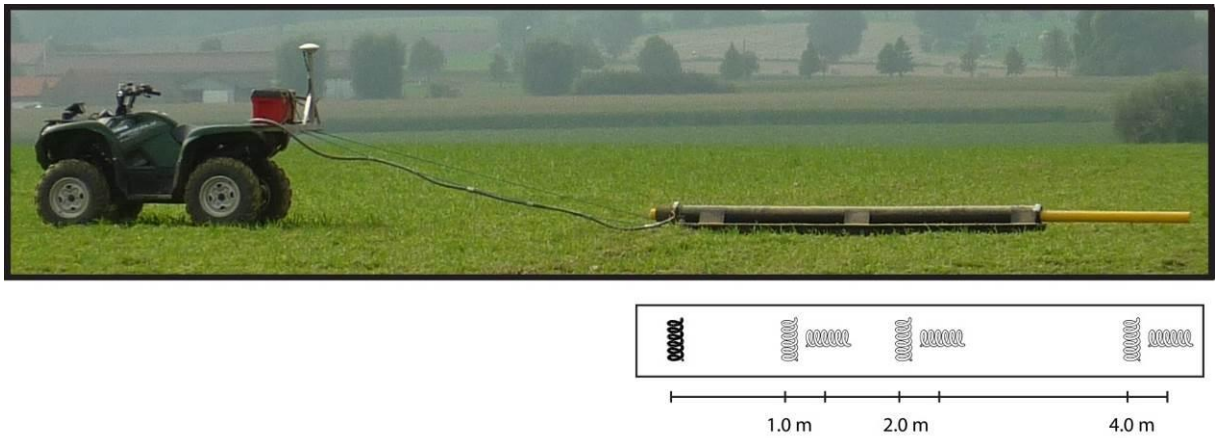

Figure 56: Top: mobile survey setup for the Dualem 421s sensor, consisting of the sensor in a sled which is pulled by a DGNSS located quad bike; bottom left: transmitter coil (black) and six receiver coils (white)

Processing of the survey data included position shift- and sensor drift correction using the methodology developed by Delefortrie et al. (2014a). The data points of the various configurations were recalculated to common coordinates and interpolated using ordinary kriging (Goovaerts, 1997).

6.4.2 Calibration and validation data

Calibration and validation data of the subsurface lithostratigraphy were available from recent CPTs (Missiaen et al., 2015), archaeological sampling drillings (Verhegge et al., submitted-a) and legacy hand augerings (Klinck et al., 2007). Conductivity CPTs have shown that the peat acts as an electrical conductor in a resistive medium if no brackish groundwater is present outside the peat layer (Verhegge et al., submitted-a). Therefore the depth to top (z_1) and base (z_2) of the peat layer were selected as calibration data at 11 locations across the dune (Figure 64B) and as validation data at 204 points spread across the survey area and clustering on the top of the dune (Figure 64C). The depths recorded from CPTs can be considered very accurate to about 0.2 m (Missiaen et al., 2015). Larger inaccuracies (0.2-0.5 m) have to be kept in mind to account for the depths derived from corings, due to coring difficulties imposed by the variability of the sediments (Verhegge et al., submitted-a).

6.4.3 Subsurface modelling

The cumulative electrical conductivity response (expressed as % of the measured signal, relative to 1) from the soil volume above a depth *z* (in m) was given by McNeill (1980) for the vertical ($R_{HCP}(z)$) dipole mode and by Wait (1962) for the perpendicular ($R_{PRP}(z)$) dipole mode:

$$R_{sHCP}(z) = 1 - (4 \cdot \frac{z^2}{s^2} + 1)^{-0.5} \quad (1)$$

$$R_{sPRP}(z) = 2\frac{z^2}{s^2}\left(4\frac{z^2}{s^2} + 1\right)^{-0.5} \quad (2)$$

with *s* being the transmitter-receiver spacing in m.

Consequently, the depth of investigation (DOI) (or the depth at the 70 % cumulative response) values are 0.5 m, 1.0 m, 2.0 m, 1.6 m, 3.2 m and 6.4 m for the 11PRP, 21PRP, 41PRP, 1HCP, 2HCP and 4HCP coil configurations, respectively.

Based on the calibration observations, a three layered subsoil stratification model was proposed, with a top layer with variable conductivity σ_1^* above a peat layer with constant conductivity σ_2 overlying a lower layer with fixed conductivity σ_3. The interface between the top and peat layer was taken at a constant depth (z_1) of 2.1 m, or the average depth deduced from the calibration observations.

Firstly, we propose to model the variable top conductivity σ_1^*, or the conductivity up to a depth z_1 of 2.1 m, from the σ_a measurements of all 11PRP and 1HCP coil configurations.

In a three-layered soil build-up, multiplying the relative weight with the σ of each layer and adding up all the layers results in the total $\sigma_{a,sHCP}$ and $\sigma_{a,sPRP}$ of the investigated medium:

$$\sigma_{a,sPRP} = [R_{sPRP}(z_1) - R_{sPRP}(z_d)] \cdot \sigma_1 + [R_{sPRP}(z_2) - R_{sPRP}(z_1)] \cdot \sigma_2 + [1 - R_{sPRP}(z_2)] \cdot \sigma_3 \quad (3)$$

$$\sigma_{a,sHCP} = [R_{sHCP}(z_1) - R_{sHCP}(z_d)] \cdot \sigma_1 + [R_{sHCP}(z_2) - R_{sHCP}(z_1)] \cdot \sigma_2 + [1 - R_{sHCP}(z_2)] \cdot \sigma_3 \quad (4)$$

with z_d the distance of the instrument above the soil surface (0.16 m).

Next, we considered a two-layered soil model with the boundary between both layers at 2.1 m.

$$\sigma_{a,sPRP} = [R_{sPRP}(z_1) - R_{sPRP}(z_d)] \cdot \sigma_1^* + [1 - R_{sPRP}(z_1)] \cdot \sigma_2^* \quad (5)$$

$$\sigma_{a,sHCP} = [R_{sHCP}(z_1) - R_{sHCP}(z_d)] \cdot \sigma_1^* + [1 - R_{sHCP}(z_1)] \cdot \sigma_2^* \quad (6)$$

The resulting conductivity of a top layer with variable conductivity σ_1^* and the conductivity of the layer deeper than 2.1 m (σ_2^*) was modelled at the 122 803 σ_a measurement locations separately. All simultaneous σ_a measurements of the Dualem-421S HCP

and PRP configurations were combined to model σ_1^* and σ_2^*. This system of equations was solved with Matlab using the Levenberg–Marquardt algorithm (Marquardt, 1963).

At the 11 calibration locations on Figure 64C, both the depth between both top and peat layer z_1 and between the peat and the sub layers z_2 were measured. With these calibration observations, the fixed conductivities of both peat and sub layers were modeled separately for both the 4HCP and 4HCP coil configurations, or the configurations with the largest DOI, by fitting the modeled z_2^* to the measured z_2 from the soil auger observations, given the above modelled values of σ_1^*.

From Equation (4), $z_{2,\mathrm{sHCP}}^*$ could be modeled given the $\sigma_{\mathrm{a,sHCP}}$ measurements. Therefore, $R_{\mathrm{s,HCP}}(z_{2,\mathrm{sHCP}}^*)$ was calculated for both HCP2 and HCP4 coil configurations given the $\sigma_{\mathrm{a,sHCP}}$ measurements, the conductivities σ_1 modeled from Equations (5) and (6) and the unknown conductivities $\sigma_{2,\mathrm{sHCP}}$ and $\sigma_{3,\mathrm{sHCP}}$, different for both coil configurations 2HCP and 4HCP and fixed to a constant value across the study site:

$$R_{\mathrm{s,HCP}}(z_{2,\mathrm{sHCP}}^*) = \frac{\left(\sigma_{\mathrm{a,sHCP}} - [R_{\mathrm{sHCP}}(z_1) - R_{1\mathrm{HCP}}(z_{\mathrm{d}})]\cdot\sigma_1 + R_{\mathrm{sHCP}}(z_1)\cdot\sigma_{2,\mathrm{sHCP}} - \sigma_{3,\mathrm{sHCP}}\right)}{[\sigma_{2,\mathrm{sHCP}} - \sigma_{3,\mathrm{sHCP}}]} \quad (7)$$

This was inserted into Eq. (1):

$$z_{2,\mathrm{sHCP}}^* = s\cdot\left(\frac{1}{4\cdot\left[1 - R_{\mathrm{s,HCP}}(z_{2,\mathrm{sHCP}}^*)\right]^2} - 0.25\right)^{0.5} - 0.16 \quad (8)$$

To obtain the constant model parameters $\sigma_{2,\mathrm{sHCP}}$ and $\sigma_{3,\mathrm{sHCP}}$, the sum of the squared differences between $z_{2,\mathrm{sHCP}}^*$ and observed z_2 was minimized at the 11 calibration locations, separately for both 2HCP and 4HCP coil configurations:

$$\sum_{i=1}^{n}\left[z_{2,\mathrm{sHCP}}^*(i) - z_2(i)\right]^2 = \min \quad (10)$$

with i the number of the measurement n the total amount of measurements (11). Finally, the $\sigma_{2,\mathrm{sHCP}}$ and $\sigma_{3,\mathrm{sHCP}}$ for the HCP2 coil configuration proved to be 151.6 mS m^{-1} and 51.1 mS m^{-1}, while these values for the 4HCP coil configuration showed to be 166.0 mS m^{-1} and 49.2 mS m^{-1}.

Finally, both the deepest HCP measurements were integrated within a three-layered soil model, to model both the variable σ_1^* and the interface depth between both peat and sub layer z_2^* given a constant z_1 of 2.1 m and a $\sigma_{2,\mathrm{sHCP}}$ and $\sigma_{3,\mathrm{sHCP}}$ for both HCP coil configurations as was calculated from the minimization procedure in Equation (10).

$$\sigma_{\mathrm{a,sHCP}} = [R_{\mathrm{sHCP}}(z_1) - R_{\mathrm{sHCP}}(z_{\mathrm{s}})]\cdot\sigma_1^* + [R_{\mathrm{sHCP}}(z_2^*) - R_{\mathrm{sHCP}}(z_1)]\cdot\sigma_{2,\mathrm{sHCP}} + [1 - R_{\mathrm{sHCP}}(z_2^*)]\cdot\sigma_{3,\mathrm{sHCP}} \quad (11)$$

At each of the 122 803 measurement locations, the nonlinear Equations (11) for both 2 and 4 m coil configurations were combined to model the unknown parameters σ_1^* and z_2^*. This system was again solved using the Levenberg – Marquardt algorithm (Marquardt, 1963).

The resulting z_2^* was interpolated to a 0.2 m grid using ordinary kriging, and the interpolated values extracted at the validation points for validation.

6.4.4 Chronological evolution of the peat base

Diachronic peat rise was a major factor delimiting prehistoric occupation space. Therefore, the changing elevation of the base of this peat layer should be reconstructed through time. Only dates at the base of the peat can be used to reflect the age-depth position of the peat, because peat samples further above are not located at the elevation of their original formation due to, often differential, peat compression.

Two approaches were used to reconstruct the rising peat at Doelpolder Noord. The first and most obvious method was to sample the base of the peat at different elevations along the flank of the modelled dune. Short-lived terrestrial macrofossils were selected for subsequent radiocarbon dating. Alternatively, a more regional age-depth model of the base of the peat using legacy- and new radiocarbon dates from the wider region, developed by Verhegge et al. (2014), was queried, and related to the elevation model of the peat base.

Based on the relationship between the age-depth position and elevation model of the peat base, paleogeographic maps can be created at significant geoarchaeological dates throughout the period of peat formation (e.g. Vos and van Heeringen, 1997). As a case study, we aim at reconstructing the paleogeography of the survey area at the time of the end of the Final Mesolithic/Early Neolithic Swifterbant occupation on the nearby dune sites of Doel Deurganckdok sector B & M, dated 6170-5950 cal BP (95%). Implications for human occupation between this date and the end of peri-marine tidal influence, dated 6085-5770 cal BP (95%), are still unknown due to a lack of well dated sites (Crombé et al. 2015, Verhegge et al. 2014).

Calibration, Bayesian modelling and querying of the radiocarbon dates were performed using Oxcal 4.2 (Bronk Ramsey, 2009a) and the IntCal13 curve (Reimer et al., 2013). The chronological relation between the available end of the Swifterbant date and the age-depth model of the peat base peat were queried using the order and difference function to retrieve contemporaneous peat base elevations.

6.5 Results

6.5.1 Dualem 421s survey

The descriptive statistics of the σ_a data are summarized in Table 11. The negative minimal values and the maximal values were recorded near metallic objects. The mean and median values increase with the DOI indicating that the topsoil is less conductive than the deeper subsoil, due to conductive peat layers and brackish groundwater at larger depths.

Table 11: Descriptive statistics of the measured σ_a data (mS/m), 212,001 measurement points: PRP11: 1.1 m perpendicular configuration; PRP21: 2.1 m perpendicular configuration; HCP1: 1 m horizontal coplanar configuration; PRP41: 4.1 m perpendicular configuration; HCP2: 2 m horizontal coplanar configuration; HCP4: 4 m horizontal coplanar configuration

	PRP11	PRP21	HCP1	PRP41	HCP2	HCP4
Mean	33.49	54.84	66.38	82.31	89.53	100.06
Median	31.79	49.84	61.23	70.64	78.52	87.80
Standard deviation	10.28	19.70	21.56	35.59	34.34	37.19
Minimum	-92.78	23.96	-232.66	29.21	6.13	-107.76
Maximum	228.82	316.13	336.00	343.23	304.41	284.04

An increasing brackish water influx from the nearby Scheldt estuary is visible in the northeastern edge of the color-scale plots of the datasets (Figure 57-62) and is superimposing the geological σ_a variability (Verhegge et al. submitted). The increased σ of this brackish groundwater prohibits the LIN approximated interpretation of the measured QP signal. As such the plotted σ_a deviates from the real conductivity, increasingly with increasing coil separation (Beamish, 2011; McNeill, 1980; Reynolds, 2011). Nevertheless, despite a reduced depth of exploration (Delefortrie et al., 2014b), qualitative interpretations were still possible through comparison with borings (Verhegge et al., submitted-a). The most noticeable feature within this highly conductive zone is a conductive gully flanked by more resistive splay deposits (Figure 61.1). Smaller gullies and linear drainage ditches are recognizable throughout all data layers, as negative σ_a anomalies in PRP11 and PRP21, but positive anomalies in the other datasets. A low conductivity anomaly centrally within the survey area (Figure 61.2) revealed and is geoarchaeologically most important. Its shape in the dataplot and laminated, medium fine (aeolian) sand observed in the borings suggests interpretation as a Late Weichsel dune.

Subsequent manual and mechanical coring of the base of the peat and top of the dune sands on a small part of the ridge resulted in the identification of prehistoric remains,

such as burnt bone fragments and small lithic- artefacts (chips) were found in a small part of the samples (Verhegge et al., 2012, submitted-a).

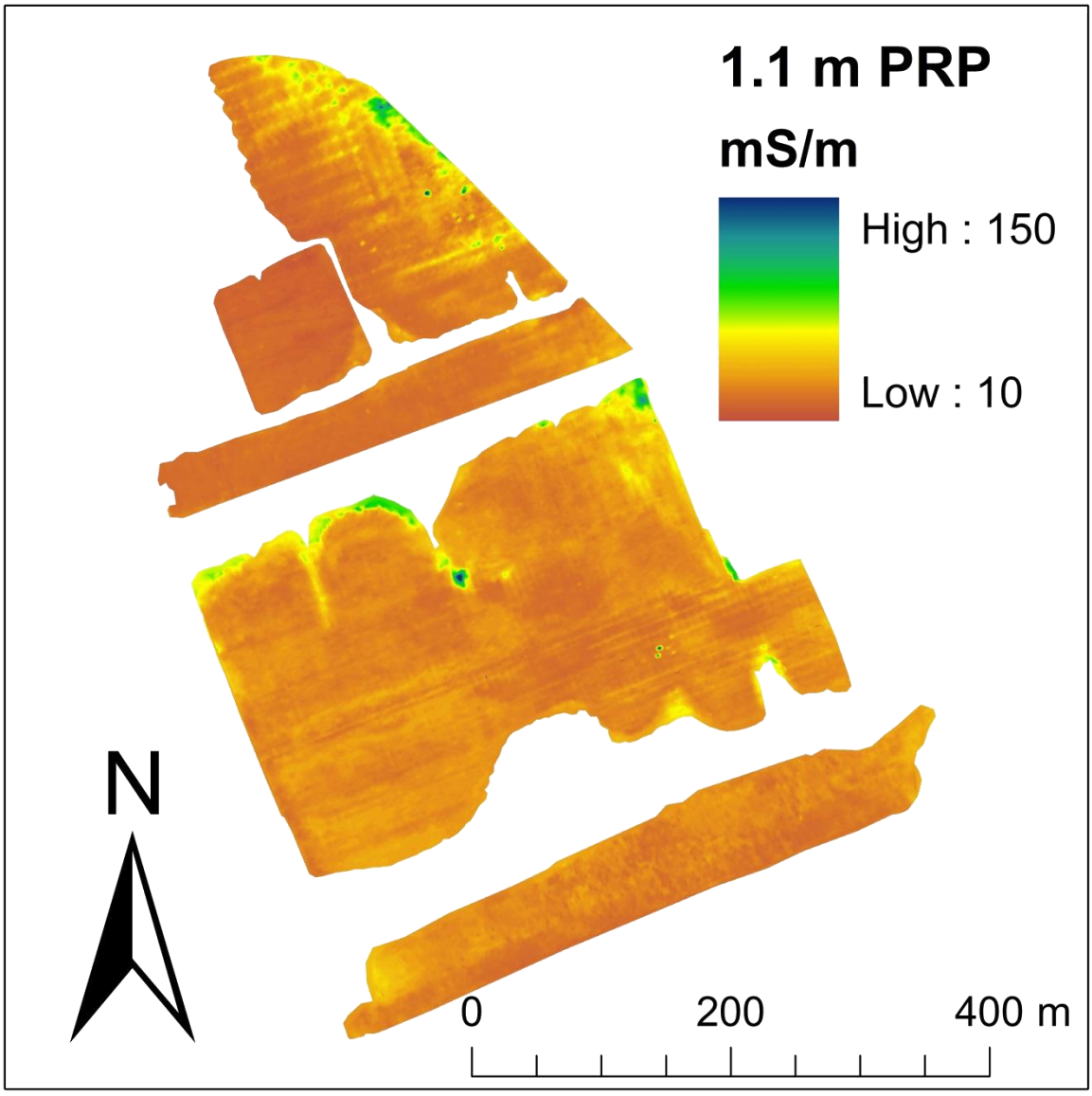

Figure 57: Interpolated σ_a data plot of the Dualem 421s survey in Doelpolder Noord in the 1.1 m perpendicular coil configuration.

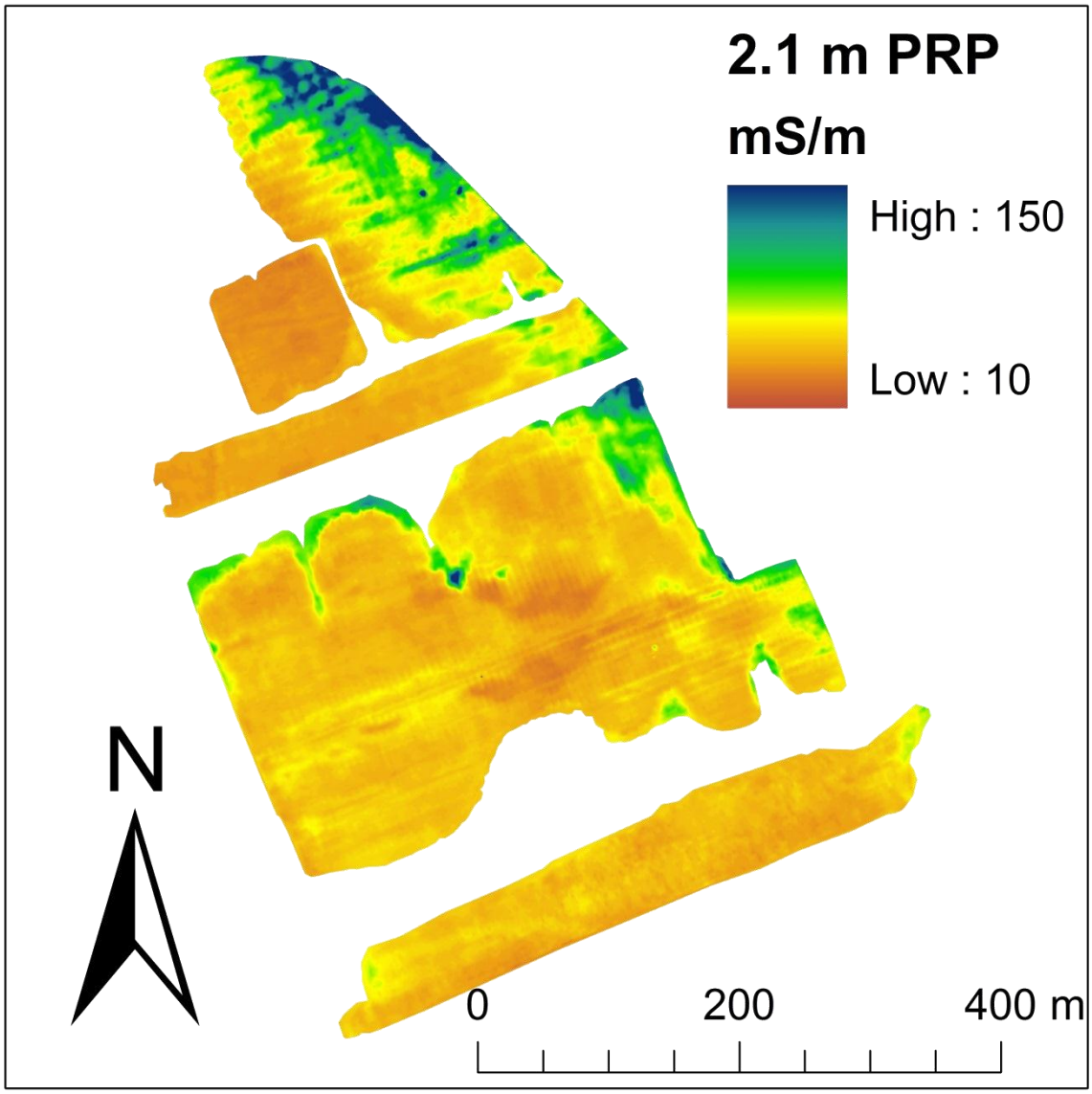

Figure 58: Interpolated σ_a data plot of the Dualem 421s survey in Doelpolder Noord in the 2.1 m perpendicular coil configuration.

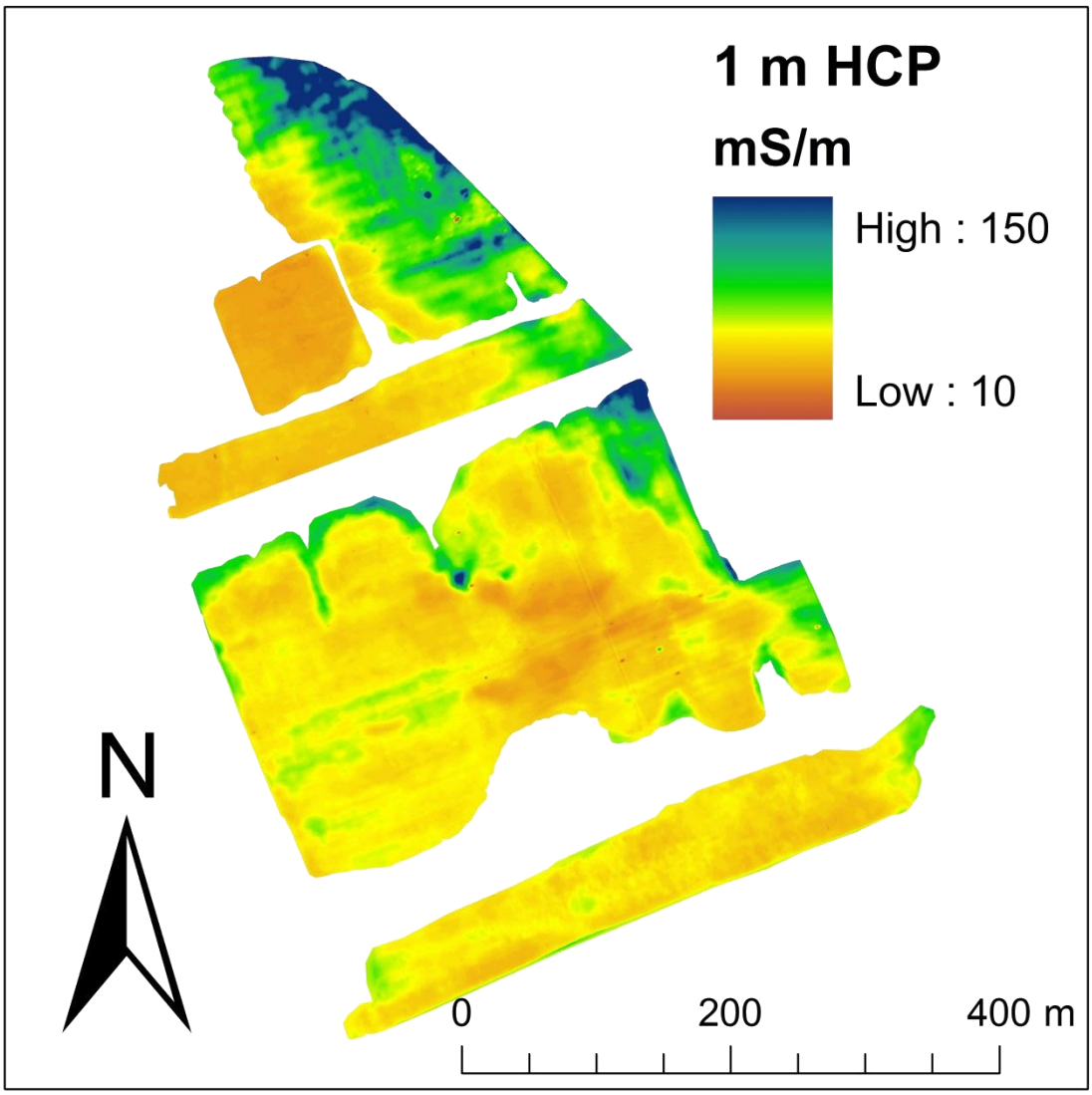

Figure 59: Interpolated σ_a data plot of the Dualem 421s survey in Doelpolder Noord in the 1 m horizontal coplanar coil configuration.

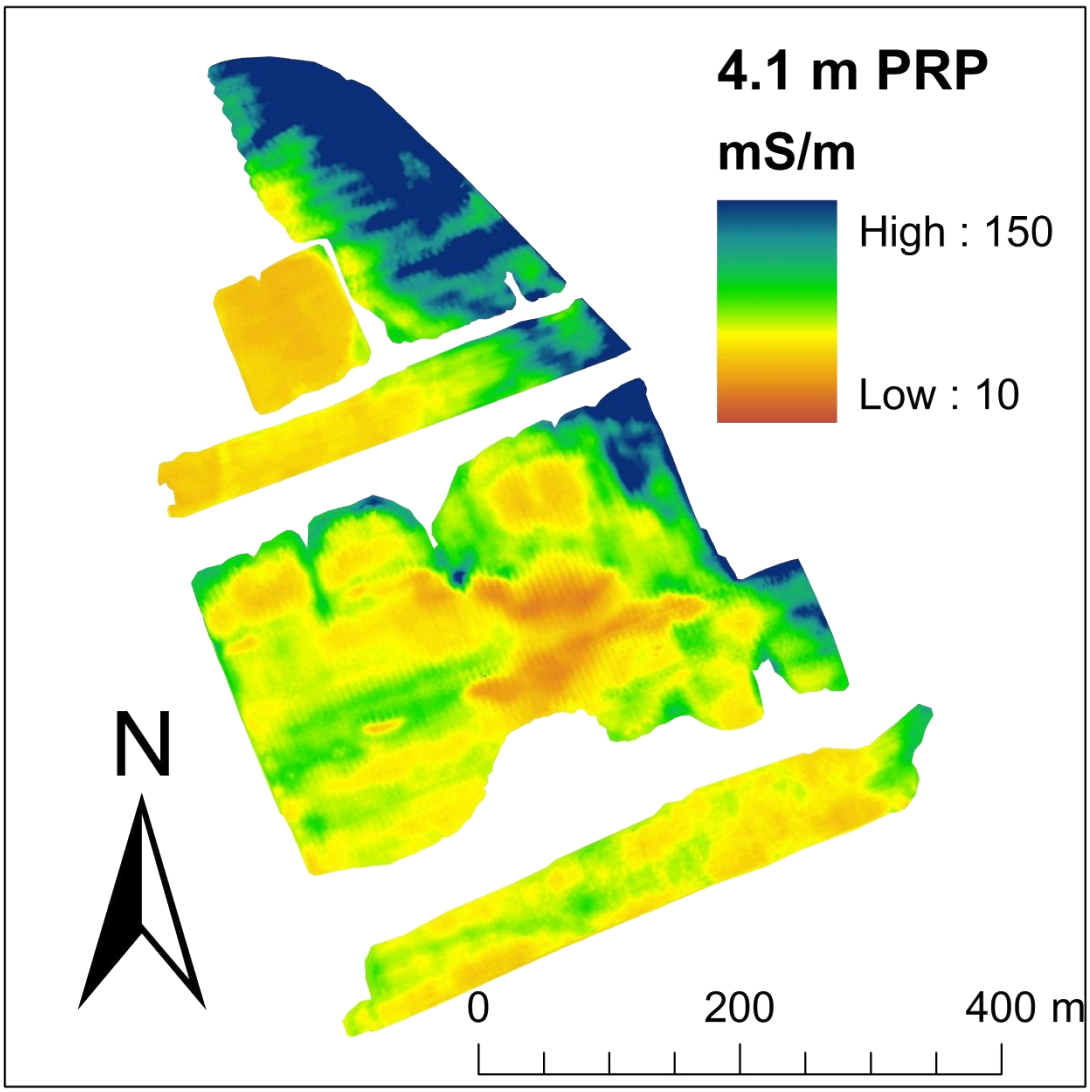

Figure 60: Interpolated σ_a data plot of the Dualem 421s survey in Doelpolder Noord in the 4.1 m perpendicular coil configuration.

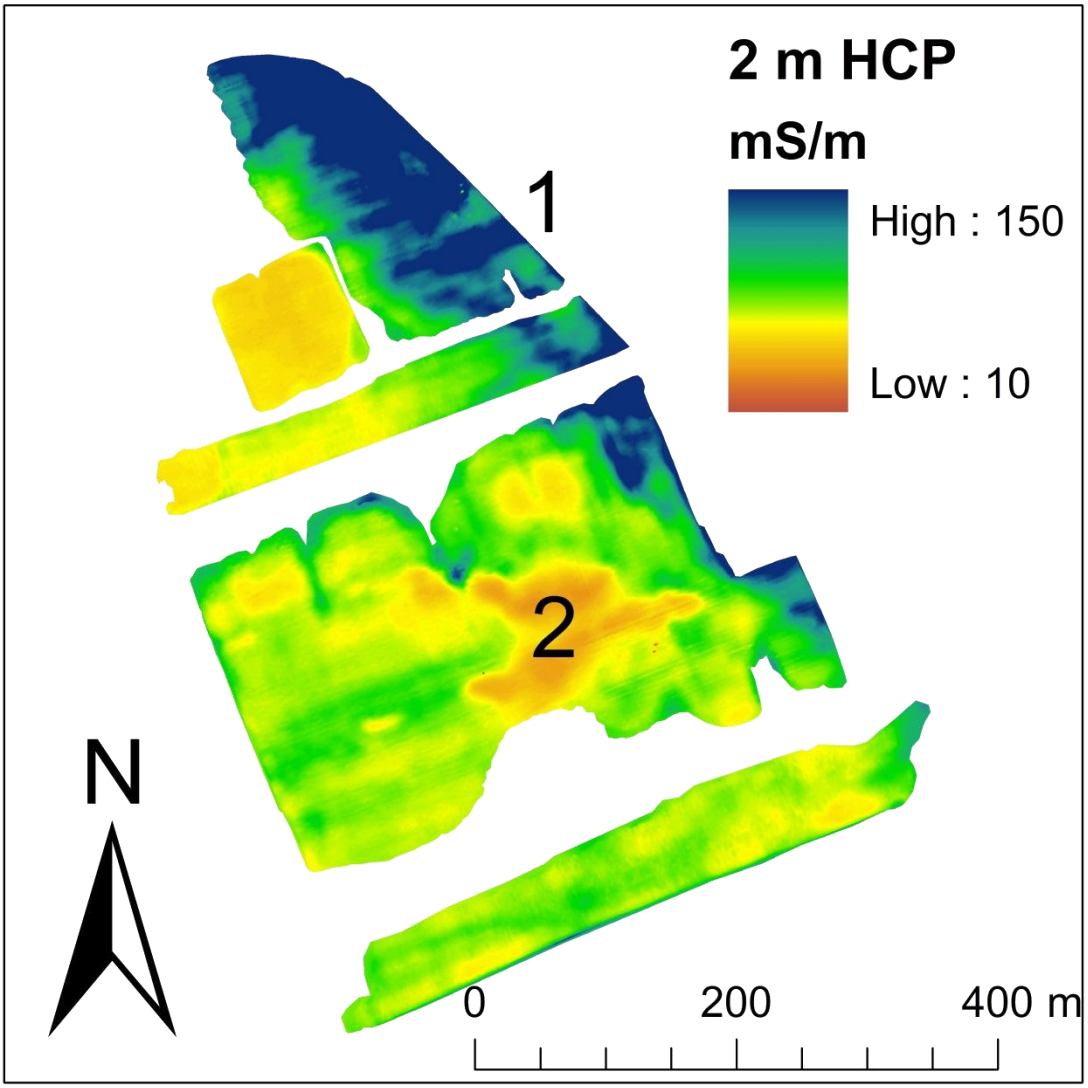

Figure 61: Interpolated σ_a data plot of the Dualem 421s survey in Doelpolder Noord in the 2 m horizontal coplanar coil configuration; 1: gully/crevasse and splays, 2: (river) dune.

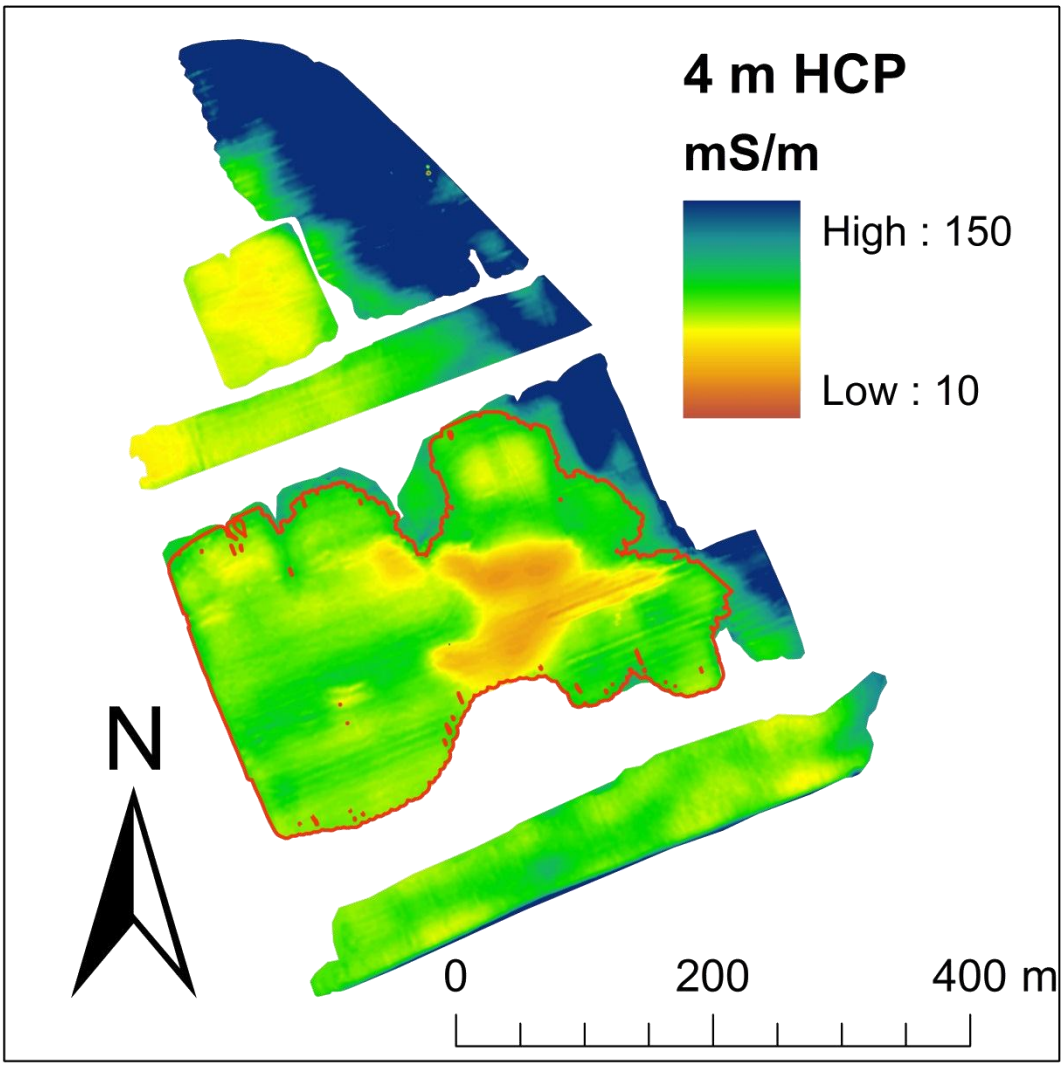

Figure 62: Interpolated σ_a data plot of the Dualem 421s survey in Doelpolder Noord in the 4 m horizontal coplanar coil configuration; red: area of the dataset selected for subsurface modelling (Figure 64).

6.5.2 EMI based subsurface modelling

The brackish groundwater influence of the Scheldt was noticeable in the data at the western edge of the survey area (Figure 61.1). Furthermore, the burial depth of the prehistoric landscape was well beyond the approximated depth of investigation of the sensor in the most southern part. Therefore, only the central parcel of the survey area was assessed suitable for subsurface modelling. Measurements in all configurations were clipped to 100 mS/m, the value suggested by McNeill (1980) as the limit of LIN condi-

tions, to exclude most superficial ferrous materials or brackish water influences from the dataset. The remaining data, used for modelling, are shown on Figure 62.

The greyscale plot of σ_1^* (Figure 64A) includes the modelled variability within the first 2.1 m. The low conductivity anomaly created by the dune is still included in this 'depth slice' because its top is situated within the modelled top layer and because the top layer of the dune up to 2.1 m depth is presumably also less conductive compared to the surroundings. Furthermore, linear anomalies caused by modern drainage pipes can be recognized as well as broader (Post) Medieval filled drainage ditch systems. Both are oriented in the SW-NE orientation. Finally, some remnant effects of the brackish water in the modern tidal ditches (Figure 55) surrounding the survey area are visible at the edges of the σ_1^* plot.

The modelled depth to the base of the peat still included anomalies caused by drainages pipes. This is a consequence of the larger width of the measured anomalies in the 2HCP and 4HCP coil configurations due to the deduplication of the signal. Therefore, the interpolated grid was smoothened using a Gaussian low-pass filter for visualization purposes (Figure 64B). Validation and further processing were applied on the unfiltered z_2^* data, however.

Table 12: Validation indices (r: Pearson correlation coefficient, MEE: mean estimation error, RMSEE: root mean squared estimation error, MAEE: mean absolute estimation error) of z_2 compared to z_2^* at the 204 validation locations and the 155 validation points within the 3.75 m z_2^* contour of the dune

	All validation points	Validation points within z_2^* contour 3.75 m
r	0.73	0.48
MEE (m)	0.01	0.01
RMSEE (m)	1.05	0.73
MAEE (m)	0.78	0.57

Many validation data were available, because firm calibration was possible using only 11 locations spread across the range of the σ_a values(Figure 64B). The statistics (Table 12) of the remaining validation points, are clustered on the dune and indicated that the model is unbiased (MEE: 0.1 m). Therefore the Pearson correlation coefficient (r) of 0.73 indicates a good linear correlation between the observed depth of the basis of the peat (z_2) and the modelled z_2^* (Figure 63). The RMSEE suggest an accuracy of 1.05 m. The MAEE of 0.78 in comparison with the RMSEE suggests that some outlying errors exist, however. Figure 63 illustrates that, in practice, such high number of clustered validation calibration points on the top of the dune is not required for paleotopographical modelling.

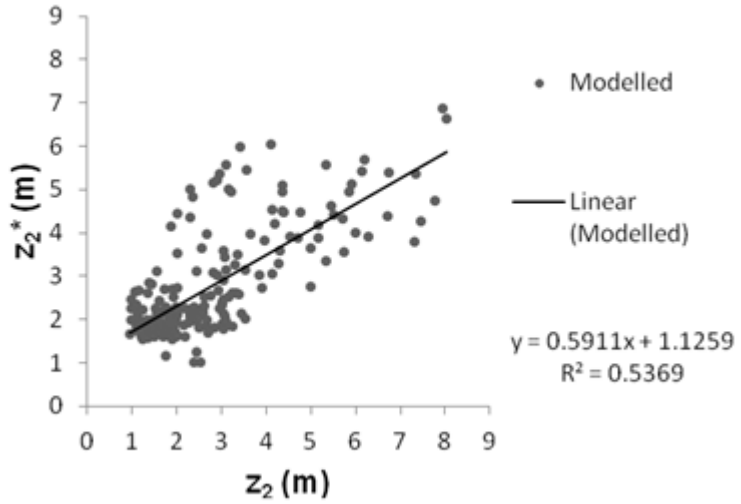

Figure 63: Modelled z_2* as a function of the observed z_2 at the 204 validation locations

The z_2^* was mainly underestimated where the observed z_2 was beyond the measurement range of the HCP4 configuration. At larger depths, the σ variability of the third layer could not be recorded, because of the preferential creation of eddy currents in the conductive second layer (i.e. the peat). Figure 64C illustrates the locations of the classified errors on the local DEM and reveals that underestimation errors were mainly located in the topographic lower areas of (Post) Medieval drainage ditches. It is hypothesized that the latter are still focal zones for runoff of local surface- and/or groundwater, resulting in an increased conductivity

Because of these spatially coherent and outlying errors, the areas where these old ditches occurred were not suited for further paleogeographic modelling. Therefore, only z_2^* points within the 3.75 m contour of the dune (Figure 64D) were selected for the final model, as this contour included a smaller difference between the RMSEE and MAEE (Table 12). Outside this contour, merely the validation points were used as depth data for the final base of the peat depth model (Figure 64E). Both datasources were interpolated to a 5 m grid using ordinary kriging. The peat base depth model was subtracted from the DEM (AGIV, 2001-2004) to obtain a peat base elevation model (Figure 64F).

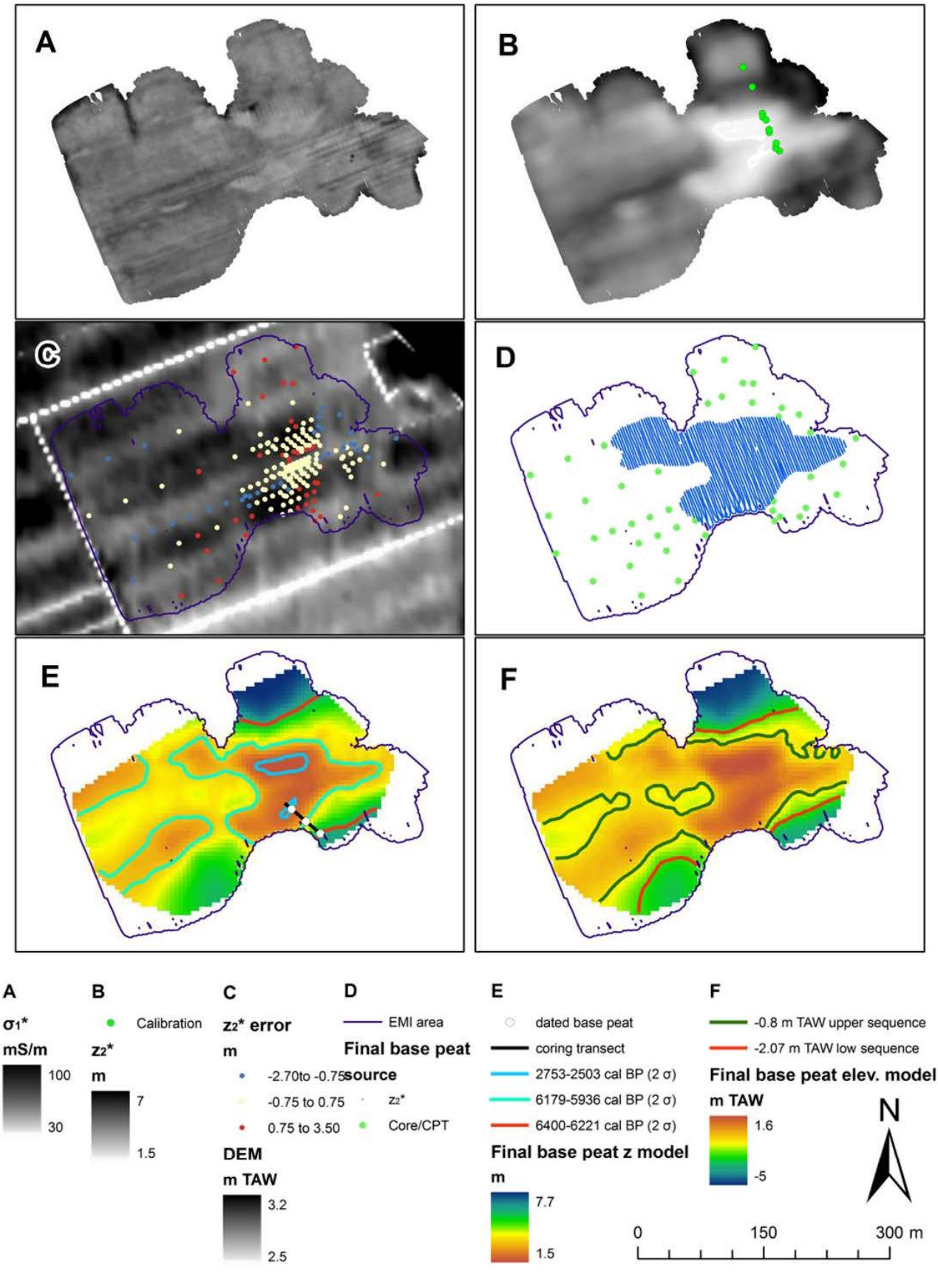
A
B
C
D
E
F
A
σ1*
mS/m
100
30
B
Calibration
z2*
m
7
1.5
C
z2* error
m
-2.70to -0.75
-0.75 to 0.75
0.75 to 3.50
DEM
m TAW
3.2
2.5
D
EMI area
Final base peat
source
z2*
Core/CPT
E
dated base peat
coring transect
2753-2503 cal BP (2 σ)
6179-5936 cal BP (2 σ)
6400-6221 cal BP (2 σ)
Final base peat z model
m
7.7
1.5
F
-0.8 m TAW upper sequence
-2.07 m TAW low sequence
Final base peat elev. model
m TAW
1.6
-5
N
0
150
300 m

Figure 64: A: Modelled electrical conductivity (σ_a^*) of layer 1. B: modelled depth (z^*) of layer 2 (peat) and the calibration locations of the base of the peat (z_2). C: DEM of the survey area and the classified errors of the modelled base of the peat (z_2^*) at the validation locations. D: the locations of the peat base depth data used for final base of peat elevation model: the modelled base of the peat depths (z_2^*) within the 3.75 m contour of the model and depths of the base of the peat at the validation points (corings and CPTs) outside this contour. E: Final peat base depth model combining the modelled base of the peat depth (z_2^*) and the base of the peat depths derived from the validation points (z_2), the location of the coring transect on Figure 65 is marked in black and the depth contours of the dated peat base on Figure 65 are marked in blue (2753-2503 cal BP (2σ)), green (6179-5936 cal BP (2 σ)) and red (6400-6221 cal BP (2 σ)); F: Final peat base elevation model combining the modelled base of the peat elevation ($z-z_2^*$) and the base of the peat elevations derived from the validation points ($z-z_2$)and the elevation contours of the modelled dates in Figure 67 are marked in green (-0.8 m TAW/upper sequence) and red (-2.07 m TAW/lower sequence).

6.5.3 Dating local peat development

Within the survey area, three radiocarbon dates were obtained on terrestrial macro-remains as suggested by Tornqvist et al. (1992) (Table 13). These were recovered from the base of the peat layer in corings distributed along the flank of the dune (Figure 65). A third date was obtained from the base of the peat in a deep depression to the south of the survey area (Figure 66-black dates). The z_2^* contours at the locations of the dated samples can simply interpreted as 'age' contours (Figure 64E). This resulted in the contours enveloping the approximate area of the dune which was not covered by peat between 6400-6221, 6179-5936 and 2753-2503 cal yr BP (95 %). The area outside the base of the peat contour was covered by river- or tidal floodplains deposits and/or peat at that contoured date. A precise local age-depth model can only be constructed if 6-10 more radiocarbon dates are acquired along the dune flank. This increases costs of coring, selection of terrestrial macro-remains and radiocarbon dating significantly. Instead, a series of available legacy dates reflecting the initiation of peat development in the wider and an age-depth model, developed by Verhegge et al. (2014), were used.

Table 13: Dated terrestric macroremains from base of peat in coring locations (Lambert ’72 coordinates) on transect from top to flank of dune

NAME	X (m Lambert ‘72)	Y (m Lambert ‘72)	Z (m TAW)	Depth base peat (m)	z2* (m)	Error	14C sample	lab-code	$\delta^{13}C$ (‰)	Age (^{14}C yr BP)	Age error (68 %) (^{14}C yr BP)	Calibrated age (cal yr BP) (95 %)
mb40	141620.37	224694.15	2.91	6.73	5.40	1.33	*Alnus* femal cone 1x	RICH-20208	-30	5515	36	6400-6221
mb39	141603.33	224708.64	3.107	5.73	3.56	2.17	*Carex* sp. 2x; *Urtica dioica* 5x; bud scales 37x	RICH-20057	-26	5265	30	6179-5936
mb16	141586.30	224723.12	3.186	1.31	1.84	-0.53	*Calluna vulgaris* flower (charred) 7x; *Calluna vulgaris* leave 4x; charred twig 3x	RICH-20046	-30	2555	28	2753-2503

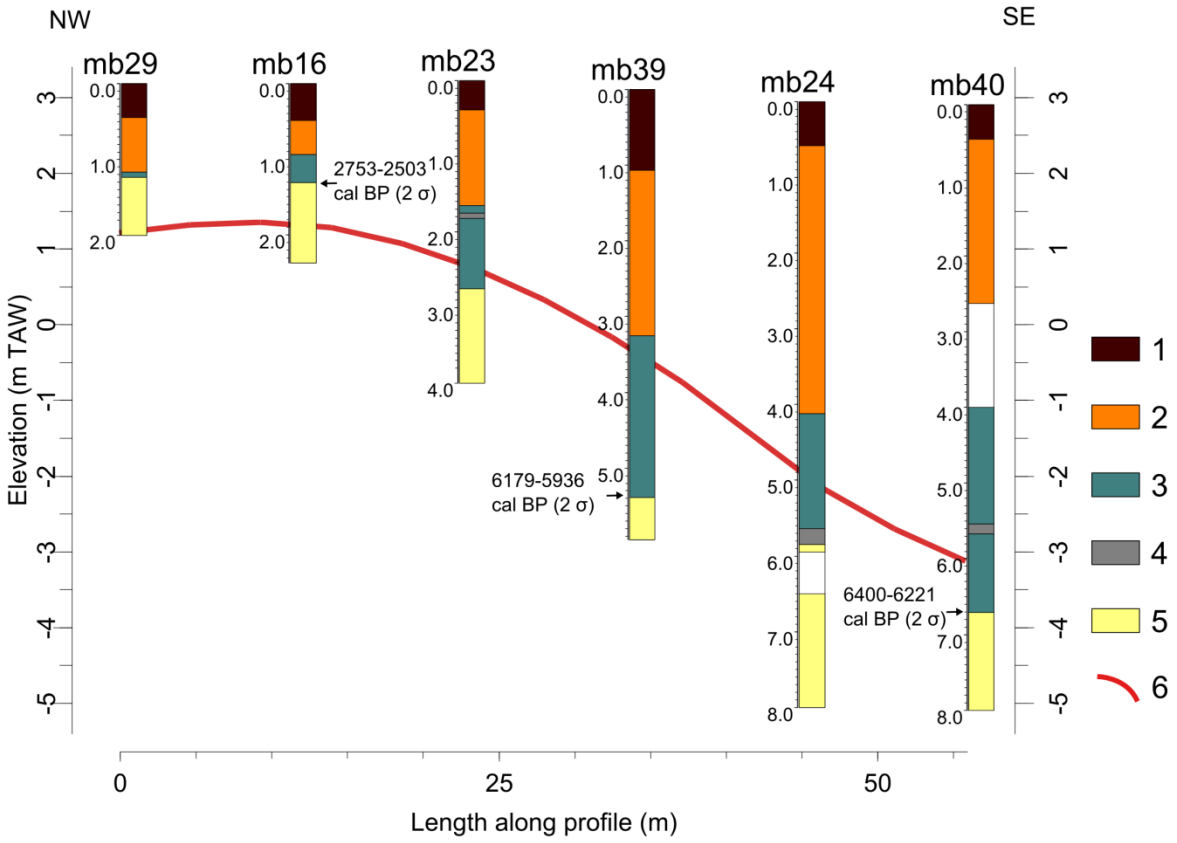

Figure 65: Coring transect with lithological interpretation (1: topsoil clay, 2: marine clayey-sand, 3: peat, 4: OM rich clay, 5: dune sand, empty space: no sediment retrieved) along transect on Figure 64E with calibrated dates from the base of the peat layer and modelled base of the peat layer (6).

6.5.4 Regional age depth of the peat

The peat base dates, collected in the wider region, reflect an 'error envelope' (Vos and van Heeringen, 1997), including all sources and scale of age-depth variability within the region (Kiden et al., 2008). Therefore Verhegge et al. (2014) decided to model an 'upper'(/older) (Figure 66-green dates, blue interpolation) and 'lower'(/younger) (Figure 66-blue dates, green interpolation) age depth deposition sequence, including a maximal number of dates, while reaching sufficient overall model agreement. Dates in between both sequences are outlying to the modelled sequences but belong within the 'error envelope' (Figure 66-purple dates). An Oxcal P_Sequence was selected because its underlying deposition (or peat rise) is mediated by a Poisson process (Bronk Ramsey, 2008). This type of sequence is selected by Verhegge et al. (2014) to account for possible elevation

errors of the peat base dates. In this paper, a small improvement to the existing model (Verhegge et al., 2014- Figure 3) includes a variable 'k' parameter (the number of random events per meter of peat rise). This allows a better assessment of the randomness in the deposition rate according to Bronk Ramsey and Lee (2013).

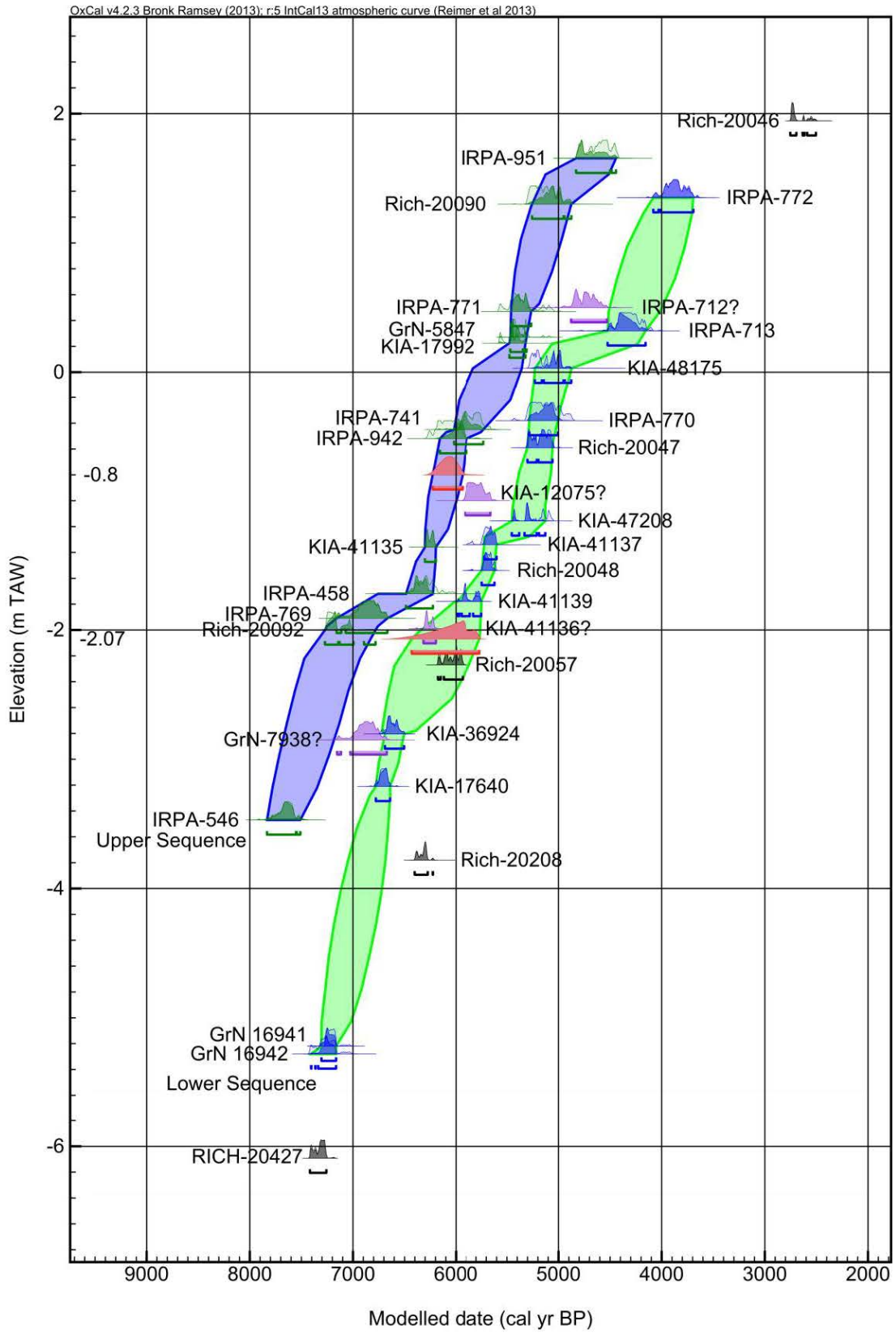

Figure 66: Age-depth plot of upper P_Sequence (blue interpolation) and lower P_Sequence model (green interpolation) enveloping the dates excluded from the sequences in between (marked with '?', purple); modelled dates contemporaneous with end Swifterbant occupation at -0.80 and -2.07 m TAW (red); radiocarbon dates at Doelpolder Noord (black) (calibrated date ranges at 2σ).

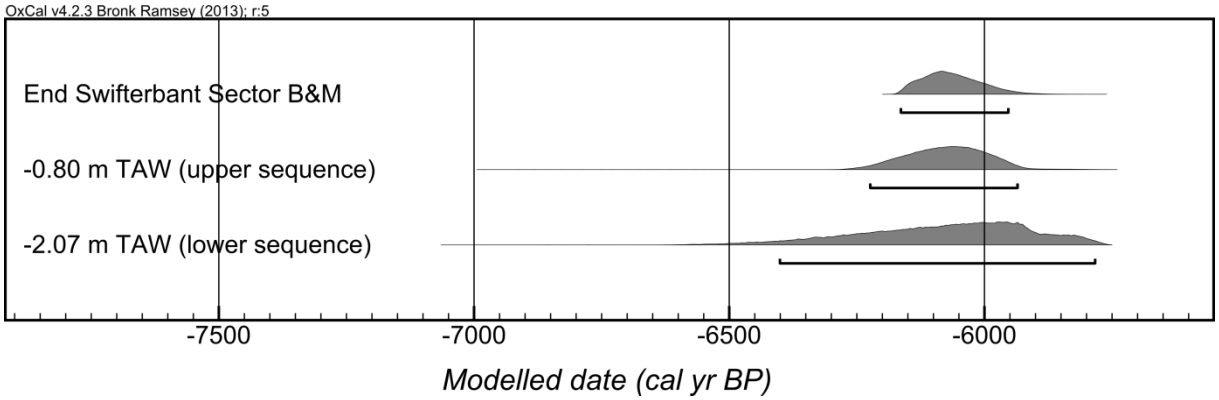

Figure 67: Modelled date for the end of Swifterbant occupation at sites of Doel Deurganckdok sector B & M and modelled dates with upper sequence and lower sequence elevations of the contemporaneous base of the peat from Figure 66

The elevation of the regional peat base at the end of the occupation of the Doel Deurganckdok sector B & M sites was derived by iteratively calculating the order and difference between end boundary of the occupation dates and multiple queried probability distribution functions (Oxcal C_date) of the modelled P_sequence. These data are plotted in the age-depth model in Figure 66 (red dates).

As such, the upper level of the peat base was modelled at -0.80 m TAW because the probability of the end of Swifterbant occupation being earlier was 0.47 and the difference between both modelled dates was -200 to 171 cal yr (95%) with a mean of -9.5 cal yr. Similarly, the lower sequence elevation was modelled at -2.07 m TAW, with the probability of the end of Swifterbant occupation being earlier at 0.50 and the difference ranging from -372.5 to 305 cal yr (95%) with a mean of -16.2 cal yr.

Therefore the possible area of the level of the peat or floodplain deposits at the end of the Swifterbant occupation is determined by the -2.07 and -0.80 m TAW contour of the final peat base elevation model (Figure 67F).

When the dates and elevations of the base of the peat within the survey area are compared to the regional age-depth model, their relation can be assessed. The most recent date (RICH-20046) is also the most recent and elevated date of the peat base in the region, impeding comparison. RICH-20057 is located within the lower sequence of the regional age-depth model, suggesting good accuracy of the latter predicting local peat rise. RICH-20208 is located below the regional peat model. This date was based on a sample, located 0.1 m above the base of the peat. If peat compaction is considered, its original position might have been more elevated. An elevation error could also have been introduced during the coring itself as no continuous sediment sequence could be retrieved (Figure 65- mb40).

If the locally date samples, closeness to the Scheldt and the downstream location of the survey area within the sample region of Verhegge et al. (2014 Figure 1) are taken

into consideration. The lower sequence of the age-depth model seems to be more representative for the start of local peat development at Doelpolder Noord indeed.

6.5.5 Paleogeography

Based on the chronological modelling results a tentative paleogeographic classification of the base of the peat elevation model can be proposed at the end of the Swifterbant dune site occupation at Doel Deurganckdok Sector B and M (Figure 67).

The age-depth modelled elevations (-2.05 and -0.80 m TAW) were selected as contour class ranges for the paleogeographic maps, the paleolandscape classes were identified based on the observed lithostratigraphy in corings, on the approach used by Vos and van Heeringen (1997) and on paleo-environmental reconstructions by Deforce et al. (2014b).

On the one hand, no peat formation was registered in the wider region above the base of the peat age depth 'error envelope', because those elevations were above groundwater level and above the floodplain. These dry ridges were vegetated with an (upper) alluvial hardwood forest (Deforce et al., 2014a; Deforce et al., 2014b). On the other hand, peat had already formed below this 'error envelope'. During the studied period, occasional flooding covered the existing peat with OM rich clay. A thin layer of OM rich clay (0.19 m), directly on top of the riverdune, was encountered in a core within the survey area (Figure 65-mb24). In this coring, the base of these supra-tidal flood deposits was at an elevation of -2.90 m TAW. This core is also located 1 m to the inside of the -2.07 m TAW contour i.e. the level of the lower peat sequence at the end of the Swifterbant occupation. The lack of peat below it and its limited thickness suggest that it was deposited near the end of the occurrence of the occasional flooding in the survey area. As such this core confirms the approximation that areas below the peat base 'error envelope', consisted of a supra-tidal floodplain landscape, vegetated with alder carr forest (Deforce et al., 2014a; Deforce et al., 2014b).

Alder carr peat could only be formed on the flanks of the dune if locally groundwater surfaces above the level at which the supratidal OM rich floodplain clay was deposited. This means that if peat was formed at all at the end of Swifterbant occupation, it would have formed within the error enveloped of the regional age-depth model of the base of the peat. Regarding the dates from within the survey area, this seems unlikely. Alternatively, if no peat was formed, lower alluvial hardwood forest is known to cover the flanks of ridges during this period (Deforce et al., 2014a; Deforce et al., 2014b).

The paleogeographic map of the survey area (Figure 68) was derived from Figure 64F following these interpretations. The exact class boundaries are still tentative because this map does not include vertical age-depth errors or depth modelling errors of the

EMI data. Nevertheless it proved relatively consistent when compared with the lithostratigraphy observed in borings (e.g. Figure 65).

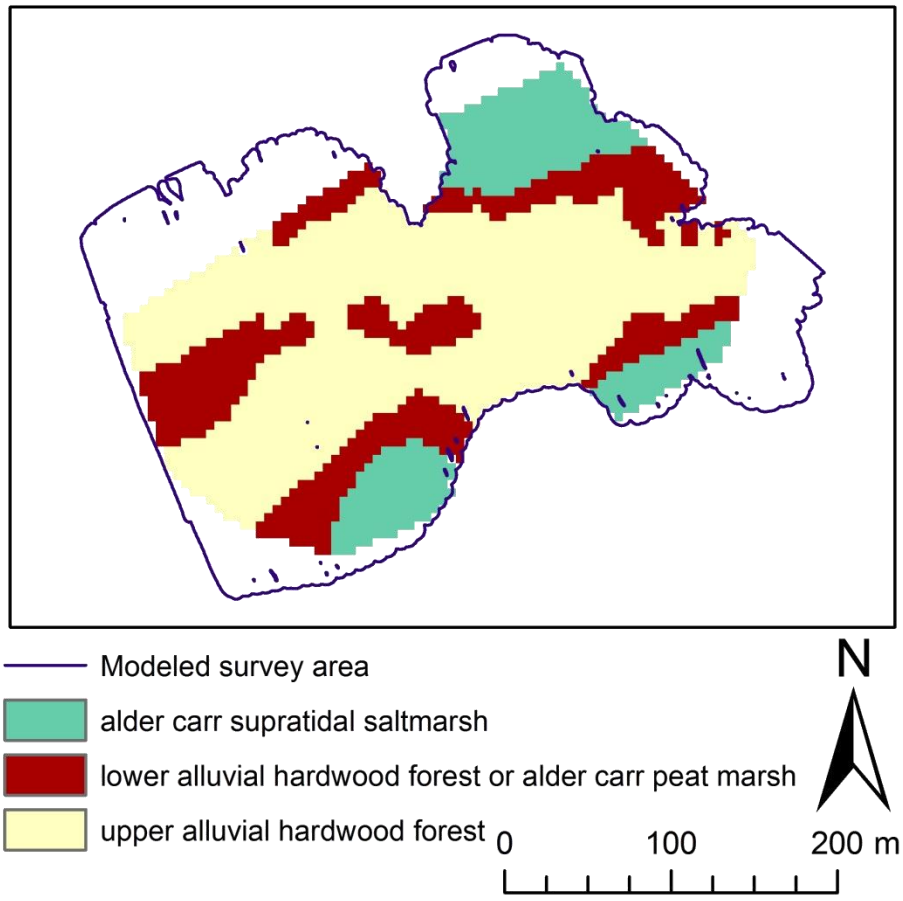

Figure 68: Tentative paleogeographic reconstruction of Doelpolder Noord at the time of the end of the Swifterbant occupation on Doel Deurganckdok Sector B & M (6164-5953 cal yr BP), the contour between upper alluvial hardwood forest and lower alluvial hardwood forest/alder carr peat marsh is derived from the calculated elevation in the upper chronological sequence of the base of the peat (-0.8 m TAW) and the countour between the contour between the lower alluvial hardwood forest and the alder carr supratidal saltmarsh is derived from the lower sequence of the base of the peat (-2.07 m TAW) (Figure 64F).

6.6 Conclusion

In Doelpolder Noord, 1-D modelling of Dualem 421s QP data, using a 3-layered system, succeeded in separating σ_a variations created by shallow (Post) Medieval and modern landscape structures from the underlying topography of the peat base covering a sand dune. This model was validated to investigate the suitability for discontinuous archaeological core sampling. Within the proposed assumptions (0.5 m vertical find spreading, 2 m core sampler), cost-saving discontinuous mechanical coring of the archaeological strata is only possible within the 3.75 m depth contour of the reconstructed dune with an overall error below 0.75 m (Figure 64C-D, Table 12). Areas outside this contour had larger z_2^* errors. Here, continuous core sampling is required for archaeological core sampling. For the final peat base model, the modelled peat base values (z_2^*) outside the 3.75 m contour of the dune were replaced with more accurate but less densely spaced interpolated validations points originating from corings and CPTs. These corings and CPTs have the ability to register locally more complicated lithostratigraphic sequences (Figure 65) with better precision than the simplified 3-layer model used for the EMI inversion. A dense coring/CPT grid is required to create an interpolated model of the small dune with the overall accuracy of the peat base model of the dune (within the 3.75 m contour) based on the EMI data however.

The development of peat over the dune was reconstructed using local radiocarbon dates and an existing regional age-depth model of the initiating peat development within the Waasland Scheldt polder' region (Verhegge et al., 2014). The elevation of the peat base at the end of the dated Swifterbant occupation of the nearby Doel Deurganckdok sector B & M sites was reconstructed and used in combination with the peat base elevation model (Figure 64F) to create a paleogeographic map of the period (Figure 68). This map is a useful prospection tool to fill up this archaeological knowledge gap of undated dune sites of the Late Swifterbant or early Michelsberg period. In such case, at least the area of the upper alluvial hardwood forest, and preferably also the area of the lower alluvial hardwood forest or alder carr peat peat marsh should be core sampled archaeologically using the variables proposed by Crombé and Verhegge (2014). This was already partly done resulting in the discovery of a new buried prehistoric site (Verhegge et al., 2012, submitted-a). Alternatively, this paleogeographic map could be used to contextualize the existing archaeological finds from the dune (Verhegge et al., submitted-a) or sites in the region.

More generally, it can be concluded that using electromagnetic induction sensors with multiple coil spacings and configurations, such as the the Dualem 421s, the prehistoric landscape (i.e. the paleotopography of the base of the Holocene peat blanket) could be reconstructed quantitatively despite the challenging and complex soil conditions of the study region, at least on important prehistoric landscape units. Therefore, if a desk-

top study does not reveal variables, such as modern metallic disturbances, recent land raising or brackish groundwater, which could hinder the success of an EMI survey, instruments such as the Dualem 421s can be used as a suitable method for a high resolution quantification of the lithological (sub-)soil variability up to a depth of 3.75 m. Based on these results, well thought-out calibration and validation data have to be acquired (based on the EMI data) using more detailed, invasive lithological mapping methods such as coring or CPTs. If brackish groundwater or a burial depth beyond the DOI of the employed instrument's depth of investigation is encountered, additional gridded coring or CPTs were proposed to account for a reliable paleotopographical model of the soil. The application of larger multi coil instruments such as the Dualem 642s to increase the vertical extent of the inversion method has to be investigated.

The regional age-depth 'error envelope' of the initiating peat development was usable for chronological prehistoric landscape reconstruction. If sufficient budget is available, it is advised to sample and date a range of peat base elevations along the flank of a dune to account for more local sources of age-depth variability.

Paleogeographic maps of other significant archaeological dates, during the period of peat formation, can be made depending on archaeological research questions using the proposed methodology. The peat base elevation data can be retrieved in high-resolution from subsurface models based on inverting multi-signal EMI signals or other sources.

6.7 Acknowledgments

The presented research was funded by Research Foundation Flanders (FWO) (Grant number G024911N) and the Interreg IVA 2 Seas project "Archaeology, Art and coastal Heritage" (08-019 Arch-Manche). Dr. Ian Hill is thanked for providing us with the Dualem 421s sensor. Valentijn Van Parys is kindly acknowledged for assistance during geophysical fieldwork. All staff and students are kindly acknowledged for their assistance with coring field work. CPTs and Sonic drill Aqualock cores were carried out by SGS. Selection of the dated macro remains was performed by Hanneke Bosch (ADC) and Luc Allemeersch (GATE). Radiocarbon dating was carried out by the Royal Institute for Cultural Heritage. The nature and forest agency of the Flemish government is thanked for allowing us access to Doelpolder Noord.

Chapter 7 In search of sealed Paleolithic and Mesolithic sites using core sampling: the impact of grid size, meshes and auger diameter on discovery probability

This chapter is adapted after Crombé and Verhegge (2014).

Since the 1990s core sampling, particularly within Dutch and Belgian wetland research, has increasingly become important for detecting covered prehistoric hunter-gatherer sites, comprised mainly of scatters of lithic artifacts of variable size and find density. Several methodological studies (Tol et al., 2004; Verhagen et al., 2013) have tried to develop standard sampling protocols differentiating grid size, core diameter and sieving mesh width according to the expected site-types. These studies are all based on a statistical analysis of excavation data, using simulations. However, these theoretical models have never been fully tested against empirical data coming from augering projects. In this paper core sampling data from eleven cored sites, some of which were subsequently excavated, are used in view of developing a core sampling strategy which allows the detection of the broadest possible range of prehistoric sites. The study concludes that in most cases, augering within a 10 m grid with a 10 cm–12 cm core and sieving through 1 mm–2 mm meshes allows the detection of buried sites, eventually even small and low-density ones. In order to further increase the discovery chances a two-step gridding approach is recommended.

Highlights

- We estimate the discovery rate using core sampling in order to detect buried prehistoric sites using data from eleven coring projects.
- Cores need to be minimal 10 cm in diameter to obtain enough positive hits.
- Grid sizes larger than 10 m will considerably reduce the discovery chances to a point that some sites can be missed.
- The discovery probability can be considerably increased when sieving through small meshes (1–2 mm).
- If the above recommendations are followed, even sites with (very) low find-densities can eventually be discovered.

Keywords

Paleolithic; Mesolithic; core sampling; discovery rate; grid size; core diameter; sieving mesh size

7.1 Introduction

In the last few decades core sampling has become the most frequently applied survey method for detecting prehistoric sites in the lowlands of the Netherlands and Belgium, especially in river floodplains and coastal plains. In these wetland environments prehistoric remains, mostly consisting of lithic artifacts, are usually situated at considerable depths, covered by younger deposits such as peat and alluvial/marine clay. As a result traditional survey techniques, e.g. field-walking, test-pitting and trial-trenching, are generally inappropriate for these areas. In the framework of his PhD dissertation Groenewoudt (1994) developed in the mid-1990s an augering strategy, which was based on the theoretical statistical models of shovel probes sampling, also called shovel testing, a technique frequently used in the United States (Banning, 2002; Krakker et al., 1983; Lovis, 1976; Orton, 2000; Shott, 1985). These models calculate the probability of

intersection and detection of archaeological sites of a certain dimension and find density. Based on his findings, Groenewoudt (1994) recommended the use of large cores (preferably 25 cm diameter) within a staggered grid of 22.5 × 22.5 m and sieving of the soil samples. The latter should be done through small meshes (1–2 mm) if cores with a diameter smaller than 20 cm are used. Since Groenewoudt's study, core sampling has increasingly been applied within Dutch archaeology, not only within wetland contexts but also for surveying areas covered by vegetation (forests, meadows), aeolian sediments or anthropogenic soils (so called 'eerdgronden').

In an attempt to refine the core sampling strategy, two major studies were performed based on simulations of excavation data from the Netherlands and Belgium. A first study conducted by Tol et al. (2004) suffered from a lack of mutually comparable data as only nine prehistoric sites, some of them partially excavated, were available. Almost a decade later Verhagen et al. (2013) could select twelve Paleolithic and Mesolithic sites which were well enough excavated to be suited for a statistical approach of grid size and core diameter. In the latter study simulations were performed by placing an equilateral triangular grid randomly placed on top of each site 100,000 times, and for each "virtual" core sample hitting the site, detection probabilities were calculated on the basis of the counted flint fragments per 50 × 50 cm (Verhagen et al., 2013). Both studies resulted in the formulation of different core sampling strategies depending on the expected size and find-density of prehistoric sites (Table 14 and Table 15).

Table 14: Core sampling strategies according to Tol et al. (2004).

Site type	Low density<40 per m²	Medium density40–125 per m²			(Very) high density>125 per m²		
		Grid	Core diam	Sieve mesh	Grid	Core diam	Sieve mesh
Small <200 m²	Test-pits	4 × 5	15–20	3–4	7.5 × 10	15–20	1–2
Medium 200–2000 m²	Test-pits	10 ×12.5 15 × 20	15–20	3–4	15 × 20	15–20	1–2
Large >2000 m²	Test-pits	30 × 40 40 × 50	15–20	3–4	40 × 50	15–20	1–2

Table 15: Core sampling strategies according to Verhagen et al. (2013).

Site type	Very low density (<40 per m²)			Low density (40–80 per m²)			Medium density (80–160 per m²)		
	Grid	Core diam.	Sieve mesh	Grid	Core diam.	Sieve mesh	Grid	Core diam	Sieve mesh
Very small <50 m²	–	–	–	–	–	–	–	–	–
Small 50–200 m²	4x5 + test-pits	–	–	4 × 5	15	3	–	–	–
Medium 200–1000 m²	4x5 + test-pits	–	–	8 × 10	15	3	13 × 15	12	3
Large >1000 m²	–	–	–	13 × 15	12	3	20 × 25	12	3

Although both simulation studies yielded interesting insights into the intersection and detection probability of stone age sites, they are hampered by a number of limitations and problems inherent to simulations and the type of data used. First, the simulations have been conducted on excavation data with a spatial resolution of 0.25 m², corresponding to the smallest excavation unit. They are based on the assumption that artifacts are distributed randomly and uniformly within each square. However, a test performed at one of the sites included in Verhagen's study, Oudenaarde-Donk (Bats, 2007; Bats et al., 2006), has demonstrated that some core samples that hardly contained lithic finds yielded a high number of finds during subsequent excavation of the related square, or vice-versa. The percentage of drilled artifacts in relation to the excavated finds on this site varies from just 1% to a maximum of ca. 40%. This clearly demonstrates the uneven or clustered distribution of finds not only on site level but even within a small unit of 0.25 m², something which undoubtedly has an important effect on the discovery rate.

Second, the effects of sieving on the detection of lithic artifacts, although recognized in both simulation studies as being one of the major determining factors, has not yet been investigated properly. This is mainly due to the fact that the prehistoric sites included in these studies were sieved using different meshes ranging between 1 mm and 4 mm, which so far has hindered a reliable intersite comparison. As Verhagen et al. admit (2013, p. 246) the data are not extremely accurate allowing only to make an educated guess of the effect of sieving on detection probabilities.

Third, both studies aim at a detection rate of 75%, obtained by summing all positive core samples per site, meaning the sum of all cores yielding artifacts. However, as Verhagen et al. (2013, 246–247) correctly state, one may seriously question whether this high rate is really necessary. Theoretically one just needs a single positive borehole to detect a site.

Fourth, there is a serious problem of feasibility with respect to some of the core sampling strategies proposed by Tol et al. (2004) and Verhagen et al. (2013). In particular the use of manual cores with a diameter of 15 cm or larger can be problematic due to soil

conditions (e.g. watersaturated sands, dry compact clay, woody peat, etc.) or the depth of the potential prehistoric level (>3 m). Furthermore, in these specific situations nowadays manual augering is often replaced by mechanical drilling, using e.g. a sonic drill aqualock system (Hissel et al., 2005), but these are generally limited to 7–10 cm diameter. Also the use of large cores can cause serious damage to the site, prior to its excavation, so optimizing the core diameter is most desirable.

Last but not least one can question whether it is desirable to adjust the core sampling strategy according to the site type which can be expected in a given project area. Due to post-depositional burial by fluvial and/or aeolian sediments there is often no prior knowledge about the types of sites, so how to choose the right sampling strategy? Furthermore this predictive approach includes a certain risk in just finding what is "expected" based on current knowledge about the prehistoric settlement system and the paleoenvironment and missing what is not known or not expected. In the end this may lead to a totally biased reconstruction of the prehistoric land-use, as the sampling strategies are mainly oriented towards finding what is expected.

In this paper we will investigate whether it is possible to develop an optimal core sampling strategy, which allows the detection of an as broad as possible spectrum of Paleolithic and Mesolithic sites and which is applicable to all environmental circumstances, even the deeper contexts. Contrary to all mentioned earlier studies, this investigation will not be based on simulations of excavation data but will use empirical data from several augering projects on prehistoric sites, some of which were subsequently partially excavated. By doing this we hope to encompass some of the above stated problems and limitations related to simulation models.

7.2 Dataset

Augering data from eleven prehistoric sites were available for this study, ten of which are situated in the floodplains of the Scheldt river in NW Belgium and the Netherlands (Figure 69). Prior to the archaeological survey all sites were drilled with a 3 cm gouge within a grid of 30 m–50 m in order to reconstruct the covered paleotopography and acquire litho-stratigraphical data. These data were used to define zones and levels in which sealed prehistoric sites could reasonably be expected, such as sand dunes, river banks, scroll bars, etc. These smaller areas were subsequently drilled in order to detect sealed prehistoric sites. The latter was done more or less in the same way on all sites, i.e. within a 5 × 5 m or 10 × 10 m staggered (isosceles triangular) grid, using a manual Edelman (spiral) auger with a diameter of 10 cm–12 cm and subsequent wet sieving through 1 mm meshes (Table 16). Selection of archaeological finds (lithic artifacts, carbonized

plant remains, bone fragments, etc.) was carried out by a stone-age specialist after the sample residues were completely dry. Due to particular project circumstances (some projects were conducted within the context of developer-led salvage operations, others within scientific research projects), some sites were surveyed in a slightly different way. For example, at Verrebroek-Dok 1 a 15 cm auger was used, while at Kerkhove-Stuw the grid was enlarged to 15 × 15 m.

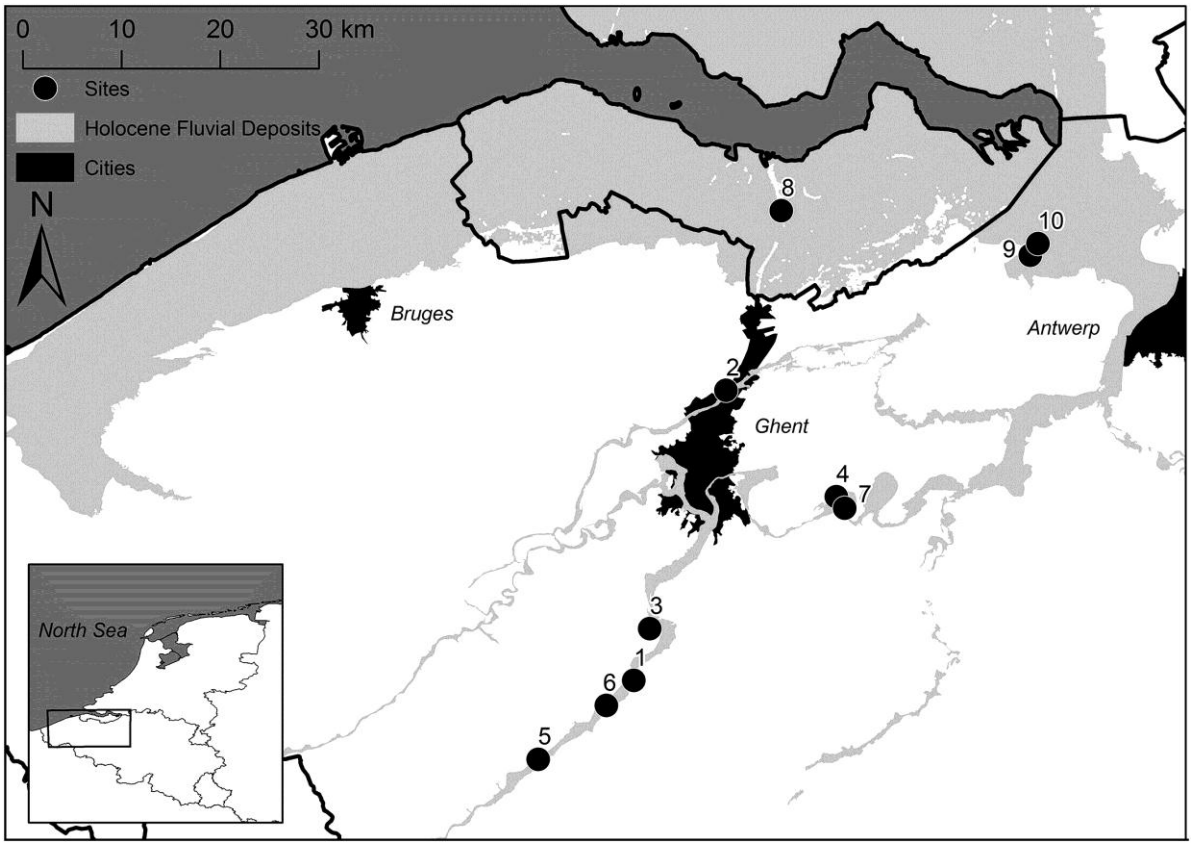

Figure 69: Map of the Scheldt floodplain with all drilled sites (1: Eine, 2: Evergem, 3: Gavere, 4: Kalken, 5: Kerkhove, 6: Oudenaardeexcept Hempens), major cities and the areas covered with Holocene fluvial sediments. Bottom left: Overview map with inset rectangle.

Table 16: List of prehistoric sites surveyed by means of core sampling within the present study, the applied coring survey variables (core diameter & grid size) and the coring results.

	Core diameter	Grid size	N Core samples	N Positive cores	% Positive cores
Eine	10	10 × 10	108	5	4.6
Evergem-Nest	12	5 × 5	408	35	8.6
Gavere-Donk	10	10 × 10	342	27	7.9
Hempens-Waldwei	10	5 × 5	41	23	56.1
Kalken-Molenmeers	10	10 × 10	78	6	7.7
Kerkhove-Stuw	12	15 × 15	143	26	18.2
Oudenaarde-Donk	10	10 × 10	74	54	73
Schellebelle-Aard	10	10 × 10	587	52	8.9
Sluiskil-Kanaalkruising	12	10 × 10	198	5	2.5
Verrebroek-Aven Ackers	10	10 × 10	356	57	16
Verrebroek-Dok 1	15	5 × 5	702	154	21.9

Five of these drilled sites were also partially excavated, which provided detailed information on the intrasite spatial distribution of the lithic artifacts (Table 17). Chronologically these sites belong to different stages of the Mesolithic (ca. 8700–4500/4000 cal BC) (Crombé and Cauwe, 2001), from the Early Mesolithic (Evergem, Oudenaarde, Verrebroek-Aven Ackers, Verrebroek- Dok1) to the Middle Mesolithic (Verrebroek-Aven Ackers), and on through the Late Mesolithic (Hempens, Verrebroek-Aven Ackers). All excavated sites yielded spatially distinct artifact clusters, separated by zones with either no artifacts or very low densities of artifacts (Figure 70). The number of scatters identified is clearly dependent on the excavated surface. It is clear that most Mesolithic sites consist of numerous scatters of varying size and density. Detailed chronological analyses on some of these sites, using multiple radiocarbon samples, have proven these scatters were formed at different moments, most likely as a result of repeated re-occupation of the same locations sometimes over very long time-periods (Crombé et al., 2006; Crombé et al., 2013b). As such these sites should be interpreted as cumulative and/or spatial palimpsests, according to the definitions of Bailey (2007).

Table 17: List of excavated sites that were core sampled prior to the excavations and the excavation results.

	Total excavated surface (m²)	N of clusters	Area (m²) per cluster	Find-density per cluster (0.25 m²)	Sieve mesh (mm)
Evergem-Nest	2600	6	2.75–29.25 (mean 10.45)	23.0–39.4 (mean 28.4)	2
Hempens-Waldwei	443	3	5.25–64 (mean 36.16)	69.2–133.4 (mean 106.16)	3
Oudenaarde-Donk	145	2	3.25–11.5 (mean 7.37)	86.0–112.5 (mean 99.25)	1
Verrebroek-Aven Ackers	365	4	13.25–142 (mean 49.56)	14.6–38.2 (mean 26.25)	2
Verrebroek-Dok 1	2091	28	1.5–186.5 (mean 37.16)	13.5–158.4 (mean 42.5)	2

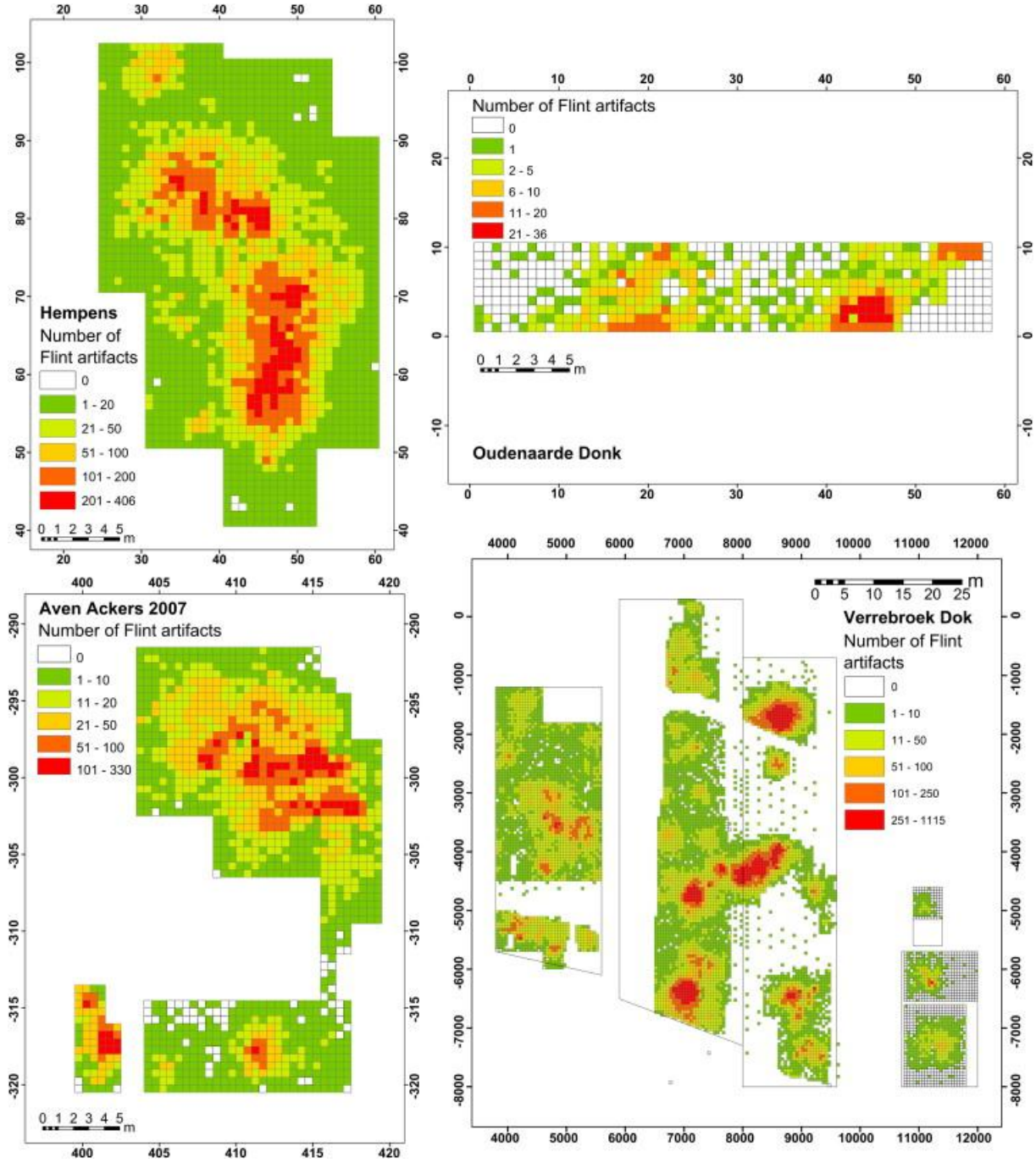

Figure 70: Distribution maps expressed in number of lithic artifacts per 1/4 m² for the excavated sites used in this study (from Verhagen et al., 2011). 1. Hempens-Waldwei; 2. Oudenaarde-Donk (2 mm mesh); 3. Verrebroek-Aven Ackers (trench VAA 2007 WP1); 4. Verrebroek-Dok 1 (local coördinate systems in varying units, varying orientation).

Despite the existence of some obvious intrasite and intersite spatial differences, we believe it is unrealistic to develop a reliable site classification based on size and find density following the example of Tol et al. (2004) and Verhagen et al. (2013) (Table 14 and Table 15). Establishing the total surface of covered sites is arduous as in most cases sites are only partially excavated or surveyed, or can be partially eroded. This also holds for the sites used in the present study. Even the extensive excavations at the site of Verre-

broek-Dok 1, covering ca. 6200 m² (Crombé, 2005), did not reach the limits of the site. In fact, augering combined with field-walking indicated this site is part of an extensive site-complex running for many kilometers without real boundaries between the different sites (cf. lithic landscape) (Crombé et al., 2011c; Perdaen et al., 2004). Another problem with site classification systems is the use of mean find-densities per site as a criterion. The data from Table 17 and Figure 71 clearly demonstrate that find-densities considerably vary even on an intrasite level. The analysis of Verrebroek-Dok 1 (Figure 71), being the most extensively excavated site, has pointed out convincingly that there is an almost infinite variation in size and density between the lithic clusters (Crombé et al., 2013b). Furthermore, the data related to site surface and density is affected by intersite differences in sieving, varying from 1 mm (Oudenaarde) to 2 mm or even 3 mm (Hempens). Taking all these limitations into account, still the Late Mesolithic site of Hempens stands out as to its find density; with a mean of 106 artifacts per 0.25 m² (= ca. 400 artifacts per 1 m²) this site definitely needs to be classified as a high-density site. Detailed spatial analysis (Noens, 2011) has proven this site to be a dense cumulative palimpsest. On the other hand, the sites of Evergem and Verrebroek-Aven Ackers are very similar with an overall find-density between ca. 26 and 28 artifacts per 0.25 m² (= ca. 100 artifacts per 1 m²). Most likely the site of Oudenaarde falls within the same "category". Referring to our sieving experiment in this paper (cf 7.4.3), we can assume that the high artifact density at this site is mainly caused by the predominance of microdebitage, consisting mainly of flint items smaller than 2 mm. Clearly Verrebroek-Dok 1 is a site of another category due to its extensive occupation surface (cf above).

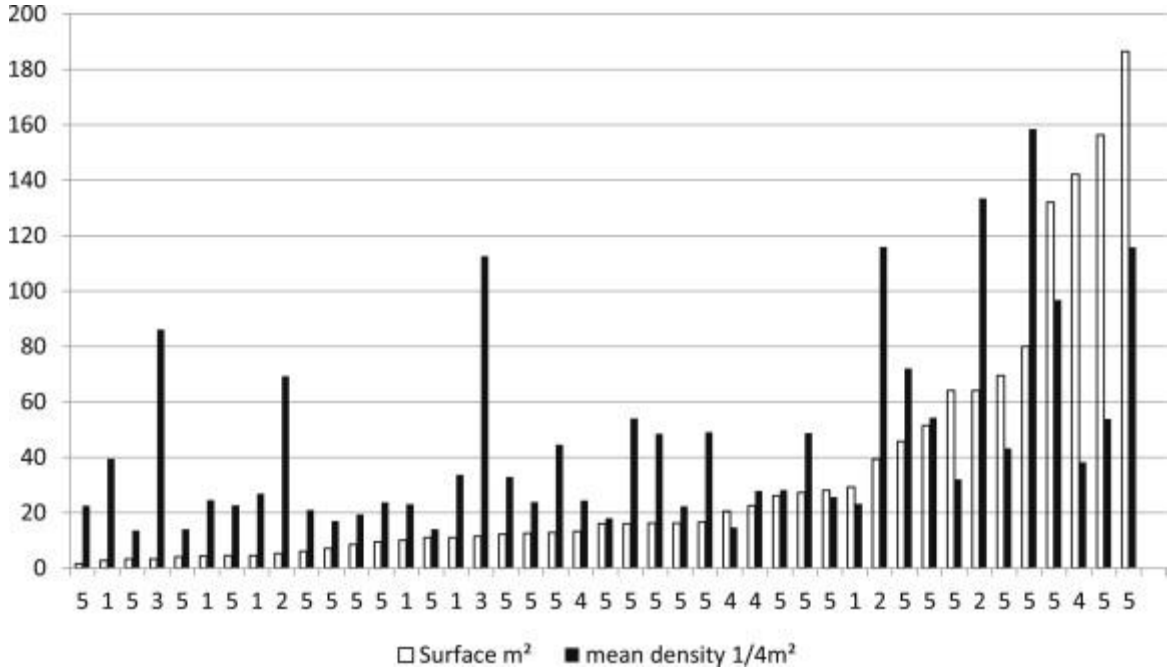

Figure 71: Variability in the size (m²) and find-density (artifacts per 0.25 m²) among the 42 excavated lithic scatters used in this study (cf. Table 17). 1. Evergem-Nest; 2. Hempens-Waldwei; 3. Oudenaarde-Donk; 4. Verrebroek-Aven Ackers; 5. Verrebroek-Dok 1.

7.3 Methodology

Starting from the augering data several estimations have been made in relation to grid size, sieving meshes, and also core diameter.

Enlarging the grid size was simulated by systematically reducing the number of boreholes and quantifying the number of remaining positive hits, following all possible arrangements. This resulted in a minimum and maximum discovery rate, based on the arrangements yielding resp. the lowest and highest number of positive hits. These were compared to the triangular grid area because this has a direct linear relation to the sampling 'costs'. The site of Oudenaarde had to be excluded since the augering project was limited to just two parallel rows of boreholes running over a distance of ca. 300 m. At Kerkhove, on the other hand, no such simulation was needed as the site was first drilled in a 30 × 30 m grid. As no lithic finds were collected, but just some carbonized hazelnut shells and small calcined bone fragments, it was decided to narrow the grid to 15 m, which resulted in several positive boreholes.

A second test aimed at quantifying the effects of mesh width during the sieving process. All lithics initially obtained through 1 mm meshes were sieved again, albeit in dry conditions, using meshes of 2 mm, 3 mm and 4 mm. This enabled us to estimate the degree of loss of positive boreholes and at the same time quantify the amount of artifacts that would be missed when enlarging the meshes. The former is relevant in terms of discovery probabilities, while the latter informs us about the possible impact of sieving meshes on the site assessment. The proportions of the positive boreholes using various mesh sizes were compared using a two tailed two sample Z-test for proportions (LeBlanc, 2004). p-values smaller than 0.1 were considered sufficiently high to suggest a significant difference between proportions. A minimum of ten positive and negative boreholes were reckoned to be required to calculate a reliable p-value.

Finally, one case-study allowed us to evaluate the impact of auger diameter on the discovery rate of prehistoric sites. At the site of Verrebroek-Aven Ackers cores with four different diameters (7–10–12–15 cm) were used next to each other within the same 0.25 m² at 69 different locations set within a grid of 5 m. This was done in the trenches of 2006 and 2007, right before the excavations started (Figure 72). The proportions of the total positive boreholes using various auger diameters were compared using the Z-test for population proportions (see above). Afterwards, these drilled squares were excavated using a 1 mm mesh, which allowed further assessment of the augering results.

Figure 72: Testing cores with different diameters at the Mesolithic site of Verrebroek-Aven Ackers (photo M. Bats, UGent): a 0,25 m² excavation unit, a 7 cm, 10 cm, 12 cm and 15 cm diameter Dutch handauger.

7.4 Results

7.4.1 Overall discovery rate

From Table 16 it can be deduced that the frequency of positive boreholes (i.e. the discovery rate) varies considerably from one site to the next. It ranges from a minimum of 2.5% at Sluiskil to a maximum 60%/73%, resp. at Hempens and Oudenaarde. However, on the majority of sites (8/11) the frequency of positive hits is situated between ca. 5% and 22%. A comparison with the excavation data helps us in explaining this large intersite variability. The extremely high number of positive boreholes at Hempens results most likely from the fact that, contrary to all other sites, the drilling project, which was conducted during the excavation, was very much focused on the lithic scatters and much less on the surrounding area. In addition, at Hempens many more artifacts occur in between the lithic clusters (so called 'background finds') compared to the other excavated sites (Figure 70). In some areas up to 55 artifacts per 0.25 m², including all categories of finds, have been reported (Noens, 2011). This is also the case at Oudenaarde, however,

here these background finds almost exclusively consist of very small artifacts, so called microdebitage (cf. discussion in 7.4.3). To date we cannot explain this phenomenon, but it may be assumed that post-depositional processes, such as fluvial erosion, may be responsible at Oudenaarde. If we exclude the sites of Hempens and Oudenaarde on the basis of the above arguments, it can be concluded that Mesolithic sites with an average find-density ranging from low to medium/high (following the definition of Tol et al., 2004; Verhagen et al., 2013) cannot be missed, at least if they cover a surface of minimum ca. 100–150 m². Sites of smaller dimensions and/or lower density eventually can be overlooked.

7.4.2 Grid size

The results of the grid spacing simulations (Table 18) demonstrate a considerable loss of positive boreholes when doubling the interval between the cores. Enlargement of the grid from 5 m (25 m²) to 10 m (100 m²) (Figure 73a–b) or from 10 m (100 m²) to 20 m (400 m²) (Figure 73c–d) induces a general decrease between roughly 60/70% to 80/90% of successful boreholes, except at Eine. Further broadening of the grid up to 30 m even reduces the discovery rate to more than 90%, eventually even 100%, for most sites. Of course in terms of site detection, what really counts is the real number of positive boreholes rather than their frequency. In the worst case scenario, enlarging the grid from 10 m (100 m²) to 20 m (400 m²) results at half of the sites in 5 or less positive boreholes; one site (Evergem) is not touched at all and another 3 (Hempens, Kalken, Sluiskil) by just 1 borehole. In more favorable situations, a 20 m (400 m²) grid leads to generally around 10 to 16 positive hits per site, a few sites excluded. The situation really becomes problematic when a 30 m (900 m²) grid is applied (Table 18). Except the extensive site of Verrebroek-Dok 1, the number of positive boreholes drops well below 10, in most cases even below 5. The chance of completely missing sites becomes very realistic as most sites are only touched by 1 or 2 or even not a single positive borehole. This increased risk is nicely illustrated by the coring project conducted at Kerkhove. As mentioned earlier, this site was first drilled in a 30 m (900 m²) grid leading to the discovery of not a single borehole yielding lithic artifacts. Subsequent narrowing of the grid to 15 m (225 m²) resulted in 26 positive hits. From this it can be concluded that augering in a grid larger than 10/15 m drastically reduces the discovery rate to a point where sites are only touched by a few positive boreholes or not at all.

Table 18: Minimal and maximal number of positive cores with simulated grids of 5 m, 10 m, 15 m, 20 m and 30 m spacing between coring locations.

	5 × 5 m 25 m²		10 × 10 m 100 m²		15 × 15 m 225 m²		20 × 20 m 400 m²		30 × 30 m 900 m²	
	Min.	Max.	Min.	Max.	Min.	Max.	Min.	Max.	Min.	Max.
Eine	–	–	5	5	–	–	3	4	0	2
Evergem-Nest	35	35	4	16	–	–	0	9	0	4
Gavere-Donk	–	–	27	27	–	–	5	8	2	7
Hempens-Waldwei	23	23	5	7	1	5	1	3	1	1
Kalken-Molenmeers	–	–	6	6	–	–	1	2	0	2
Kerkhove-Stuw	–	–	–	–	26	26	–	–	0	0
Schellebelle-Aard	–	–	52	52	–	–	11	14	2	10
Sluiskil-Kanaalkruising	–	–	5	5	–	–	1	2	0	4
Verrebroek-Aven Ackers	–	–	57	57			8	12	2	4
Verrebroek-Dok 1	154	154	34	40	–	–	12	16	5	9

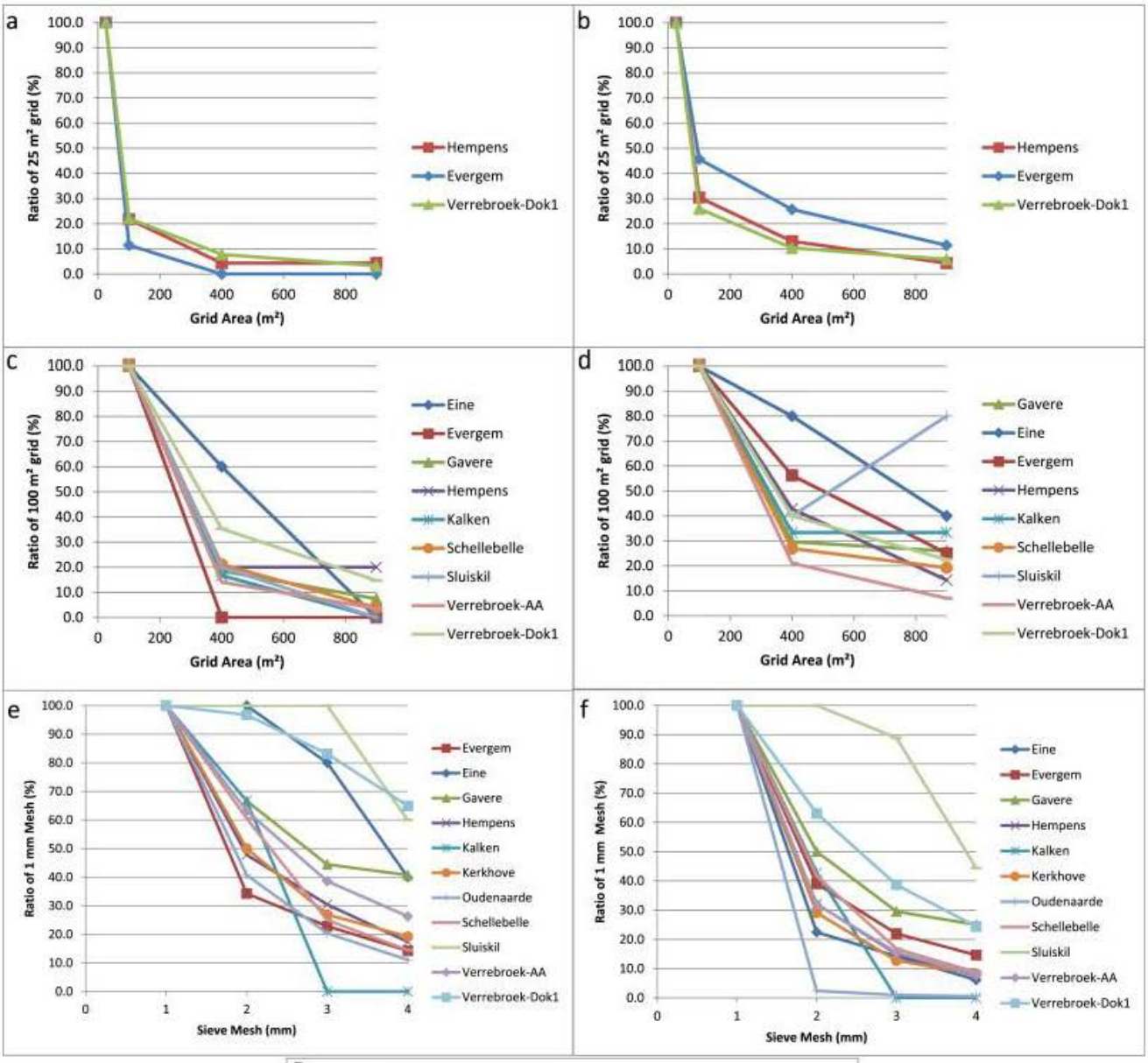
a
Ratio of 25 m² grid (%)
Grid Area (m²)
Hempens
Evergem
Verrebroek-Dok1
b
Ratio of 25 m² grid (%)
Grid Area (m²)
Hempens
Evergem
Verrebroek-Dok1
c
Ratio of 100 m² grid (%)
Grid Area (m²)
Eine
Evergem
Gavere
Hempens
Kalken
Schellebelle
Sluiskil
Verrebroek-AA
Verrebroek-Dok1
d
Ratio of 100 m² grid (%)
Grid Area (m²)
Gavere
Eine
Evergem
Hempens
Kalken
Schellebelle
Sluiskil
Verrebroek-AA
Verrebroek-Dok1
e
Ratio of 1 mm Mesh (%)
Sieve Mesh (mm)
Evergem
Eine
Gavere
Hempens
Kalken
Kerkhove
Oudenaarde
Schellebelle
Sluiskil
Verrebroek-AA
Verrebroek-Dok1
f
Ratio of 1 mm Mesh (%)
Sieve Mesh (mm)
Eine
Evergem
Gavere
Hempens
Kalken
Kerkhove
Oudenaarde
Schellebelle
Sluiskil
Verrebroek-AA
Verrebroek-Dok1
g
Positive Borehole Ratio
Core Diameter (cm)
VAA 2007 WP2
VAA 2006
VAA 2007 WP1
total

Figure 73: Fig. a–b: Intersite comparison of the minimum (a) and maximum (b) frequency of positive boreholes obtained with a 10/12 cm core and 1 mm sieve meshes, using different grid areas (25 m² = 5 m grid; 100 m² = 10 m grid; 400 m² = 20 m grid; 900 m² = 30 m grid). The results from the 5 m/25 m² grid are set at 100%.
Fig. c–d: Intersite comparison of the minimum (c) and maximum (d) frequency of positive boreholes obtained with a 10/12 cm core and 1 mm sieve meshes, using different grid areas (the results from the 10 m/100 m² grid are set at 100%).
Fig. e: Intersite comparison of the frequency of positive boreholes obtained with a 10/12 cm core within a 10 m grid, using different meshes (the results from the 1 mm mesh are set at 100%).
Fig. f: Intersite comparison of the frequency of lithic artifacts obtained with a 10/12 cm within a 10 m grid, using different meshes (the results from the 1 mm mesh are set at 100%).
Fig. g: Comparison of the frequency of positive boreholes within the different trenches at Verrebroek-Aven Ackers (the total amount of boreholes is set at 100%).

7.4.3 Mesh size

The above observations are all based on fine wet sieving with 1 mm meshes, assuming a 100% artifact retrieval. It can be expected that broadening the meshes will further decrease the discovery rate. The results of the sieving experiments (Table 19, Figure 73e) indicate a significant difference in the proportion of positive boreholes between 1 and 2 mm (p-value<0.1) at 6 sites (Evergem, Hempens, Kerkhove, Oudenaarde, Schellebelle and Verrebroek-Aven Akkers). At these sites just 35% to ca. 65% of the boreholes still yield artifacts when a 2 mm mesh is used. However, in real numbers they still yield a sufficient amount of positive boreholes in order to be detected. The situation changes drastically when meshes larger than 2 mm are used. At 3 mm the frequencies drop further to just ca. 20% to ca. 40%, now also including the sites of Gavere, Verrebroek-Dok 1 and Kalken (p-value<0.1). Still most sites yield at least 5 successful hits, except for Kalken which was not hit at all. At 4 mm only 5 sites are identified at least 5 times. The sites of Sluiskil and Eine have insufficient positive cores to perform a reliable Z-test of the proportions.

Table 19: Results and statistical significance of the sieving experiments based on data obtained within a 10 m grid and 10–12 cm core diameter of the sites survey using archaeological coring.

Site	Total number of cores	1 mm			2 mm				3 mm				4 mm			
		Positive cores	N artifacts	% Positive Cores	Positive cores	N artifacts	% Positive Cores	p-value (Z score proportions compared to 1 mm)	Positive cores	N artifacts	% Positive Cores	p-value (Z score proportions compared to 1 mm)	Positive cores	N artifacts	% Positive Cores	p-value (Z score proportions compared to 1 mm)
Eine	108	5	49	4.6	5	11	4.6	1	4	7	3.7	0.74	2	3	1.9	0.27
Evergem-Nest	408	35	41	8.6	12	16	2.9	0.001	8	9	2	0	5	6	1.2	0
Gavere-Donk	342	27	44	7.9	18	22	5.3	0.172	12	13	3.5	0.014	11	11	3.2	0.008
Hempens-Waldwei	41	23	53	56.1	11	17	26.8	0.01	7	8	17.1	0.001	4	4	9.8	0.001
Kalken-Molenmeers	78	6	7	7.7	4	3	5.1	0.509	0	0	0	0.015	0	0	0	0.015
Kerkhove-Stuw	143	26	110	18.2	13	32	9.1	0.025	7	14	4.9	0.001	5	9	3.5	0
Oudenaarde-Donk	74	54	1507	73	22	36	29.7	0	11	15	14.9	0	6	8	8.1	0
Schellebelle-Aard	587	76	137	12.9	46	57	7.8	0.004	19	23	3.2	0	11	12	1.9	0
Sluiskil-Kanaalkr.	198	5	9	2.5	5	9	2.5	1	5	8	2.5	1	3	4	1.5	0.478
Verrebroek-Aven Ackers	356	57	219	16	36	70	10.1	0.02	22	34	6.2	0	15	17	4.2	0
Verrebroek-Dok 1	702	154	693	21.9	149	437	21.2	0.75	128	268	18.2	0.084	100	169	14.2	0

The results are very variable when looking at the total amount of artifacts in relation to the mesh width (Table 19; Figure 73f). With a 2 mm mesh the loss of artifacts ranges between 0% (Sluiskil) and almost 100% (Oudenaarde). In the latter case the number of lithic finds drops from 1507 to 36! Yet, the loss on most sites situates generally between ca. 50% and 80%. This loss increases generally until ca. 80%–90% with 3 mm meshes and ca. 90% with 4 mm meshes, a few sites excluded. Although this in most cases has little impact on the discovery rate, the extremely small amount of drilled artifacts (<10–15 artifacts per site) considerably impedes the assessment of the discovered site in terms of its chronology, internal spatial patterning, and extent.

7.4.4 Auger diameter

The results of the tests with different core diameters (Table 20) conducted at Verrebroek-Aven Ackers within a 5 m grid need to be addressed with some caution. Referring to our introduction, we need to take into account the uneven distribution of lithics within the soil, even within a small unit as 0.25 m², which certainly will affect the data. However, the large sample of our test case (69 corings per core type) weakens these biases to a certain degree allowing us to observe some general trends, which need to be further verified by means of future studies.

Trenches	N cores	7 cm		10 cm			12 cm			15 cm		
		N positive cores	%	N positive cores	%	p-value (Z-score proportions compared to 7 cm)	N positive cores	%	p-value (Z-score proportions compared to 10 cm)	N positive cores	%	p-value (Z-score proportions compared to 12 cm)
VAA 2006	29	8	27.6	13	44.8		12	41.4		12	41.4	
VAA 2007-WP1	23	17	73.9	17	73.9		21	91.3		20	87	
VAA 2007-WP2	17	1	5.9	3	17.6		3	17.6		6	35.3	
Total	69	26	37.7	33	47.8	0.23	36	52.2	0.64	38	55.1	0.72

Table 20: Frequency of positive boreholes for different core diameters, listed per excavation trench, at Verrebroek-Aven Ackers (5 m grid and 1 mm sieving mesh).

The p-values (Table 20) demonstrate that there are no significant differences in detection rate between the different core diameters. However, from Figure 74a it is clear that the greatest gain is obtained when using a 10 cm instead of a 7 cm auger; the number of positive hits increases by almost a fifth (18.4%). The difference with the 12 cm and 15 cm is clearly less pronounced. The opposite seems true for the total yield of artifacts (Figure 74b); here the biggest gain is reached when changing a 12 cm auger into a 15 cm auger (ca. 37%).

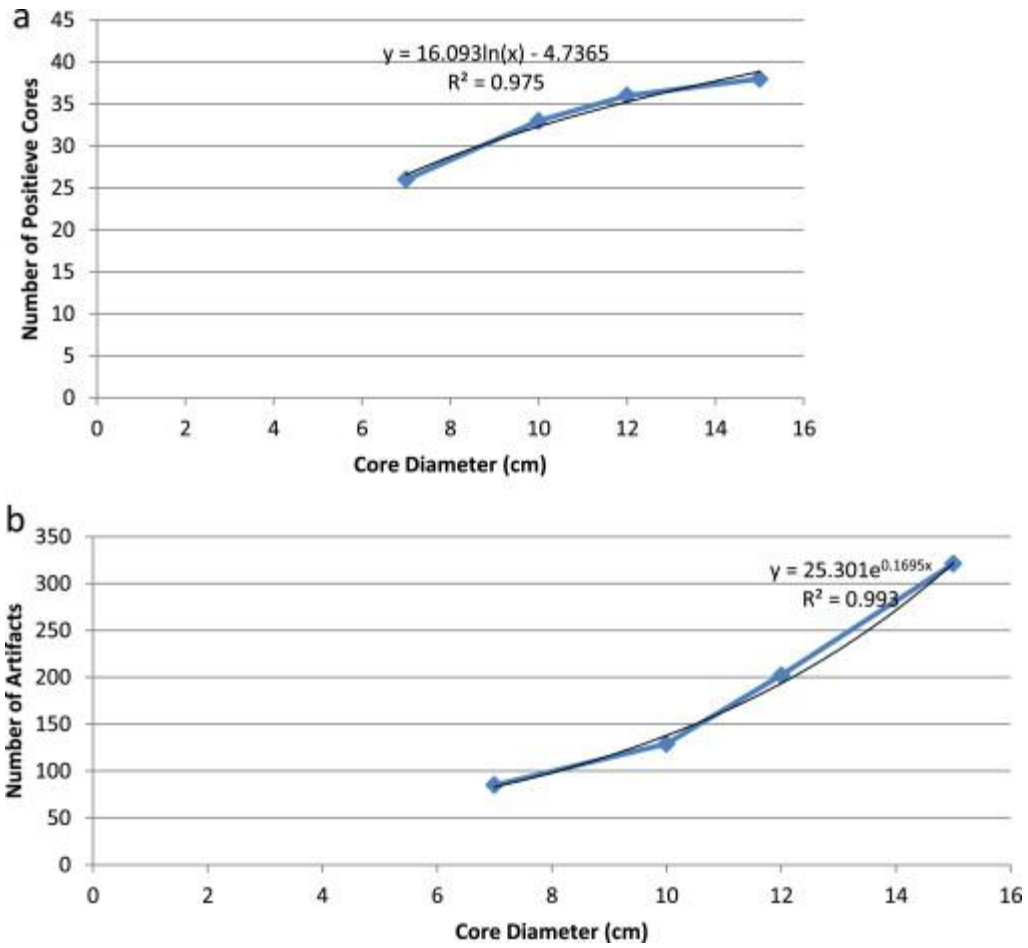

Figure 74: a: Comparison of the relative occurrence of positive boreholes per core diameter (the results from the 15 cm core are set at 100%) at Verrebroek-Aven Ackers; b: Comparison of the amount of lithic artifacts within boreholes per core diameter (the results from the 15 cm core are set at 100%) at Verrebroek-Aven Ackers.

This experiment is also interesting in terms of the overall discovery rate when using a grid of 5 × 5 m. Indeed, the data from Table 20 demonstrate that all auger diameters reach high scores, situated between ca. 38% (7 cm) and ca. 55% (15 cm), with respect to the totality of performed cores. The difference in discovery rate with the 10 cm core applied in a 5 m (Table 20; ca. 48%) or a 10 m grid (Table 16; ca. 16%) is considerable. However, similar to Hempens (cf. 7.4.1) this is partially caused by the focus of this coring experiment on the dune tops where the density of lithics is highest. As such these data

give a somewhat biased view compared to a prospection project without prior knowledge.

7.5 Discussion

The present study was set up to evaluate different core sampling strategies in order to develop the most optimal strategy for detecting an as broad as possible spectrum of Paleolithic and Mesolithic sites in covered contexts. Due to post-depositional burial by fluvial and/or aeolian sediments there is often no prior knowledge about the types of sites to be expected within project areas. Hence, we question the recommendations of former studies (Tol et al., 2004; Verhagen et al., 2013) in which specific sampling strategies for each type of site have been proposed, while favoring the use of a standard sampling strategy which can be applied in all conditions. If, however, reliable prior information is available one can decide to adapt the sampling strategy accordingly in order to obtain the best results.

Our study, albeit still preliminary, has clearly demonstrated that from the three variables – grid size, mesh size and core diameter – the latter has the least effect on the discovery rate of lithic sites. Choosing between a 10 cm, 12 cm or 15 cm core apparently does not lead to substantial differences in number of positive hits. This is an important observation especially for surveying deeper contexts, which are technically difficult to sample with cores of ≥10 cm due the considerable depth (>3 m) and/or soil characteristics (texture, moisture, etc.) of the potential archaeological strata, even when augering is done mechanically. Our observations also show that even in shallow situations the general use of 15 cm–20 cm cores, as recommended by Tol et al. (2004) and to a certain degree by Verhagen et al. (2013) (cf Table 14), is not really necessary. A comparison between the augering and excavation data from the site of Verrebroek-Aven Ackers allows us to study the relationship between core diameter and the size and density of the excavated lithic scatters in more detail. At this site three trenches were excavated, two situated on the top of small dunes (VAA 2006; VAA 2007 WP1) and one on a dune flank (VAA 2007 WP2) (Figure 75). The former two trenches revealed a dense pattern of lithic clusters of varying sizes (from 15 to 142 m²) and densities (from ca. 60 to 185 per/m²) (Table 17, Figure 70), typical of palimpsest sites (Crombé et al., 2013b; Sergant et al., 2007). On the other hand trench VAA 2007 WP2, investigated by means of test-pits (Figure 76), rather yielded a low density artifact distribution in which four discrete clusters of 3–4 m in diameter and a low-density (<80 per m²) can be discerned. This pattern, which was also observed on the dune flanks of other excavated sites (e.g. Verrebroek-Dok), is typical for peripheral zones of Mesolithic camp-sites (Figure 77). A comparison

of the effectiveness of different core diameters between these three trenches (Figure 73g) demonstrates some important differences related to find-density and size of the lithic clusters. As a matter of fact there is a difference in discovery frequency of ca. 50% to ca. 75%, depending on the core diameter used, between the trenches on the dune tops, in particular VAA 2007-WP1, and the dune flank trench VAA 2007-WP2. The high score in VAA 2007-WP1, even with a 7 cm core, clearly is due to the presence of medium sized and medium density scatters. In contrast, a 7 cm auger is not appropriate at all for finding small, low-density areas or sites, as clearly demonstrated by trench VAA 2007 WP2 (Figure 73g). Here the use of larger cores, preferably up to 15 cm, is strongly recommendable, as it increases the discovery rate exponentially up to a factor of 6.

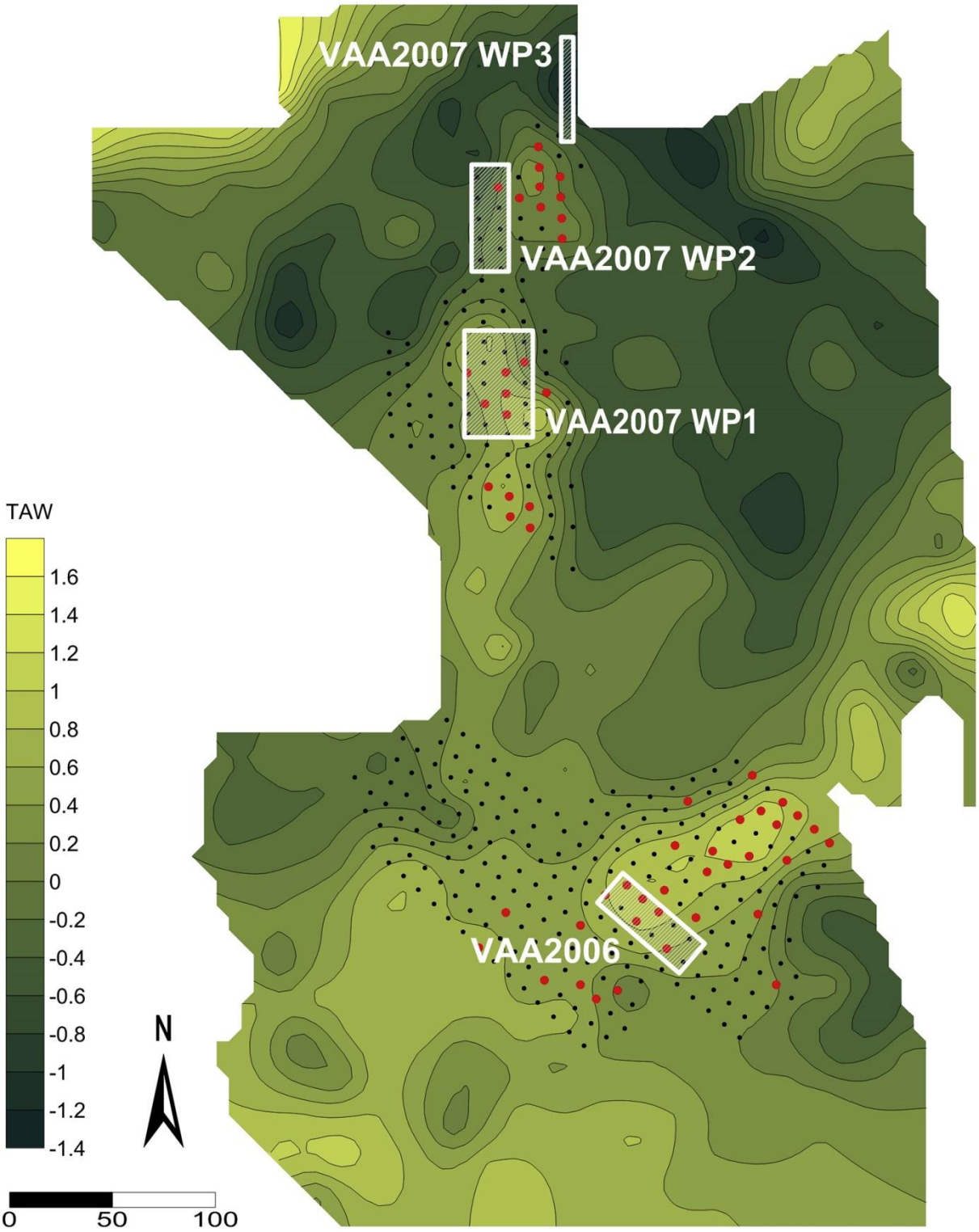

Figure 75: Map of the buried Pleistocene coversand topography with the positioning of the excavation trenches investigated in 2006 and 2007 at Verrebroek-Aven Ackers. The black dots represent negative boreholes, the red dots the positive ones within a 10 × 10 m grid.

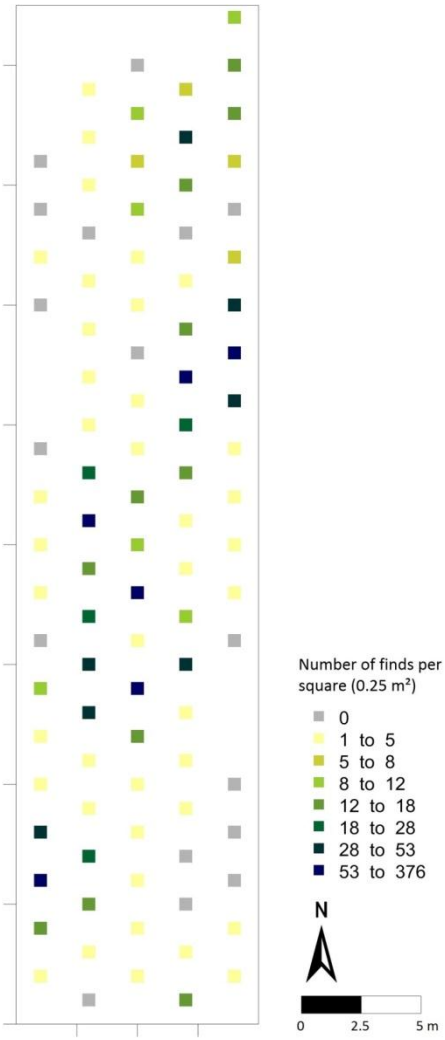

Figure 76: Density map of the lithic finds from test pitting within trench VAA 2007 WP2 at Verrebroek-Aven Ackers, expressed in number of lithic artifacts per 1/4 m².

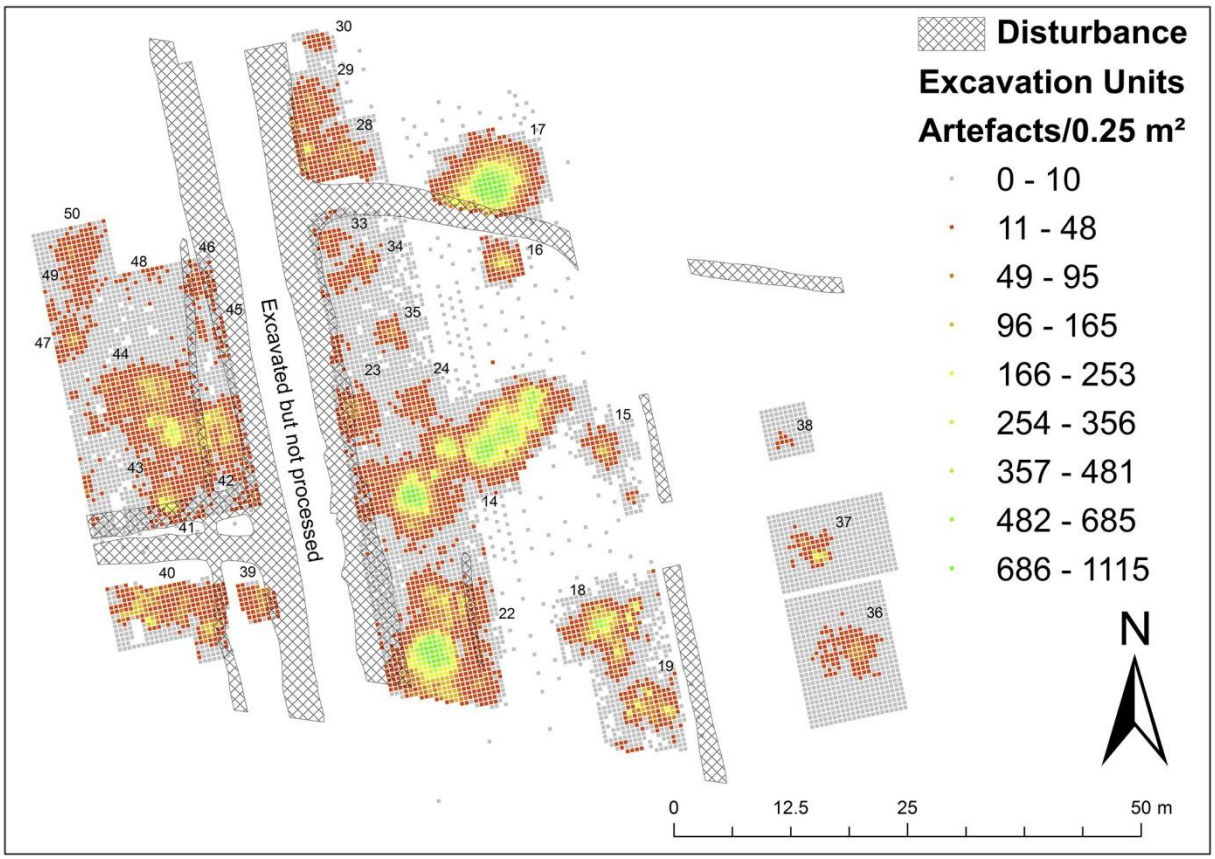

Figure 77: Artefact distribution map of the site of Verrebroek-Dok 1, labelled with the number codes of the individual lithic scatters mentioned in the text.

The analysis of the sampling grid size conducted in this study has demonstrated that 10 m or smaller interdistance between the boreholes, especially when working with 10/12 cm augers, is to be strongly encouraged. The effectiveness of a 15 m grid needs further testing as in this study the dataset is restricted to just three sites. Enlarging the grid to 20 m or 30 m generally induces a loss of positive hits between 60% and 90%, except for extensive site-complexes such as Verrebroek-Dok 1; in fact, some sites (Evergem, Kerkhove) would not have even been detected at all. Again, small and low-density sites or scatters turn out to be the most difficult to detect, as demonstrated by the available excavation data. Comparison of the augering and excavation data from the extensive site of Verrebroek-Dok 1 (Figure 77 and Figure 78) allows us to conclude that very small scatters occupying less than ca. 15 m² and having a find-density between ca. 80 and 100 artifacts per m² (e.g. clusters 15, 30, 33, 34, 35, 38) are missed even when sampling is done in a 5 m grid and with a 15 cm core. Although some of these very small clusters were touched by the core, the drilled sample did not yield prehistoric finds. All this confirms Tol et al. (2004) and Verhagen et al. (2013), who state that very small sites with densities <40 artifacts per m² are as good as untraceable by means of core sampling but need to be addressed by means of test-pits eventually combined with coring in a 5 m grid. However, slightly larger scatters, such as clusters 16, 23, 24, and 37 at Verrebroek-Dok, covering between ca. 15 and 25 m² but having a similar low find-density can even-

tually be hit within a 5 m grid, although not systematically (e.g. cluster 36). This is also demonstrated by the data from the nearby site of Verrebroek-Aven Ackers. Core sampling in the peripheral trench VAA 2007 WP2 within a 10 m grid revealed only one positive borehole, yielding 8 artifacts, despite the presence of at least 4 low-density clusters, comparable to the ones at Verrebroek-Dok (cf. supra). Yet, reducing the grid size to 5 m (Table 18) resulted in an increase of positive hits up to 3 (10 and 12 cm core) and even 6 (15 cm core). So, contrary to Tol et al. (2004) and Verhagen et al. (2013) our data suggests that core sampling within a 5 m grid may be successful in detecting low-density scatters smaller than <50 m², albeit not with a 75% detection probability.

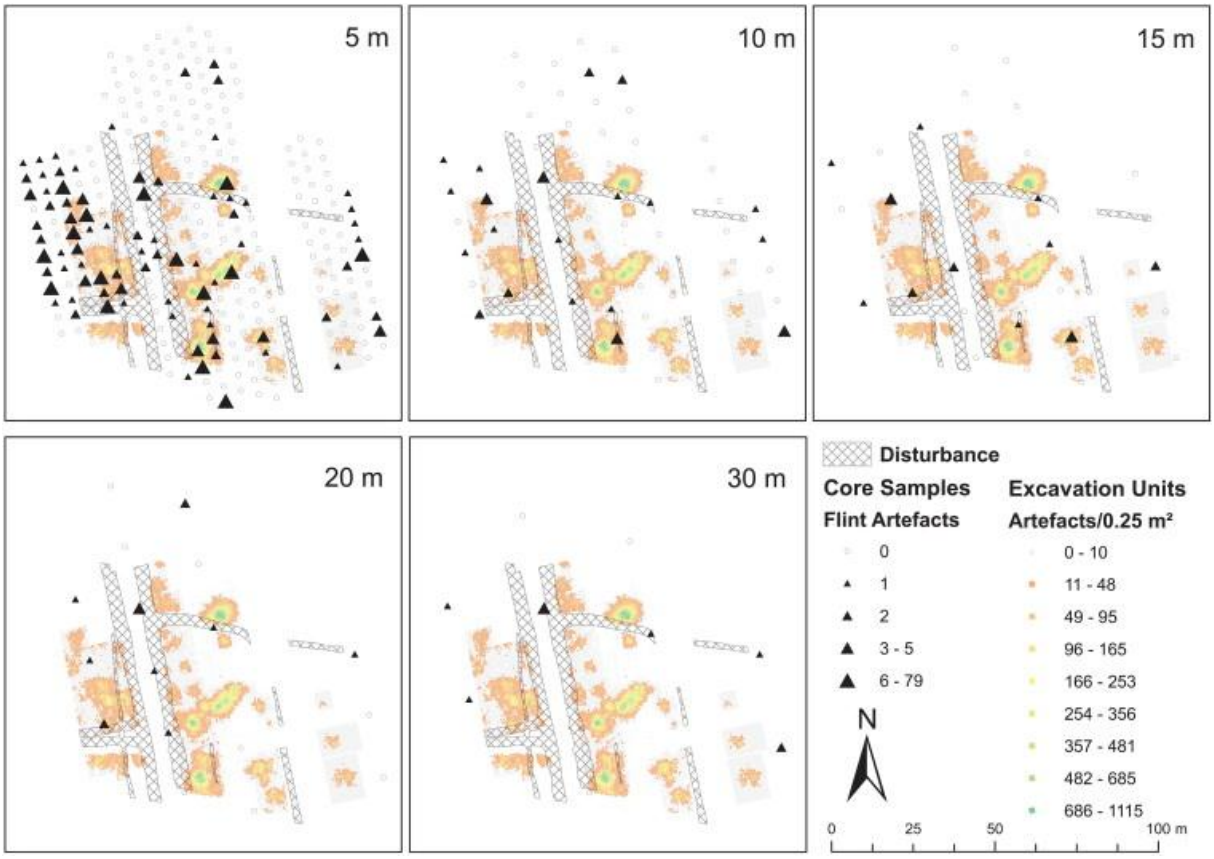

Figure 78: Simulation of the core sampling grid at Verrebroek-Dok 1 (15 cm core and 1 mm meshes) in relation to the excavated lithic scatters. The simulations yielding the highest amount of positive hits have been selected per grid.

The comparative analysis of the Verrebroek-Dok excavation data allows us to assess the existing core sampling strategies even further. Following Tol et al. (2004), the site, which can be classified as a large and high-density site, should be sampled in a 40x50 grid with a 15–20 cm core and sieved with 1 or 2 mm meshes. From our simulations of the augering data (Figure 78) it is clear that this would result in an absolute minimum of positive hits, as the 30 m simulation already did not result in a single positive hit within the excavated area, despite the presence of several extensive and high-density clusters. Enlarging the grid to 40/50 m would most likely result in missing the site completely. The strategy proposed by Verhagen et al. (2013) for this type of site, consisting of coring

in a 20 × 25 m grid with a 12 cm core would yield better results if applied to Verrebroek (Figure 78), however without reaching the expected 75%. In addition the spatial resolution is seriously affected, as large parts of the site, in particular the SE and central parts of the excavated sector, are not touched at all. So, the comparison of excavation and augering data at Verrebroek-Dok leads us to conclude that, although this extensive site would have been detected using a grid up to 30 m, the spatial resolution reaches a critical point once the spacing between the boreholes is enlarged to >10 m.

The discovery rate and spatial resolution are further impacted by the size of the sieving mesh. Our tests have shown a reduction of 60%–80% of positive hits when using a 3 mm sieving mesh, as generally recommended by Verhagen et al. (2013) and Tol et al. (2004) (Table 14 and Table 15). At the site of Verrebroek-Dok (Figure 79) enlarging the mesh size in combination with a sampling grid >5 m would result in hardly any positive hits (between 6 and 2) and lithic finds (1–2 per borehole), complicating the assessment of the site considerably. Apparently the use of a 3 mm mesh on this particular extensive and high-density site is justifiable only when applied in a 5 m sampling grid. It is questionable whether this also holds for smaller and less dense sites, given the considerable loss of artifacts per borehole when increasing the mesh size.

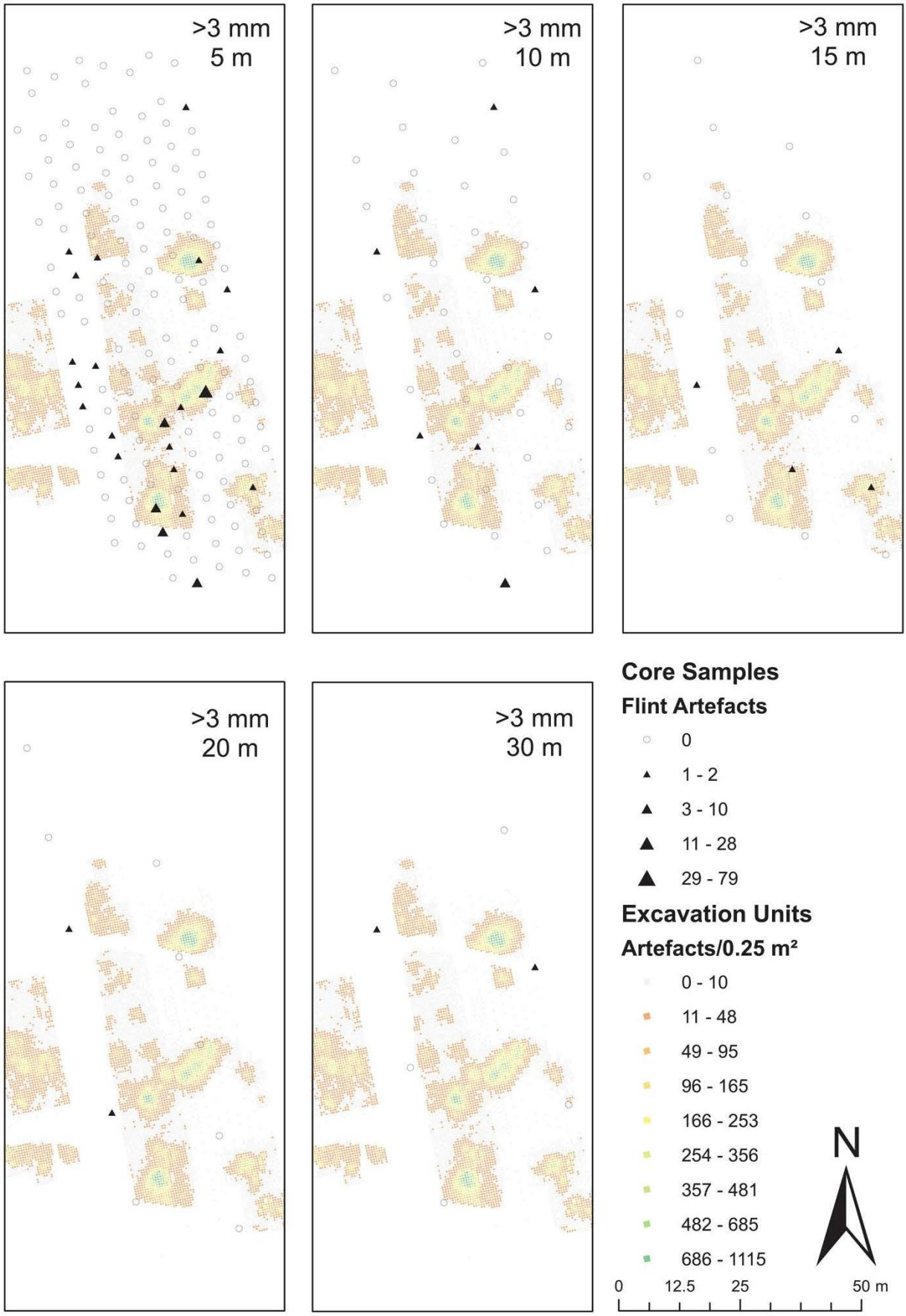

Figure 79: Simulation of positive coring results with 3 mm sieving in relation to different sampling grids at Verrebroek-Dok (central part of the excavated area).

The importance of the finest lithic fraction is also demonstrated by experimental and excavation data (Noens et al., 2013). Recent experimental work has shown that the 1 mm fraction on sites where flint knapping has been conducted amounts to a mean of 61% of all artifacts, whereas the 2 mm fraction is situated around 19% mean. Similar observations have been gathered at various excavations in the Scheldt valley where 2 mm wet sieving has been systematically applied. At the Early Mesolithic site of Doel, for example, the 2 mm fraction has been quantified at ca. 48% of the total industry recovered. So, all this implies that if sieving is done with meshes >2 mm between 50% and 80% of the finds can be lost, which considerably reduces the discovery rate even when sampling in a small grid and with a large core. This mainly applies to sites where flint knapping was an important activity, as is the case on nearly all known Paleolithic and Mesolithic sites within the study-area and even beyond. Despite the obvious advantages, the use of small meshes is often dissuaded based on the argument that it generates extra costs as more finds have to be processed, i.e. selected and analyzed (Peeters, 2007; Tol et al., 2004). Tol et al. (2004) estimate that the costs per borehole increases with ca. 60%, however without mentioning how this was calculated. Based on personal experience this seems highly exaggerated. Sieving through 1 mm instead of 3 or 4 mm will not induce that much extra time on the condition that it is done by means of water, except when one is dealing with highly organic (e.g. peaty) or fine-grained soil material (e.g. clay, loam). However, most Paleolithic and Mesolithic sites in the Dutch and Belgian lowlands are situated in sandy soils, which are easy to sieve wet. In addition it is sometimes claimed that fine sieving renders the selection and identification of small artifacts, chips or microdebitage, more difficult due to the presence of natural mineral material, so called pseudo-artifacts (Tol et al., 2004; Wansleeben and Laan, 2012). Based on our experience, however, these problems can be avoided or at least minimized if the selection process is done by a trained prehistorian. Other researchers have also emphasized the importance of experienced staff and their influence on survey results (Banning, 2002; Kildea and Musch, 2006; Peeters, 2007). Peeters (2007) rightly states that "there is no point in having (core) samples processed by people who are not able to distinguish between naturally formed flint and small flint knapping debris". Furthermore admixture with pseudo-artifacts is generally related to the sieving of fluviatile sediments (e.g. scroll-bar sediments) and does not occur or much less within aeolian sediments (e.g. coversands). From the eleven sampled sites within our project, serious admixture has only been attested at the site of Oudenaarde. If, however, the selection of pseudo-artifacts is rendering too much problems or costs due to the fine screening, one can always decide to dry sieve the recovered lithic assemblages again through a larger mesh, as we have done in our mesh test (cf. 7.4.3). This is a fast procedure, which will not induce too much extra costs but provides a backup control. Contrary, if sieving is done immediately with larger meshes (>2 mm) there is no possibility at all to assess the loss of information afterwards.

One could of course argue that all these efforts in reducing grid size and meshes are superfluous as theoretically one positive borehole is sufficient to find a site. In practice, however, the lesser the amount of successful boreholes, the more difficult it becomes to fully assess the site in terms of its extent, chronology and spatial lay-out, while this information is crucial in view of further research, e.g. finer coring and/or excavations. Sampling in a wide grid and/or with larger meshes inevitably results in the detection of a few positive boreholes, characterized by a scattered distribution and very limited finds (Figure 78 and Figure 79).

Especially within developer-led archaeology augering survey projects yielding only few scattered hits often lead to long and tough discussions with project financers and/or heritage managers whether such "sites" are really important for further investigation. In most cases a decision against further research is taken, despite there being no real guarantee of a lack of worthwhile sites. It is obvious that mainly sites with the smallest surface and lowest find-density are threatened by such decisions. In the best-case scenario, core sampling would be extended by adding a few boreholes around each positive borehole in order to check for its relevance. However, this too leads to a totally biased view of artifact distribution within sites, as one assumes that the negative boreholes from the initial coring phase are effectively negative, and by consequence the entire zone around them. The best strategy seems to be a step-wise approach, starting with sampling in a 10 m grid that allows the detection of sites and first assessments, such as defining site boundaries. Within the limits of the site(s) a second sampling stage within a 5 m grid can be performed with special focus on the edges of the site(s). The excavations at both Verrebroek sites have taught us that low-density areas within or at the periphery of sites can only be traced when using a fine grid (5 × 5 m), preferably combined with a 15 cm core, although some results can also be achieved with a 10/12 cm core. If the survey-area is small, one can even decide to skip the first stage and directly auger within a 5 m grid.

7.6 Conclusions

The outcome of this simulation study is that core sampling with a core diameter of 10 cm is sufficient for the detection of Paleolithic and Mesolithic camp-sites, from low/medium to high-density, and from rather small (>100 m²) to very extensive. The potential of a 7 cm auger must still be further investigated, but certainly will allow detection of some types of sites, most likely the larger and denser ones (e.g. Verrebroek-Dok 1, Verrebroek-Aven Ackers WP1, Hempens). These new insights open new perspectives for surveying in deeply buried landscapes and sampling of prehistoric levels situ-

ated at great depths. However, two conditions must always be fulfilled: the grid size may not exceed 10 m and sieving has to be done with meshes of preferably 1 mm, if not a maximum of 2 mm. Even better would be a step-wise approach in which a 10 m initial stage is followed by a 5 m sampling in order to also define areas with lower densities of artifacts. We are aware of the financial implications of this strategy compared to earlier recommendations by Tol et al. (2004) and Verhagen et al. (2013), but it seems to be the best method for avoiding surveys that result in finding the same types of sites over and over again, i.e. the large and dense "palimpsests" ones, while the smaller sites with a lower artifact density, which might represent less mixed or less frequently re-occupied locations, slip through the nets. In the end it will prevent the reconstruction of prehistoric settlement systems and land-use based on biased information, as the detection of a greater diversity of prehistoric sites will enable a better capturing of human behavioral variability. As M. Shott (1985) rightly states "the costs of surveys, however, should follow their goals, not place limits on what they can accomplish. If such increases are needed to produce more reliable results, then we should be prepared to accept them".

7.7 Acknowledgments

This study was conducted within the framework of a research project funded by the Special Research Fund of Ghent University (BOF 011/052/04), entitled "The Flemish wetlands. An archaeological survey of the Scheldt floodplains". Most fieldwork was done by M. Bats in collaboration with numerous colleagues and students from Ghent University, who all are kindly acknowledged. We also want to thank our UGent colleagues, Erick Robinson and Joris Sergant, as well as two anonymous reviewers for the critical reading of our paper and their most valuable comments.

Conclusions and perspectives

Methodological progress in context

In Chapter 2, geophysical and geotechnical techniques were explored as an alternative for coring to spatially reconstruct buried prehistoric landscapes in the Scheldt polders. Although previously only employed in fresh water river plains (Bates et al., 2007; Howard et al., 2008), EMI and CPT were evaluated in an area with both fresh and salt groundwater conditions. This showed the reliability of CPT and revealed that EMI data were more complex to interpret in salty groundwater conditions. When both fresh and salty groundwater are present, subsurface modelling was impossible using EMI data. Nevertheless, important qualitative interpretations were possible in these challenging conditions if the EMI data are backed up by a limited number of coring or CPTs. This proved a reliable combined survey strategy to map paleolandscape units for subsequent archaeological core sampling by hand coring. The results also showed that multifrequency EMI, did not increase or provide multiple DOIs, confirming McNeill (1996) and contrasting to claims made by Won et al. (1996). ERI and land seismics did not give the required results (i.e. high resolution maps of small buried floodplain geomorphic units), mainly because of the slow data acquisition speed and data processing. In the study region, ERI and land seismic can be used to characterize known features units however, e.g. to interpret parts of an EMI dataset. This application contrasts with Gourry et al. (2003) and (Bates et al., 2007), who use ERI equally to EMI.

In Chapter 3, CPT was further evaluated as a direct replacement for gridded coring. To the author's knowledge, this has not yet been done in an archaeological context. It is already widely used to fill gaps in coring transects however (e.g. Amorosi and Marchi, 1999). CPT was also tested as a calibration tool for near surface geophysical data. Rather than using simple CPT-E or CPT-U data and infer geophysical properties indirectly as done by Bates et al. (2007), CPT-S and CPT-C were employed to directly measure respectively seismic velocity and electrical conductivity. This illustrated that CPT-E records subtle lithological differences such as intercalating OM rich clay intercalating the peat

layer which are not recorded in the electrical data of the CPT-C. On the other hand, CPT-E could not explain saltwater variations which are recorded in the electrical conductivity data of CPT-C, EMI and ERI, which makes CPT-E less suitable as a geophysical data calibration. In addition CPT was tested at Kerkhove, where it recorded subtle differences in the OM rich clayey sediments and peats, which could not be recorded using near-surface geophysics. This chapter also highlights the difficulties in quantitatively interpreting peats (Robertson, 2010). These could not be solved using pore pressure data as suggested by Fellenius and Eslami (2000).

Whilst previously constructed ground water or peat level rise curves only used mean and range values of dates (e.g. Van De Plassche et al., 2010), the latter was modelled for the first time using the full probability distribution functions of the radiocarbon dates and Bayesian analysis in Chapter 4. In combination with Chapter 5, Chapter 4 is amongst the rare case studies integrating geological and archaeological chronological models using Bayesian methods (e.g. Gearey et al., 2009). This combined analysis allows us to propose chronological hypotheses such as the correlation between the start of a tidal influence intercalating peat formation and the appearance of the first Neolithic 'Swifterbant' cultural tradition in the study region with unprecedented precision.

Paleogeographic maps are mostly based on national or regional coring databases (Vos et al., 2011; Vos and van Heeringen, 1997). In Chapter 6, a local scale paleogeographic reconstruction is made for the first time using a three layer subsurface model of a complex lithostratigraphic sequence, derived from EMI data, using the depth of investigation curves proposed by (McNeill, 1980). This provides a methodology to split shallow (Post) Medieval soil features from the underlying geological variability. Recently similar local palaeogeographical maps, derived from geophysical data, have also been produced in archaeological evaluations by Vos et al. (in press). Bayesian analysis of the chronological data also allowed that archaeological research question oriented paleogeographic maps were made. This forms a significant progress compared to previous EMI based (prehistoric) paleolandscape mapping strategies (Bates et al., 2007; Conyers et al., 2008). The developed evaluation strategy is directly applicable to individual archaeological projects in the study area.

It has to be emphasized that the proposed archaeological evaluation strategy is not suited to map discrete features such as posthole structures from younger periods. Regional paleogeographic maps show that significant areas of the landscape were not yet covered by peat in the Bronze Age (Heirman et al., 2013; Vos and van Heeringen, 1997). Therefore, the Scheldt polders region was theoretically suitable for longterm (Neolithic or) Bronze Age occupation and exploitation. In addition, van Dinter and van Zijverden (2010) have shown that crevasse splay deposits have formed attractive locations for Neolithic to Bronze Age settlement in the Rhine-Meuse estuary. Indeed, for the period after their formation these crevasse splays were temporary dry, elevated locations in the floodplain until they were permanently flooded or overgrown by peat. Bronze- and Iron

Age settlement sites have been found in nearby Sint-Gillis-Waas, just outside the Scheldt polder area (Bourgeois and Hageman, 1998; Bourgeois et al., 1996; Lauwers and De Reu, 2011). Such sites could also be present on locations within the Scheldt polder region, which were only overgrown with peat after this period. The subtle soil features of the Bronze- and Iron Age structures, dug into the peat covered sands, can not be detected using the proposed coring, CPT or geophysical survey strategy and require more invasive techniques such as trial trenching. De Clercq (2009); De Clercq and Van Dierendonck (2008) and Sier (2003) have presented that at least from Roman times onwards the top of the contemporaneous top of the peat was inhabited and/or exploited extensively. The archaeological remains of this occupation are hard to detect, even with more invasive methods such as trial trenches at Ellewoutsdijk, because they consisted of wood, the same material as (and possibly recovered from) the peat itself (Sier, 2003). In general, if archaeological sites don't consist of relatively large and dense artefact clusters, they are hard to detect using coring. Prospecting these small soil feature sites remains problematic at the large depths of possible archaeological levels in the Scheldt polders. These depths are beyond the range of most near surface geophysical instruments.

Larger Medieval land division structures, such as dikes, raised roads or ditches, and moated sites have proven to be detectable in trial trenches and in the results of multiple coil spaced EMI survey with 2-3 m line spacing (e.g. De Smedt et al., 2013a) but are often not recognized in coring survey (e.g. unpublished results from Verrebroek Schoorhavenweg).

Even if they are detected using (non-) or limited invasive methods at all, an accurate evaluation of the degree of preservation of archaeological feature of structure sites will always require (targeted) invasive archaeological excavation (e.g. De Smedt et al., 2013c).

A spatial and chronological prehistoric landscape reconstruction strategy

The main aim of this PhD research is the development of a spatial and chronological prehistoric landscape reconstruction strategy for the archaeological prospection of a diverse range of stone age sites, mainly composed of scatters of lithic artifacts, buried below the Lower Scheldt polders and floodplain. An archaeological evaluation procedure is proposed consisting of a paleolandscape reconstruction in view of subsequent archaeological prospection, namely detecting buried Stone Age artifact scatter sites in the study area.

The proposed prehistoric paleolandscape reconstruction consists of a decision schema in various steps: desktop study and geological mapping followed by archaeological prospection in the strict meaning of archaeological site mapping (Figure 80). Based on this PhD research, conclusions on the diverse choices to be made during this process are discussed and opportunities for further research developments proposed.

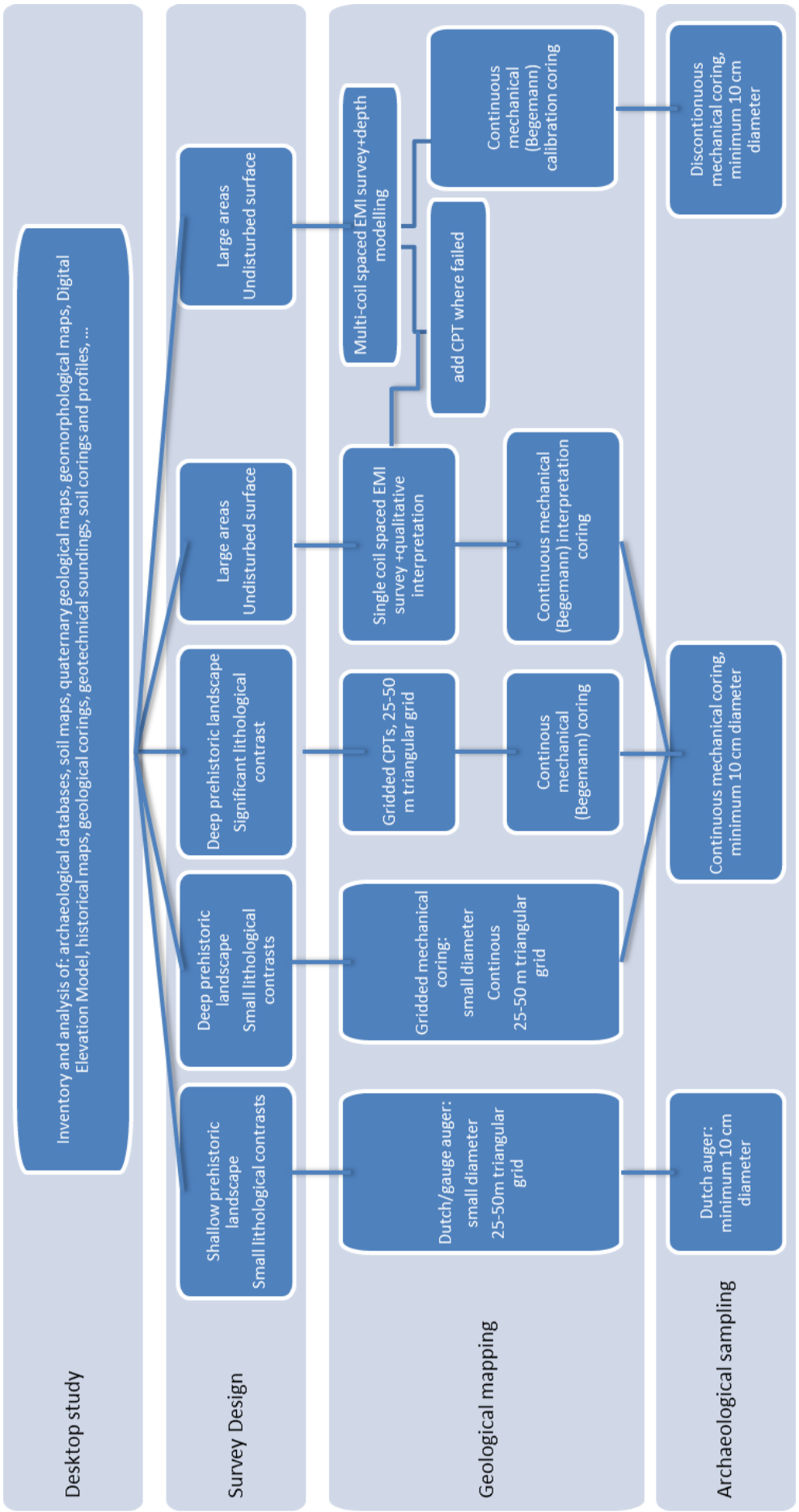

Figure 80: Proposed archaeological evaluation decision scheme for alluvial plains or polders for detecting prehistoric sites.

Desktop study and survey design

The importance of a thorough desktop study at the start of the archaeological evaluation process cannot be underestimated. It is of paramount importance to create an inventory of all relevant data allowing an assessment of all possible suitable paleolandscape reconstruction methods.

Relevant aboveground factors to consider are the state of the terrain surface, overgrowth and modern (metallic) disturbances, such as constructions, metal fences, pillars, power lines, etc. These can be assessed on the basis of cartographic information (e.g. orthophotos) but often a terrain visit prior to the survey provides the most recent view on the state of the terrain.

Furthermore, the nature of the top soil is also of importance. Heavily plowed or badly drained soils impede mobility. Natural topsoil clay impedes the use of ground penetrating radar, but a conductive topsoil is advantageous for EMI methods. The presence of an anthropological topsoil also has to be investigated. Over the last century, many polders and floodplains, especially in the expansion area of the Antwerp harbor, have been raised e.g. with dredging sediments or construction waste materials. These increase burial depth of archaeological levels and may influence geophysical and geotechnical results. This was experienced at the archaeological site of Kerkhove-Stuw, where the EMI and ERE surveys gave negative results (unpublished data) while CPTs were very successful in mapping the deeply buried paleolandscape (cf chapter on CPTs). However, in some cases bricks or stones may impede CPT cones and require pre-augering until the undisturbed soil is reached. An unsaturated topsoil also hampers CPT data interpretation, which has to be taken into account when interpreting shallow (prehistoric) lithostratigraphic layers.

In addition, the complexity of the lithostratigraphy in the study area, ranging from sand to clay and peat, has to be considered. All of these can be attested within a single core sequence and in various possible orders. This can be a hindrance for many near surface geophysical methods. At the same time, the lateral complexity of the sediments also hampers near surface geophysical methods and requires denser coring or CPT grids to encompass the subsoil variability. For example, large (Post) Medieval gullying can simply overwhelm the subtle topographic variability of thin peat layers in EMI data. Similarly, the groundwater level and its brackish nature can hinder the interpretation of EMI data. In some parts of Doelpolder-Noord, it was found that the variability due to intrusions from the Scheldt estuary overwhelmed sedimentary variability. This impeded quantitative interpretation and subsurface modeling of the EMI data, but some qualitative interpretations were nevertheless still possible using validation data.

Taking all these considerations into account, it is highly advisable to collect as much information as possible before designing the survey strategy for the archaeological evaluation. If the available desktop data do not allow to make a sufficient choice of

methodology, a preliminary field test, in which various methods are tested on a small scale, should be organized during or shortly after the desktop based assessment.

Spatial prehistoric landscape reconstruction through geological mapping

Geological (lithostratigraphic) mapping aims at an inventory of the lithology and topographic variability of transitions and stratigraphic interpretation. Within the Lower Scheldt floodplain, the topography of the Pleistocene substrate and/or the basis of the basal peat are the most important references for mapping the paleolandscape. Interrupted stratigraphy or truncated paleotopography are indications of the preservation potential of archaeological strata as well.

Hand coring is widely used because its equipment is cheap and low tech. However, this method is only effective when the prehistoric landscape is buried shallowly (< 2-3 m). As a consequence of the combination of peat, clay and sand geology, even small diameter hand cores do not always allow rapid coring prospection of deeper horizons. In Doelpolder-Noord, the prehistoric surface could hardly be reached manually beyond 6-8 m using a combination of gauge and Dutch augers but only with large efforts due to the groundwater causing sand to clog up the borehole. A fully clay or peat lithostratigraphic sequence can be cored more easily using manual gauge augers. Similar conclusions have been drawn by Soens et al. (2012) after testing hand coring in nearby polders.

The physical boundaries of manual coring methods can be solved using mechanical coring techniques. Sonic Drill Aqualock sampler coring was tested during this research project. The main advantage of this technique lies in the fact that large depths are reached more quickly and cored sediments can be described in the field. In addition, larger diameter samples are recovered than using a manual gauge auger, which is advantageous to evaluate thin layers of discontinuous horizons. This also allows to retrieve archaeological remains. However, the Sonic Drill Aqualock sampler has some drawbacks. Due to the mechanics of the sampler, 20 cm of the sediment sequence is generally lost between every 2 or 4 m core, dependent on the corer sampler tube used. This problem can be resolved by placing two cores next to each other with staggered transitions between the core samplers, using the Aqualock to stop the first meter of soil from entering the sampler. Peat also tends to get stuck after being forced into the Aqualock sampler, resulting in parts of the sedimentary sequence which cannot be sampled, and consequently a lower depth accuracy. If the corings is not encased, the borehole can also clog up by sand flowing, together with the groundwater, into the borehole, similar to manual (unencased) augering (see above). Encased mechanical coring methods can address parts of these issues but decrease coring speed significantly while increasing the operating costs. The Begemann coring method provides the most continu-

ous sampling in soft clays and peats and is therefore most suited to detect the finest sediment layers in an undisturbed way (Hissel and Van Londen, 2004). However, the high costs exclude the systematic use of this coring technique on a large scale for paleolandscape mapping.

In general, manual or mechanical coring is therefore most suitable for linear trajectories, transects or small areas (e.g. less than 10 ha).

Electric cone penetration testing (CPT) could serve as a direct (and less costly) alternative to coring below groundwater (Chapter 3). The CPT-E method has a high depth accuracy recording the soil behavior parameters (tip resistance and sleeve friction) every 2 cm, at a speed of 2 cm per second. The equipment can be operated by a single worker and does not require the presence of a geologist or archaeologist during the field data collection. Interpretation can be done afterwards in the office by a geologist or geoarchaeologist. Qualitative interpretation and paleosol mapping is possible through comparison with a limited number of well-aimed borings. At Doelpolder-Noord, peat layers could be easily identified in comparison with the sandy layer above and below. Even OM rich clay intercalating the peat could be mapped through its relative contrast with the latter. However, quantitative interpretation is rather problematic. First of all, the interpretation charts classify the measurements to soil behavior units which is not exactly the same as the lithology (Robertson and Cabal, 2012). In addition, the measured mechanical values of peats partly do not fall within soil behavior charts.

Further research is needed to automate quantitative CPT interpretation through the development of regional CPT classification methods by comparison with high resolution corings. Detecting and interpreting thin sediment layers (< 0.2 m) or paleosol horizons within non-contrasting lithology was also problematic as the CPT conus measured a volume up to 20 cm ahead of the cone. More suitable paleosol mapping sensors integrated in CPT cones, apart from the piezocone, seismic cone or conductivity cone, should also be subjected to further research. The latter did form a suitable interpretation tool for EMI and ERI. CPT-C confirmed the assumed correlations between lithology and electrical conductivity. They were even more important to indicate where this correlation was not the case, e.g. if saltwater intrusion causes segregation between the electrical and lithological variability, due to an increased conductivity outside of the peat layer in its turn recognizable by the thinner zone of high friction ratio.

As the area to be evaluated increases and the size of the paleolandscape units to be mapped decreases (e.g. small dunes in a buried floodplain), the number of gridded corings or geotechnical soundings required to map these palaeolandscape units increase. In such cases, EMI measures large numbers of data points, many locations and at a high data collection speed. The time needed to process a larger survey area does not necessarily increase with the same factor as the survey area, however. The EMI electrical conductivity data points can be related to lithological variability resulting in interpretation with more horizontal data than using interpolations derived from a 25 to 50 m

gridded coring or CPT survey. As a consequence, less corings or CPTs are needed to map a buried paleolandscape unit in sufficient detail. If a near surface geophysical survey is done as a starting inventory of the lithological variability, coring locations for detailed description can be located even better in order to optimally capture the lithological variability of the subsoil.

GPR has the possibility to reveal most vertical information but is of little use in polder areas due to signal attenuation by the shallow and possibly salty groundwater table and clay top soil. 2-D ERI and shear wave land seismic survey provided usable results in Doelpolder-Noord but the slow data collection and/or required data processing make the information delivered by these methods barely more efficient than a transect of CPT-E's collected during the same time interval (Chapter 1). In one working day about 300 to 400 electrode or geophone locations could be measured using respectively ERI and shear wave land seismics at Doelpolder-Noord. Both methods still required calibration corings and significant processing time.

In contrast, EMI does not require soil contact, allows a mobile configuration and collection of far more spatially dispersed data which can be related to lithology. Depending on the distance between the transmitting and receiving coil and their orientation relative to each other, various soil volumes can be measured. Using instruments with a single coil spacing, a significant improvement could be made in mapping the apparent conductivities of the total subsoil variability within the measured soil volume. Because this includes both prehistoric and later lithological variations as well as hydrological influences, qualitative interpretations could be done of the conductivity data using well located corings or CPT's as interpretation tools (Chapter 1). A multiple frequency single coil pair sensor (GEM-2) did not prove advantageous over single frequency single coil spaced instruments based on our tests in Doelpolder-Noord.

The use of multiple coil pairs with differing spacing and orientation (e.g. the Dualem 421s sensor) proved significantly advantageous. Because the apparent electrical conductivity is recorded in multiple soil volumes, the depth to the base of the peat could be modelled using a 3-layer model and separated from shallow modern or (Post) Medieval archaeological land division features. After validation, the final peat base depth model could be related to an age-depth model of the basal peat to create paleogeographic maps. Alternatively, it can be used to decrease the costs of archaeological sampling, because discontinuous mechanical sampling is possible (see further).

However, EMI has also some limiting factors, which reduced its applicability. First there is the DOI, which is limited to 5 to 6 m using the Dualem 421s and sufficient to reconstruct a small river dune in Doelpolder Noord. Furthermore, we were faced with the high electrical conductivity of the peats in Doelpolder Noord and the maximal coil spacing of 4 m in HCP configuration. However, longer sensors were recently developed with coil spacing up to 6 m (e.g. Dualem 642s), extending the depth range of detectable prehistoric landscapes. Other limiting factors are the presence of overlying recent and pol-

luted dumps or land raising. This was the case in Kerkhove. The variable influence of brackish groundwater can also impede results, as was experienced at Doelpolder-Noord. Furthermore it should be stressed that the lithostratigraphical resolution is less compared to coring and CPT. EMI for example was not successful in mapping the peat intercalated flooding sediments, which constitutes an important reference level in the context of prehistoric research into the Mesolithic-Neolithic transition (cf. below).

Based on the geological mapping, parts of the survey area can be selected for archaeological sampling if the prehistoric surface is preserved. The selection procedure of these paleolandscape parts was further developed by adding the chronological aspect and by integration of the dated paleolandscape evolutions with the dated prehistoric land use (see further).

Chronological prehistoric landscape reconstruction

Diachronic landscape reconstruction is based on reconstructing the lithostratigraphy of the corings and CPT. The lithostratigraphy has to be simplified into three layers during the subsurface modelling procedure of EMI data. Secondly, because of the diachronic and continuous nature of the basal peat development (Vos and van Heeringen, 1997), an age-depth model was to be developed in Chapter 4. Only dates of the base of the basal peat directly on top of the Pleistocene substrate are used for the age-depth model of the initiation of peat development in order to avoid age-depth errors caused by peat compression. The Oxcal P-sequence proved a useful tool to model this age-depth relation, including the full distribution of the dates, rather the mean value and/or standard deviation. The inclusion of the elevation errors of the dated samples was still partly problematic.

An age-depth model could be constructed during the deceleration of relative sea level rise in the Middle Holocene. This model can be considered as an error envelope including the regional variability in initiating peat development (Vos and van Heeringen, 1997). It fills the gaps within existing models (Kiden, 2006) and confirms the lower age-depth location of the basal peat in the Scheldt paleovalley compared to Zeeland (Chapter 4). In Chapter 6 this model is integrated with the geological subsoil model at Doelpolder-Noord. Higher resolution dating of the bottom of the basal peat along the flanks of single landscape units within the Scheldt paleovalley could provide more accurate local age-depth models of the basal peat in the future as well as further elaborate the drowning history of the river floodplain (e.g. Berendsen and Stouthamer, 2002).

Kiden (2006 fig. 6) illustrates that while intercalations of the Middle Holocene peat with marine or estuarine sediments is also a diachronic evolution, its expansion into the Belgian Scheldt polder was rather sudden and possibly related to the formation of a new Scheldt trajectory (Vos and van Heeringen, 1997). The timing of this expansion had to

be defined accurately to investigate the chronological relation with the appearance of two Early Neolithic archaeological sites from the Swifterbant culture (Doel Deurganckdok Sector B and M). As a result, the start of this tidal influence in the wider floodplain was modelled as an 'event' dated 6535-6410 cal BP (2 σ) rather than a diachronic evolution. Similarly the retreat of this influence was dated 6085 -5770 cal BP (2 σ) (Chapter 4). Dating the peat rise and occurrence of the tidal environment allows reconstructing of paleogeography at the Mesolithic-Neolithic transition period if combined with the subsurface models from geological and paleosol mapping.

Based on pollen and microfossil analysis, Deforce (2014) interprets the tidal influence as occasional floodings (spring tides/storm surges), bringing estuarine sediments exceptionally far upstream to the study region. This would make the areas covered with these sediments part of the supratidal zone at the edge of a newly formed Scheldt estuary. The relative distribution of alluvial hardwood forest on the dunes and alder woodland in lower parts of the landscape was derived from archaeological finds from Swifterbant hearths, while pollen and microfossil evidence from the OM rich clay deposits points towards an estuarine environment. This would have positioned the study region at the ecotonal zone between estuarine saltwater mudflat landscapes downstream and the river and freshwater alluvial hardwood forest in the wider floodplain.

Prehistoric land use during the Mesolithic-Neolithic transition

Archaeological landscape occupation during the Mesolithic-Neolithic period in the Lower Scheldt floodplain was chronologically and spatially modelled by integrating the radiocarbon dates and locations of the archaeological sites in our model.

The earliest known sites, dating back to the Final Paleolithic and Early Mesolithic, are located on the inland cover sand ridges and slightly later also on the smaller ridges (levees and point bars) closer to the Scheldt river.

So far no Middle to Late Mesolithic sites were found on the inland river dunes during the period of basal peat formation. As soon as occasional (supratidal) flooding starts, however, these ridges started to be re-occupied by Final Mesolithic/Early Neolithic Swifterbant people. These occupations ended before this intertidal influence had ceased, because some sites were covered with flooding sediments and as soon as the modelled basal peat curve reached the site elevations (Chapter 4, Chapter 5). The clustered occupation of the dune sites resulted in spatial palimpsest sites according to Bailey (2007) (Crombé et al., in press-b), as the available occupation surfaces decreased drastically as a result of flooding and peat formation.

In contrast, the sites along the Scheldt located on levees or point bars, have a different nature and occupation pattern (Chapter 5). The site occupation at Bazel started earlier and ended later than the Doel Deurganckdok Sector B and M dune sites. The long

occupation period of these river flanking sites resulted in the formation of cumulative palimpsest sites according to Bailey (2007), with a hardly distinguishable stratigraphy. At Bazel, Bayesian modelling allowed distinguishing part of the site chronology using environmental and archaeological dates within respectively the different lithostratigraphic units and waste deposits flanking the site.

On both dune and levee sites discussed in Chapter 5, Bayesian modelling in Oxcal provided a chronological framework for chronological integration of the prehistoric sites and the sedimentary or organic deposits, reflecting the surrounding landscape.

Further research can focus on the chronological relation between the disappearance of the Swifterbant culture, the appearance of the Michelsberg culture and the retreating (supra-)tidal environment. The dated site of Doel Deurganckdok sector M is covered with a thin layer of OM rich clay and its dates also indicate that occupation stopped before the (supra-)tidal influence ceased. Sites with an elevation above the peat level at that time have not yet been found and dated. A survey strategy to prospect such sites and answer such scientific questions is proposed in Chapter 6 and could be adopted in further evaluations.

Finally, it has to be emphasized that prehistoric landscape paleogeography and archaeological occupation modelling is an iterative process with continuously information exchange.

Archaeological core sampling

Archaeological prospection *sensu stricto* can be done using core sampling. Chapter 7 has shown that a minimal coring grid of 10 m, a minimal core diameter of 10 cm Dutch auger and a 1 to 2 mm sieving mesh is required to find the broad range of sites such as those already found during completed coring and excavation projects. A similar diameter would be suggested as a minimum for mechanical coring. The mechanical coring samples should be undisturbed and unmixed to evade admixture of over- or underlying strata.

If high resolution models to depth of prehistoric surface are available (horizontally < 5-10 m grid, absolute depth accuracy < 0.75 m), discontinuous mechanical coring is possible, using the 2 m Aqualock sampler employed at Doelpolder-Noord (Chapter 6). This decreases cost, time and effort required and could decrease sample losses encountered during continuous uncased Sonic Drill Aqualock coring at Doelpolder-Noord.

Due to improved quality of sample retrieval using mechanical cores compared to Dutch augers, the soil samples of the various paleosol horizons can be sieved separately. This allows a better evaluation of the preservation and vertical find spreading of identified sites. Such additional information is valuable to decide about further test pitting or excavation.

Several archaeological research questions and hypotheses were formed based on archaeological sites and paleolandscape relations. Future research has to investigate how effective the latter can be included during cost/effort allocation during the archaeological sampling phase. If sites are not threatened, only certain parts of prehistoric sites or landscape units can be cored archaeologically to answer scientific research questions (Chapter 6).

Alternatively, archaeological sampling grids can be adapted to the archaeological sites expected on prehistoric landscape locations in an development-led evaluation context. Smaller grids can be employed effectively to find spatial palimpsests with small separate lithic concentrations on aeolian dunes or coversand ridges. Conversely, coarser grids can be employed to simply delineate large area cumulative palimpsest sites on levees. If no large palimpsests are identified using this adaptive archaeological sampling, the grid has to be densified in order to find unexpected smaller lithic concentrations on these levees using a broad range of archaeological sampling strategies (Chapter 7). This additional effort is required to avoid circle reasoning of hypothetic human-landscape relations determining field archaeological evaluation. In turn, such archaeological evaluations would limit our knowledge about the past to the current hypothesis rather than extend it beyond what is already known.

Bibliography

Adams, R., S. Vermeire, G. De Moor, P. Jacobs, S. Louwye, and T. Polfliet, 2002, Toelichting bij de Quartairgeologische kaart. Kaartblad 15: Antwerpen, V. o. D. N. Rijkdommen., ed., Haecon & Universiteit Gent.

ADW, 2010, Paleolandschappelijk en archeologisch onderzoek van de te realiseren ontpoldering in Prosperpolder in het kader van de uitvoering van het Sigmaplan (gemeente Beveren) – uitvoering onderzoeksfase 1: Paleolandschappelijke en archeologische screening aan de hand van boringen en inventarisatie. Eindrapport: synthese van de onderzoeksresultaten. , 48, Archeologische Dienst Waasland, Sint Niklaas.

AGIV, 2001-2004, DHM-Vlaanderen-Digitaal Hoogtemodel Vlaanderen (CD-ROM). (Ondersteunend centrum GIS-Vlaanderen, 2004).

Amorosi, A., and N. Marchi, 1999, High-resolution sequence stratigraphy from piezocone tests: an example from the Late Quaternary deposits of the southeastern Po Plain, *Sedimentary Geology*, **128(1)**, 67-81.

Antrop, M., 1995-2000, Traditionele landschappen, U.-v. geografie, ed., AGIV, Gent.

Antrop, M., 2000, Structures physiques, régions géographiques et paysages traditionnels en Belgique, *Hommes et Terres du Nord*, **3**, 204-212.

Baeteman, C., 2004, A discussion of Gullentops, F. & De Moor, G. (2001) :Quaternary lithostratigraphic units (Belgium). 2.2 Remaining marine-estuarine deposits. Geologica Belgica, 2001, 4/1-2: 153-164, *Geologica Belgica*, **7(1-2)**, 77-78.

Baeteman, C., 2005a, How subsoil morphology and erodibility influence the origin and pattern of late Holocene tidal channels: case studies from the Belgian coastal lowlands, *Quaternary Science Reviews*, **24(18-19)**, 2146-2162.

Baeteman, C., 2005b, The Streif classification system: a tribute to an alternative system for organising and mapping Holocene coastal deposits, *Quaternary International*, **133-134**, 141-149.

Baeteman, C., 2008, Radiocarbon-dated sediment sequences from the Belgian coastal plain: testing the hypothesis of fluctuating or smooth late-Holocene relative sea-level rise, *The holocene*, **18(8)**, 1219-1228.

Bailey, G. N., 2007, Time perspectives, palimpsests and the archaeology of time, *Journal of Anthropological Archaeology*, **26**, 198-223.

Baines, D., D. G. Smith, D. G. Froese, P. Bauman, and G. Nimeck, 2002, Electrical resistivity ground imaging (ERGI): a new tool for mapping the lithology and geometry of channel-belts and valley-fills, *Sedimentology*, **49**, 441-449.

Bakker, M. A. J., D. Maljers, and H. J. T. Weerts, 2007, Ground-penetrating radar profiling on embanked floodplains, *Netherlands Journal of Geosciences*, **86(1)**, 55.

Banning, E. B., 2002, Archaeological Survey: Manuals in Archaeological Method, Theory and Technique: New York, Kluwer Academic/Plenum Publishers.

Barentsen, P., 1936, Short description of a field testing method with cone-shaped sounding apparatus: Proceedings 1st International Conference on Soil Mechanics and Foundation Engineering, p. 6-10.

Bastiaens, J., K. Deforce, B. Klinck, L. Meersschaert, C. Verbruggen, and L. Vrydaghs, 2005, Features: palaeobotanical analyses, *The last hunter-gatherer-fishermen in Sandy Flanders (NW Belgium) : the Verrebroek and Doel excavation projects, volume 1 : palaeo-environment, chronology and features*, **3**, 251-278.

Bates, M. R., 1998, Locating and evaluating archaeology below the alluvium: the role of sub-surface stratigraphic modelling, *Lithics*, **19**, 4-18.

Bates, M. R., 2000, Problems and procedures in the creation of an integrated stratigraphic database for the Lower Thames region: a geoarchaeological contribution., in *IGCP 437 Coastal environmental change during Sea-level highstands the Thames Estuary.*, J. Sidell, and A. Long, eds., Research Publication, **4**, University of Durham, Durham.

Bates, M. R., and A. J. Barham, 1995, Holocene alluvial stratigraphic architecture and archaeology in the Lower Thames area., in *The Quaternary of the Lower Reaches of the Thames. Field Guide.*, 85-98, D. R. Bridgeland, P. Allen, and B. A. Haggart, eds., Quaternary Research Association, Cambridge.

Bates, M. R., A. J. Barham, C. A. Pine, and V. D. Williamson, 2000, The use of borehole stratigraphic logs in archaeological evaluation strategies for deeply stratified alluvial areas., in *Interpreting stratigraphy. Site evaluation, recording procedures and stratigraphic analysis. Papers presented to the interpreting stratigraphy conferences 1993-1997.* , 49-69, S. Roskams, ed., BAR International Series, **910**, Archaeopress, Oxford.

Bates, M. R., and C. R. Bates, 2000, Multidisciplinary approaches to the geoarchaeological evaluation of deeply stratified sedimentary sequences: examples from pleistocene and holocene deposits in Southern England, United Kingdom, *Journal of Archaeological Science*, **27**, 845–858.

Bates, M. R., C. R. Bates, and J. E. Whittaker, 2007, Mixed method approaches to the investigation and mapping of buried Quaternary deposits: examples from southern England, *Archaeological Prospection*, **14(2)**, 104-129.

Bates, M. R., and E. Stafford, 2013, Thames Holocene: A geoarchaeological approach to the investigation of the river floodplain for High Speed 1, 1994-2003, Wessex Archaeology, 280 p.

Bates, M. R., and K. Whittaker, 2004, Landscape evolution in the Lower Thames Valley: implications for the archaeology of the earlier Holocene period., in *Towards a New Stone Age aspects of the Neolithic in south-east England.*, 50-70, J. Cotton, and D. Field, eds., CBA Reasearch Reports, **137**, Council for British Archaeology, York.

Bats, M., 2007, The Flemish wetlands. An archaeological survey of the valley of the River Scheldt, in *Archaeology from the wetlands. Recent perspectives. Proceedings of the 11th WARP conference*, 93-100, J. Barber, C. Clark, M. Cressy, A. Crone, A. Hale, J. Henderson, R. Housley, R. Sands, and A. Sheridan, eds., Society of Antiquaries, Edinburgh.

Bats, M., J. Bastiaens, and P. Crombé, 2006, Prospectie en waardering van alluviale gebieden langs de Boven-Schelde. CAI project 2003-2004., in *CAI-II: Thematisch inventarisatie en evaluatieonderzoek*, 75-100, K. Cousserier, and E. Meylemans, eds., VIOE rapport Brussel.

Bats, M., and P. Crombé, 2007, Bovenschelde, vernieuwen en ontdubbelen van de stuw te Kerkhove. Archeologisch vooronderzoek: UGent Archeologische Rapporten, v. 2: Gent, UGent.

Bats, M., P. Crombé, W. Gheyle, and J. Jacops, 2008, Bovenschelde, vernieuwen en ontdubbelen van de stuw te Kerkhove. Fase 2b: Aanvullend Archeologisch Onderzoek, *UGent Archeologische Rapporten*, **11**.

Bats, M., J. De Reu, P. De Smedt, M. Antrop, J. Bourgeois, M. Court-Picon, P. De Maeyer, P. Finke, M. Van Meirvenne, J. Verniers, I. Werbrouck, A. Zwertvaegher, and P. Crombé, 2009, Geoarchaeological research of the large palaeolake of the Moervaart (municipalities of Wachtebeke and Moerbeke-Waas, East Flanders, Belgium): from Late Glacial to Early Holocene, *Notae Praehistoricae*, **29**, 105-112.

Bats, M., P. De Smedt, I. Werbrouck, A. Zwertvaegher, M. Court-Picon, J. De Reu, L. Serbruyns, H. Demiddele, M. Antrop, J. Bourgeois, P. De Maeyer, P. Finke, M. Van Meirvenne, J. Verniers, and P. Crombé, 2010, Continued geoarchaeological research at the Moervaart palaeolake area (East Flanders, Belgium): preliminary results, *Notae Praehistoricae*, **30**, 15-21.

Beamish, D., 2011, Low induction number, ground conductivity meters: A correction procedure in the absence of magnetic effects, *Journal of Applied Geophysics*, **75(2)**, 244-253.

Beets, D. J., and A. F. J. van der Spek, 2000, The Holocene evolution of the barrier and back-barrier basins of Belgium and the Netherlands as a functionof late Weichselian morphology, relative sea-level rise and sediment supply, *Geologie en Mijnbouw*, **79(1)**, 3-16.

Bell, M., 2007, Prehistoric coastal communities: the Mesolithic in western Britain, Council for British Archeology.

Bell, M., A. Caseldine, and H. Newmann, 2000, Prehistoric Intertidal Archaeology in the Welsh Severn Estuary, CBA Research Report, **120**.

Bell, M., and H. Neumann, 1997, Prehistoric intertidal archaeology and environments in the severn estuary, Wales, *World Archaeology*, **29(1)**, 95-113.

Berendsen, H. J. A., and E. Stouthamer, 2000, Late Weichselian and Holocene palaeogeography of the Rhine–Meuse delta, The Netherlands, *Palaeogeography, Palaeoclimatology, Palaeoecology*, **161(3)**, 311-335.

Berendsen, H. J. A., and E. Stouthamer, 2002, Palaeographic evolution and avulsion history of the Holocene Rhine-Meuse delta, The Netherlands, *Geologie en Mijnbouw*, **81(1)**, 97-112.

Berendsen, M. A., B. Makaske, O. Van De Plassche, M. H. M. Van Ree, S. Das, M. van Dongen, S. Ploumen, and W. Schoenmakers, 2007, New groundwater-level rise data from the Rhine-Meuse delta - implications for the reconstruction of Holocene relative mean sea-level rise and differential land-level movements, *Netherlands Journal of Geosciences-Geologie En Mijnbouw*, **86(4)**, 333-354.

Björck, S., M. J. C. Walker, L. C. Cwynar, S. Johnsen, K. L. Knudsen, J. J. Lowe, and B. Wohlfarth, 1998, An event stratigraphy for the Last Termination in the North Atlantic region based on the Greenland ice-core record: a proposal by the INTIMATE group, *Journal of Quaternary Science*, **13(4)**, 283-292.

Blaauw, M., R. Bakker, J. Andres Christen, V. A. Hall, and J. van der Plicht, 2007, A Bayesian framework for age modeling of radiocarbon-dated peat deposits: Case studies from the Netherlands, *Radiocarbon*, **49(2)**, 357-367.

Blaauw, M., and J. A. Christen, 2005, Radiocarbon peat chronologies and environmental change, *Journal of the Royal Statistical Society: Series C (Applied Statistics)*, **54(4)**, 805-816.

Bogemans, F., 1997, Toelichting bij de Quartairgeologische kaart, kaartblad 1-7 Essen-Kapellen: Quartairgeologische Kaart, Vrije Universiteit Brussel; Departement Leefmilieu, Natuur en Energie, Dienst Natuurlijke Rijkdommen, Vlaamse overheid, 38 p.

Bogemans, F., E. Meylemans, J. Jacops, Y. Perdaen, A. Storme, I. Verdurmen, and K. Deforce, 2012, The evolution of the sedimentary environment in the lower River Scheldt valley (Belgium) during the last 13,000 a BP, *Geologica Belgica*, **15(1-2)**, 105-112.

Bogemans, F., and D. Vandenberghe, 2011, OSL dating of an inland dune along the lower River Scheldt near Aard (East Flanders, Belgium), *Netherlands Journal of Geosciences-Geologie En Mijnbouw*, **90(1)**, 23-29.

Boon, J. J., F. P. M. Bunnik, H. Cremer, D. C. Brinkhuizen, K. M. Cohen, R. P. Exaltus, K. van Kappel, L. Kooistra, H. Koolmees, H. de Kruyk, L. Kubiak-Martens, J. M. Moree, M. Niekus, J. H. M. Peeters, D. Schiltmans, A. Verbaas, F. Verbruggen, P. Vos, and J. T. Zeiler, 2014, Twintig meter diep! Mesolithicum in de Yangtzehaven-Maasvlakte te Rotterdam. Landschapsontwikkeling en bewoning in het Vroeg Holoceen, in *BOORrapporten*, J. M. Moree, and M. M. Sier, eds., Burau Oudheidkundig Onderzoek Rotterdam, Rotterdam.

Bos, J. A., F. Verbruggen, S. Engels, and P. Crombé, 2013, The influence of environmental changes on local and regional vegetation patterns at Rieme (NW Belgium): implications for Final Palaeolithic habitation, *Vegetation History and Archaeobotany*, **22(1)**, 17-38.

Boudin, M., M. Van Strydonck, and P. Crombé, 2009, Radiocarbon Dating of Pottery Food Crusts: Reservoir Effect or not? The case of the Swifterbant pottery from Doel "Deurganckdok", in *Chronology and Evolution within the Mesolithic of North-West Europe: Proceedings of an International Meeting*, 727-745, P. Crombé, M. Van Strydonck, J. Sergant, and M. Bats, eds., Cambridge Scholars Publishing.

Boudin, M., M. Van Strydonck, P. Crombe, W. De Clercq, R. M. van Dierendonck, H. Jongepier, A. Ervynck, and A. Lentacker, 2010, Fish Reservoir Effect on Charred Food Residue C-14 Dates: Are Stable Isotope Analyses the Solution?, *Radiocarbon*, **52(2)**, 697-705.

Bourgeois, J., and B. Hageman, 1998, Sint-Gillis-Waas (O.-Vl.) 1997: verder noodonderzoek van de ijzertijdnederzetting, *Lunula. Archaeologia protohistorica*, **6**, 88-93.

Bourgeois, J., M. Meganck, J. Van Roeyen, and K. Verlaeckt, 1996, Noodopgravingen 1995 te Sint-Gillis-Waas-Reepstraat (O.-Vl.): nederzettingssporen uit de late bronstijd, de vroege ijzertijd en de Romeinse periode, *LUNULA (BRUSSEL)*, **4**, 29-32.

Brandenberg, S., J. Coe, R. Nigbor, and K. Tanksley, 2009, Different Approaches for Estimating Ground Strains from Pile Driving Vibrations at a Buried Archeological Site, *Journal of Geotechnical and Geoenvironmental Engineering*, **135(8)**, 1101-1112.

Bronk Ramsey, C., 1995, Radiocarbon calibration and analysis of stratigraphy: The OxCal program, *Radiocarbon*, **37(2)**, 425-430.

Bronk Ramsey, C., 2001, Development of the radiocarbon calibration program, *Radiocarbon*, **43(2A)**, 355-363.

Bronk Ramsey, C., 2008, Deposition models for chronological records, *Quaternary Science Reviews*, **27(1-2)**, 42-60.

Bronk Ramsey, C., 2009a, Bayesian analysis of radiocarbon dates, *Radiocarbon*, **51(1)**, 337-360.

Bronk Ramsey, C., 2009b, Dealing with outliers and offsets in radiocarbon dating, *Radiocarbon*, **51(3)**, 1023-1045.

Bronk Ramsey, C., C. E. Buck, S. W. Manning, P. Reimer, and H. van der Plicht, 2006, Developments in radiocarbon calibration for archaeology, *Antiquity*, **80(310)**, 783-799.

Bronk Ramsey, C., and S. Lee, 2013, Recent and planned developments of the program OxCal, *Radiocarbon*, **55(2–3)**, 720-730.

Brown, A. G., 1997, Alluvial geoarchaeology. Floodplain archaeology and environmental change: Cambridge manuals in Archaeology: Cambridge, Cambridge University Press.

Buck, C. E., J. B. Kenworthy, C. D. Litton, and A. F. M. Smith, 1991, COMBINING ARCHAEOLOGICAL AND RADIOCARBON INFORMATION - A BAYESIAN-APPROACH TO CALIBRATION, *Antiquity*, **65(249)**, 808-821.

Buck, C. E., C. D. Litton, and A. F. M. Smith, 1992, CALIBRATION OF RADIOCARBON RESULTS PERTAINING TO RELATED ARCHAEOLOGICAL EVENTS, *Journal of Archaeological Science*, **19(5)**, 497-512.

Canti, M. G., and F. M. Meddens, 1998, Mechanical Coring as an Aid to Archaeological Projects, *Journal of Field Archaeology*, **25(1)**, 97-105.

Challis, K., and A. J. Howard, 2006, A Review of Trends within Archaeological Remote sensing in Alluvial Environments, *Archaeological Prospection*, **13(4)**, 231-240.

Chapman, H., and B. R. Gearey, 2013, Modelling archaeology and palaeoenvironments in wetlands: The hidden landscape archaeology of Hatfield and Thorne Moors, eastern England: Oxford, Oxbow Books, 216 p.

Chiverrell, R. C., V. R. Thorndycraft, and T. O. Hoffmann, 2011, Cumulative probability functions and their role in evaluating the chronology of geomorphological events during the Holocene, *Journal of Quaternary Science*, **26(1)**, 76-85.

Claerhout, J., 1921a, Glanes ethnographiques, *Bulletin de la Société archéologique de Belgique*, **36**, 298-299.

Claerhout, J., 1921b, Une pointe de lance de l'âge de bronze, *Mémoires de Cercle archéologique et historique de Courtrai*, **1**, 13.

Cohen, K. M., 2003, Differential Subsidence within a Coastal Prism: Late-Glacial - Holocene tectonics in the Rhine-Meuse Delta, The Netherlands, *Netherlands Geographical Studies*, **316**, 1-172.

Coles, J. M., 1987, Preservation of the past: the case for wet archaeology, in *European wetlands in prehistory*, 1-22, J. M. Coles, and A. J. Lawson, eds., Clarendon Press Oxford.

Conyers, L. B., 2013, Ground-penetrating radar for archaeology, AltaMira Press.

Conyers, L. B., E. G. Ernenwein, and K. M. Lowe, 2008, Electromagnetic conductivity mapping for site prediction in meandering river floodplains, *Archaeological Prospection* **15(2)**, 81-91.

Coutinho, R. Q., and P. W. Mayne, 2012, Geotechnical and Geophysical Site Characterization 4: London, Taylor & Francis Group.

Craig, O. E., M. Forster, S. H. Andersen, E. Koch, P. Crombe, N. J. Milner, B. Stern, G. N. Bailey, and C. P. Heron, 2007, Molecular and isotopic demonstration of the processing of aquatic products in northern European prehistoric pottery, *Archaeometry*, **49**, 135-152.

Crombé, P., 1986, Een Prehistorische site te Kerkhove (Mesolithicum Neolithicum), *Westvlaamse Archaeologica*, **2(1)**, 3-39.

Crombé, P., 2005, The last hunter-gatherer-fishermen in Sandy Flanders (NW Belgium). The Verrebroek and Doel excavation Projects. Vol.1: Archaeological Reports Ghent University, v. 3: Gent, UGent.

Crombé, P., 2006, The wetlands of Sandy Flanders (Northwest Belgium): potentials and prospects for prehistoric research and management, in *Preserving the Early Past. Investigation, selection and preservation of Palaeolithic and Mesolithic sites and landscapes*, 41-54, E. Rensink, and H. Peeters, eds., Nederlandse Archeologische Rapporten, **31**, Rijksdienst voor het Oudheidkundig Bodemonderzoek, Amersfoort.

Crombé, P., submitted, Federmesser hunter-gatherer land use in the Scheldt basin (NW Belgium), in *From the Atlantic to beyond the Bug river. Finding and defining the Federmesser-Gruppen / Azilian*, S. B. Grimm, L. Mevel, I. Sobkowiak-Tabaka, and M.-J. Weber, eds.

Crombé, P., M. Boudin, and M. Van Strydonck, 2011a, Swifterbant pottery in the Scheldt basin and the emergence of the earliest indigenous pottery in the sandy lowlands of Belgium, in *Early Pottery in the Baltic – Dating, Origin and Social Context, International Workshop at Schleswig on 20-21 October 2006*, 465-483, S. Hartz, F. Lüth, and T. Terberger, eds., Bericht der Römisch-Germanischen Kommission, **89**, Frankfurt.

Crombé, P., and N. Cauwe, 2001, The Mesolithic, in *Prehistory in Belgium. Special issue on the occasion of the XIVth congress of the International Union for Prehistroic and Protohistoric Sciences*, 49-62, Anthopologica et Praehistorica.

Crombé, P., P. De Smedt, N. Davies, V. Gelorini, A. Zwertvaegher, R. Langohr, D. Van Damme, H. Demiddele, M. Van Strydonck, M. Antrop, J. Bourgeois, P. De Maeyer, J. De Reu, P. Finke, M. Van Meirvenne, and J. Verniers, 2013a, Hunter-gatherer responses to the changing environment of the Moervaart palaeolake (NW Belgium) during the Late Glacial and Early Holocene, *Quaternary International*, **308**, 162-177.

Crombé, P., Y. Perdaen, and J. Sergant, 2006, Extensive artefact concentrations: single occupations or palimpsests? The evidence from the Early Mesolithic site of Verrebroek "Dok" (Belgium). in *After the Ice-Age. Settlements, subsistence and social development in the Mesolithic of Central Europe. Proceedings of the International Conference 9th to 12th September 2003. Rottenburg/Neckar, Baden-Württemberg, Germany.*, 237-243, C. J. Kind, ed., Konrad Theiss Verlag, Stuttgart.

Crombé, P., Y. Perdaen, J. Sergant, J.-P. Van Roeyen, and M. Van Strydonck, 2002, The Mesolithic-Neolithic transition in the sandy lowlands of Belgium: new evidence., *Antiquity*, **76**, 699-706.

Crombé, P., and J. Sergant, 2008, Tracing the Neolithic in the lowlands of Belgium: the evidence from Sandy Flanders, in *Between foraging and farming. An extended broad spectrum of papers presented to Leendert Louwe Kooijmans*, 75-84, H. Fokkens, B. J. Coles, A. L. Van Gijn, J. P. Kleijne, H. H. Ponjee, and C. G. Slappendel, eds., Analecta Praehistorica Leidensia, **40**, Leiden University, Leiden.

Crombé, P., J. Sergant, and J. De Reu, 2013b, La contribution des dates radiocarbone pour démêler les palimpsestes mésolithiques: exemples provenant de la région des sables de couverture en Belgique du Nord-Ouest: Seances de la societé prehistorique française, p. 235-249.

Crombé, P., J. Sergant, and L. Lombaert, 2011b, L'occupation du nord-ouest de la Belgique aux IVe et IIIe millénaires: bilan des recherches récentes en région sablonneuse: Revue Archeologique De Picardie : Numero Special, p. 103-118.

Crombé, P., J. Sergant, and Y. Perdaen, 2009a, The neolithisation of the Belgian lowlands: new evidence from the Scheldt Valley, in *Mesolithic Horizons. Papers presented at the Seventh International Conference on the Mesolithic in Europe*, 564-569, S. B. McCartan, R. Schulting, G. Warren, and P. Woodman, eds., Oxbow books, Oxford.

Crombé, P., J. Sergant, Y. Perdaen, E. Meylemans, and K. Deforce, in press-a, Neolithic pottery finds at the wetland site of Bazel-Kruibeke (Flanders, Belgium): evidence of long-distance forager-farmer contact during the 5th millennium cal BC in the Rhine-Meuse-Scheldt area, *Archäologisches Korrespondenzblatt*.

Crombé, P., J. Sergant, E. Robinson, and J. De Reu, 2011c, Hunter-gatherer responses to environmental change during the Pleistocene-Holocene transition in the southern North Sea basin: Final Palaeolithic-Final Mesolithic land use in northwest Belgium, *Journal of Anthropological Archaeology*, **30(3)**, 454-471.

Crombé, P., J. Sergant, A. Verbrugge, A. De Graeve, B. Cherretté, J. Mikkelsen, V. Cnudde, T. De Kock, H. D. J. Huisman, and B. J. H. van Os, 2014, A sealed flint knapping site from the Younger Dryas in the Scheldt valley (Belgium): Bridging the gap in human

occupation at the Pleistocene–Holocene transition in W Europe, *Journal of Archaeological Science*, **50**, 420-439.

Crombé, P., M. van Strydonck, and M. Boudin, 2009b, Towards a refinement of the absolute (typo) chronology for the Early Mesolithic in the coversand area of northern Belgium and the southern Netherlands: Chronology and Evolution within the Mesolithic of North-West Europe, p. 95-112.

Crombé, P., M. Van Strydonck, M. Boudin, T. Van den Brande, C. Derese, D. Vandenberghe, P. Van den haute, M. Court-Picon, J. Verniers, V. Gelorini, J. Bos, F. Verbruggen, M. Antrop, M. Bats, J. Bourgeois, J. De Reu, P. De Maeyer, P. De Smedt, P. Finke, M. Van Meirvenne, and A. Zwertvaegher, 2012, Absolute dating (14C and OSL) of the formation of coversand ridges occupied by prehistoric hunter-gatherers in NW Belgium, *Radiocarbon*, **54(3-4)**, 715-726.

Crombé, P., and B. Vanmontfort, 2007, The neolithisation of the Scheldt and Basin in western Belgium, *Proceedings of the British Academy*, **144**, 261-283.

Crombé, P., and C. Verbruggen, 2002, The Late Glacial and Early Post Glacial occupation of northern Belgium: the evidence from Sandy Flanders., in *Recent studies in the Final Palaeolithic of the European plain. Proceedings of a U.I.S.P.P. Symposium, Stockholm, 14.-17. October 1999.*, 165-180, B. V. Eriksen, Bratlund, B., ed., Jutland Archaeological Society Publications, **39**, Jutland Archaeological Society, Stockholm.

Crombé, P., and J. Verhegge, 2014, In search of sealed Palaeolithic and Mesolithic sites using core sampling: The impact of grid size, meshes and auger diameter on discovery probability, *Journal of Archaeological Science*.

Crombé, P., J. Verhegge, K. Deforce, E. Meylemans, and E. Robinson, in press-b, Wetland landscape dynamics, Swifterbant land use systems, and the Mesolithic-Neolithic transition in the southern North Sea basin, *Quaternary International*.

Crombé, P. H., E. Robinson, M. Van Strydonck, and M. Boudin, 2013c, Radiocarbon dating of Mesolithic open-air sites in the coversand area of the North-West European plain: problems and prospects, *Archaeometry*, **55(3)**, 545-562.

De Bie, M., and P. M. Vermeersch, 1998, Pleistocene-Holocene transition in Benelux., *Quaternary International*, **49**, 29-43.

De Clercq, W., 2009, Lokale gemeenschappen in het Imperium Romanum: transformaties in de rurale bewoningsstructuur en de materiële cultuur in de landschappen van het noordelijk deel van de civitas Menapiorum (Provincie Gallia-Belgica, ca. 100 v. Chr.–400 n. Chr.), Ghent University.

De Clercq, W., M. Bats, J. Bourgeois, P. Crombé, G. De Mulder, J. De Reu, D. Herremans, P. Laloo, L. Lombaert, G. Plets, J. Sergant, and B. Stichelbaut, 2012, Development-led archaeology in Flanders: an overview of practives and results in the period 1990-2010, in *Development-led archaeology in Northwest Europe*, L. Webley, M. Vander Linden, C. Haselgrove, and R. Bradley, eds., Oxbow Books, Oxford and Oakville.

De Clercq, W., M. Bats, P. Laloo, J. Sergant, and P. Crombé, 2011, Beware of the known. Methodological issues in the detection of low density rural occupation in large surface archaeological landscape assessment in Northern-Flanders (Belgium), in *Understanding the Past: A Matter of Surface-Area. Acts of the XIIIth Session of the EAA Congress, Zadar 2007*, 73-89, G. Blancquaert, F. Malrain, H. Stäuble, and J. Vanmoerkerke, eds., BAR International Series, 2194, Archeaopress, Oxford.

De Clercq, W., and R. Van Dierendonck, 2008, Extrema Galliarum: Noordwest-Vlaanderen en Zeeland in het Imperium Romanum, *Zeeuws Tijdschrift*, **58(3-4)**, 6-34.

De Ferraris, J.-J.-F., 1771-1778, Kabinetskaart van de Oostenrijkse Nederlanden, in *Kaarten en plannen*, KBR, Brussel.

De Moor, G., 1963, Bijdrage tot de kennis van de Vlaamse Vallei, Ghent University, Ghent, 172 p.
De Moor, G., and I. Heyse, 1978a, De morfologische evolutie van de Vlaamse vallei, *De Aardrijkskunde*, **4**, 343-375.
De Moor, G., and I. Heyse, 1978b, Dépôts quaternaires et géomorphologie dans le nord-ouest de la Flandre, *Bulletin de la Société Belge de Géologie*, **87(1)**, 37-47.
De Moor, G., and A. Pissart, 1992, Het reliëf, in *Geografie van België*, 129-215, J. Denis, ed., Gemeentekrediet, Brussel.
De Moor, G., and D. van de Velde, 1995, Quartairgeologische Kaart van België, Vlaams Gewest, Verklarende tekst bij het Kaartblad (14) Lokeren (1/50.000), 119, V. o. D. N. Rijkdommen., ed., Universiteit Gent, Gent.
De Smedt, P., T. Saey, A. Lehouck, B. Stichelbaut, E. Meerschman, M. M. Islam, E. Van De Vijver, and M. Van Meirvenne, 2013a, Exploring the potential of multi-receiver EMI survey for geoarchaeological prospection: a 90 ha dataset, *Geoderma*, **199**, 30-36.
De Smedt, P., M. Van Meirvenne, N. Davies, M. Bats, T. Saey, J. De Reu, E. Meerschman, V. Gelorini, A. Zwertvaegher, M. Antrop, J. Bourgeois, P. De Maeyer, P. Finke, J. Verniers, and P. Crombé, 2013b, A multidisciplinary approach to reconstructing Late Glacial and Early Holocene landscapes, *Journal of Archaeological Science*, **40(2)**, 1260-1267.
De Smedt, P., M. Van Meirvenne, D. Herremans, J. De Reu, T. Saey, E. Meerschman, P. Crombé, and W. De Clercq, 2013c, The 3-D reconstruction of medieval wetland reclamation through electromagnetic induction survey, *SCIENTIFIC REPORTS*, **3**.
De Smedt, P., M. Van Meirvenne, E. Meerschman, T. Saey, M. Bats, M. Court-Picon, J. De Reu, A. Zwertvaegher, M. Antrop, J. Bourgeois, P. De Maeyer, P. Finke, J. Verniers, and P. Crombé, 2011a, Reconstructing palaeochannel morphology with a mobile multicoil electromagnetic induction sensor, *Geomorphology*, **130(3-4)**, 136-141.
De Smedt, P., M. Van Meirvenne, and D. Simpson, 2011b, Multi-signal EMI and geoarchaeology: evaluating integrated magnetic susceptibility measurements for archaeological prospection: Archaeological prospections, p. 54-57.
Deforce, K., 2011, Middle and late Holocene Vegetation and landscape evolution of the Scheldt estuary. A palynological study of a peat deposit from Doel (N-Belgium), *Geologica Belgica*, **14(3-4)**, 277-287.
Deforce, K., 2014, Middle Holocene vegetation and woodland exploitation of the lower Scheldt valley, Ghent University. Faculty of Arts and Philosophy, Ghent, Belgium.
Deforce, K., J. Bastiaens, and P. Crombé, 2014a, A reconstruction of middle Holocene alluvial hardwood forests (Lower Scheldt River, Northern Belgium) and their exploitation during the Mesolithic-Neolithic transition period (Swifterbant culture, ca. 4,500-4,000 BC), *Quaternaire*, **25(1)**, 9-21.
Deforce, K., J. Bastiaens, W. Van Neer, A. Ervynck, A. Lentacker, J. Sergant, and P. Crombe, 2013, Wood charcoal and seeds as indicators for animal husbandry in a wetland site during the late mesolithic-early neolithic transition period (Swifterbant culture, ca. 4600-4000 BC) in NW Belgium, *Vegetation History and Archaeobotany*, **22(1)**, 51-60.
Deforce, K., A. Storme, J. Bastiaens, S. Debruyne, L. Denys, A. Ervynck, E. Meylemans, H. Stieperaere, W. Van Neer, and P. Crombé, 2014b, Middle-Holocene alluvial forests and associated fluvial environments: A multi-proxy reconstruction from the lower Scheldt, N Belgium, *The Holocene*.
Delefortrie, S., P. De Smedt, T. Saey, E. Van De Vijyer, and M. Van Meirvenne, 2014a, An efficient calibration procedure for correction of drift in EMI survey data, *Journal of Applied Geophysics*, **110**, 115-125.

Delefortrie, S., T. Saey, E. Van De Vijver, P. De Smedt, T. Missiaen, I. Demerre, and M. Van Meirvenne, 2014b, Frequency domain electromagnetic induction survey in the intertidal zone: Limitations of low-induction-number and depth of exploration, *Journal of Applied Geophysics*, **100(0)**, 14-22.

Denys, L., and C. Baeteman, 1995, Holocene evolution of relative sea level and local mean high water spring tides in Belgium - a first assessment, *Marine Geology*, **124(1-4)**, 1-19.

Denys, L., and C. Verbruggen, 1989, A Case of Drowning - the End of Subatlantic Peat Growth and Related Palaeoenvironmental Changes in the Lower Scheldt Basin (Belgium) Based on Diatom and Pollen Analysis, *Review of palaeobotany and palynology*, **59(1-4)**, 7-36.

Eslami, A., and B. H. Fellenius, 2004, CPT and CPTu data for soil profile interpretation: review of methods and a proposed new approach, *Iranian journal of science and technology*, **28(B1)**, 69-86.

Fellenius, B. H., and A. Eslami, 2000, Soil profile interpreted from CPTu data: Proceedings of Year 2000 Geotechnics Conference, Southeast Asian Geotechnical Society, Asian Institute of Technology, Bangkok, Thailand, p. 163-171.

Gaffney, C., and J. Gater, 2003, Revealing the buried past. Geophysics for archeaologists: Gloucestershire, Tempus.

Gearey, B. R., P. Marshall, and D. Hamilton, 2009, Correlating archaeological and palaeoenvironmental records using a Bayesian approach: a case study from Sutton Common, South Yorkshire, England, *Journal of Archaeological Science*, **36(7)**, 1477-1487.

Gelorini, V., E. Verleyen, C. Verbruggen, and L. Meersschaert, 2006, Paleo-ecologisch onderzoek van een Holocene sequentie uit het Deurganckdok te Doel (Wase Scheldepolders, Noord-België), *Belgeo*, **3**, 243-264.

Geuze, E., 1953, Résultats d'essais de pénétration en profondeur et de mise en charge de pieux-modèle, *Annales Inst Tech Bâtiment Travaux Publics Paris*, **63**, 313-319.

Ghose, R., 2003, High-frequency shear-wave reflections to monitor lateral variations in soil, supplementing downhole geotechnical tests., in *Proceedings of ITA world tunneling.*, J. Saveur, ed.

Ghose, R., V. Nijhof, J. Brouwer, Y. Matsubara, Y. Kaida, and T. Takahashi, 1998, Shallow to very shallow, high-resolution reflection seismic using a portable vibrator system, *Geophysics*, **63(4)**, 1295-1309.

Gilot, E., 1997, Index Général des dates Lv, laboratoire du carbone 14 de Louvain/Louvain-la-Neuve, publisher not identified.

Goes, B. J. M., G. H. P. Oude Essink, R. Veness, and F. Sergi, 2009, Estimating the depth of fresh and brackish groundwater in a predominantly saline region using geophysical and hydrological methods, Zeeland, the Netherlands, *Near Surface Geophysics*, **7(5-6)**, 401-412.

Goovaerts, P., 1997, Geostatistics for natural resources evaluation, Oxford university press.

Gourry, J.-C., F. Vermeersch, M. Garcin, and D. Giot, 2003, Contribution of geophysics to the study of alluvial deposits: a case study in the Val d'Avaray area of the River Loire, France, *Journal of Applied Geophysics*, **54**, 35-49.

Groenewoudt, B. J., 1994, Prospectie, waardering en selectie van archeologische vindplaatsen: een beleidsgerichte verkenning van middelen en mogelijkheden: Nederlandse Archeologische Rapporten, v. 17: Amersfoort, Rijksdienst voor het Oudheidkundig Bodemonderzoek.

Gullentops, F., F. Bogemans, G. De Moor, E. Paulissen, and A. Pissart, 2001, Quaternary lithostratigraphic units (Belgium), *Geologica Belgica*, **4(1/2)**, 153-164.

Haoping, H., and I. J. Won, 2003, Real-time resistivity sounding using a hand-held broadband electromagnetic sensor, *Geophysics*, **68(4)**, 1224-1231.

Haslett, J., and A. Parnell, 2008, A simple monotone process with application to radiocarbon-dated depth chronologies, *Journal of the Royal Statistical Society: Series C (Applied Statistics)*, **57(4)**, 399-418.

Heirman, K., T. Missiaen, and P. C. Vos, 2013, Holocene palaeogeographical evolution of the Waasland Scheldepolders, in *Internal Report*, 37.

Heyse, I., 1979, Bijdrage tot de geomorfologische kennis van het noordwesten van Oost-Vlaanderen (België): Brussel.

Heyse, I., 1983, Cryoturbation Types in Eolian Würm Late Glacial Sediments in Flanders, Belgium, *Polarforschung* **53(2)**, 87-95.

Hijma, M. P., and K. M. Cohen, 2011a, Comment on: Mid-Holocene water-level changes in the lower Rhine-Meuse delta (western Netherlands): implications for the reconstruction of relative mean sea-level rise, palaeoriver-gradients and coastal evolution by Van de Plassche et al. (2010), *Netherlands Journal of Geosciences-Geologie En Mijnbouw*, **90(1)**, 51-54.

Hijma, M. P., and K. M. Cohen, 2011b, Holocene transgression of the Rhine river mouth area, The Netherlands/Southern North Sea: palaeogeography and sequence stratigraphy, *Sedimentology*, **58(6)**, 1453-1485.

Hijma, M. P., K. M. Cohen, W. Roebroeks, W. E. Westerhoff, and F. S. Busschers, 2012, Pleistocene Rhine-Thames landscapes: geological background for hominin occupation of the southern North Sea region, *Journal of Quaternary Science*, **27(1)**, 17-39.

Hilgers, A., 2007, The chronology of Late Glacial and Holocene dune development in the northern Central European lowland reconstructed by optically stimulated luminescence (OSL) dating, Universität zu Köln.

Hilhorst, M. A., 1998, Dielectric characterisation of soil, Landbouwuniversiteit Wageningen (Wageningen Agricultural University).

Hissel, M., and H. Van Londen, 2004, De kwaliteit van de waarneming. Een vergelijking van boormethoden voor archeologisch inventariserend veldonderzoek. Project TSA02001: AAC publicaties, v. 70: Amsterdam, Amsterdams Archeologisch Centrum.

Hissel, M., H. Van Londen, L. Tiggelman, and J. K. van Deen, 2005, Een oog voor de archeoloog, *Geotechniek*, **oktober 2005**, 30-35.

Hoek, W. Z., 2001, Vegetation response to the ~14.7 and ~11.5 ka cal. BP climate transitions: is vegetation lagging climate?, *Global and Planetary Change*, **30**, 103-115.

Howard, A. J., 2005, The contribution of geoarchaeology to understanding the environmental history and archaeological resources of the Trent Valley, UK, *Geoarchaeology: an International Journal*, **20(2)**, 93-107.

Howard, A. J., A. G. Brown, C. J. Carey, K. Challis, L. P. Cooper, M. Kincey, and P. Toms, 2008, Archaeological resource modelling in temperate river valleys: a case study from the Trent Valley, UK, *Antiquity*, **82(318)**, 1040-1054.

Howard, A. J., and M. G. Macklin, 1999, A generic geomorphological approach to archaeological interpretation and prospection in British river valleys: a guide for archaeologists investigating Holocene landscapes, *Antiquity*, **73(281)**, 527-541.

Jacobs, P., T. Polfliet, M. de Ceukelaire, and G. Moerkerke, 2010a, Geologische kaart van België, Vlaams gewest, Kaartblad (1-7) Essen - Kapellen Schaal 1: 50 000, Departement Leefmiliue, Natuur en Energie, Dienst Natuurlijke Rijkdommen.

Jacobs, P., T. Polfliet, M. de Ceukelaire, and G. Moerkerke, 2010b, Geologische kaart van België, Vlaams gewest, Kaartblad (15) Antwerpen Schaal 1: 50 000, Departement Leefmiliue, Natuur en Energie, Dienst Natuurlijke Rijkdommen.

Janssens, W., and D. K. Ferguson, 1985, The palaeoecology of the Holocene sediments at Kallo, Northern Belgium, *Review of Palaeobotany and Palynology*, **46**, 81-95.

Jelgersma, S., 1961, Holocene Sea Level Changes in the Netherlands. Thesis Leiden: Mededelingen Geologische Stichting, v. CVI-7: Leiden, Leiden University.

Jelgersma, S., J. de Jong, W. H. Zagwijn, and J. F. van Regteren Altena, 1970, The coastal dunes of the western Netherlands; geology, vegetational history and archaeology, *Mededelingen van de Rijks Geologische Dienst*, **21**, 93-167.

Johnson, W. J., and J. C. Clark, 1992, High resolution shear wave reflection surveying for hydrogeological investigations, in *Report No. DOE/CH-9211 (Contract No. 02112405 with Argonne National Laboratory)*, U.S. Department of Energy, Washington DC.

Jongepier, I., C. Wang, T. Missiaen, T. Soens, and S. Temmerman, 2015, Intertidal landscape response time to dike breaching and stepwise re-embankment: A combined historical and geomorphological study, *Geomorphology*, **236(0)**, 64-78.

Kasse, C. K., 2002, Sandy aeolian deposits and environments and their relation to climate during the Last Glacial Maximum and Lateglacial in northwest and central Europe, *Progress in Physical Geography*, **26(4)**, 507-532.

Kattenberg, A. E., and G. Aalbersberg, 2004, Archaeological prospection of the Dutch perimarine landscape by means of magnetic methods, *Archaeological Prospection*, **11(4)**, 227-235.

Keller, G. V., and F. C. Frischknecht, 1966, Electrical methods in geophysical prospecting.

Kiden, P., 1991, The Late Glacial and Holocene evolution of the Middle and Lower river Scheldt, Belgium, in *Temperate Palaeohydrology*, 283, L. Starkel, Gregory, and Thornes, eds., Wiley and Sons Ltd., Chichester.

Kiden, P., 1995, Holocene relative sea-level change and crustal movement in the southwestern Netherlands, *Marine Geology*, **124(1-4)**, 21-41.

Kiden, P., 2006, De evolutie van de Beneden-Schelde in België en Zuidwest-Nederland na de laatste ijstijd, *Belgeo*, **3**, 279-294.

Kiden, P., and C. Baeteman, 1989, Holocene water level movements in the Lower Scheldt perimarine area, Geologische Dienst van België.

Kiden, P., L. Denys, and P. Johnston, 2002, Late Quaternary sea-level change and isostatic and tectonic land movements along the Belgian-Dutch North Sea coast: geological data and model results, *Journal of Quaternary Science*, **17(5-6)**, 535-546.

Kiden, P., Denys, L. & Johnston, P., 2002, Late Quaternary sea-level change and isostatic and tectonic land movements along the Belgian - Dutch North Sea coast: geological data and model results., *Journal of Quaternary Science*, **17(5-6)**, 535-546.

Kiden, P., B. Makaske, and O. Van De Plassche, 2008, Waarom verschillen de zeespiegelreconstructies voor Nederland?, *Tijdschrift Grondboor en Hamer*, **3/4**, 54-61.

Kiden, P., and C. Verbruggen, 2001, Het verhaal van een rivier: de evolutie van de Schelde na de laatste ijstijd, in *Een duik in het verleden. Schelde, Maas en Rijn in de pre- en protohistorie*, 11-35, J. Bourgeois, P. Crombé, G. De Mulder, and M. Rogge, eds., Zottegem.

Kildea, F., and J. Musch, 2006, Developing methods for the assessment of artefacts densities on Mesolithic sites in central France, in *Preserving the Early Past. Investigation, selection and preservation of Palaeolithic and Mesolithic sites and landscapes.*, 141-150, E. Rensink, and H. Peeters, eds., Nederlandse Archeologische Rapporten, **31**.

Klinck, B., L. Meersschaert, and J.-P. Van Roeyen, 2007, Paleolandschappelijk en archeologisch onderzoek van de te realiseren natuurcompensatiezones "Weidevogelgebied Doelpolder Noord en Kreek" in het kader van de bouw van het containergetijdendok-west (gemeente Beveren). Interimrapport 1: paleolandschappelijke en archeologische screening aan de hand van boringen en inventarisatie (parentheses 1 en 2).

Knight, D., and A. J. Howard, 2004, Trent Valley Landscapes. The arcaeology of 500,000 years of change.: King's Lynn, Heritage Marketing and Publications Ltd.
Krakker, J. J., M. J. Shott, and P. D. Welch, 1983, Design and Evaluation of Shovel-Test Sampling in Regional Archaeological Survey, *Journal of Field Archaeology*, **10(4)**, 469-480.
Kuijper, W. J., 2006, Flora en fauna in en rond een Scheldegeul bij Kallo op het einde van het atlanticum (Beveren, prov. Oost-Vlaanderen), *Relicta, Archeologie, Monumenten en Landschapsonderzoek in Vlaanderen*, **1**, 29-48.
Laga, P., S. Louwye, and S. Geets, 2001, Paleogene lithostratigraphic units (Belgium), *Guide to a revised lithostratigraphic scale of Belgium. Geologica Belgica*, **4**, 135-152.
Landva, A. O., E. O. Korpijaakko, and P. E. Pheeney, 1983, Geotechnical classification of peats and organic soils, *Testing of peats and organic soils, ASTM STP*, **820**, 37-51.
Lauwers, B., and J. De Reu, 2011, Een midden-bronstijdbewoning te Sint-Gillis-Waas–Kluizenmolen (prov. Oost-Vlaanderen, België), *LUNULA (BRUSSEL)*, **19**, 27-33.
LeBlanc, D. C., 2004, Statistics: Concepts and Applications for Science, Jones and Bartlett.
Lespez, L., M. Clet-Pellerin, R. Davidson, G. Hermier, V. Carpentier, and J.-M. Cador, 2010, Middle to Late Holocene landscape changes and geoarchaeological implications in the marshes of the Dives estuary (NW France), *Quaternary International*, **216(1-2)**, 23-40.
Loke, M. H., 2014, Tutorial: 2-D and 3-d electrical imaging surveys, Geotomosoft.
Loke, M. H., J. E. Chambers, D. F. Rucker, O. Kuras, and P. B. Wilkinson, 2013, Recent developments in the direct-current geoelectrical imaging method, *Journal of Applied Geophysics*, **95(0)**, 135-156.
Long, M., 2005, Review of peat strength, peat characterisation and constitutive modelling of peat with reference to landslides.
Long, M., 2008, Design parameters from in situ tests in soft ground - recent developments, in *Geotechnical and Geophysical Site Characterization*, 89-116, A. B. Huang, and P. W. Mayne, eds.
Long, M., and N. Boylan, 2012, In situ testing of peat–a review and update on recent developments, *Geotechnical Engineering Journal of the SEAGS & AGSSEA* **43**, 41-55.
Lousberg, M., L. Calembert, and e. al., 1974, Penetration testing in Belgium: Proceedings of the European Symposium on Penetration Testing ESOPT. Stockholm (5–7 June, 1974), p. 7-17.
Louwe Kooijmans, L. P., 2010, Mesolithic Europe: diversity in uniformity, *Antiquity*, **84(323)**, 241-246.
Lovis, W. A., 1976, Quarter Sections and Forests: An Example of Probability Sampling in the Northeastern Woodlands, *American Antiquity*, **41(3)**, 364-372.
Lunne, T., and K. H. Andersen, 2007, Soft clay shear strength parameters for deepwater geotechnical design: Proceedings of the 6th International Conference: Society for Underwater Technology, Offshore Site Investigation and Geotechnics (SUT-OSIG), London, p. 11-13.
Lunne, T., P. K. Robertson, and J. J. M. Powell, 1997, Cone penetration testing in Geotechnical Practice: London, Spon Press Taylor & Francis Group.
Makaske, B., D. G. van Smeerdijk, H. Peeters, J. R. Mulder, and T. Spek, 2003, Relative water-level rise in the Flevo lagoon (The Netherlands), 5300-2000 cal. yr BC: an evaluation of new and existing basal peat time-depth data, *Geologie en Mijnbouw*, **82(2)**, 115-131.
Marquardt, D. W., 1963, An algorithm for least-squares estimation of nonlinear parameters, *Journal of the Society for Industrial & Applied Mathematics*, **11(2)**, 431-441.
McNeill, J. D., 1980, Electromagnetic terrain conductivity measurement at low induction numbers, Geonics Limited Ontario, Canada.

McNeill, J. D., 1996, Why doesn't Geonics Limited build a Multi-Frequency EM31 or EM38?, *Geonics Limited Techical Notes*, **TN-30**.

Meersschaert, L., J.-P. Van Roeyen, and C. Verbruggen, 2006, Geomorfologisch, geoarcheologisch, paleoecologisch en paleobotanisch onderzoek van de havenuitbreidingswerken op de linker Scheldeoever ten noorden van Antwerpen, *Belgeo*, **3**, 183-203.

Meier-Uhlherr, R., C. Schulz, and V. Luthardt, 2011, Steckbriefe Moorsubstrate, *Berlin*.

Meigh, A. C., 2013, Cone penetration testing: methods and interpretation, Elsevier.

Meylemans, E., E. Bogemans, A. Storme, Y. Perdaen, I. Verdurmen, and K. Deforce, 2013, Lateglacial and Holocene fluvial dynamics in the Lower Scheldt basin (N-Belgium) and their impact on the presence, detection and preservation potential of the archaeological record, *Quaternary International*, **308**, 148-161.

Minnaert, G., and C. Verbruggen, 1986, Palynologisch onderzoek van een veenprofiel uit het Doeldok te Doel, *Buitengewone uitgaven van de Koninklijke Oudheidkundige Kring van het Land van Waas Bijdragen van de Archaeologische Dienst Waasland I*, **19**, 201-208.

Missiaen, T., E. Slob, and M. E. Donselaar, 2008, Comparing different shallow geophysical methods in a tidal estuary, Verdronken Land van Saeftinge, Western Scheldt, the Netherlands, *Netherlands Journal of Geosciences-Geologie En Mijnbouw*, **87(2)**, 151-164.

Missiaen, T., J. Verhegge, K. Heirman, and P. Crombé, 2015, Potential of cone penetrating testing for mapping deeply buried palaeolandscapes in the context of archaeological surveys in polder areas, *Journal of Archaeological Science*, **55(0)**, 174-187.

Montafia, A., 2013, Influence of Physical Properties of Marine Clays on Electric Resistivity and Basic Geotechnical Parameters, Norwegian University of Science and Technology, 148 p.

Morin, E., F. Hinschberger, J.-J. Macaire, I. Gay-Ovéjéro, and C. Chartin, 2009, Significance of the correlation between the electrical conductivity dataset and lithology in Pleni-Lateglacial and Holocene alluvial archives. A case study: the Choisille catchment (SW Paris Basin, France), *ArcheoSciences. Revue d'archéométrie*, **(33 (suppl.))**, 191-194.

MOW, 2010, Verslag over de resultaten van de boringen met bijhorend laboratoriumonderzoek uitgevoerd ten behoeve van de studie van het vernieuwen en ontdubbelen van de stuw op de Bovenschelde te Avelgem (Kerkhove), in *MOW Geotechniek internal report* Mobiliteit & Openbare Werken.

Mys, M., 1973, De landschapsgeschiedenis van de Scheldepolders ten noorden van Antwerpen, *Tijdschrift van de Belgische vereniging voor aardrijkskundige studies*, **42**, 39-124.

Nanson, G. C., and A. D. Knighton, 1996, ANABRANCHING RIVERS: THEIR CAUSE, CHARACTER AND CLASSIFICATION, *Earth surface processes and landforms*, **21(3)**, 217-239.

National Committee of Geography of Belgium, I., 2012, A concise geography of Belgium: Ghent, Academic Press, 46 p.

Nicholas, G. P., 1998, Wetlands and Hunter-Gatherers: A Global Perspective, *Current ANthropology*, **39(5)**, 720-733.

Noens, G., 2011, Een afgedekt mesolithisch nederzettingsterrein te Hempens/N31 (gemeente Leeuwarden, provincie Friesland, Nl.). Algemeen kader voor de studie van een lithische vindplaats: ARGU 7: Gent, Academia Press.

Noens, G., M. Bats, A. Van Baelen, and P. Crombé, 2013, Archeologische (lithische) indicatoren met geringe afmetingen en hun rol bij het opsporen van afgedekte prehistorische vindplaatsen: experimentele en archeologische observaties, *Notae Praehistoricae*, **33**, 193-215.

Olhoeft, G. R., 2003, Electromagnetic field and material properties in ground penetrating radar: Advanced Ground Penetrating Radar, 2003. Proceedings of the 2nd International Workshop on, p. 144-147.

Orbons, J., 2011, Electromagnetic survey for paleo-lanscape analyses in sedimentation areas: 9th international conference on Archaeological Prospection.

Orton, C., 2000, Sampling in Archaeology, 261, Cambridge Manuals in Archaeology, Cambridge University Press, Cambridge.

Parnell, A. C., C. E. Buck, and T. K. Doan, 2011, A review of statistical chronology models for high-resolution, proxy-based Holocene palaeoenvironmental reconstruction, *Quaternary Science Reviews*, **30(21–22)**, 2948-2960.

Parnell, A. C., J. Haslett, J. R. M. Allen, C. E. Buck, and B. Huntley, 2008, A flexible approach to assessing synchroneity of past events using Bayesian reconstructions of sedimentation history, *Quaternary Science Reviews*, **27(19–20)**, 1872-1885.

Pavlopoulos, K., M. Triantaphyllou, P. Karkanas, K. Kouli, G. Syrides, K. Vouvalidis, N. Palyvos, and T. Tsourou, 2010, Paleoenvironmental evolution and prehistoric human environment, in the embayment of Palamari (Skyros Island, Greece) during Middle-Late Holocene, *Quaternary International*, **216(1–2)**, 41-53.

Peeters, H., 2007, Hoge Vaart-A27 in Context: towards a Model of Mesolithic - Neolithic Land Use Dynamics as a Framework for Archaeological Heritage Management: Amersfoort, RACM.

Peeters, H., 2008, Een nieuwe archeologische verwachtings-kaart voor het mesolithicum en neolithicum van Flevoland, in *De indicatieve kaart van Archeologische Waarden, derde generatie*, 13, J. deeben, ed., RACM, Amersfoort.

Perdaen, Y., J. Sergant, and P. Crombé, 2004, Early mesolithic land-use and site-use in northwestern Belgium: the evidence from Verrebroek "Dok", *BAR International Series*, **1302**, 11-18.

Perdaen, Y., J. Sergant, E. Meylemans, A. Storme, K. Deforce, J. Bastiaens, S. Debruyne, A. Ervynck, R. Langohr, and A. Lentacker, 2011, Noodonderzoek van een wetland site in Bazel-Sluis (Kruibeke, Oost-Vlaanderen, B): een nieuwe kijk op de neolithisatie in Vlaanderen, *Notae Praehistoricae*, **31**, 31-45.

Pillans, B., and P. Gibbard, 2012, The Quaternary Period, in *The Geologic Time Scale 2012. The Geological Time Scale, 2*, Elsevier.

Raemaekers, D. C. M., 1999, The articulation of a 'New Neolithic'. The meaning of the Swifterbant Culture for the process of neolithisation in the western part of the North European Plain (4900-3400 BC). Archaeological Studies Leiden University, Leiden University Press, Leiden.

Reimer, P. J., M. G. L. Baillie, E. Bard, A. Bayliss, J. W. Beck, P. G. Blackwell, C. B. Ramsey, C. E. Buck, G. S. Burr, R. L. Edwards, M. Friedrich, P. M. Grootes, T. P. Guilderson, I. Hajdas, T. J. Heaton, A. G. Hogg, K. A. Hughen, K. F. Kaiser, B. Kromer, F. G. McCormac, S. W. Manning, R. W. Reimer, D. A. Richards, J. R. Southon, S. Talamo, C. S. M. Turney, J. van der Plicht, and C. E. Weyhenmeye, 2009, INTCAL09 and MARINE09 radiocarbon age calibration curves, 0-50,000 years CAL BP, *Radiocarbon*, **51(4)**, 1111-1150.

Reimer, P. J., E. Bard, A. Bayliss, J. W. Beck, P. G. Blackwell, C. Bronk Ramsey, C. E. Buck, H. Cheng, R. L. Edwards, and M. Friedrich, 2013, IntCal13 and Marine13 radiocarbon age calibration curves 0-50,000 years cal BP.

Reynolds, J. M., 2011, An introduction to applied and environmental geophysics, John Wiley & Sons.

Rippon, S., 2000, The transformation of coastal wetlands: exploitation and management of marshland landscapes in north west Europe during the Roman and Medieval periods, Oxford University Press Oxford.

Robertson, P. K., 2010, Soil behaviour type from the CPT: an update, in *2nd International Symposium on Cone Penetration Testing*, Huntington Beach, CA, USA, May 2010.

Robertson, P. K., and K. L. Cabal, 2012, Guide to Cone Penetration Testing for Geotechnical Engineering (5th edition): Signal Hill, California, USA, Gregg Drilling & Testing, Inc.

Robertson, P. K., R. G. Campanella, D. Gillespie, and J. Greig, 1986, Use of Piezometer Cone data, *In-Situ'86 Use of In-situ testing in Geotechnical Engineering GSP 6 , ASCE, Reston, VA, Specialty Publication*, 1263-1280.

Robinson, E., L. Lombaert, J. Sergant, and P. Crombé, 2011, Armatures and the question of forager-farmer contact along the North-Western fringe of LBK: the site of "Verrebroek-Aven Ackers" (East Flanders, Belgium), *Archäologisches Korrespondenzblatt*, **41**(**4**), 473-490.

Robinson, E., M. Van Strydonck, V. Gelorini, and P. Crombe, 2013, Radiocarbon chronology and the correlation of hunter-gatherer sociocultural change with abrupt palaeoclimate change: the Middle Mesolithic in the Rhine-Meuse-Scheldt area of northwest Europe, *Journal of Archaeological Science*, **40**(**1**), 755-763.

Roeleveld, W., 1974, The Holocene evolution of the Groningen Marine-Clay District, *Berichten van de Rijksdienst voor het Oudheidkundig Bodemonderzoek*, **24**(**Supplement**), 8-132.

Roozen, S., S. Kluiving, and S. Soetens, 2013, A lithostratigraphic geo-archaeological 3D model of the subsurface of a medieval mound in the city center of Vlaardingen (The Netherlands): EGU General Assembly Conference Abstracts, p. 6244.

Saey, T., P. De Smedt, E. Meerschman, M. M. Islam, F. Meeuws, E. Van De Vijver, A. Lehouck, and M. Van Meirvenne, 2012a, Electrical conductivity depth modelling with a multireceiver EMI sensor for prospecting archaeological features, *Archaeological Prospection*, **19**(**1**), 21-30.

Saey, T., M. M. Islam, P. De Smedt, E. Meerschman, E. Van De Vijver, A. Lehouck, and M. Van Meirvenne, 2012b, Using a multi-receiver survey of apparent electrical conductivity to reconstruct a Holocene tidal channel in a polder area, *Catena*, **95**, 104-111.

Saey, T., D. Simpson, U. W. A. Vitharana, H. Vermeersch, J. Vermang, and M. Van Meirvenne, 2008, Reconstructing the paleotopography beneath the loess cover with the aid of an electromagnetic induction sensor, *Catena*, **74**(**1**), 58-64.

Saey, T., M. Van Meirvenne, D. Simpson, U. W. A. Vitharana, L. Cockx, and H. Vermeersch, 2010, Reconstructing palaeotopography at the beginning of the Weichselian glacial stage using an electromagnetic induction sensor: Progress in Soil Science, p. 423-434.

Samouëlian, A., I. Cousin, A. Tabbagh, A. Bruand, and G. Richard, 2005, Electrical resistivity survey in soil science: a review, *Soil and Tillage Research*, **83**(**2**), 173-193.

Santos, F. A. M., J. Triantafilis, K. E. Bruzgulis, and J. A. E. Roe, 2010, Inversion of Multiconfiguration Electromagnetic (DUALEM-421) Profiling Data Using a One-Dimensional Laterally Constrained Algorithm, *Vadose Zone Journal*, **9**(**1**), 117-125.

Schirmer, W., 1999, The Symposium „Dunes and fossil soils", *GeoArchaeoRhein*, **3**, 5-9.

Schmidt, A., 2001, Geophysical Data in Archaeology: A Guide to Good Practice: Oxford, Oxbow Books.

Schuldenrein, J., 1991, Coring and the Identity of Cultural-Resource Environments: a comment on Stein, *American Antiquity*, **56**(**1**), 131-137.

Sergant, J., M. Bats, G. Noens, L. Lombaert, and D. D'Hollander, 2007, Voorlopige resultaten van noodopgravingen in het afgedekte dekzandlandschap van Verrebroek - Aven Ackers (Mesolithicum, Neolithicum), *Notae Praehistoricae*, **27**, 101-107.

Sergant, J., P. Crombé, and Y. Perdaen, 2006a, The 'invisible' hearths: a contribution to the discernment of Mesolithic non-structured surface hearths, *Journal of Archaeological Science*, **33**(**7**), 999-1007.

Sergant, J., Y. Perdaen, and P. Crombé, 2006b, The Site of Doel "Deurganckdok" and the Neolithisation of the Sandy Lowland of Belgium., in *La Neolithisation/The Neolithisation Process. Acts of the XIVth UISPP Congress, University of Liège, Belgium, 2-8 September 2001.*, 53-60, J. Guilaine, and J. P. van Berg, eds., BAR International Series, **1520**, Archeopress, Oxford.

Shennan, I., and B. Horton, 2002, Holocene land-and sea-level changes in Great Britain, *Journal of Quaternary Science*, **17(5-6)**, 511-526.

Sheriff, R. E., and L. P. Geldart, 1995, Exploration seismology, Cambridge university press.

Shott, M., 1985, Shovel-Test Sampling as a Site Discovery Technique: A Case Study from Michigan, *Journal of Field Archaeology*, **12(4)**, 457-468.

Sier, M. M., 2003, Ellewoutsdijk in de Romeinse tijd: ADC Rapport: Amersfoort ADC.

Silva, A. J., and H. G. Brandes, 1998, Geotechnical properties and behavior of high-porosity, organic-rich sediments in Eckernförde Bay, Germany, *CONTINENTAL SHELF RESEARCH*, **18(14)**, 1917-1938.

Simpson, D., A. Lehouck, M. van Meirvenne, J. Bourgeois, E. Thoen, and J. Vervloet, 2008, Geoarchaeological prospection of a medieval manor in the Dutch Polders using an electromagnetic induction sensor in combination with soil augerings, *Geoarchaeology*, **23**, 1-14.

Simpson, D., A. Lehouck, L. Verdonck, H. Vermeersch, M. Van Meirvenne, J. Bourgeois, E. Thoen, and R. Docter, 2009a, Comparison between electromagnetic induction and fluxgate gradiometer measurements on the buried remains of a 17th century castle, *Journal of Applied Geophysics*, **68(2)**, 294-300.

Simpson, D., M. V. Meirvenne, T. Saey, H. Vermeersch, J. Bourgeois, A. Lehouck, L. Cockx, and U. W. A. Vitharana, 2009b, Evaluating the multiple coil configurations of the EM38DD and DUALEM-21S sensors to detect archaeological anomalies, *Archaeological Prospection*, **16(2)**, 91-102.

Simpson, D., M. Van Meirvenne, T. Saey, H. Vermeersch, J. Bourgeois, A. Lehouck, L. Cockx, and U. V. Wellewatte Arachchige, 2009c, Evaluating the Multiple Coil Configurations of the EM38DD and DUALEM-21S Sensors to Detect Archaeological Anomalies, *Archaeological Prospection*, **16(2)**, 91-102.

Sjoerd, J. K., A. L. Michel, M. J. d. K. Adriaan, R. Hans, J. B. Guus, and A. S. Steven, 2013, Potential and use of archaeological and historical data for a reconstruction of the sea level curve of the last 3000 years in the coastal zone of the southern North Sea. Results of a case study, in *Landscapes or seascapes?*, 61-84.

Soens, T., J. Sergant, E. Wauters, I. Jongepier, H. Masure, F. Cruz, P. Laloo, L. Lombaert, J. Mikkelsen, and G. Noens, 2012, Ruraal erfgoed Linkeroever- Onderzoek naar het ruraal erfgoed in de Wase polders, Technicum, Universiteit Antwerpen, Gate Archaeology.

Spikins, P., 1999, Mesolithic Northern England. Environment, population and settlement: BAR British Series 283: Oxford, Archeopress.

Steier, P., and W. Rom, 2000, The use of Bayesian statistics for C-14 dates of chronologically ordered samples: A critical analysis, *Radiocarbon*, **42(2)**, 183-198.

Stein, J. K., 1986, Coring archaeological sites, *American Antiquity*, **51(3)**, 505-527.

Stuiver, M., and P. J. Reimer, 1993, Extended C-14 Data-base and revised CALIB 3.0 C-14 age calibration program, *Radiocarbon*, **35(1)**, 215-230.

Svenning, J.-C., 2002, A review of natural vegetation openness in north-western Europe, *Biological Conservation*, **104(2)**, 133-148.

Svensson, A., K. K. Andersen, M. Bigler, H. B. Clausen, D. Dahl-Jensen, S. M. Davies, S. J. Johnsen, R. Muscheler, S. O. Rasmussen, and R. Röthlisberger, 2006, The Greenland

ice core chronology 2005, 15–42ka. Part 2: comparison to other records, *Quaternary Science Reviews*, **25(23)**, 3258-3267.

Tavernier, R., 1946, L'évolution du Bas-Escaut au Pléistocene supérieur, *Bulletin Societé Belge Géologique, Paléontologique, Hydrologique*, **55**, 106-125.

Terberger, T., N. Barton, and M. Street, 2006, The Late Glacial reconsidered - recent progress and interpretations, in *Humans, environment and chronology of the Late Glacial of the North European Plain. Proceedings of Workshop 14 (Commission XXXII "The Final Palaeolithic of the Great European Plain / Le paléolithique Final de la Grande Plaine Européenne") of the 15th U.I.S.P.P. congress, Lisbon, September 2006*, 189-207, M. Street, N. Barton, and T. Terberger, eds., Verlag des Römisch-Germanischen Zentralmuseums, Mainz.

Tol, A. J., J. W. H. P. Verhagen, A. Borsboom, and M. Verbruggen, 2004, Prospectief boren: een studie naar de betrouwbaarheid en toepasbaarheid van booronderzoek in de prospectiearcheologie: RAAP-rapport, v. 1000: Amsterdam, RAAP Archeologisch Adviesbureau.

Tol, A. J., J. W. H. P. Verhagen, and M. Verbruggen, 2006, Leidraad inventariserend veldonderzoek. Deel: karterend booronderzoek, SIKB.

Tornqvist, T. E., A. F. M. Dejong, W. A. Oosterbaan, and K. Vanderborg, 1992, Accurate dating of organic deposits by AMS C-14 measurement of macrofossils, *Radiocarbon*, **34(3)**, 566-577.

Tornqvist, T. E., and M. P. Hijma, 2012, Links between early Holocene ice-sheet decay, sea-level rise and abrupt climate change, *Nature Geoscience*, **5(9)**, 601-606.

Triantafilis, J., and F. A. Monteiro Santos, 2013, Electromagnetic conductivity imaging (EMCI) of soil using a DUALEM-421 and inversion modelling software (EM4Soil), *Geoderma*, **211–212(0)**, 28-38.

Van Berg, P. L., L. H. Keeley, J.-P. Van Roeyen, and R. Van Hove, 1992, Le gisement mésolithique de Melsele (Flandrien-Orientale, Belgique) et le subnéolithique en europe occidentale., in *Paysans et bâtisseurs. L'émergeence du Néolithique atlantique et les origins du Mégalithisme. Actes du 17ème Colloque interrégional sur le Néolithique, Vannes, 23-31 octobre 1990*, 93-99, C.-T. Le Roux, ed., Revue Archéologique de l'Ouest, Rennes.

Van De Plassche, O., 1982, Sea-level change and water-level movements in the netherlands during the holocene, *Mededelingen Rijks Geologische Dienst Nederland*, **36(1)**, 1-93.

Van De Plassche, O., S. J. P. Bohncke, B. Makaske, and J. van der Plicht, 2005, Water-level changes in the Flevo area, central Netherlands (5300–1500 BC): implications for relative mean sea-level rise in the Western Netherlands, *Quaternary International*, **133-134(77-93)**.

Van De Plassche, O., B. Makaske, W. Z. Hoek, M. Konert, and J. van der Plicht, 2010, Mid-Holocene water-level changes in the lower Rhine-Meuse delta (western Netherlands): implications for the reconstruction of relative mean sea-level rise, palaeoriver-gradients and coastal evolution, *Netherlands Journal of Geosciences-Geologie En Mijnbouw*, **89(1)**, 3-20.

van der Spek, A. J. F., 1997, Tidal asymmetry and long-term evolution of Holocene tidal basins in The Netherlands: simulation of palaeo-tides in the Schelde estuary, *Marine Geology*, **141(1-4)**, 71-90.

Van Dijk, G. J., H. J. A. Berendsen, and W. Roeleveld, 1991, Holocene water level development in the Netherlands' river area; implications for sealevel reconstruction, *Geologie en Mijnbouw*, **70**, 311-326.

van Dinter, M., and W. K. van Zijverden, 2010, Settlement and land use on crevasse splay deposits; geoarchaeological research in the Rhine-Meuse Delta, the Netherlands, *Netherlands Journal of Geosciences*, **89(01)**, 21-34.

Van Eetvelde, V., and M. Antrop, 2009, A stepwise multi-scaled landscape typology and characterisation for trans-regional integration, applied on the federal state of Belgium, *Landscape and urban planning*, **91(3)**, 160-170.

Van Neer, W., A. Ervynck, A. Lentacker, J. Bastiaens, K. Deforce, E. Thieren, J. Sergant, and P. Crombé, 2013, Hunting, gathering, fishing and herding: Animal exploitation in Sandy Flanders (NW Belgium) during the second half of the fifth millennium BC, *Environmental Archaeology*, **18(2)**, 87-101.

Van Ranst, E., and C. Sys, 2000, Eenduidige legende voor de Digitale Bodemkaart van Vlaanderen (Schaal 1:20.000): Gent, Laboratorium voor Bodemkunde UGent.

Van Roeyen, J.-P., G. Minnaert, M. Van Strydonck, and C. Verbruggen, 1991, Melsele-Hof ten Damme: prehistorische bewoning, landschappelijke ontwikkeling en kronologisch kader, *Notae Praehistoricae*, **11**, 41-49.

Van Roeyen, J. P., C. Verbruggen, B. Klinck, and L. Meersschaert, 2001, Het Deurganckdok te Doel (Beveren, O.-Vl.). Paleo-landschappelijk en archeolgisch onderzoek, *Annalen van de Koninklijke Oudheidkundige Kring van het Land van Waas (ook in Bijdragen van de Archeologische Dienst Waasland 5)*, **104**, 437-484.

Van Strydonck, M., 2005, Radiocarbon dating, in *The last hunter-gatherer-fischermen in Sandy Flanders (NW Belgium). the Verrebroek and Doel excavation projects (vol.1)*, 127-138, P. Crombé, ed., Archaeological Reports Ghent University, **3**, Ghent University, Gent.

Van Strydonck, M., and P. Crombé, 2005, Features: radiocarbon dating, *The last hunter-gatherer-fishermen in Sandy Flanders (NW Belgium): the Verrebroek and Doel excavation projects, volume 1: palaeo-environment, chronology and features*, **3**, 180-212.

Van Strydonck, M., and K. van der Borg, 1990-1991, The construction of a preparation line for AMS-targets at the Royal Institute for Cultural Heritage Brussels, *Bulletin of the Royal Institute for Cultural Heritage*, **23**, 2258-234.

Van Strydonck, M., J. P. Van Roeyen, G. Minnaert, and C. Verbruggen, 1995, Problems in dating stone-age settlements on sandy soils: the Hof ten Damme site near Melsele, Belgium, *Radiocarbon*, **37(2)**, 291-297.

Vandenberghe, J., and R. A. van Overmeeren, 1999, Ground penetrating radar images of selected fluvial deposits in the Netherlands, *Sedimentary Geology*, **128(3–4)**, 245-270.

Verbruggen, C., L. Denys, and P. Kiden, 1996, Belgium, in *Palaeoecological events during the last 15000 years: regional syntheses of palaeoecological studies of lakes and mires in Europe*, 553-574, B. E. Berglund, H. J. B. Birks, M. Ralska-Jasiewiczowa, and H. E. Wright, eds., John Wiley & sons, Chichester.

Verhagen, P., E. Rensink, M. Bats, and P. Crombé, 2011, Optimale strategieën voor het opsporen van Steentijdvindplaatsen met behulp van booronderzoek: een statistisch perspectief, v. 197, Rijksdienst voor het cultureel erfgoed.

Verhagen, P., E. Rensink, M. Bats, and P. Crombé, 2013, Establishing discovery probabilities of lithic artefacts in Palaeolithic and Mesolithic sites with core sampling, *Journal of Archaeological Science*, **40(1)**, 240-247.

Verhart, L. B. M., 2000, Times fade away.The neolithization of the southern Netherlands in an anthropological and geographical perspective: Archaeological Studies Leiden University: Leiden, Universiteit Leiden.

Verhegge, J., T. Missiaen, and P. Crombé, 2012, Preliminary results of an archaeological survey of the land-sea transition at Doelpolder Noord (prov. Of Antwerp, B.), *Notae Praehistoricae*, **32**, 165-174.

Verhegge, J., T. Missiaen, and P. Crombé, submitted-a, Exploring integrated geophysics and geotechnics as a palaeolandscape reconstruction tool: archaeological prospection of (prehistoric) sites buried deeply below the Scheldt polders (NW Belgium), *submitted to Archaeological Prospection*.

Verhegge, J., T. Missiaen, M. Van Strydonck, and P. Crombe, 2014, Chronology of Wetland Hydrological Dynamics and the Mesolithic-Neolithic Transition Along the Lower Scheldt: A Bayesian Approach, *Radiocarbon*, **56**(2), 883-898.

Verhegge, J., T. Saey, M. Van Meirvenne, T. Missiaen, and P. Crombé, submitted-b, Reconstructing Early Neolithic paleogeography: EMI-based subsurface modelling and chronological modelling of Holocene peat below the lower Scheldt floodplain (NW Belgium), *submitted to Geoarchaeology-An International Journal*.

Vermeersch, P., 1994, Increasing Destruction of prehistoric Settlements in Flanders, in *Aspekte Europaischer Bodendenkmalpflege*, 17-27, R. Habelt, ed., Köln.

Vermeersch, P. M., 2011, The human occupation of the Benelux during the Younger Dryas, *Quaternary International*, **242**(2), 267-276.

Vink, A., H. Steffen, L. Reinhardt, and G. Kaufmann, 2007, Holocene relative sea-level change, isostatic subsidence and the radial viscosity structure of the mantle of northwest Europe (Belgium, the Netherlands, Germany, southern North Sea), *Quaternary Science Reviews*.

Vos, J. D., 1982, The practical use of CPT in soil profiling: Proceedings of the Second European Symposium on Penetration Testing, ESOPT-2, Amsterdam, May, p. 24-27.

Vos, P., J. G. A. Bazelmans, H. J. T. Weerts, and M. J. van der Meulen, 2011, Atlas van Nederland in het Holoceen: landschap en bewoning vanaf de laatste ijstijd tot nu, Bert Bakker.

Vos, P., M. van den Berg, D. Maljers, and S. de Vries, 2009, Geoarcheologische bureaustudie ten behoeve van het Yangtzehavenproject (1e onderzoeksfase in het verkennend inventariserend veldonderzoek), Deltares.

Vos, P. C., 2006, Toelichting bij de nieuwe paleogeografische kaarten van Nedeerland (versie 1.0, geaccepteerd maart 2006).

Vos, P. C., F. P. M. Bunnik, K. M. Cohen, and H. Cremer, in press, A staged geogenetic approach to underwater archaeological prospection in the Port of Rotterdam (Yangtzehaven, Maasvlakte, The Netherlands): A geological and palaeoenvironmental case study for local mapping of Mesolithic lowland landscapes, *Quaternary International*, (**0**).

Vos, P. C., and R. M. van Heeringen, 1997, Holocene geology and occupation history of the province of zeeland, *Mededelingen Nederlands Instituut voor Toegepaste Geowetenschappen TNO*, **59**, 5-109.

Wait, J. R., 1962, A note on the electromagnetic response of a stratified earth, *Geophysics*, **27**(3), 382-385.

Wansleeben, M., and W. Laan, 2012, The archaeological practice of discovering Stone Age sites, *The End Of Our Fifth Decade, Leiden*, 254-261.

Waters, M. R., 1992, Principles of Geoarchaeology: Tucson, University of Arizona Press.

Watlab, 2013, Getijtafels Prosperpolder TAW 2013, **24-04-2015**.

Webster, R., and R. M. Lark, 2013, Field sampling for environmental science and management, Routledge.

Weerts, H., P. Cleveringa, W. Westerhoff, and P. Vos, 2006, Nooit meer: afzettingen van Duinkerke en Calais, *Archeobrief*, 28-34.

Weerts, H. J. T., A. Otte, B. I. Smit, P. Vos, D. Schiltmans, W. Waldus, and W. Borst, 2012, Finding the Needle in the Haystack by Using Knowldge of Mesolithic Human Adaptation in a Drowning Delta, *eTopoi, Journal for Ancient Studies*, **3**, 17-24.

Weston, D. G., 2001, Alluvium and geophysical prospection, *Archaeological Prospection*, **8**(4), 265-272.

Whitehouse, N. J., and D. Smith, 2010, How fragmented was the British Holocene wildwood? Perspectives on the "Vera" grazing debate from the fossil beetle record, *Quaternary Science Reviews*, **29**(**3-4**), 539-553.

Won, I., D. Keiswetter, G. Fields, and L. Sutton, 1996, GEM-2: A New Multifrequency Electromagnetic Sensor, *Journal of Environmental and Engineering Geophysics*, **1**(**2**), 129-137.

Won, I. J., 1980, A wide-band electromagnetic exploration method-Some theoretical and experimental results, *Geophysics*, **45**(**5**), 928-940.

Yeloff, D., K. D. Bennett, M. Blaauw, D. Mauquoy, U. Sillasoo, J. van der Plicht, and B. Geel, 2006, High precision C-14 dating of Holocene peat deposits: A comparison of Bayesian calibration and wiggle-matching approaches, *Quaternary geochronology*, **1**(**3**), 222-235.

Zwertvaegher, A., P. Finke, J. De Reu, A. Vandenbohede, L. Lebbe, M. Bats, W. De Clercq, P. De Smedt, V. Gelorini, J. Sergant, M. Antrop, J. Bourgeois, P. De Maeyer, M. Van Meirvenne, J. Verniers, and P. Crombé, 2013, Reconstructing phreatic palaeogroundwater levels in a geoarchaeological context: a case study in Flanders, Belgium, *GEOARCHAEOLOGY-AN INTERNATIONAL JOURNAL*, **28**(**2**), 170-189.

Appendix

Appendix 1: List of all used radiocarbon dated archaeological samples used.

Site	Latitude	Longitude	Elevation (mTAW) (top ridge)	Lab n°	BP	Error	δ13C	Sample composition	Context	Bibliography; Map number on Figure 39 and Figure 48
Bazel-Sluis	51°08′09″	4°19′23″	−0.25	KIA-47396	6060	40	−24.6	Skull fragment with horncore (Bos, auroch)	OM rich Clay/Peat (2)	http://radiocarbon.kikirpa.be; Figure 48-6
Bazel-Sluis	51°08′09″	4°19′23″	−0.25	KIA-47399	6045	45	−22.9	Antler fragment (Cervus)	OM rich Clay/Peat (2)	
Bazel-Sluis	51°08′09″	4°19′23″	−0.25	KIA-47327	5900	40	−24.6	Skull fragment with horncore (Bos, auroch)	OM rich Clay/Peat (2)	
Bazel-Sluis	51°08′09″	4°19′23″	−0.25	KIA-47403	5865	55	−23.0	Antler tip: lower part cut off (Cervus)	OM rich Clay/Peat (2)	
Bazel-Sluis	51°08′09″	4°19′23″	−0.25	KIA-47400	5855	40	−25.00	Wood shafted in metatarsus Bos	OM rich Clay/Peat (2)	
Bazel-Sluis	51°08′09″	4°19′23″	−0.25	KIA-47402	5835	60	−22.8	Antler: pierced and flattened (Cervus)	OM rich Clay/Peat (2)	

Bazel-Sluis	51°08′09″	4°19′23″	−0.25	KIA-47411	5835	45	−24.0	Skull fragment with horncore (Bos)	OM rich Clay/Peat (2)
Bazel-Sluis	51°08′09″	4°19′23″	−0.25	KIA-47408	5830	50	−23.6	Wood shafted in metatarsus Bos	OM rich Clay/Peat (2)
Bazel-Sluis	51°08′09″	4°19′23″	−0.25	KIA-47329	5830	35	−21.3	Mandibule, male animal (Sus)	OM rich Clay/Peat (2)
Bazel-Sluis	51°08′09″	4°19′23″	−0.25	KIA-47328	5790	35	−22.0	Human clavicula	OM rich Clay/Peat (2)
Bazel-Sluis	51°08′09″	4°19′23″	−0.25	KIA-47407	5790	45	−23.1	Antler: pierced and used (Cervus)	OM rich Clay/Peat (2)
Bazel-Sluis	51°08′09″	4°19′23″	−0.25	KIA-47326	5715	40	−23.8	Auroch subadult sacrum fragment (Bos)	OM rich Clay/Peat (2)
Bazel-Sluis	51°08′09″	4°19′23″	−0.25	KIA-47410	5320	45	−23.5	Upper skull, horned (Ovis)	Coarse Sand (3)
Bazel-Sluis	51°08′09″	4°19′23″	−0.25	KIA-47405	5050	60	−21.4	Scapula fragment (Sus, boar)	Coarse Sand (3)
Bazel-Sluis	51°08′09″	4°19′23″	−0.25	KIA-47412	5030	55	−22.3	Metatarsus, worked and pierced (Cervus)	Coarse Sand (3)
Bazel-Sluis	51°08′09″	4°19′23″	−0.25	KIA-47568	4985	35	−25.66	Triticum aestivum charred remains	Shell-/OM rich Clay (4)
Bazel-Sluis	51°08′09″	4°19′23″	−0.25	KIA-47721	4925	35	−24.99	Triticum aestivum/Spelta charred remains	Shell-/OM rich Clay (4)
Bazel-Sluis	51°08′09″	4°19′23″	−0.25	KIA-47723	4810	30	−21.66	Hordeum charred remains	Shell-/OM rich Clay (4)
Bazel-Sluis	51°08′09″	4°19′23″	−0.25	KIA-47404	7260	50	−23.4	Cranium and mandible (Canis)	unclear (2/3/4)
Bazel-Sluis	51°08′09″	4°19′23″	−0.25	KIA-47401	6075	45	−23.3	Humerus? Worked, usage patina (Bos)	unclear (2/3/4)

Bazel-Sluis	51°08′09″	4°19′23″	−0.25	KIA-47406	6045	40	−23.3	Antler tip: chopped at basis (Cervus)	unclear (2/3/4)	
Bazel-Sluis	51°08′09″	4°19′23″	−0.25	KIA-47426	6030	45	−23.2	Antler fragments, 1 tip (Cervus)	unclear (2/3/4)	
Bazel-Sluis	51°08′09″	4°19′23″	−0.25	KIA-47409	5955	50	−22.9	Antler fragments (Cervus)	unclear (2/3/4)	
Bazel-Sluis	51°08′09″	4°19′23″	−0.25	KIA-47398	5910	50	−23.9	Thrown antler fragment (Cervus)	unclear (2/3/4)	
Bazel-Sluis	51°08′09″	4°19′23″	−0.25	KIA-47395	5895	40	−20.8	Ulna (Sus, domesticated)	unclear (2/3/4)	
Bazel-Sluis	51°08′09″	4°19′23″	−0.25	KIA-47325	5855	35	−24.4	Skull fragment with horncore (Bos, auroch)	unclear (2/3/4)	
Bazel-Sluis	51°08′09″	4°19′23″	−0.25	KIA-47425	5330	45	−24.2	Calcaneus (Ovis)	unclear (2/3/4)	
Bazel-Sluis	51°08′09″	4°19′23″	−0.25	KIA-47397	5150	40	−23.3	Os centrotarsale, adult (Bos)	unclear (2/3/4)	
Bazel-Sluis	51°08′09″	4°19′23″	−0.25	KIA-47413	5105	40	−23.3	Metatarsus adult animal (Bos)	unclear (2/3/4)	
Bazel-Sluis	51°08′09″	4°19′23″	−0.25	KIA-47330	5040	40	−20.2	Ulna, proximal fragment (Sus)	unclear (2/3/4)	
Doel-Deurganckdok-B	51°18′10″	4°15′59″	−0.55	KIA-17995	5635	30	−25.3	Sorbus charcoal	Surface-hearth	(Boudin et al., 2009) and Boudin et al. (2010); Figure 39-8 and Figure 48-1
Doel-Deurganckdok-B	51°18′10″	4°15′59″	−0.55	KIA-17996	5595	35	−26.3	Quercus charcoal	Surface-hearth	
Doel-Deurganckdok-B	51°18′10″	4°15′59″	−0.55	KIA-32618	5595	35	−28.29	Carbonized hazelnut shell	Surface-hearth	
Doel-Deurganckdok-B	51°18′10″	4°15′59″	−0.55	KIA-17994	5575	35	−24.3	Cornus charcoal	Surface-hearth	
Doel-Deurganckdok-B	51°18′10″	4°15′59″	−0.55	KIA-17987	5570	30	−24.3	Carbonized seeds	Surface-hearth	

Doel-Deurganckdok-B	51°18′10″	4°15′59″	−0.55	KIA-17997	5550	35	−27.1	Carbonized Hedera helix seeds	Surface-hearth	
Doel-Deurganckdok-B	51°18′10″	4°15′59″	−0.55	KIA-17986	5400	30	−25.8	Carbonized Prunus spinosa seed	Surface-hearth	
Doel-Deurganckdok-B	51°18′10″	4°15′59″	−0.25	NZA-12076	5220	55	−26.4	Carbonized hazelnut shell	Surface-hearth	
Doel-Deurganckdok-M	51°19′00″	4°16′00″	−0.62	KIA-35774	5700	35	−28.31	Hedera helix charcoal	Surface-hearth	Deforce et al. (2013); Figure 39-4 and Figure 48-4
Doel-Deurganckdok-M	51°19′00″	4°16′00″	−0.62	KIA-35804	5570	35	−27.80	Quercus hilum	Surface-hearth	
Doel-Deurganckdok-M	51°19′00″	4°16′00″	−0.62	KIA-35770	5490	40	−27.75	Viscum album charcoal	Surface-hearth	
Doel-Deurganckdok-M	51°19′00″	4°16′00″	−0.62	KIA-35771	5490	40	−30.00	Hedera helix seeds	Surface-hearth	
Doel-Deurganckdok-M	51°19′00″	4°16′00″	−0.62	KIA-36257	5385	30	−24.17	Viburnum opulus seed	Surface-hearth	
Doel-Deurganckdok-M	51°19′00″	4°16′00″	−0.62	KIA-35769	5350	40	−24.32	Carbonized hazelnut shell	Surface-hearth	
Doel-Deurganckdok-M	51°19′00″	4°16′00″	−0.62	KIA-35772	5325	35	−26.91	Cornus sanguinea seed	Surface-hearth	
Doel-Deurganckdok-M	51°19′00″	4°16′00″	−0.62	KIA-36231	5305	50	−27.27	Carbonized hazelnut shell	Surface-hearth	
Doel-Deurganckdok-M	51°19′00″	4°16′00″	−0.62	KIA-35786	5280	40	−26.65	Carbonized hazelnut shell	Surface-hearth	

Appendix 2: List of all used radiocarbon dated geological samples.

Site	Coring/Profile n°	Latitude	Longitude	Litho-Strat. position	Elevation (mTAW)	Lab n°	BP	Error	Sample composition	Bibliography; Map number on Figure 39 and Figure 48
Antwerpen-Droogdokken	40	51°14′14″	4°24′09″	top peat	−0.08	RICH-20052	2703	30	wood	Verhegge et al., 2014; Figure 39-15
Antwerpen-Droogdokken	40	51°14′14″	4°24′09″	basis peat	−0.59	RICH-20047	4522	29	Alnus glutinosa fruits; Alnus glutinosa male catkin scale; Alnus glutinosa catkin; twigs	
Antwerpen-Droogdokken	46	51°14′12″	4°24′05″	basis peat	−1.54	RICH-20048	4957	30	Alnus glutinosa catkins	
Antwerpen-Liefkenshoek	14	51°18′50″	4°20′30″	top peat	0.63	KIA-48174	3200	30	peat bulk	Verhegge and Laloo, 2010; Figure 39-5
Antwerpen-Liefkenshoek	14	51°18′50″	4°20′30″	middle peat	0.28	KIA-48173	4300	30	peat bulk	
Antwerpen-Liefkenshoek	14	51°18′50″	4°20′30″	basis peat	0.03	KIA-48175	4460	30	peat bulk	
Antwerpen-Regatta	11	51°13′10″	4°22′03″	basis peat	−1.36	KIA-41135	5450	35	peat bulk	Smit and Timmerman, 2009; Figure 39-16
Antwerpen-Regatta	135	51°12′60″	4°22′16″	basis peat	−1.99	KIA-41136	5470	35	peat bulk	
Antwerpen-Regatta	24	51°13′08″	4°21′42″	basis peat	−1.34	KIA-41137	4955	40	peat bulk	
Antwerpen-Regatta	24	51°13′08″	4°21′42″	top peat	−0.49	KIA-41138	2970	30	peat bulk	
Antwerpen-Regatta	56	51°13′06″	4°21′59″	basis peat	−1.78	KIA-41139	5140	35	Alnus glutinosa catkin	
Antwerpen-Regatta	56	51°13′06″	4°21′59″	middle peat	−1.33	KIA-41151	4580	35	Alnus glutinosa catkin	

Antwerpen-Regatta	56	51°13′06″	4°21′59″	top peat	−0.83	KIA-41152	3675	40	Oenanthe aquatica seeds	
Bazel-sluis	A	51°08′09″	4°19′23″	peat (5)	−0.53	Beta-343983	4500	30	Urtica dioica (1 seed), Alnus glutinosa (1 cone, 4 seeds, 6 seed fragments)	Deforce et al., 2014b; Figure 48-6
Bazel-sluis	A	51°08′09″	4°19′23″	shell-/OM rich clay (4)	−0.7	KIA-47570	4575	35	Ilex aquifolium (1 seed), Alnus glutinosa (cone fragment), Quercus sp. (6 bud fragments)	
Bazel-sluis	A	51°08′09″	4°19′23″	shell-/OM rich clay (4)	−0.91	Beta-342273	4790	30	Unidentified (1 bud, 22 bud fragments)	
Bazel-sluis	A	51°08′09″	4°19′23″	shell-/OM rich clay (4)	−1.11	KIA-47722	4660	30	Alnus glutinosa (1 cone)	
Bazel-sluis	B	51°08′09″	4°19′23″	shell-/OM rich clay (4)	−2.8	KIA-47571	4950	35	Betulaceae (2 catkin fragments), Quercus sp. (1 bud fragment) 2, Alnus glutinosa (1 seed)	
Bazel-sluis	B	51°08′09″	4°19′23″	coarse sand (3)	−3.13	KIA-47567	5035	35	Tilia sp. (1 seed)	
Bazel-sluis	B	51°08′09″	4°19′23″	OM rich clay/peat (2)	−3.35	KIA-47720	6155	40	Unidentified twig	
Bazel-sluis	B	51°08′09″	4°19′23″	(sandy) clay (1)	−3.43	KIA-47572	6145	35	Quercus sp. (1 seed)	
Berendrechtsluis	1	51°21′00″	4°16′00″	basis basal peat	−1.91	IRPA-769	6000	75	peat bulk	Kiden, 1989; Figure 39-1
Berendrechtsluis	2	51°21′00″	4°16′00″	basis basal peat	−0.38	IRPA-770	4480	70	peat bulk	
Berendrechtsluis	3	51°21′00″	4°16′00″	basis basal peat	0.47	IRPA-771	4630	70	peat bulk	
Berendrechtsluis	4	51°21′00″	4°16′00″	basis basal peat	1.35	IRPA-772	3570	65	peat bulk	

Doel-Deurganckdok-A		51°18′15″	4°16′04″	basis basal peat	−3.21	KIA-17640	5885	35	peat bulk	Van Strydonck, 2005; Figure 39-7
Doel-Deurganckdok-A		51°18′15″	4°16′04″	top basal peat	−2.84	KIA-17639	5740	35	peat bulk	
Doel-Deurganckdok-A		51°18′15″	4°16′04″	basis holland peat	−1.89	KIA-17638	4955	30	peat bulk	
Doel-Deurganckdok-A		51°18′15″	4°16′04″	top holland peat	0.01	KIA-17637	1340	25	peat bulk	
Doel-Deurganckdok-B		51°18′10″	4°15′59″	basis peat	−1	KIA-12075	5050	55	peat bulk	Van Strydonck, 2005; Figure 39-8, Figure 48-1
Doel-Deurganckdok-M	1	51°19′00″	4°16′00″	basis basal peat	−1.655	RICH-20092	6269	37	charcoal	Verhegge et al., 2014; Figure 39-4, Figure 48-4
Doel-Deurganckdok-M	1	51°19′00″	4°16′00″	top basal peat	−1.37	RICH-20091	5477	42	Urtica dioica	
Doel-Deurganckdok-M	1	51°19′00″	4°16′00″	basis holland peat	−0.82	RICH-20093	4856	36	Urtica dioica (wood)	
Doel-Deurganckdok-M	3	51°19′00″	4°16′00″	basis holland peat	−0.6	RICH-20087	4695	68	Urtica dioica; Alisma plantago-aquatica; Oenantha aquatica; Solanum dulcamara; Carex cf. pseudocyperus; Carex cf. vesicaria	
Doel-Dok		51°18′15″	4°15′10″	basis basal peat	−1.72	IRPA-458	5490	80	peat bulk	Minnaert and Verbruggen, 1986; Figure 39-6,
Doel-Dok		51°18′15″	4°15′10″	top basal peat	−1.1	IRPA-454	4900	60	peat bulk	
Doel-Dok		51°18′15″	4°15′10″	basis holland peat	−0.98	IRPA-457	5350	70	peat bulk	
Doel-Dok		51°18′15″	4°15′10″	middle holland peat	NoData	IRPA-456	3000	70	peat bulk	
Doel-Dok		51°18′15″	4°15′10″	top holland peat	−0.385	IRPA-455	2050	70	peat bulk	

Doel-NPP		51°19′16″	4°14′43″	basis basal peat	−2.805	KIA-36924	5820	35	peat bulk	Deforce, 2011; Figure 39-3
Doel-NPP		51°19′16″	4°14′43″	top basal peat	−2.43	Beta-261806	5750	40	peat bulk	
Doel-NPP		51°19′16″	4°14′43″	Calais sedi-ments	−2.065	Beta-261805	5530	40	peat bulk	
Doel-NPP		51°19′16″	4°14′43″	basis holland peat	−1.675	KIA-36912	5025	30	peat bulk	
Doel-NPP		51°19′16″	4°14′43″	middle holland peat	−1.205	Beta-261804	4340	40	peat bulk	
Doel-NPP		51°19′16″	4°14′43″	middle holland peat	−0.845	KIA-36911	3770	30	peat bulk	
Doel-NPP		51°19′16″	4°14′43″	middle holland peat	−0.575	Beta-261803	3130	40	peat bulk	
Doel-NPP		51°19′16″	4°14′43″	top holland peat	−0.245	KIA-33610	1400	25	peat bulk	
Doel-Polder Noord	16	51°19′56″	4°14′53″	basis peat	1.945	RICH-20046	2555	28	Calluna vulgaris (charred flowers, leaves, charred twigs)	Verhegge et al., 2014; Figure 39-2
Doel-Polder Noord	16	51°19′56″	4°14′53″	top peat	2.215	RICH-20050	3365	30	wood	
Doel-Polder Noord	39	51°19′56″	4°14′54″	basis peat	−2.27	RICH-20057	5265	30	Carex sp.; Urtica dioica (budscales)	
Doel-Polder Noord	39	51°19′56″	4°14′54″	top peat	−0.135	RICH-20045	1095	29	Sphagnum leaves	
Doel-Polder Noord	40	51°19′55″	4°14′55″	basis basal paet	−3.776	RICH-20208	5515	36	Alnus female cone	
Doel-Polder Noord	40	51°19′55″	4°14′55″	basis holland peat	−1.615	RICH-20079	5153	36	wood	
Kallo-Vrasenedok		51°15′45″	4°14′31″	basis peat	−3.47	IRPA-546	6790	80	peat bulk	Janssens and Ferguson, 1985;

Kallo-Vrasenedok		51°15′45″	4°14′31″	middle peat	−2.27	IRPA-545	4240	70	peat bulk	Figure 39-11
Kallo-Vrasenedok		51°15′45″	4°14′31″	top peat	−1.3	IRPA-544	2810	60	peat bulk	
Kallo-Zeesluis		51°16′02″	4°16′22″	basis peat	−2.85	GrN-7938	6020	70	peat bulk	
Kallo-Zeesluis		51°16′02″	4°16′22″	basis Calais gully	−6.2	GrN-7898	5750	40	peat bulk	
Kallo-Zeesluis		51°16′02″	4°16′22″	top holland peat	−0.75	GrN-7937	4630	60	peat bulk	Kuijper, 2006; Figure 39-9
Kreekrak		51°25′48″	4°13′45″	A-horizon top pleistocene	−5.28	GrN-16942	6330	70	peat bulk	Vos, 1992; outside the map
Kreekrak		51°25′48″	4°13′45″	basis basal peat	−5.22	GrN-16941	6290	45	peat bulk	
Melsele-Hof ten Damme	3	51°15′01″	4°17′40″		−0.52	IRPA-942	5300	70	organic layer bulk	Van Strydonck et al., 1995; Figure 39-13, Figure 48-5
Melsele-Hof ten Damme	3	51°15′01″	4°17′40″		−0.235	IRPA-943	5160	60	organic layer bulk	
Melsele-Hof ten Damme	3	51°15′01″	4°17′40″	basis peat	−0.175	IRPA-944	5350	50	peat bulk	
Melsele-Hof ten Damme	3	51°15′01″	4°17′40″	top peat	0.22	IRPA-946	5000	40	peat bulk	
Melsele-Hof ten Damme	3	51°15′01″	4°17′40″	basis holland peat	0.51	IRPA-947	4300	60	peat bulk	
Melsele-Hof ten Damme	3	51°15′01″	4°17′40″	middle peat	1.1	IRPA-949	2900	50	peat bulk	
Melsele-Hof ten Damme	3	51°15′01″	4°17′40	top holland peat	1.83	IRPA-950	1915	40	peat bulk	
Melsele-Hof ten Damme	2	51°15′01″	4°17′40″	basis peat	1.655	IRPA-951	4080	60	peat bulk	

Melsele-Hof ten Damme	2	51°15′01″	4°17′40″	middle peat	1.76	IRPA-952	3540	50	peat bulk	
Melsele-Hof ten Damme	2	51°15′01″	4°17′40″	middle peat	1.87	IRPA-953	3500	45	peat bulk	
Melsele-Hof ten Damme	2	51°15′01″	4°17′40″	middle peat	1.95	IRPA-954	3300	40	peat bulk	
Melsele-Hof ten Damme	2	51°15′01″	4°17′40″	middle peat	2.07	IRPA-955	2800	45	peat bulk	
Melsele-Hof ten Damme	2	51°15′01″	4°17′40″	middle peat	2.13	IRPA-956	2310	40	peat bulk	
Melsele-Hof ten Damme	2	51°15′01″	4°17′40″	top peat	2.29	IRPA-957	1770	40	peat bulk	
Moerzeke-Kastel	1	51°03′00″	4°10′00″	basis basal peat	0.27	IRPA-5847	4620	40	peat bulk	Kiden, 1989; outside the map
Moerzeke-Kastel	2	51°03′00″	4°10′00″	top peat	1.1	IRPA-9711	1585	80	peat bulk	
Oosterweel	1	51°14′35″	4°23′10″	basis basal peat	0.32	IRPA-713	3890	65	peat bulk	Kiden, 1989; Figure 39-14
Oosterweel	2a	51°14′35″	4°23′10″	top peat	1.27	IRPA-714a	1840	55	peat bulk	
Oosterweel	2b	51°14′35″	4°23′10″	top peat	1.27	IRPA-714b	1300	55	peat bulk	
Oosterweel	3	51°14′35″	4°23′10″	top peat	0.83	IRPA-652	1630	55	peat bulk	
Verrebroek-Aven Ackers	14	51°15′14″	4°11′55″	basis peat	−1.157	KIA-47208	4565	35	Alnus glutinosa twigs	Verhegge et al., 2014; Figure 39-12
Verrebroek-Aven Ackers	13	51°15′14″	4°11′55″	middle peat	−0.277	KIA-47207	3870	30	Betula (fruit fragments, female catkin scales, male catkin scales); Carex rostrata	

Verrebroek-Aven Ackers	12	51°15′14″	4°11′55″	top peat	0.393	KIA-47206	725	20	Ranunculus flammula; Alisma plantago-aquatica; Elecharis palus-tris/uniglumis; Hydro-cotyle vulgaris; Plantago major; Stellaria media	
Verrebroek-Dok 1	1	51°15′53″	4°12′40″	basis peat	0.225	KIA-17992	4690	30	peat bulk	Van Strydonck, 2005; Figure 39-10
Wintham	1	51°07′01″	4°18′15″	basis basal peat	0.5	IRPA-712	4220	65	peat bulk	Kiden, 1989; outside the map
Wintham	2	51°07′01″	4°18′15″	basis basal peat	−0.45	IRPA-741	5110	70	peat bulk	
Wintham	3	51°07′01″	4°18′15″	basis basal peat	−1.25	IRPA-740	5550	75	peat bulk	
Wintham	4	51°07′01″	4°18′15″	top peat	−2.07	IRPA-768	5740	75	peat bulk	
Zwijndrecht-Stellae Scaldis	A15	51°12′19″	4°21′16″	basis peat	1.3	RICH-20090	4484	49	Sambucus nigra (seed), Juncus	Verhegge et al., 2014; Figure 39-17